GEORG-AUGUST-UNIVERSITÄT
GÖTTINGEN

Dynamics of Neutrophil Extracellular Trap (NET) Formation

DISSERTATION

for the award of the degree
"Doctor rerum naturalium"
of the Georg-August-Universität Göttingen

within the doctoral program
"Molecular Medicine"
of the Georg-August University School of Science (GAUSS)

submitted by

Elsa Neubert
from Berlin, Germany

Göttingen, 2019

Thesis Committee

Prof. Dr. Michael P. Schön
Department of Dermatology, Venereology and Allergology
University Medical Center Göttingen

Prof. Dr. Jürgen Wienands
Institute for Cellular and Molecular Immunology
University Medical Center Göttingen

Dr. Sebastian Kruss
Institute for Physical Chemistry
Georg-August University Göttingen

Members of the Examination Board

Referee: Prof. Dr. Michael P. Schön
Department of Dermatology, Venereology and Allergology
University Medical Center Göttingen

2nd Referee: Prof. Dr. Jürgen Wienands
Institute for Cellular and Molecular Immunology
University Medical Center Göttingen

Further members of the Examination Board

Dr. Sebastian Kruss
Institute for Physical Chemistry
Georg-August University Göttingen

Prof. Dr. Alexander Flügel
Institute of Neuroimmunology and Multiple Sclerosis Research
University Medical Center Göttingen

Prof. Dr. Holger Reichardt
Institute for Cellular and Molecular Immunology
University Medical Center Göttingen

Prof. Dr. Alexander Egner
Laser Laboratory Göttingen

Date of oral examination: 07/05/2019

Affidavit

I hereby declare that this doctoral thesis “Dynamics of Neutrophil Extracellular Trap (NET) Formation” has been written independently with no other aids or sources than quoted.

Göttingen, March 2019

Elsa Neubert

Table of content

Abstract I (English)

Neutrophil granulocytes are the largest group of white blood cells and play a significant role in the innate immune system. With the discovery of a vast number of thus far unknown functions, neutrophil granulocytes became a focus in biomedical research. One of the most remarkable findings are neutrophil extracellular traps (NETs), fibril networks of decondensed chromatin with attached antimicrobial proteins that can be released as a response to various stimuli in order to defend pathogens. The process of NET formation (NETosis) is evolutionarily highly conserved and involved in many pathological conditions. A detailed analysis of NETosis can, therefore, contribute to a better understanding of such diseases and therapeutic strategies.

So far, the biophysical forces driving the morphological alternations that underlie chromatin decondensation and subsequent NET release are poorly understood. This issue is addressed in the first manuscript of this thesis. The results of this study show that NETosis occurs in three distinct phases of which only the first depends on enzymatic activity and energy consumption. The second phase is primarily driven by material properties and entropic swelling of chromatin. Therefore, the start of chromatin decondensation with nuclear envelope breakdown (onset of phase 2) represents a point of no return in NETosis. Complete chromatin decondensation is followed by NET release through rupture of the plasma membrane at a predetermined breaking point (phase 3). This biophysical characterization facilitates our understanding of the precise mechanisms of NETosis and highlights the extent by which complex biological processes can be driven by material properties.

In vitro NETosis studies are being conducted by an ever-increasing number of groups. They use highly diverse amounts of serum and serum albumin in their culture media. This is problematic, as these supplements interfere with NETosis depending on their concentration, used stimulus and neutrophil donor species (human vs. mouse). Details are analyzed in the second manuscript, which contributes to the comparability of research conditions.

Furthermore, ultraviolet-visible (UV-Vis) light can massively alter cell functions. The third manuscript investigates the effect of UVA and blue light on NETosis. Light activates a neutrophil elastase (NE)- and myeloperoxidase (MPO)-dependent pathway of ‘suicidal’ NETosis, which requires the riboflavin-mediated generation of reactive oxygen species (ROS). External factors, therefore, have a crucial impact on NET formation, which has to be considered for *in vitro* studies. Additionally, light-induced NETosis may be of particular interest in the pathogeneses of light-sensitive disorders (“photodermatoses”) including autoimmune diseases such as lupus erythematosus.

Together, these studies provide detailed insight into the mechanisms of NET formation and their regulation.

Abstract II (German)

Neutrophile Granulozyten sind die größte Population weißer Blutzellen und ein essentieller Bestandteil des angeborenen Immunsystems. Durch die Entdeckung einer Vielzahl neuer Funktionen sind neutrophile Granulozyten in den Fokus der biomedizinischen Forschung gerückt. Die Bildung neutrophiler extrazellulärer Traps (NETosis), einem Netzwerk aus dekondensiertem Chromatin dekoriert mit antimikrobiellen Substanzen, welches zur Abwehr von Pathogenen freigegeben werden kann, ist eine der eindrucksvollsten Funktionen. Interessanterweise ist dieser Prozess evolutionär konserviert und involviert in verschiedenste Pathologien. Daher kann eine detaillierte Analyse dieses Prozesses zu einem tieferen Verständnis der damit assoziierten Erkrankungen und zur Entwicklung möglicher therapeutischer Strategien beitragen.

Bisher sind die biophysikalischen Kräfte hinter den massiven morphologischen Veränderungen, welche die vollständige Chromatindekondensation und Freigabe der NETs ermöglichen, nur wenig verstanden. Die Beantwortung dieser Frage steht im Fokus des ersten Manuskriptes dieser Arbeit. Die Bildung von NETs kann in drei Phasen unterteilt werden. Davon ist jedoch nur die erste abhängig von enzymatischen Prozessen und Energieverbrauch. Die zweite Phase hingegen wird von den Materialeigenschaften der Zelle, insbesondere dem entropischen Schwellen des Chromatins, bestimmt. Der Beginn der Dekondensation geht hierbei mit der Ruptur der Kernhülle Hand in Hand und repräsentiert einen „*point of no return*“. Nachdem das Chromatin vollständig dekondensiert ist, bricht die Plasmamembran an einer vorbestimmten Position (Phase 3). Diese biophysikalische Charakterisierung erleichtert unser Verständnis der der NETose zugrundeliegenden Mechanismen maßgeblich. Sie hebt auch hervor, in welchem Ausmaß Materialeigenschaften einer Zelle komplexe Vorgänge steuern können.

In vitro Studien der NETose werden von einer stetig steigenden Zahl von Forschungsgruppen durchgeführt. Sie verwenden die unterschiedlichsten Serum- und Serumalbuminzusätze in ihren Kulturmedien. Allerdings beeinflussen Serumzusätze die NETose abhängig von ihrer Konzentration, dem verwendeten Stimulus und der Neutrophilenspezies (human vs. murin). Diese Mechanismen werden detailliert im zweiten Manuskript analysiert, was zu einer verbesserten Vergleichbarkeit von experimentellen Konditionen beitragen kann.

Auch Licht aus dem ultravioletten und sichtbaren Bereich kann Zellfunktionen massiv beeinflussen. Der Effekt von UVA und blauem Licht auf Neutrophile wurde im dritten Manuskript untersucht. Licht aktiviert die „suizidale“ NETose über einen Neutrophilen Elastase (NE)- und Myeloperoxidase (MPO)-abhängigen Weg, der die Bildung von reaktiven Sauerstoffspezies (ROS) über Riboflavin voraussetzt. Demnach können externe Faktoren die NETose massiv beeinflussen, was von großer Bedeutung für *in vitro* Untersuchungen ist. Darüberhinaus ist es denkbar, dass lichtinduzierte NETose in der Pathogenese von Erkrankungen mit erhöhter Photosensibilität, beispielsweise Autoimmunerkrankungen wie des Lupus erythematodes, beteiligt ist.

Die Ergebnisse dieser Arbeit erlauben einen detaillierten Einblick in die Mechanismen der NETose sowie in deren Regulierung.

List of abbreviations

aggNETs: aggregated Neutrophil extracellular traps
AGs: Azurophilic granules
ANCAs: Anti-neutrophil cytoplasmic antibodies
APC: Antigen-presenting cells
ATP: Adenosine triphosphate
AZU: Azurocidin
BSA: Bovine serum albumin
CaI: Calcium ionophore
CCR: C-C motif chemokine receptor
CD: Cluster of differentiation
CDK4/6: Cyclin-dependent kinases 4 and 6
CG: Cathepsin G
CGD: Chronic granulomatous disease
CR1/3: Complement receptor 1/3
CRISPR/Cas9: Clustered regularly interspaced short palindromic repeats/CRISPR-associated protein 9
CXCL: CXC chemokine ligand
CXCR: CXC chemokine receptor
DCs: Dendritic cells
DNA: Deoxyribonucleic acid
DNase: Deoxyribonuclease
DPPI: Dipeptidyl peptidase I
EETs: Eosinophil extracellular traps
ERK: Extracellular signal-regulated kinase
ETs: Extracellular traps
fMLPR: N-formyl-methionyl-leucyl-phenylalanine receptor
G-CSF: Granulocyte-colony stimulating factor
GGs: Gelatinase granules
G-MDSCs: Granulocytic myeloid-derived suppressor cells
GPCR: G protein-coupled receptor
H3K9me2/3: Histone 3 lysine 9 methylated 2/3
H3S10: Histone 3 serine 10
H3Cit: Citrullinated histone 3
HEPES: 4-(2-Hydroxyethyl)-1-piperazineethanesulfonic acid
hiFCS: Heat-inactivated fetal calf serum
HP1: Heterochromatin protein 1
HSA: Human serum albumin
HSCs: Hematopoietic stem cells
ICAM-1/2: Intercellular adhesion molecule-1/2
LED: Light-emitting diode

IgG: Immunoglobulin G
IL: Interleukin
INFα: Interferon alpha
INM: Inner nuclear membrane
JNK: c-Jun N-terminal kinase
LBR: Lamin B receptor
LDNs: Low-density neutrophils
LDGs: Low-density granulocytes
LFA-1: Lymphocyte function-associated antigen 1
LINC: Linker of nucleoskeleton and cytoskeleton complex
LPS: Lipopolysaccharides
Mac-1: Macrophage-1 antigen
MAPK: Mitogen-activated protein kinase
MEK: MAPK/ERK kinase
METs: Monocyte and/or macrophage extracellular traps
MHC: Major histocompatibility complex
MLKL: Mixed lineage kinase domain-like protein
MMP-25: Matrix metalloproteinase-25
MPO: Myeloperoxidase
MSU: Monosodium urate
mtDNA: mitochondrial Deoxyribonucleic acid
MTOC: Microtubule organizing center
NADPH oxidase: Nicotinamide adenine dinucleotide phosphate oxidase
NE: Neutrophil elastase
NETs: Neutrophil extracellular traps
NK cells: Natural killer cells
NPC: Nuclear pore complex
NSP4: Neutrophil serine protease 4
ONM: Outer nuclear membrane
P1-3: Phase 1-3
PAD: Peptidylarginine deiminase
PAMPs: Pathogen-associated molecular patterns
PDT: Photodynamic therapy
PKC: Protein kinase C
PMA: Phorbol 12-myristate 13-acetate
PNS: Perinuclear space
PSGL1: P-selectin glycoprotein ligand 1
Rac: Ras-related C3 botulinum toxin substrate
RIPK1: Receptor-interacting protein kinase 1
RIPK3: Receptor-interacting protein kinase 3
ROCK: Rho-associated protein kinase
ROS: Reactive oxygen species

SGs: Specific granules
SK3: Small-conductance calcium-activated potassium channel 3
SLE: Systemic lupus erythematosus
SLPI: Secretory leukocyte protease inhibitor
SVs: Secretory vesicles
SVV: Small-vessel vasculitis
TLR4: Toll-like receptor 4
TNFR1: Tumor necrosis factor receptor 1
UV-Vis light: Ultraviolet-Visible light
VAMP2: Vesicle-associated membrane protein 2
VCAM-1: Vascular cell adhesion molecule-1
VLA-4: Very late antigen-4

Motivation and outline

In the past decades, the idea of neutrophils changed from purely short-lived, mature killing cells to highly sophisticated modulators of immune responses. This development has been accelerated by the discovery of new neutrophil functions such as the release of neutrophil extracellular traps (NETs) and the regulation and modulation of innate and adaptive immunity and of multiple neutrophil phenotypes behind these tasks. Hence, the detailed molecular analysis of these new functions in physiological and pathological conditions is the focus of ongoing research. However, only a small number of studies have considered and explored the underlying biophysical mechanisms, which can substantially augment the understanding of their complex sequences and driving forces.
During the formation of neutrophil extracellular traps, neutrophils can release a fibril network of decondensed chromatin in combination with antimicrobial peptides and other mediators to disarm and subsequently attack pathogens. The generation of NETs, apart from phagocytosis and degranulation, thus represents a newly discovered defense strategy. While studying NET release (NETosis) in detail, it became increasingly clear that the deregulation of NETosis is deeply implicated in a variety of diseases including chronic and acute inflammation as well as cancer and autoimmune diseases. Additionally, several groups reported the formation of extracellular traps (ETs) among different cell types, species, and organisms such as earthworms and plants. ET formation is, therefore, a highly conserved, fascinating phenomenon. During NETosis, the neutrophil cell body undergoes profound changes as the cell decondenses its chromatin and dissolves its inner membranes in response to a stimulus. This process leads to a unique mixture of cytoplasmic and granular content along with the decondensed chromatin. In only a few hours, this mixture leaves the cell through the cell membrane in a yet not fully understood manner.

How the cell can perform such extensive cell alterations, as well as the underlying biophysical mechanisms, remains unknown. The first and largest part of this thesis focuses in-depth on the biophysical and biological characterization of NETosis (**Manuscript I**).

The second part of this thesis targets the influence of two external factors on NETosis: serum and serum albumin in cell culture media (**Manuscript II**) and the effect of UVA and blue light on *in vitro* NET formation (**Manuscript III**). The latter is of particular interest regarding the involvement of light sensitivity in autoimmune disorders and may serve as a starting point to understand the contribution of neutrophils to these still largely enigmatic mechanisms.

CHAPTER 1 - Scientific background

1.1 Neutrophils in the human immune system

1.1.1 Functions of neutrophils

To protect itself from intruders, the human body employs a complex system of surface barriers, antimicrobial substances, biochemical cascades, and highly specialized cells: the immune system. Dysregulation of this finely tuned network leads to uncontrolled inflammation with severe tissue damage and is implicated in a variety of severe diseases. Therefore, a detailed understanding of single components of this complex system is essential to ameliorate defective regulation and the host's defense against pathogens.

Classically, the immune system is divided into an innate and an adaptive defense, which builds a finely regulated, closely linked system to protect the organism from pathogens and allow the body to return to physiological conditions. The innate immune system represents the first line defense against pathogens and is characterized by a broad and fast response with the overall goal to stop invading pathogens directly and to activate the adaptive immune response. It comprises physical, chemical and biological barriers, the complement system and multiple cells such as professional phagocytes (neutrophils, macrophages, dendritic cells and mast cells), eosinophils/basophils, innate lymphoid cells as well as natural killer cells (NK cells). In contrast, the adaptive immune response is characterized by a rather slow antigen-specific answer and is responsible for the development of long-term protection against reinfection in the form of memory cells. This precise response is regulated by T cells (T helper cells, T killer cells, γδ T cells, regulatory T cells and natural killer T cells) and B cells, which are located in the secondary lymphoid organs such as lymph nodes, spleen and mucosal lymphoid follicles. Here, T cells are mainly responsible for the antigen-specific cell-mediated response, while B cells mediate the humoral immune response through production of antibodies. Thereby, the presentation of antigens by innate immune cells, so-called antigen-presenting cells (APCs), to lymphocytes in the lymph nodes bridges innate and adaptive immunity [1].

During the last decades, this strict division into two distinct branches has been challenged. More and more researchers report new closely related or overlapping immune functions, thus highlighting considerable flexibility of the immune system. For instance, innate immune cells like NK cells and macrophages can be altered by histone modifications or DNA methylation and thereby obtain short-time immunological memory, referred to as "trained immunity" [2, 3].

Neutrophils are classically assigned to the innate immune system. After their production in the bone marrow, they enter the blood circulation and patrol for infection to exert their primary function, the fast elimination of invading pathogens. For this purpose, they are equipped with an arsenal of innate defense strategies: phagocytosis, degranulation, and the recently discovered NETosis, extensively discussed in **paragraph 1.1.5 and 1.2**. The classical innate functions, phagocytosis and degranulation have already been addressed in many

detailed studies and have led to a profound understanding of neutrophils as a short-lived, terminally differentiated "*unsophisticated thugs*" [4]. During the last two decades, however, this one-sided and narrow view has been challenged, not insignificantly, as a consequence of the invention of new technics such as CRISPR/Cas9, super-resolution microscopy, next-generation sequencing or intravital imaging [4]. Thus, so far unexplored functions like the formation of NETs [5] shifted into the focus of neutrophil research.

Furthermore, the dogma of neutrophils as exclusively short-lived cells has been questioned, as they are able to perform more sophisticated functions than initially anticipated. A recent study confirmed a half-life time of around 19 h [6], which can be increased after cell activation in the context of inflammation by cytokines or bacterial products [7]. In a selective study, even lifetimes of 5.4 days were reported [8], however, this finding is a matter of ongoing debate [9].

Additionally, in contrast to long-lasting opinions, neutrophils do not get fully terminally differentiated and inactive. Upon stimulation, neutrophils can modulate gene expression profiles towards transcriptional regulators as well as proteins for cell survival, proliferation and T cell activation to modulate the immune response actively [10-12].

Among the remarkable discovery of NETosis, whose underlying mechanisms are the main focus of this thesis, neutrophils are able to closely communicate with cells of the innate and adaptive immune system and build a 'social network' to regulate and modulate the immune response [13, 14]. These functions are presumably carried out by phenotypically different neutrophils (see also **paragraph 1.1.3**) [15, 16]. Even direct modulation of T and B cell functions at the site of infection and within lymphatic organs has been reported [17-19]. Neutrophils can express major histocompatibility complexes (MHC) as well as co-stimulating molecules by translocation or *de novo* synthesis in response to various stimuli [20-23] characterizing neutrophils as APCs. In response to severe infection, they can infiltrate into the lymph nodes [19], most likely guided by C-C motif chemokine receptor 7 (CCR7) expression [24], and present antigens to cluster of differentiation 4 positive ($CD4^+$) T cells [25]. Neutrophils can also transport viral antigens to bone marrow or lung and directly influence memory $CD8^+$ T cell-priming [26-28]. Even a modulation of B cell function by cytokine production [29] or by so-called B cell helper neutrophils has been described. The latter can alter immunoglobulin class switch, somatic hypermutation as well as antibody generation in the marginal zone of the spleen [30]. In addition, neutrophils can affect the function of innate immune cells such as monocytes, dendritic cells (DCs) or NK cells [31-34]. However, a major part of these studies has been carried out in mice. Therefore, their role in humans requires further investigation [15].

Altogether, these findings indicate that neutrophils are complex cells performing multiple innate and adaptive functions to kill pathogens and modulate immune responses. As a consequence, the role of neutrophils in pathophysiological conditions has also been reconsidered. They appear to have an underestimated immense role in severe and chronic inflammation [35, 36], autoimmune diseases [37] and cancer [38, 39].

1.1.2 Architecture and development of neutrophil granulocytes

Around 10^{11} neutrophils are produced in humans per day [40], which makes them the largest population among white blood cells (50-70%). Together with eosinophils and basophils, they belong to the polymorphonuclear granulocytes, aptly named by Paul Ehrlich after the lobulated structure of their nucleus (in detail discussed in **paragraph 1.1.4**) [41].
The exact morphology of these cells measuring 10-15 µm was elucidated in detail by electron microscopy [42, 43] (**Fig. 1**). Aside from their unique nuclear structure, the neutrophilic cytoplasm is characterized by several types of granules, which differ in size and content. Four major types of granules have been described, however, more subtypes are under consideration [44]: azurophilic granules (AGs), specific granules (SGs), gelatinase granules (GGs) and secretory granules/vesicles (SVs). All of them have distinct functions according to their content of dissolved and membrane-bound molecules (**Fig. 1**, see also **paragraph 1.1.5**). The different types of granules are formed during distinct stages of maturation in the bone marrow (granulopoiesis) [45]. This process lasts in total around two weeks [46] and is tightly regulated by growth factors and cytokines. Granulopoiesis takes place in three phases: 1) lineage determination starting from hematopoietic stem cells (HSCs) (stem cell pool), 2) the mitotic phase (proliferating cells) and 3) the post-mitotic phase (terminally differentiated cells) [16, 45]. The exact sequence of lineage determination is currently under discussion. It most likely proceeds directly from HSCs to granulocyte-monocyte progenitor cells [47-49]. In the proliferating phase, first myeloblasts and then promyelocytes are formed. The latter already contain AGs. These cells further proliferate to myelocytes containing SGs [46]. In the post-mitotic phase, the cells start to lose their round nucleus and develop from metamyelocytes over band cells holding GGs, to fully mature neutrophils with multilobulated nuclei and the full arsenal of granules [45]. The origin of each type of granule was confirmed by correlation of the granular proteome with the corresponding transcriptome [50]. The exact content of granules can differ slightly even within the same granule type according to the time of generation [51-53].
The onset of differentiation is closely controlled in the HSC niche of the bone marrow by HSC-surrounding cells [45]. Here, HSCs are maintained in the bone marrow mainly by the interaction of the CXC chemokine receptor 4 (CXCR4) with the CXC chemokine ligand 12 (CXCL12) [54]. Granulocyte-colony stimulating factor (G-CSF) represents one of the main inductors of granulopoiesis. In response to G-CSF, HSCs redistribute within the HSC niche [55], and transcription factors are regulated toward the granulocytic lineage. Furthermore, G-CSF controls neutrophil release into the blood by downregulation of the CXCR4-CXCL12-interaction [56, 57] and induction of the CXCR2-CXCL1-interaction with endothelial cells [58]. CXCR2 and CXCR4 are, therefore, functional antagonists in the regulation of neutrophil release from the bone marrow [59]. Additionally, the upregulation of the interleukin (IL) 23-IL17-axis in the tissue increases G-CSF and chemokine release from endothelial cells to recruit neutrophils [60-62]. Enhanced granulopoiesis, also referred to as emergency granulopoiesis, occurs in response to pathogen recognition [63, 64] in order to sufficiently defend intruders. Persistently elevated granulopoiesis, however, can lead to chronic

inflammation [35]. Downregulation of granulopoiesis can be mediated by phagocytosis of aging apoptotic neutrophils by suppression of the IL23-IL17-axis and therefore decrease in G-CSF production, as described in mice [65].
Interestingly, under physiological conditions, neutrophils are also regularly found in spleen, liver, and lung. Whether these cells are mature neutrophils, or continuously recruited to patrol the tissue for infection, remains to be clarified [66].

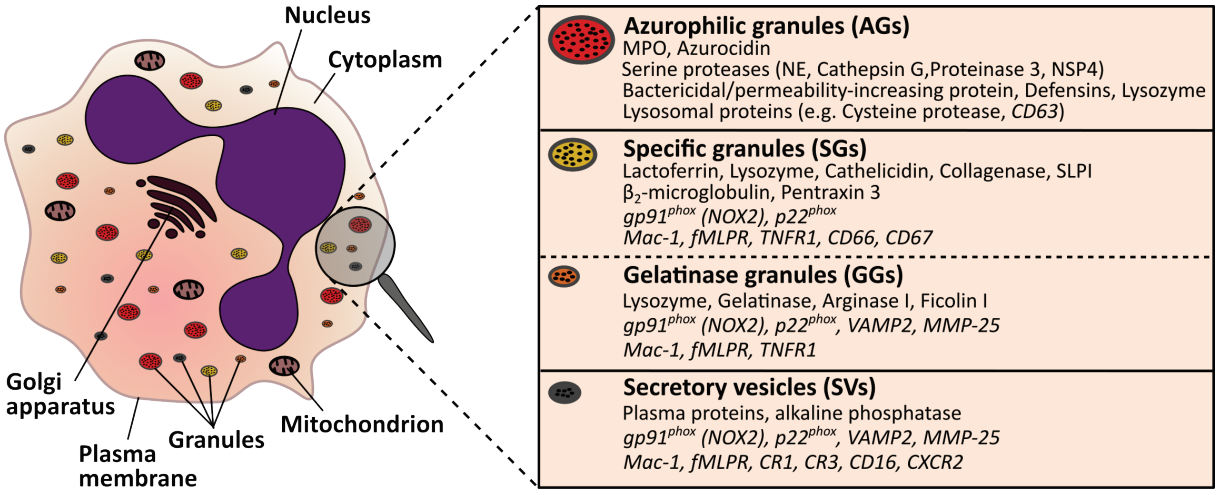

Figure 1: **Architecture of human neutrophil granulocytes.** Neutrophils display two prominent morphological characteristics: lobulated nuclei and neutrophil granules. Neutrophil granules have a unique composition of free (normal writing) and membrane-bound (italic writing) proteins. Granular types: azurophilic granules (AGs), secretory and gelatinase granules (SGs, GGs) and secretory vesicles (SVs). MPO: myeloperoxidase, NE: neutrophil elastase, NSP4: neutrophil serine protease 4, SLPI: secretory leukocyte protease inhibitor, CD: cluster of differentiation, Mac-1: macrophage-1 antigen, fMLPR: N-formyl-methionyl-leucyl-phenylalanine receptor, TNFR1: tumor necrosis factor receptor 1, VAMP2: vesicle-associated membrane protein 2, MMP-25: matrix metalloproteinase-25, CR1/3: complement receptor 1/3, CXCR2: CXC chemokine receptor 2. *Neubert et al., in preparation.*

1.1.3 Heterogeneity of neutrophil granulocytes

The concept of neutrophil heterogeneity was already proposed in 1984 [67]. With the description of new neutrophil functions, this topic moved back into focus. It is an ongoing debate whether these phenotypes represent functionally distinct subtypes or only phenotypes modified by the surrounding tissue, age and host situation. This discussion is addressed in recent reviews [15, 16, 45], but goes beyond the scope of this thesis. Nonetheless, the phenotypes/subtypes differ in neutrophil function and are important to be considered in neutrophil dysregulation (*e.g.*, NETosis). Therefore, they will be summarized shortly in this paragraph.
Clearly different phenotypes have been assigned to priming, aging, and exhaustion. Priming leads to enhanced neutrophil defense (*e.g.*, higher respiratory burst) and can be induced by activating chemotactic stimuli [35, 68]. For instance, cells are primed for NETosis in hyperglycemia [69] and systemic lupus erythematosus (SLE) [70]. In contrast, aging is a programmed change in phenotype, which occurs daily in a circadian fashion as shown in mice [71]. These cells are CXCR4 positive to easily migrate back to the bone marrow [72]. They share surface markers for adhesion and cell-to-cell-cross-talk with primed neutrophils

and act pro-inflammatory [71, 73]. Continuous stimulation can lead to exhaustion or paralysis of neutrophils, characterized by a massive decrease in granules as reported during sepsis [74]. A similar phenotype can occur in systemic inflammation or infections with resistant bacteria [75]. Interestingly, neutrophil function also changes with the host's age. Cells from aged hosts show an increasing deficiency in bioenergetics as well as altered recruitment with enhanced tissue damage and impaired defense mechanisms, such as NETosis [76-80].

Additionally, a few tissue- and disease-specific neutrophil phenotypes/subtypes have been reported [15]. Tissue-specific neutrophils include B cell helper neutrophils in the spleen [30], lymph node neutrophils [24, 81] and pro-angiogenic neutrophils [82]. Disease-specific subtypes/phenotypes have been reported particularly in inflammation, autoimmunity and cancer [83]. One prominent example are low-density neutrophils (LDNs), which show a strikingly low amount of granules. This phenotype was first described in SLE as well as rheumatic diseases [84] and verified in multiple diseases including cancer, sepsis, psoriasis, acquired immune deficiency syndrome and malaria [15]. Two different types exist among LDNs. First, pro-inflammatory LDNs, which were described especially in autoimmune diseases. These cells are prone to undergo NETosis and share multiple markers with activated or exhausted neutrophils [84-87]. Second, an immunosuppressive LDN-type is frequently observed in cancer. This type is difficult to separate from granulocytic myeloid-derived suppressor cells (G-MDSCs), which represent one of the most important types of tumor-associated neutrophils [88-91].

1.1.4 The neutrophil nucleus – structure and function

The neutrophil nucleus has unique properties, which allow the cell to rapidly migrate to its target, tightly squeeze through the endothelium [92-94] or even undergo the massive alterations during NETosis**.** It has a remarkable lobulated shape, which develops during granulopoiesis**.** Under physiological conditions, each cell has 3 to 4 lobuli connected by thin strands of nucleoplasm with little internal chromatin (**Fig. 2** (1)). The number of these lobuli can vary depending on activation or in the context of diseases [95-99].

Within the lobuli, the chromatin is distinguishable in a compact heterochromatin region in the periphery and a large inter-chromatin compartment (DNA-free) in the center of the nucleus (**Fig. 2** (2)). The large inter-chromatin regions arguably contribute to the high flexibility of the nucleus [100]. These layers are separated by euchromatin, the active nuclear compartment in neutrophils [100]. Within the chromatin, 147 base pairs [101] are tightly packed by histone octamers from H2-H4 (**Fig. 2** (3)) into nucleosomes [102, 103]. Thereby, histone H1 functions as a linker to further compact the DNA in the nucleosome [104]. The exact topology of the neutrophil nucleus was only recently described by *Zhu et al.* with respect to its alterations during differentiation [105]. Modification of histones including methylation, ubiquitinylation, acetylation, citrullination or phosphorylation can regulate chromatin functions, such as transcription and chromatin de- and condensation [106, 107].

The cell's chromatin is protected by the nuclear envelope consisting of the inner (INM) and outer (ONM) nuclear membrane separated by the perinuclear space (PNS) and stabilized by

the underlying lamina. Nuclear pore complexes (NPCs) interrupt the membrane and function as transport systems between the extracellular space and the cytoplasm [108, 109]. The nuclear lamina represents a complex protein system consisting of intermediate filaments type V (Lamin A, B1, B2, and C) [110, 111], which are anchored in the INM by several membrane proteins [112] (**Fig. 2** (2)). The lamina is connected to the heterochromatin by the lamina-associated domains [113] and *via* the linker of nucleoskeleton and cytoskeleton (LINC) complex to the cytoskeleton [114, 115]. It can adapt to the cell's requirements [116] and has been considered to contribute to nuclear shaping, mechanotransduction and overall cell mechanics [117]. Interestingly, neutrophils contain relatively low amounts of nuclear envelope proteins, which are down-regulated during granulopoiesis [118]. Mature neutrophils lack proteins of the LINC complex [119] as well as lamin A/C and contain only low remaining lamin B [118]. These alterations may constitute the mechanistic basis for the morphological plasticity of the neutrophil nucleus. For instance, lamin A/C-deficiency significantly softens the nucleus and increases its deformability [120-122].
In contrast, lamin B receptor (LBR) expression increases during maturation as shown in HL-60 cells (human leukemia cell line) and mouse models [105, 123]. LBR is a transmembrane protein that binds to chromatin, lamins (especially Lamin B) and heterochromatin binding protein 1 (HP1) as reviewed elsewhere [124-126]. Interestingly, loss of LBR leads to impaired lobulation and decreased migration in neutrophils of LBR-deficient patients [127, 128]. The exact contribution of LBR to neutrophil function especially *in vivo*, however, is a matter of ongoing debate [94, 125, 129].

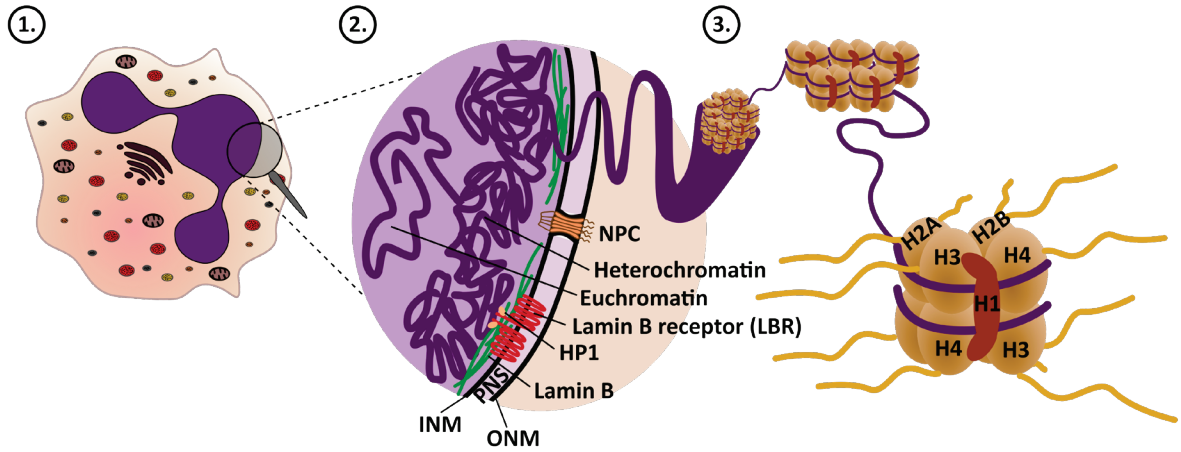

Figure 2: The neutrophil nucleus. 1) Overview of a human neutrophil. 2) Typical structure of the nuclear envelope. INM/ONM: inner and outer nuclear membrane, PNS: perinuclear space, NPC: nuclear pore complex, LBR: lamin B receptors, HP1: heterochromatin protein 1. 3) Nucleosome structure. H 1-4: histone 1-4**.** *Neubert et al., in preparation.*

The role of the cytoskeleton in the development of the lobulated nucleus is still under consideration as well. While actin is presumably not involved, a contribution of tubulin has been discussed, and a decrease of vimentin may favor a multi-lobulated nuclear shape [97, 119, 123, 130, 131]. Overall, neutrophils form an astonishingly flexible nucleus, although parts of the exact underlying mechanisms still remain unresolved [105, 119].

Remarkable are also the morphological differences between murine and human neutrophils. The nuclear lobes of human neutrophils are frequently connected with thin strands, while murine cells rather feature a "*twisted ring-shape*" [99]. Additionally, the latter show higher lamin B expression and appear less fragile than human cells [99]. In general, the morphology varies considerably among different species, possibly due to different tissue densities [92], which needs to be considered for their comparison within experimental data.

1.1.5 Defense strategies of neutrophils - degranulation and phagocytosis

To attack intruders, neutrophils have to be recruited and guided to the place of infection. This process has to be tightly regulated since uncontrolled neutrophil activation can lead to massive tissue damage as discussed in **paragraph 1.2.5** for NETosis. The complex mechanisms of neutrophil recruitment are reviewed in detail by *Kolaczkowska and Kubes* [66].

In the classical scenario of diapedesis, neutrophils have to migrate through the intact endothelium into the tissue to reach the site of infection [132]. Therefore, the cells have to show particularly high flexibility and compensate the mechanical forces due to the shear stress of the blood flow as well as pressure of the surrounding cells. This process is tightly regulated and involves characteristic changes of the nuclear morphology and its interplay with the cytoskeleton as recently extensively reviewed [94, 133]. The unique morphology of neutrophils also allows them to reach a remarkable migration speed of 19 +/-6 µm/min *in vitro* [134].

Neutrophil infiltration from the vasculature into the tissue is mainly induced by mast cells and macrophages as well as pathogens and their products recognized by receptors for pathogen-associated molecular patterns (PAMPs) [135]. To guide neutrophils to the site of infection, the endothelium, in the first step, expresses E- and P-selectin in proximity to the stimulus and neutrophils bind by glycosylated ligands such as P-selectin glycoprotein ligand 1 (PSGL1) [136] enabling them to adjustably tether and roll along the endothelium [137]. Under high shear stress, even thin membrane extensions can be built, so-called 'slings', which wrap around a neutrophil and guide the rolling cell on the endothelial lining [138]. Further stimulation of neutrophils by *e.g.*, chemokines attached to the endothelium [139], leads to activation of integrins on the cell's surface (inside-out-signaling). The main integrins involved are β_2-integrins (lymphocyte function-associated antigen 1 (LFA-1), macrophage-1 antigen (Mac-1)) and β_1-integrins (very late antigen-4 (VLA-4)). These integrins mediate the cell's binding to intercellular or vascular cell adhesion molecule-1/2 (ICAM-1/2, VCAM-1) expressed by the endothelium [140]. Subsequently, neutrophils reduce rolling speed, crawl and flatten the cell body until they attach firmly and start to migrate para- and transcellularly through the endothelium [141]. Thereafter, cells are guided to the site of infection by chemotactic gradients (*e.g.*, chemokines, leukotrienes, complement factors or bacterial products) [66, 142]. In addition to this classical way, alternative recruiting pathways of neutrophils into specific tissues such as liver, brain or spleen were reported [14, 66]. For instance, neutrophils can be recruited CD44-hyaluronan-dependently into the liver [143]. Interestingly, within the tissue, neutrophils are even able to guide themselves over large

distances in complex cell cluster movements. This process, also referred to as neutrophil swarming, can be mediated by leukotriene B4 [144].

Having arrived at the target, neutrophils attack pathogens by different strategies including degranulation, phagocytosis and NETosis (**Fig. 3**). One of the most important tools to exert these functions is the directed release of different granules. As already alluded to **paragraph 1.1.2**, neutrophils contain at least four different types of granules (AGs, SGs, GGs, VSs) with unique compositions of dissolved and membrane-bound molecules [145-147] (**Fig. 1** and below). The granules discharge their contents in a precisely defined sequence in response to multiple signals and thresholds (reviewed in [148]). In general, they are released inversely to their generation and with increasing content of antimicrobial substances (SVs → GGs → SGs → AGs). The precise regulation of degranulation is complex (**Fig. 3** (1)). The current knowledge including the underlying signaling cascades was only recently summarized by *Yin et al.* [148].

SVs [149, 150] contain a large fraction of membrane-bound proteins including receptors (*e.g.*, fMLPR, CR1/3, CD16b (FCγRIIIb), CXCR2), MMP-25, membrane fusion proteins (*e.g.*, VAMP2), integrins (Mac-1) as well as membrane-bound nicotinamide adenine dinucleotide phosphate (NADPH) oxidase components ($gp91^{phox}$/NOX2, $p22^{phox}$) (**Fig. 1**; for abbreviations see figure legend). Furthermore, they contain a surprisingly high amount of cytoplasmic proteins [149], most likely originating from an endocytotic formation of these vesicles [146]. Importantly, SVs are already mobilized during rolling [151] by the induced modest calcium increase and simultaneous activation by chemokines [152, 153]. Thereby, integrins [154] and receptors [155] are transported to the cell's surface, which modulate neutrophil activation as well as firm adhesion to the endothelium.

Specific (lactoferrin positive) and gelatinase (gelatinase positive) granules (SGs, GGs) have similar functions and overlapping contents [45, 50]. They contain moderate amounts of antimicrobials (SG > GGs) and several membrane-bound receptors and integrins (*e.g.*, fMLPR, TNFR1, Mac-1) to guide neutrophils to the site of infection and initiate the antimicrobial defense [148]. Degranulation of SGs and GGs occurs in response to stronger calcium signals (calcium flickers [156]) induced by the increasing chemotactic signal and subsequent G protein-coupled receptor activation (GPCR) [157]. Thereby, the majority of these granules is released onto the cell surface and only a few granules (mainly SGs) into the phagosome during phagocytosis (**Fig. 3** (2)) [158].

AGs contain a large number of antimicrobial effectors such as myeloperoxidase (MPO), serine proteases (neutrophil elastase (NE), proteinase 3, cathepsin G (CG) and neutrophil serine protease 4 (NSP4)), bactericidal/permeability-increasing protein, defensins and lysosomal proteins. Hence, the main function of AGs is the effective killing of pathogens. To carry out this function, AGs can be secreted onto the cell surface (membrane-targeting, actin-dependent [159]) or into the phagosome (phagosome-targeting, tubulin-dependent [160]) [161-163]. Their degranulation is triggered by an additive calcium signal induced by combinations of GPCR, phagocytic receptor [164] and complement receptor [165] activation [148, 164, 166].

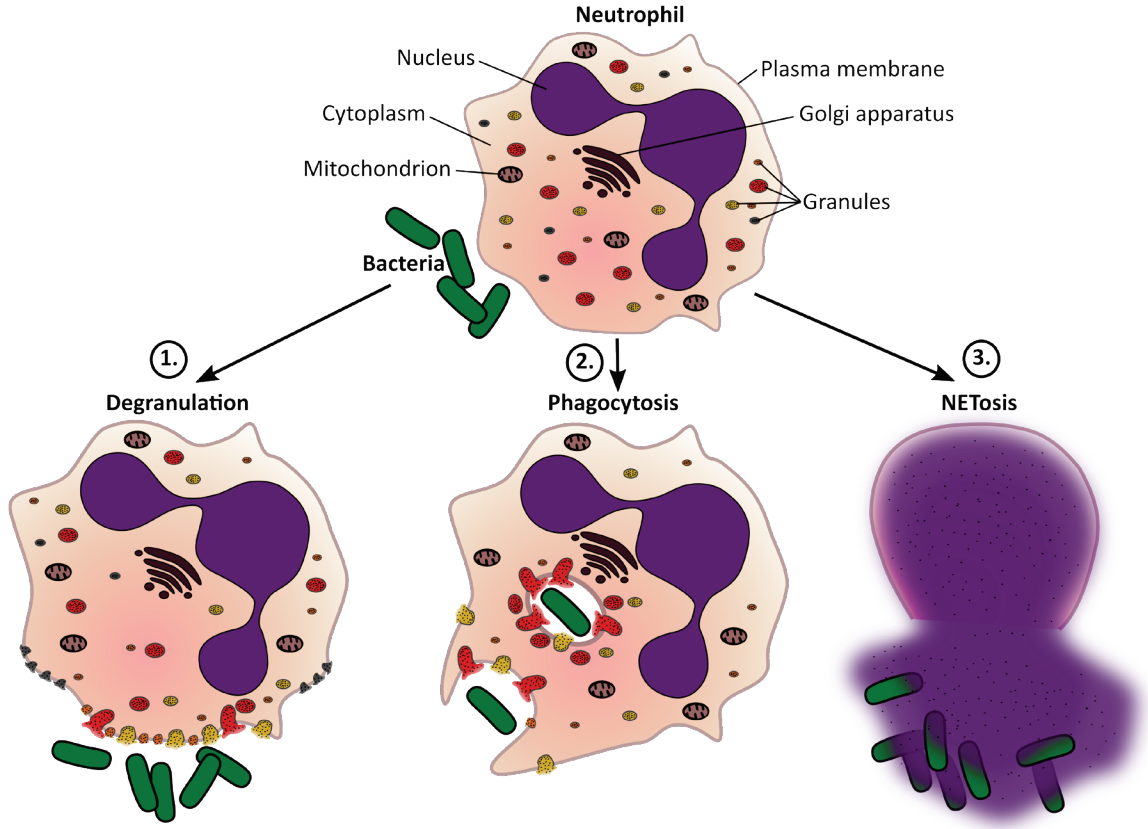

Figure 3: Defense strategies of neutrophil granulocytes. Neutrophils can attack pathogens by three main mechanisms. 1) The release of antimicrobial substances by degranulation. 2) Phagocytosis of bacteria. 3) Immobilization and attack of bacteria by the release of NETs. *Neubert et al., in preparation.*

Phagocytosis is one of the most important defense strategies of neutrophils first described by *Metchnikoff* in 1905 [167] (**Fig. 3** (2)). Neutrophils can engulf opsonized pathogens by pseudopod extension in so-called phagosomes after binding of immunoglobulin G (IgG) by phagocytic receptors (*e.g.*, FcγRIIa and FcγRIIIb) or complement factors by complement receptors [168]. Importantly, neutrophil phagocytosis is closely connected to degranulation. Unlike macrophages, they do not perform the classical endosome-lysosome pathway, but fuse AGs and partly SGs, directly with the phagosome in a remarkably fast manner within seconds [169] (reviewed in detail by *Nordenfelt and Tapper* [168]). During this process, the degranulation of granules can occur already prior to and during phagosome formation at the plasma membrane [170]. In this way, neutrophils can directly attack pathogens by antimicrobial substances from the first contact on. This antimicrobial response is supported by the generation of reactive oxygen species (ROS) (oxidative burst), one of the key steps in phagocytosis [171]. For ROS generation, the protein complex NADPH oxidase first assembles at granular, plasma and phagosomal membranes triggered by soluble agonists such as phorbol 12-myristate 13-acetate (PMA) and fMLP [172, 173] or in the context of phagocytosis activation [174]. Upon activation, the membrane-bound components (gp91^{phox}/NOX2, p22^{phox}), which are mainly localized at the membranes of SGs, GGs and to a lower extent SVs [145, 146], associate with the cytosolic components (p47^{phox}, p67^{phox}, p40^{phox}) as well as with the Ras-related C3 botulinum toxin substrate (Rac) [168] (**Fig. 1** and **Fig. 4**). The assembly of NADPH oxidase enables the reduction of O_2 to superoxide anions ($O_2^{\cdot-}$) followed by subsequent formation of several ROS types, above all hydrogen peroxide

(H_2O_2). The formation of H_2O_2 is the basis for further ROS production. It can be used for instance by MPO to generate hypochlorous acid (HClO) or in Fenton reactions to create hydroxyl radicals ($OH^{\cdot}$) catalyzed by metal ions (*e.g.*, Fe^{2+}) [175].
Furthermore, neutrophils are able to 'choose' a certain defense strategy [176]. For instance, NETosis is considered to be preferred over phagocytosis with increasing pathogen size as reported for fungi hyphae [177]. During this process, the decision for NETosis depends on multiple factors such as the accessibility of MPO and NE in granules [177], successful activation of phagocytosis *via* pathogen detection as shown for Dectin-1 [177] or cytoskeletal integrity [176, 177].
Beside the main defense pathways shown in **Fig. 3**, neutrophils can modulate the immune response by *de novo* synthesis of specific proteins or generation of microparticles [35]. Microparticles are membrane vesicles filled with heterogeneous content depending on the surrounding conditions and the activating stimulus. They can be released to carry out diverse functions in health and diseases [178]. These functions include contributions to reactions against opsonized particles [179, 180] or induction of pro-inflammatory [181] as well as anti-inflammatory [182, 183] responses.
Over time, activated neutrophils decrease their resistance against anti-apoptotic signaling [184] and, after successfully targeting the pathogen, they undergo apoptosis or, under certain circumstances, autophagy [185]. In this context, they can express 'find-me' or 'eat-me' signals and are silently cleared by phagocytosis [35, 185, 186]. According to a model of *Kennedy and DeLeo*, this process can be dysregulated by certain pathogens or in a disease-related context. Importantly, this dysregulation can induce a switch to pro-inflammatory cell death pathways such as pyroptosis, oncosis and NETosis [185, 187] accompanied by subsequent tissue damage and acute as well as chronic inflammation [35].

1.2 Neutrophil extracellular trap (NET) formation - NETosis

1.2.1 Forms and pathways of NETosis

In 1996 *Takei et al.* reported the "*rapid killing of human neutrophils by the potent activator phorbol 12-myristate 13-acetate (PMA) accompanied by changes different from typical apoptosis or necrosis*" [188]. However, this observation was initially barely acknowledged until *Brinkmann et al.* showed in 2004 that this mysterious cell death actually represents a third defense strategy of neutrophils besides phagocytosis and degranulation [189]. They reported that neutrophils could release a web-like structure of decondensed chromatin together with several attached antimicrobial proteins in response to gram-positive or -negative bacteria, IL-8, lipopolysaccharides (LPS) or PMA. In these structures, the neutrophils immobilized and attacked gram-positive (*Staphylococcus aureus*) as well as gram-negative (*Shigella flexneri*) bacteria [189]. After fixation, these structures appeared as a web of 15-17 nm long fibers with globular domains of ca. 25 nm visible in electron microscopy [189]. They termed these structures "*neutrophil extracellular traps (NETs)*" [189].
In the following years, the research on NET formation, termed NETosis [190], exploded and it turned out that this phenomenon can occur in multiple forms in a physiological as well as

pathological context, as summarized in recent reviews [191-193]. Furthermore, it is well recognized that human and mouse neutrophils are not the only cells undergoing this fascinating process. The release of extracellular traps (ETs) was reported for various immune cells [194, 195] including monocytes and macrophages (METs) [196, 197], eosinophils (EETs) [198, 199] and mast cells [200]. Additionally, ETs similar to those observed in neutrophils, were documented in many species (*e.g.*, dogs [201], cats [202], cows [203], sheep [204], carps [205], chicken [206], shrimps [207], oysters [208], social amoeba [209], earthworms [210] and root tip cells of plants [211]). Therefore, the formation of ETs is an evolutionarily highly conserved process.

NET formation in neutrophils can occur in response to many different pathogens including bacteria [98, 212-214], viruses [215, 216], fungi [177, 214, 217, 218] and parasites [219-221] as well as activated platelets [212, 222], cytokines/chemokines [98, 189, 223, 224], mitogens such as PMA [98, 189, 213, 214, 217, 225], ionophores [212, 214], monosodium urate (MSU) or cholesterol crystals [213, 226, 227], and a variety of other substances [212] triggering highly diverse signaling cascades [192]. Frequently, the activity of the azurophilic proteins MPO and NE, as well as peptidylarginine deiminase (PAD) enzymes and ROS generation, are involved [98, 214, 217, 218, 224, 228]. Additionally, analogies with pyroptosis/ inflammasome formation [229, 230], autophagy [231, 232], necroptosis [233, 234] and, only recently, mitosis [235] were reported. In most scenarios, the activation is followed by subsequent chromatin decondensation, disintegration of nuclear and granular membranes and mixing of cytoplasmic content with the decondensed chromatin. Eventually, the cell releases the NET through the cell membrane into the extracellular space, leaving the cell to die [98]. This process is clearly distinct from apoptosis, necroptosis, and necrosis [98, 214], and was termed 'suicidal' NETosis. For mechanistic studies of 'suicidal' NETosis, the direct protein kinase C (PKC) activator PMA, ionophores or LPS are frequently used. These molecules are the main activators in the studies presented in **CHAPTER 2**, and their signaling pathways will be addressed in **paragraph 1.2.2**.

In response to gram-positive bacteria, a different form of NET release was reported: 'vital' or 'non-lytic' NETosis [236]. Here, the cells actively release chromatin within 10 minutes in the form of DNA-filled vesicles, possibly to allow a rapid attack of these highly invasive pathogens *in vivo* [237]. It was postulated that these cells are multitasking and even the same cell is able to perform NETosis while crawling at the same time [238]. Apart from nuclear DNA, mitochondrial DNA was found in these NETs [239]. However, the importance of these observations has not been clarified yet [237].

The relevance of the different forms of NETosis and respective pathways *in vivo*, as well as their contribution to the pathogenesis of diseases, is the subject of ongoing research. Several reviews discuss the relevance of, for instance, 'vital' *vs.* 'suicidal' NETosis [236], NETosis *vs.* necroptosis [240], NETosis *vs.* leucocyte hypercitrullination [241], NOX-dependent NETosis *vs.* NOX-independent NETosis [193], aggregated NETs (aggNETs) [242] or the involvement of mitochondrial DNA [241].

The appearance of the released NET can be as diverse as the underlying pathway. Already in the first report of NETs, the presence of histones and granular proteins, most prominently NE, CG, and MPO, was reported [189]. In subsequent studies, the NET-attached proteome in response to PMA was added up to 24 or 29 proteins, respectively, including all four azurophilic serine proteases as well as several cytoplasmic proteins [243, 244]. In response to physiological stimuli, a NET-proteome including 28-80 variable proteins with a 'core proteome' of 33 proteins was confirmed [245, 246]. Bound to the NET, the antimicrobial histones [247, 248] and proteins are locally restricted and can contribute to a directed attack of the immobilized target [189, 244]. For instance, positively charged neutrophilic serine proteases, above all NE, have a high DNA-affinity and are proteolytically active within the NET [244, 249, 250]. Although the actual elimination of pathogens is still controversial, a contribution to pathogen-killing by NETs was confirmed in selective studies [251, 252] and their protective immune function demonstrated [253] for fungi [243, 254], bacteria [189, 214, 251], viruses [215] and parasites [219]. NETosis appears to be especially needed to clear infections involving fungi hyphae, which are too large to be cleared by phagocytosis [192]. After release, the NET can cause significant tissue damage and destroy endothelial as well as epithelial cells [87, 255]. Therefore, NETs must be removed from the tissue. This process is mainly realized by deoxyribonuclease (DNase). DNase decomposes the DNA and inhibits NE activity. The remaining fragmented DNA and proteins are then, most likely, opsonized and subsequently cleared by macrophages in a presumably immunologically silent manner [256, 257]. Inefficient clearance of NETs, as well as the dysregulation of NET formation, can contribute to the pathogenesis of several diseases.
Pathogens can also employ different strategies to escape NETs. They can degrade NETs through DNases or modify the DNA structure as shown for *Staphylococcus aureus* [258, 259], *Streptococcus pneumoniae* [260] and *Streptococcus pyogenes* [261]. Furthermore, they can develop resistance against NETs mainly by virulence factors such as D-alanylation of lipoteichoic acids [262], or suppress NETosis by the release of proteases [263], exotoxins [264] and attenuation of neutrophil adhesion [265].

1.2.2 PMA-, LPS- and calcium ionophore-induced NETosis

The PKC activator PMA is the most frequently used stimulus in mechanistic studies of 'suicidal' NETosis, and its underlying signaling cascade is, therefore, the most widely studied one (**Fig. 4**). Interestingly, NETosis involves very similar signaling pathways in response to different pathogens or crystals [227]. The activation of PKC leads to ROS generation by the assembly of the NADPH oxidase [98] induced by Raf-MEK-ERK signaling [266]. The requirement for NADPH oxidase activity in NETosis was confirmed in neutrophils isolated from chronic granulomatous disease (CGD) patients, who suffer from a defect in this protein [98, 214]. The induced oxidative burst leads to H_2O_2 formation and subsequently triggers the activation and dissociation of NE, CG, and AZU from an azurophilic complex termed azurosome [228]. This process appears to depend on MPO, but the exact mechanism behind MPO involvement requires further investigation [217, 228]. After release from the azurosome, NE starts to degrade actin and at later stages promotes chromatin

decondensation together with MPO [228]. As a consequence, the cell undergoes the characteristic morphological changes of 'suicidal' NETosis. The necessity of MPO and NE was further confirmed in studies with neutrophils isolated from patients with MPO-deficiency [214, 217] or Papillon-Lefèvre syndrome. The latter lack the NE-activating protease dipeptidyl peptidase I (DPPI) [267] and therefore fail to generate NE. Downstream or parallel to NADPH oxidase activation, p38, MAPK and ERK phosphorylation [268], receptor-interacting protein kinase 1 (RIPK1)-RIPK3-mixed lineage kinase domain-like protein (MLKL)-signaling [234] or autophagy pathways [231] were proposed, but conflicting results necessitate further investigations [192, 193]. Apoptosis signaling, however, is not involved as suggested by caspase inhibition studies [214] and absence of DNA-fragmentation [98]. In contrast, activation of NETosis can even induce apoptosis inhibition [266, 269].

Furthermore, the activity of peptidylarginine deiminase 4 (PAD4) was frequently implicated in NETosis, especially in chromatin decondensation. This deiminase converts arginine and methyl-arginine in a calcium-dependent fashion through deimination to citrulline, preferentially at the histone tail [270-273] (**Fig. 5** (6)). PAD4 involvement appears to be heterogeneous and was shown for various stimuli and in multiple mouse models, often in autoimmune diseases [192]. However, its contribution to PMA-induced NETosis especially in human neutrophils is still controversial [214, 224].

Only recently, crucial new players were described for PMA-induced NETosis. For instance, the chromatin-binding protein DEK seems to be required for successful NETosis and possibly contributes to chromatin decondensation [274]. Additionally, based on morphological similarities, a link between NETosis and mitosis was proposed [237]. This issue was addressed in a recent study by *Amulic et al.* [235]. They reported several parallels with mitosis including increased reactivity of the Ki-67 antibody and phosphorylation of retinoblastoma protein, lamin A/C and serine 10 of histone 3 (H3S10) as well as centrosome separation. In this context, NETosis appeared to depend on components of the cell-cycle machinery such as cyclin-dependent kinases 4 and 6 (CDK4/6). Interestingly, they did not observe S phase induction and emphasized the remarkable difference in temporal dynamics between both processes. Based on their results, they pictured NETosis as a "*modified*" or "*hi-jacked*" cell division [235].

Calcium ionophore (CaI)-induced NETosis proceeds more rapidly and varies profoundly in the underlying signaling cascade compared to the PMA-induced process. Most strikingly, it does not require NADPH oxidase activation but mitochondrial ROS generation, and was therefore termed NOX-independent [275, 276]. The induction of this form of NETosis is mediated by the small-conductance calcium-activated potassium channel 3 (SK3) [275] and appears to be clearly independent of NE and MPO activation [214]. Furthermore, CaI-induced formation of NETs is accompanied by a fast transient increase in cytosolic calcium concentrations within the first minutes [277] and appears to depend strongly on extracellular calcium [276]. How the chromatin decondensation in response to CaI is regulated is not fully understood. Since the NET is exceptionally rich in citrullinated histone 3 (H3Cit) [214, 278, 279], a dependency on PAD4 activation was postulated, but the actual dependency on this enzyme, especially in human cells, is also for CaI an ongoing debate [214]. Remarkably, the cell membrane starts

to lose integrity already within the first 30 min and not with the final DNA release as reported for PMA induction [212]. This observation highlights the diversity of morphological changes during NETosis in response to different stimuli.

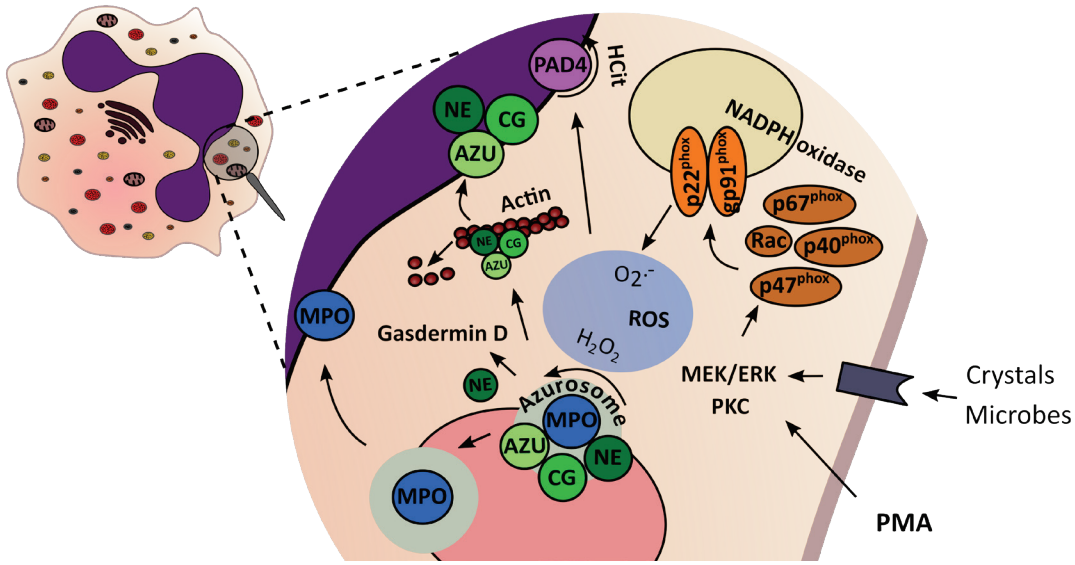

Figure 4: Mechanism of PMA-induced NETosis. PMA, similar to crystals or microbes *via* receptors, directly activates protein kinase C (PKC) and subsequently promotes the assembly of nicotinamide adenine dinucleotide phosphate (NADPH) oxidase *via* the mitogen-activated protein kinase/ERK kinase (MEK)/extracellular-signal-regulated kinase (ERK) pathway. Then, H_2O_2 generated by the induced oxidative burst triggers MPO-dependent dissociation of NE, cathepsin G (CG), and azurocidin (AZU) from the azurosome. Released from the granules, NE translocates to actin as well as to the nucleus and promotes chromatin decondensation, actin degradation and gasdermin D-cleavage. Chromatin decondensation is enhanced by MPO and histone citrullination (HCit) by peptidylarginine deiminase 4 (PAD4). *Neubert et al., in preparation*.

LPS is used in mechanistic studies as a physiologically more relevant stimulus, often together with platelets [212]. The induction of 'suicidal' NETosis with LPS depends highly on the employed bacterial species [280], and the success and extent of activation vary profoundly [212, 225]. LPS-induced NETosis depends on Mac-1 [281] and toll-like receptor 4 (TLR4) activation [282] and involves NADPH oxidase as well as c-Jun N-terminal kinase (JNK) [282]. Furthermore, NE activity [283] and autophagic pathways [280] may be required.
To defend against cytosolic LPS or intracellular infections with gram-negative bacteria (shown for *Salmonella* Δ*sifA* and *Citrobacter rodentium*), neutrophils can make use of an alternative pathway, caspase-11-driven NETosis (caspase-4 in humans), which shares key players with non-canonical pyroptosis. This pathway proceeds completely independent of NE, MPO, and PAD4, but depends on caspase-11 activation and subsequent cleavage of gasdermin D followed by pore formation on membranes [229]. Simultaneously, gasdermin D activation is involved in classical PMA-induced NETosis. Here, NE induces the cleavage of gasdermin D [230] (**Fig. 4**).

1.2.3 Chromatin decondensation in NETosis

As already alluded to**,** chromatin decondensation is an essential step in NETosis (**Fig. 5**). It is mainly initiated by histone alterations and chromatin modifications. The involved processes are highly diverse and depend largely on the used stimulus.

NE is possibly the most important player in the induction of chromatin decondensation and was extensively studied by *Papayannopoulos et al.* [218]. Upon stimulation, NE migrates into the nucleus, where it is detectable within the first hour and degrades histones H4 and H2B (**Fig. 5** (4)) [218, 228]. The decomposition of these histones correlates with the onset of decondensation. NE also degrades the linker histone H1, as shown *in vitro* with isolated nuclei, possibly allowing the onset of core histone degradation [218]. After releasing NE from the azurosome, also MPO translocates to the nucleus [218]. Importantly, the contribution of MPO to chromatin decondensation is independent of its enzymatic activity and is most likely exerted through sterical interactions [218] (**Fig. 5** (5)).

The citrullination of histones by PAD enzymes decreases positive charges and weakens the electrostatic interactions with the negatively charged DNA. This mechanism is postulated most frequently for PAD4-induced decondensation during NETosis [279, 284]. Interestingly, deimination is tightly regulated by different PKC isoforms. For instance, PKCα decreases deimination, while PKCζ is required to induce citrullination in response to PMA or LPS [279] (**Fig. 5** (6)). PAD4 was also postulated to restrict heterochromatin binding of HP1. HP1 usually maintains the heterochromatin state by binding to methylated histone H3 (H3K9me2/3) [285]. The citrullination of histone H3 at arginine 8 (H3cit8) during NETosis possibly impairs this binding, similar to a mechanism seen in fibroblasts [284]. However, since mature neutrophils have low levels of HP1 [99, 286], this requires further investigation (**Fig. 5** (7)).

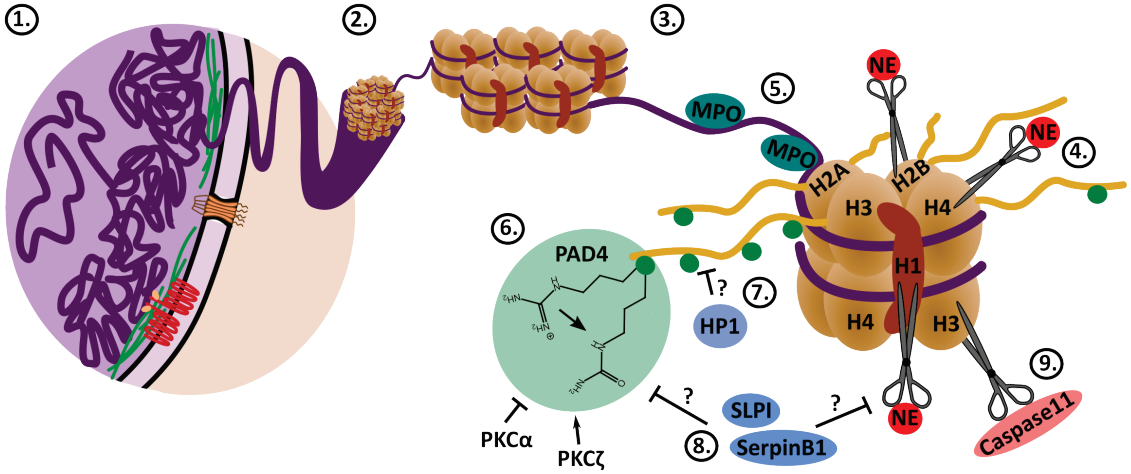

Figure 5: Chromatin decondensation in NETosis. 1-3) Structure of the neutrophil nucleus. 4) Cleavage of histone (H) 1/2B/4 by NE. 5) Sterical interaction of MPO with chromatin. 6) Citrullination of arginines of core histone tails by PAD4. PKC isoforms differentially control the activity of PAD4. 7) Citrullination of arginine 8 at histone H3 (H3Cit8) by PAD4 possibly impairs binding of HP1 to dimethylated histone H3 at lysine 9 (H3K9me2/3). 8) SerpinB1 and/or SLPI possibly regulate the activity of NE and/or PAD4. 9) Caspase-11-mediated cleavage of histone H3. *Neubert et al., in preparation.*

Overshooting decondensation can be regulated by serine protease inhibitors like SerpinB1 or secretory leukocyte protease inhibitor (SLPI) [287-289], which are frequently expressed in cytoplasm and granules of neutrophils [290, 291]. Both inhibitors translocate to the nucleus upon PMA activation, and their depletion significantly enhances NET formation as verified in deficient-mice [292, 293]. Furthermore, sterical effects of these molecules were postulated.

For instance, SerpinB1 was considered to restrict access of PAD4 to the histones tails and, therefore, subsequent histone citrullination [292] (**Fig. 5** (8)).
Caspase-11 is a newly described decondensation-inducing molecule that enters the nucleus through gasdermin D-induced pores and degrades histone H3 [229] (**Fig. 5** (9)) (see also **paragraph 1.2.2**).

1.2.4 Membrane modifications during NET formation

After initiation of chromatin decondensation, the expanding NET has to overcome two restrictive barriers until it can reach the extracellular space: the nuclear and the plasma membrane. Although several studies address the signaling cascades underlying NETosis in detail, only little is known about the modification and remodeling of neutrophil membranes. This question is one of the main motivations for the first study presented in **CHAPTER 2** (**manuscript I**). The following paragraph will summarize the current knowledge on membrane modifications during NETosis including the recently found contribution of gasdermin D-driven pore formation (**Fig. 6**).
The loss of the nuclear and plasma membranes was already reported by *Fuchs et al.* in early studies of PMA-induced NETosis [98]. According to electron microscopy images, inner and outer nuclear membranes (INM, ONM) dilate, followed by disintegration of the nuclear membrane in the form of vesicles 120 min after PMA stimulation. Simultaneously, granular membranes dissolve and NETs are released through rupture of the plasma membrane [98]. The formation of vesicles after 120 min was confirmed by *Amulic et al.* [235] (**Fig. 6** (1)). Whether these vesicles form actively to allow chromatin distribution within the cell or are formed secondary to membrane rupture within the hydrophilic surrounding of the cytoplasm is unclear.
Additionally, it is unknown how the supporting lamin layer behaves during NETosis. Only the phosphorylation of lamin A/C in PMA- or *Candida albicans*-induced NETosis was reported [235] (**Fig. 6** (2)).
Chen et al. and *Sollberger et al.* collectively reported the formation of pores induced by gasdermin D-cleavage during caspase-11/4-driven NETosis [229, 230]. The formation of membrane pores by cleaved

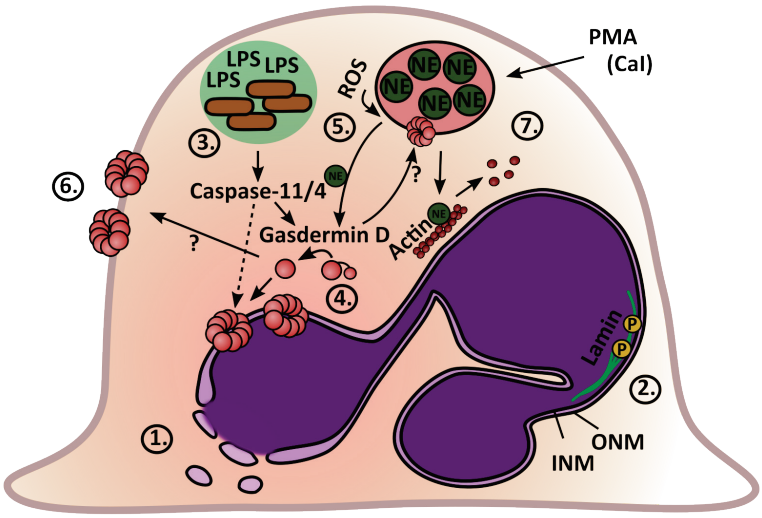

Figure 6: Membrane modifications during NETosis. 1) Vesicle formation of the nuclear membrane. 2) Lamin phosphorylation. 3) Intracellular LPS and bacteria activate Caspase-11 (murine)/4 (human). 4) Caspase-11/4 cleaves gasdermin D and induces pore formation. Pores in the nuclear envelope allow translocation of caspase-11 to the nucleus and subsequent chromatin decondensation. 5) NE, released from the azurosome, cleaves gasdermin D upon PMA/(CaI) activation. Likewise, pores in azurophilic granules further promote NE release. 6) Possible pore formation at the plasma membrane. ONM: outer nuclear membrane. INM: inner nuclear membrane. *Neubert et al., in preparation.*

gasdermin D to promote lytic cell death was studied by *Liu et al*. in pyroptosis [294]. Now, *Chen et al*. reported that upon infection, caspase-11 induces gasdermin D-cleavage to the p30 pore-forming fragment, which enriches at the nuclear membrane and allows the entry of caspase-11 into the nucleus [229] (**Fig. 6** (3-4). In response to PMA or CaI, the cleavage of gasdermin D depended on NE activity (**Fig. 6** (5)). *Sollberger et al.* correlated this observation with pore-formation in the plasma and granular membranes, but this observation requires further validation [230] (**Fig. 6** (6)).
Whether the cytoskeleton contributes to the breakdown of membranes in NETosis is largely unknown. A general involvement of the cytoskeleton in LPS-induced NETosis was proposed based on inhibition of tubulin and actin polymerization. The authors postulated that a functional cytoskeleton is required for NETosis and particularly actin for the final membrane rupture [281]. In contrast, actin degradation occurs after 30 min in response to *Candida albicans* and correlates with NE release from the azurosome. Actin-degradation by NE was likely required for further NETosis [228] (**Fig. 6** (7)). Similarly, tubulin filaments dissolve from the microtubule organizing center (MTOC) within 30 min after PMA-stimulation. However, functional consequences of this observation are unclear [235].

1.2.5 NETosis in disease and autoimmunity

The generation of NETs and its dysregulation were reported in several pathological conditions with growing evidence that NETs are "*double-edged swords of innate immunity*" [295] rather than only an additional defense strategy. Neutrophils isolated from patients with Papillon-Lefèvre syndrome or MPO-deficiency fail to form NETs. Yet, these patients do not suffer from severe immune-deficiency [267, 296]. This calls into question whether NETosis truly is an indispensable defense mechanism, and thus challenges the concept of deficient NETosis in diseases. However, this does not necessarily mean that NETosis is irrelevant in defense of acute microbial infections.
Several recent reviews [192, 193, 297] highlight the broad implications of NETosis in several widespread infectious and noninfectious diseases such as cancer [298-301], diabetes and impaired wound healing [69], lung diseases [246, 302], preeclampsia [303], sepsis [304] and cardiovascular diseases including atherosclerosis, thrombosis and myocardial infarction [227, 305, 306]. Indeed, NETs are discussed as a biomarker for disease progression for instance of cardiovascular events [307, 308] or acute myocardial infarction [309].
Of note, NET formation is not necessarily negatively associated with disease progression. In gout, NETs can form aggregates, so-called aggNETs, which enclose MSU crystals, thus preventing further tissue damage and promoting an anti-inflammatory response [226]. However, aggNETs can also lead to obstructions as shown in pancreatitis [310].

The growing understanding of NETosis opened new perspectives on the role of neutrophils in autoimmune disorders [37, 311, 312] such as rheumatoid arthritis [313, 314], SLE [86, 315], psoriasis [316, 317] or anti-neutrophil cytoplasmic antibody (ANCAs)-rich small-vessel vasculitis (SVV) [318]. Here, the immune system acts against the host itself and induces tissue damage. The exact development of autoantigens and subsequent break of immune

tolerance in these disorders is only partly understood. Possible scenarios include 'molecular mimicry', where foreign and self-peptides share structural similarities [319], as well as agglomeration of cell debris. Inefficient clearance of this debris by phagocytosis and complement activation can further enhance the reaction [311, 320, 321]. Thereby, especially antigens against nuclear content including histones and ribonucleic proteins as well as citrullinated structures were described. The development of these antigens, however, is only partly understood. Obviously, NETs are putative inducers of these antibodies [189]. Importantly, the implication of NETs in autoimmunity could also be a starting point to explain the connection between infections and the break of immune tolerance [311].
Not surprisingly, the presence of autoantigens against NET components such as citrullinated proteins, serine proteases, MPO or histones was detected in several autoimmune disorders [245, 318, 322, 323]. In line, neutrophils from patients with psoriasis [316], SLE or rheumatoid arthritis [245] are prone to NETosis, and healthy neutrophils can be activated by sera or autoantibodies isolated from these patients [70, 316, 318, 324].
NETosis was also directly implicated in the pathogenesis of autoimmune disorders. For instance, in the context of SLE, neutrophils can produce DNA-peptide (LL37)-complexes upon stimulation. These complexes can directly activate memory B cells [325] or induce interferon alpha (INFα) release by plasmacytoid DCs (pDCs) *via* TLR9 activation [70, 324, 326]. Therefore, NET generation may contribute to the exacerbation of SLE. Additionally, pro-inflammatory LDGs in SLE show spontaneous NETosis [87] and contribute to disease severity and tissue damage [87, 327]. Interestingly, NETosis of SLE-LDNs, as well as NETosis induced by immune complexes, involves mitochondrial ROS-dependent pathways. The produced NETs are rich in oxidized pro-inflammatory mitochondrial DNA (mtDNA) [86], which can further drive disease severity. Consequently, antibodies against mtDNA are elevated in sera from SLE patients and correlate with INFα levels [328]. Similar to other cell death pathways, defective or absent NET-clearance enhances autoimmune reactions. In SLE, namely the alteration or impairment of DNase activity [329, 330] was correlated with increased disease severity [331] and complement consumption [332]. The pro-inflammatory microenvironment created by inefficiently cleared NETs can facilitate disease progression by autoantibody generation, tissue damage, cytokine release and immune cell recruitment [321]. Although strong evidence points to a contribution of NETosis in autoimmune diseases, the exact mechanisms remain inconclusive and require further investigation [311].

1.3 Effect of light on human skin and neutrophils

1.3.1 Light penetration through the human skin

The human skin is one of the most important parts of the innate immune system. It defends the body from intruders by its unique composition of microbial, chemical, physical and immune cell barriers [333]. Additionally, it significantly protects the body from external factors such as mechanical stress, temperature or irradiation. Especially light of shorter wavelengths (UV-Vis light) can cause substantial harm and protection against it is, therefore, an essential function of the skin.

UV-Vis light is composed of visible (Vis, 400-700 nm) and ultraviolet light (UV light) including UVA (315-400 nm), UVB (280-315 nm) and UVC (190-280 nm). Intensity and spectrum of the sun-emitted light are altered by the earth's atmosphere through reflection and absorption. Indeed, UVC and large parts of UVB light are absorbed within the ozone layer [334]. Quality and quantity of transmitted light that reaches the skin can vary due to geographic position, season, daytime and degree of decay of the ozone layer. Within the skin, the remaining light intensity is further modified by reflection (around 4-7%), absorption, scattering and backward-scattering [335, 336] (**Fig. 7**).

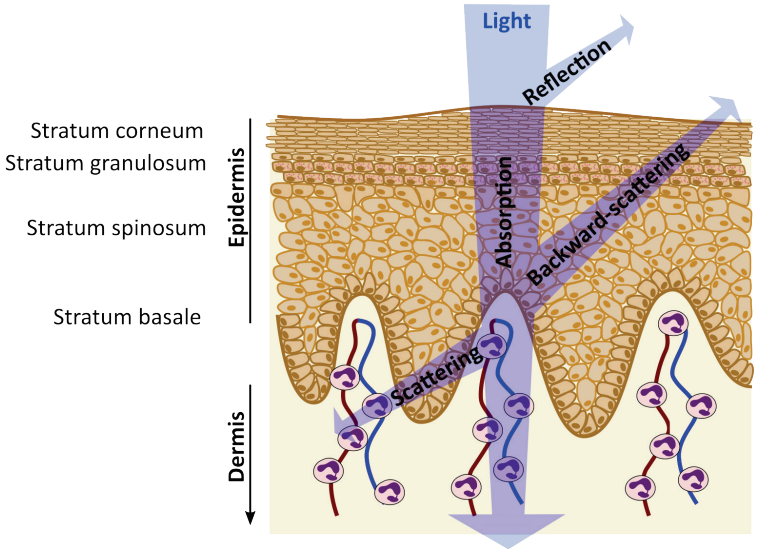

Figure 7: Light attenuation in the human skin. Light transmission can be altered within the human skin by absorption, reflection, scattering or backward-scattering. *Neubert et al., in preparation.*

Within the epidermis, light is mainly absorbed by peptide bands (< 240 nm), aromatic amino acids (tryptophan and tyrosine), nucleic acids (< 300 nm) and melanin (> 300 nm). Melanin has a very large absorption range, which is decreasing with the wavelength and is highly variable due to melanogenesis [335]. Almost no UVC/UVB, roughly 10-15% of UVA and 40-50% of blue light can pass the epidermis and reach the layers below [335, 337] (**Fig. 8**). Within the dermis, the penetration depth is mainly determined by scattering through collagen fibers [338]. Besides scattering, blood-borne chromophores such as hemoglobin, oxyhemoglobin, β-carotene and bilirubin with maxima between 350 nm and 500/600 nm can further absorb the remaining light [335]. In general, the penetration depth of light is inversely proportional to its wavelength [335, 337, 339, 340] with an optical window at around 600-1300 nm [335] (**Fig. 8**).

Overall, light alterations within the skin are complex and vary depending on body region, individual composition, skin type, pigmentation, age, gender and ethnicity. For instance, the thickness of facial skin (epidermis and dermis together) can vary from 0.4 mm (upper eyelid) to 1.4 mm (nasal tip) [341]. Most variations are observed in the dermis. However, also stratum corneum and epidermis are inhomogeneous among different body regions. As an example, around 11 µm and 70 µm were measured on the shoulder for stratum corneum and epidermis, respectively, compared to 18 µm and 57 µm measured on the forearm [342]. Although many groups have tried to measure or model [336] the penetration for each wavelength, the exact penetration depth is complex and can only be estimated.

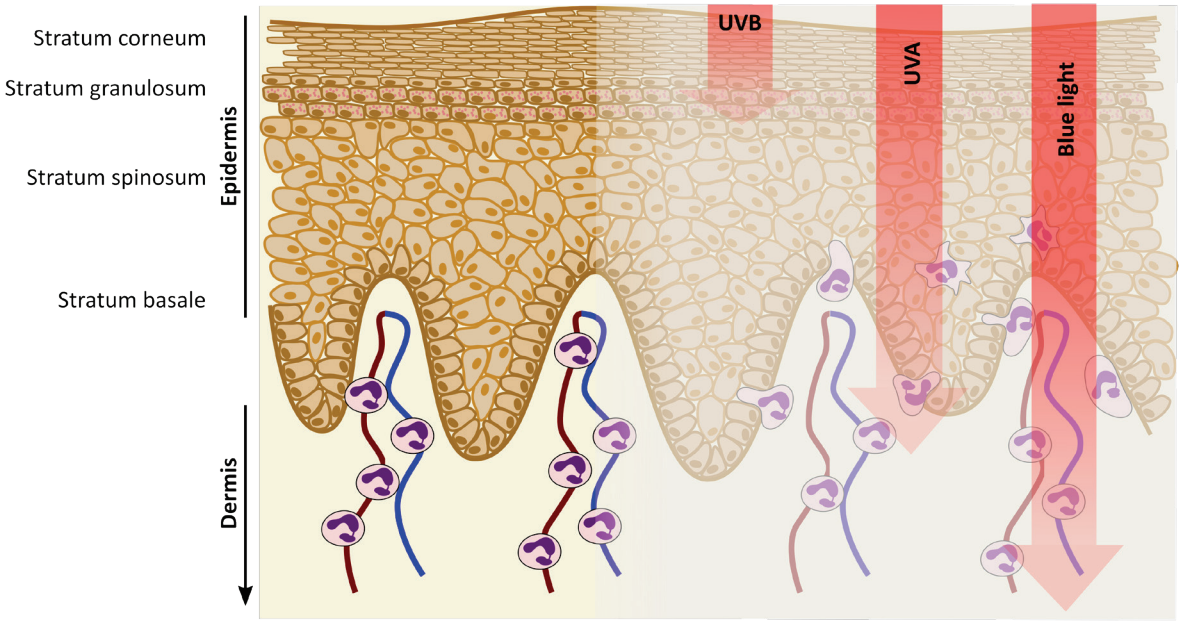

Figure 8: Penetration depth of UVB, UVA, blue light. The penetration depth of UV and blue light increases with its wavelength. Light irradiation, especially UVB, can lead to enhanced infiltration of neutrophils into the tissue. *Neubert et al., in preparation.*

1.3.2 Toxic effects of light on human skin

Light can cause massive skin damage. Its effects can be conveyed through direct alteration of target molecules or can be mediated by photo-sensitive substrates and lead, for instance, to lipid peroxidation, DNA damage, free radical production and protein destruction [343]. Due to these effects, several cell components can be damaged, with a secondary impact on cell function, expression of adhesion molecules, and release of inflammatory modulators such as ROS and cytokines [344]. The extent of destruction and subsequent skin reaction depends on light doses, wavelength and skin predisposition.

Through light absorption, light-sensitive molecules (chromophores) get excited to states of higher energy (excited state, singlet or triplet). This energy is quickly released as thermal energy, transferred to other molecules (photosensitization) or gets fed directly into photochemical reactions to form photoadducts [343, 345]. High-energy UVB light mainly causes direct molecular alterations, above all DNA damage. UVA, however, preferential causes ROS generation and secondary modifications by photosensitization [343]. Importantly, ROS generation *via* photosensitizers can also occur in response to visible light, especially blue light. Only recently, increased ROS formation was documented in mouse skin as well as human keratinocytes and attributed to blue light-excitation of flavoproteins with subsequent superoxide formation [346].

Exhaustion of DNA repair mechanisms or antioxidant systems (*e.g.*, glutathione peroxidase, catalase, melanin, vitamins C and E) can lead to enhanced tissue damage in the form of cell death and secondary inflammation [347]. Consequently, excessive irradiation evokes symptoms known as sunburn with painful erythema, edema, release of inflammatory mediators and even signs of systemic inflammation. Later, the skin develops hyperplasia and hyperkeratosis and, following chronic exposure, photoaging and skin cancer [343, 348].

Interestingly, the immune response to UV irradiation changes from an acute pro-inflammatory reaction to immunosuppression in response to chronic exposure [344]. Vascular permeability, cytokine release (*e.g.*, IL-1, IL-8, IL-6, IFNα), complement activation and influx of immune cells including neutrophils characterize the acute immune response. In contrast, immunosuppression induced by chronic exposure is mediated by anti-inflammatory cytokines (*e.g.*, IL-10) and changes in cell composition such as an increase in regulatory T cells [349]. This immune modulation towards immunosuppression was frequently correlated with enhanced photo-carcinogenesis and is exploited in phototherapy of inflammatory skin diseases [343, 344].

In photodermatoses, the skin is oversensitive to light, mainly UVA. The results are disorders induced by photosensitizers. These sensitizers can be either well-recognized inducers of phototoxic or photoallergic reactions (*e.g.*, furocoumarins, cosmetics, chemicals and pharmaceuticals), or can be idiopathic or idiosyncratic triggers of polymorphous light eruption and solar urticaria. Additionally, manifest skin diseases can be worsened by light, so-called photo-aggravated dermatoses. There are two groups of these disorders. Facultative photo-aggravated dermatoses paradoxically often improve in response to low doses of light, but can exacerbate upon high-dose irradiation (*e.g.*, psoriasis or atopic eczema). In contrast, obligatory photo-aggravated dermatoses are mandatorily correlated with skin light-sensitivity. Typical representatives are autoimmune diseases (*e.g.*, SLE, dermatomyositis), porphyria and pellagra as well as specific genodermatoses [343]. Among these diseases, SLE is arguably the most frequent one, typically with a weeks-delayed reaction to light. The exact mechanisms of SLE-related photoreactions are still enigmatic. UVB and UVA contribute differently to the erythema and cutaneous lesions as reviewed by *Kim et al*. [350]. The proposed mechanisms include increased sensitivity of keratinocytes to UVB, defective clearance of apoptotic material and appearance of autoantigens on the surface of apoptotic keratinocytes. Additionally, UVB light can induce immune cell recruitment *via* pro-inflammatory cytokines and modify the expression of adhesion molecules (*e.g.*, ICAM-1). Simultaneously, UVA enhances the release of pro-inflammatory cytokines and alters cell structures mainly by oxidative damage [350].

1.3.3 Influence of UV-Vis light on human neutrophils

In vitro irradiation of neutrophils can directly affect their functions. For instance, UVA reduces phagocytosis as well as migration in response to fMLP and enhances NADPH activity [351]. Furthermore, light of higher-energy (UVB/UVC) often leads to apoptotic cell death [352, 353]. Interestingly, UVC light can also cause the formation of ‘suicidal’ NETs [354]. In this scenario, NETosis proceeds independent of NOX but dependent on mitochondrial ROS and p38 MAPK activation. Due to the activation of Caspase-3, the authors termed this form of cell death ApoNETosis. Additionally, near-infrared light (980 nm) can activate NETosis *via* a ROS-dependent autophagy-associated pathway [355]. Whether these two forms of NETosis are related and whether UVB, UVA or Vis light can also induce NETosis is unclear.

Under physiological conditions, the most superficial neutrophils are located within the superficial arterio-venous plexus of the papillary dermis [356]. As detailed above, almost no

UVB, around 10-15% of UVA and 40-50% of blue light penetrate through the epidermis into these zones. If the skin is harmed, inflamed or pathologically predisposed, higher numbers of neutrophils can be recruited into upper skin layers or be less protected from light due to skin barrier destruction. In these cases, the intensity of UV-Vis light reaching and activating neutrophils can be enhanced. Additionally, irradiation, particularly with UVB, can directly recruit neutrophils [357]. This is presumably due to increased release of cytokines such as IL-8 and TNFα in human skin [358] or CXCL1 as shown in mice [359]. Consequently, the enhanced infiltration of neutrophils and the subsequent release of elastase, collagenase or gelatinase, were implicated into the pathogenesis of photoaging [360].

CHAPTER 2 **- Manuscripts**

2.1 Manuscript I

„Chromatin Swelling Drives Neutrophil Extracellular Trap Release“

Elsa Neubert[1,2], Daniel Meyer[2,3], Francesco Rocca[3,4], Gökhan Günay[1,2], Anja Kwaczala-Tessmann[1], Julia Grandke[1], Susanne N. Senger-Sander[1], Claudia Geisler[3,4], Alexander Egner[3,4], Michael P. Schön[1,5], Luise Erpenbeck[1] & Sebastian Kruss[2,3]

These authors contributed equally: Elsa Neubert and Daniel Meyer.

[1]Department of Dermatology, Venereology and Allergology, University Medical Center, Göttingen University, Göttingen 37075, Germany
[2]Institute of Physical Chemistry, Göttingen University, Göttingen 37077, Germany
[3]Center for Nanoscale Microscopy and Molecular Physiology of the Brain (CNMPB) Göttingen 37073, Germany
[4]Optical Nanoscopy, Laser-Laboratorium Göttingen e.V., Göttingen 37077, Germany
[5]Lower Saxony Institute of Occupational Dermatology, University Medical Center Göttingen and University of Osnabrück, Göttingen 37075, Germany

The following paragraph was published in *Nature Communications*.
DOI: 10.1038/s41467-018-06263-5

Received: 2 January 2018
Accepted: 11 August 2018
Published online: 14 September 2018

nature COMMUNICATIONS

ARTICLE

DOI: 10.1038/s41467-018-06263-5 OPEN

Chromatin swelling drives neutrophil extracellular trap release

Elsa Neubert[1,2], Daniel Meyer[2,3], Francesco Rocca[3,4], Gökhan Günay[1,2], Anja Kwaczala-Tessmann[1], Julia Grandke[1], Susanne Senger-Sander[1], Claudia Geisler[3,4], Alexander Egner[3,4], Michael P. Schön[1,5], Luise Erpenbeck[1] & Sebastian Kruss[2,3]

Neutrophilic granulocytes are able to release their own DNA as neutrophil extracellular traps (NETs) to capture and eliminate pathogens. DNA expulsion (NETosis) has also been documented for other cells and organisms, thus highlighting the evolutionary conservation of this process. Moreover, dysregulated NETosis has been implicated in many diseases, including cancer and inflammatory disorders. During NETosis, neutrophils undergo dynamic and dramatic alterations of their cellular as well as sub-cellular morphology whose biophysical basis is poorly understood. Here we investigate NETosis in real-time on the single-cell level using fluorescence and atomic force microscopy. Our results show that NETosis is highly organized into three distinct phases with a clear point of no return defined by chromatin status. Entropic chromatin swelling is the major physical driving force that causes cell morphology changes and the rupture of both nuclear envelope and plasma membrane. Through its material properties, chromatin thus directly orchestrates this complex biological process.

[1] Department of Dermatology, Venereology and Allergology, University Medical Center, Goettingen University, Göttingen 37075, Germany. [2] Institute of Physical Chemistry, Göttingen University, Göttingen 37077, Germany. [3] Center for Nanoscale Microscopy and Molecular Physiology of the Brain (CNMPB), Göttingen 37073, Germany. [4] Optical Nanoscopy, Laser-Laboratorium Göttingen e.V., Göttingen 37077, Germany. [5] Lower Saxony Institute of Occupational Dermatology, University Medical Center Göttingen and University of Osnabrück, Göttingen 37075, Germany. These authors contributed equally: Elsa Neubert, Daniel Meyer. Correspondence and requests for materials should be addressed to L.E. (email: luise.erpenbeck@med.uni-goettingen) or to S.K. (email: skruss@uni-goettingen.de)

Neutrophilic granulocytes are the most abundant immune cells in humans and essential to defeat invading pathogens[1]. Their mechanisms to target invading microbes include well-known processes such as phagocytosis and generation of reactive oxygen species (ROS). A third defense pathway is the release of neutrophil extracellular traps (NETs)[2]. The formation of NETs (NETosis) can be triggered by organisms such as bacteria or different chemicals and was originally described as an additional form of cell death apart from apoptosis and necrosis[3–5]. NETosis has been reported not only for neutrophils but also other immune cells[6,7], amoebas[8] and plant cells[9] indicating an evolutionary conserved process[3].

During NETosis, cells can release three-dimensional meshworks (NETs) consisting of chromatin[2], antimicrobial components including myeloperoxidase (MPO)[5], neutrophil elastase (NE)[10], and LL37 of the cathelecidin family[11]. These fibrous networks were initially described as a mechanism to catch and eliminate bacteria, fungi, as well as viral particles[2]. However, it is becoming increasingly clear that the role of NETs in the immune system is far more complex than originally estimated. On the one hand, accumulating data suggests that the immediate role of NETs in immunoprotection against pathogens may be smaller than originally anticipated, as mice that cannot form NETs do not suffer from severe immunosuppression[12,13]. On the other hand, dysregulated or excessive NETosis appears to be implicated in an ever growing number of diseases, including cancer[14], thrombosis and vascular diseases[15–17], preeclampsia[18], chronic inflammatory diseases[19], and ischemia-reperfusion injury after myocardial infarction[16].

Various stimuli such as bacteria, fungi, viruses, platelets, as well as small compounds including lipopolysaccharides (LPS), calcium ionophores (CaI), or phorbol-myristate acetate (PMA) induce NETosis and release of NETs[20]. In many settings, NETosis appears to rely on the adhesion of neutrophils, in particular on the engagement of neutrophilic integrin receptors such as Mac-1[21–23], in others, adhesion via Mac-1 seems to be dispensable[24–26]. It has also been described that hemodynamic forces can trigger shear-induced NETosis[27].

While these triggers—biochemical or mechanical—engage diverse pathways, they all converge to a uniform outcome, namely histone modification, chromatin decondensation and NET release[28]. Cells dramatically rearrange their contents (cytoskeleton, organelles, membranes, nucleus) during NETosis; in most scenarios, they eventually die[4]. Chromatin decondensation has been described qualitatively since the discovery of NETs[4,29,30] and NET formation has been evaluated both in high-throughput approaches, as well as on the single-cell level[29–31]. Yet, the mechanistic basis of these fundamental changes, as well as the underlying dynamic forces remain poorly characterized. Here, we investigate NETosis from a biophysical perspective, particularly looking at the forces and dynamics driving this process, and provide functional links between chromatin dynamics and biochemical behavior. We show that NETosis is organized into well-defined phases orchestrated by entropic swelling of chromatin, which finally ruptures the membrane.

Results

NETosis is organized into distinct phases. To better understand how the cell's interior is rearranged and how NETs are released we studied human neutrophils in real-time. First, we imaged chromatin and cell membranes of human neutrophils stimulated by 100 nM PMA (Fig. 1a, b, Supplementary Movies 1, 2). NETosis was confirmed by co-localization of chromatin and MPO within the expelled NETs (Fig. 1f).

The chromatin-filled area inside the cells followed a characteristic time course (Fig. 1a, b) that consistently allowed the assignment of three distinct phases. As can be seen later this phase classification allows us to distinguish active biological processes from materials driven processes and to identify a point of no return. Cells were stimulated ($t = 0$) and during the first phase P1 ($0 < t < t_1$ = start of chromatin expansion) the lobular structure of the nucleus was still intact (34 min in Fig. 1a) and the corresponding chromatin area stayed constant. In the second phase P2 ($t_1 < t < t_3$ = NET release) chromatin expanded within a few minutes until it reached the cell membrane as a barrier (t_2 = maximal chromatin expansion in Fig. 1a). Simultaneously, the cell rounded up (t_2 to t_3 in Fig. 1a and Supplementary Fig. 1a, b). In the third and final phase (P3, $t > t_3$) the cell membrane is ruptured (t_3) and the NET released into the extracellular space. Additionally, released NETs were also visualized by stimulated emission depletion (STED) nanoscopy to reveal the architecture of hydrated NETs below the resolution limit of normal fluorescence microscopy (Supplementary Fig. 2). The observed architecture was in good agreement with previous electron microscopy images of NETs[2].

The above-mentioned phase classification was applied to multiple cells ($n = 139$ cells) from five different donors (Fig. 1c, Supplementary Fig. 3a-c, Supplementary Movies 3–6). Although the onset time points for the different phases of all individual cells followed a broad distribution (Fig. 1c), average onset values for all five donors were remarkably reproducible, indicating low inter-individual variability for the three distinct phases under standardized conditions (Supplementary Fig. 3c). Decondensation of chromatin started at $t_1 = 56 \pm 4$ min (standard error of the mean, SEM) and reached a maximum at $t_2 = 82$ min (±3 min). After $t_3 = 116$ min (±4 min) the cytoplasmic membrane ruptured and the NETs were released. In summary, P1, as well as P2, require around 60 min in our experimental setup.

The three distinct phases of chromatin decondensation were not only elicited by PMA but also by LPS (Fig. 1d) or calcium ionophores (Fig. 1e), albeit with different onset times, particularly with respect to P1 (Supplementary Fig. 3d, Supplementary Movie 7), which is most likely an expression of the distinct signaling pathways engaged by different stimuli[28].

To understand biophysical events during NETosis in detail, we analyzed chromatin shape with special regard to the most relevant internal and external boundaries (i.e., nuclear envelope and cell membrane). In P1, cells first adhered to the surface, flattened and showed filopodia activity (Supplementary Fig. 4a, b, Supplementary Movies 1, 2, 8). During P2, the cell retracted its cell body as shown by CLSM (Fig. 1a, Supplementary Fig. 4a, b) and time-resolved reflection interference contrast microscopy (RICM) (Supplementary Fig. 4c, d and Supplementary Movies 9–11), the cells rounded up and their height increased as demonstrated by both three-dimensional CLSM stacks (side view, Fig. 2a) and atomic force microscopy (AFM) (Fig. 2b).

Interestingly, NETotic cells reached approximately the same height as non-stimulated round cells (Fig. 2b), suggesting that chromatin expansion/decondensation is a swelling process and the swelling pressure caused the energetically most favorable spherical shape.

To address the question of how chromatin exits the nucleus, we labeled lamin B1, a constitutive component of the nuclear envelope that surrounded all individual lobuli of the nucleus (Fig. 2c, Supplementary Fig. 5). Over time, those lobuli merged and became less distinctive, indicating profound changes in the separation between chromatin. Around the onset of P2 (t_1; i.e., the start of chromatin expansion), the lamin B1 layer tore on at least one site of the nucleus. Often, several rupture events of this layer were discernable (arrows Fig. 2c, see also comparison

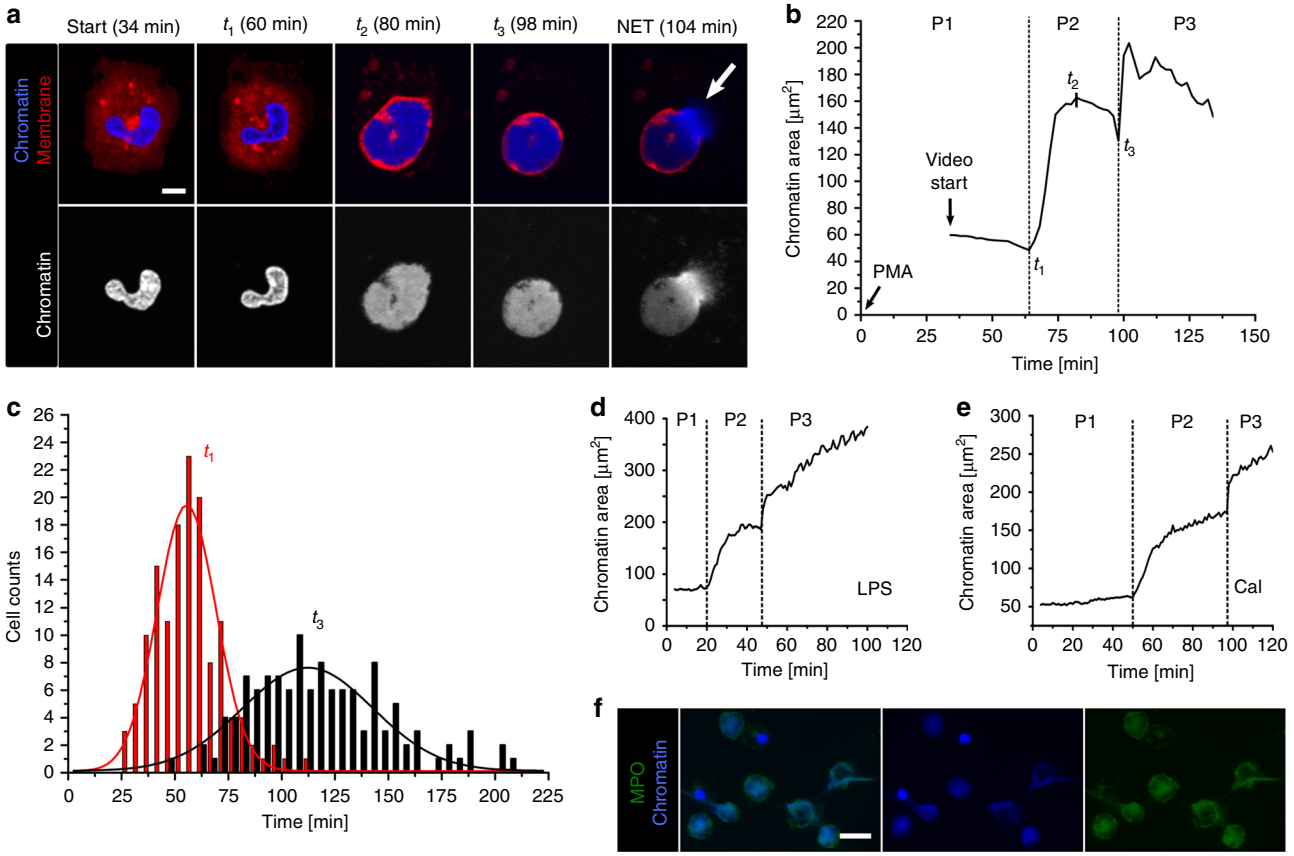

Fig. 1 Phases of NETosis. **a** Morphological changes of chromatin (blue) and cell membrane (red) during NETosis of human neutrophils (stimulated with 100 nM PMA) imaged by live-cell confocal laser scanning microscopy (CLSM). The lobular nucleus loses its shape and chromatin decondenses until it fills the entire cell. Finally, the cell rounds up and releases the NET (white arrow). Scale bar = 5 µm. **b** Corresponding chromatin area of a NETotic neutrophil (**a**) as a function of time reveals three distinct phases. P1: Activation, lobulated nucleus. P2: Decondensation/expansion of chromatin within the cell (t_1 = start of chromatin expansion, t_2 = maximal chromatin expansion within the cell); cell rounding. P3: Rupture of the cell membrane (arrow **a**) and NET release (t_3 = NET release). **c** Histogram of onset times of the different phases. $n = 139$ cells. $N = 5$ donors. Lines represent Gaussian distribution function fits. **d** Time course of chromatin area for stimulation with LPS (Lipopolysaccharide, from Pseudomonas aeruginosa, 25 µg ml^{-1}). **e** Time course of chromatin area for stimulation with calcium ionophore (4 µM). **c**–**e** data acquired with live-cell wide field fluorescence microscopy. **f** Colocalization of decondensed neutrophil chromatin (blue) and myeloperoxidase (green). Fixed cells imaged by wide field fluorescence microscopy. Scale bar = 20 µm

of chromatin area at t_1 in Supplementary Fig. 5). Similar fluorescent labeling methods have been used by others to quantify nuclear envelope rupture events[32]. Previous publications have described the modification of nuclear lamins by phosphorylation as an early event, which would affect rigidity and could facilitate the here-described breakage of the nuclear envelope[33]. It should be noted that the breakage of the nuclear envelope appears to be a distinct process from the previously described dissolution of the nuclear envelope, which is a hallmark of late stages of NETosis[13,33].

In line with these previously published observations, we could show that the nuclear envelope further decomposed during P2 and P3 and lamin B1 was found distributed throughout the cytoplasm (Fig. 2c, P2/3). Subsequently, nuclear envelope breakdown allowed further expansion and swelling of chromatin within the cell (Fig. 2d). Consequently, the temporal correlation between t_1 and the rupturing of the nuclear envelope indicates that chromatin swelling is the physical driving force of this event.

The dissection of NETosis into distinct phases allowed us to identify and distinguish active (biological/biochemical) and passive (material properties) events. In the next step, we linked the phase classification to biochemical processes.

Active and passive mechanisms during NETosis. The initial steps of NETosis are thought to rely on several enzymes, with the exact progression depending greatly on the activator used to initiate NET formation[28]. In most scenarios, NETosis depends on the activity of typical neutrophil enzymes such as neutrophil lactase (NE) and myeloperoxidase (MPO)[34], as well as histone citrullination by the enzyme peptidyl-arginine deiminase 4 (PAD4). However, it is unclear at which time point during NETosis signaling and activity by these players are essential, and whether they initiate or maintain the process. If they were required in P1, and later phases were governed by passive mechanisms such as swelling of chromatin, then P2 and P3 should not depend on an active cellular energy supply. Indeed, ATP levels of (PMA) activated neutrophils quickly decreased in P1 by up to 70%, particularly within the first 30 min, indicating energy-dependent processes (Fig. 3a). In contrast, ATP levels then remained constant throughout P2 on a low level (Fig. 3a). To corroborate the hypothesis that energy supply is not necessary for P2, the main energy source in neutrophils, glycolysis[35,36], was cut off by inhibiting glucose metabolism with 2-Deoxy-D-glucose (2-Deox-Gluc)[37–40], which quickly and durably reduced ATP levels of neutrophils as early as 15 min in PMA-stimulated cells

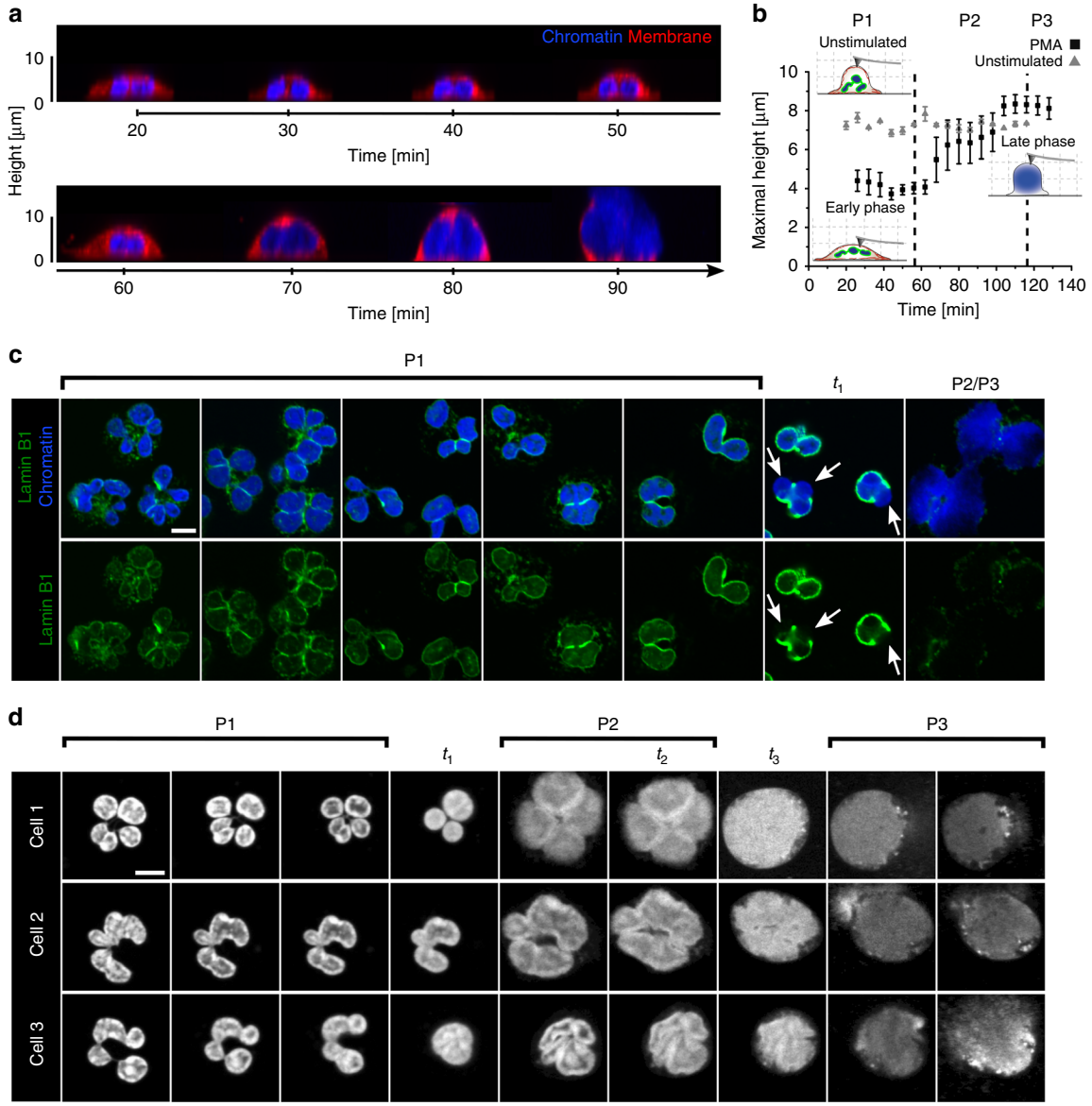

Fig. 2 Chromatin swelling drives morphological changes. **a** Live-cell CLSM side view of a neutrophil during NETosis. Chromatin (blue) decondenses/expands, reaches the membrane (red) and the cell rounds up until the membrane ruptures. z-stack depth: 1 µm. **b** Cell height as measured by atomic force microscopy (AFM) on life neutrophils. PMA stimulated cells adhere and flatten (compared to the control cells that stay more or less round) and then round up (>8 µm) in P2. $n = 3$. Mean ± SEM. **c** Characteristic distribution of lamin B1 (green) in the three phases, CSLM images of fixed cells. Lamin B1 first surrounds single lobuli of the nucleus/chromatin (blue). When chromatin starts to expand corresponding to the start of P2 (around t_1), the lamin B1 layer/nuclear envelope ruptures on at least on one side of the nucleus. During P2 and P3 lamin B1 further decomposes. White arrows indicate rupture sites of the lamin B1 layer. Scale bar = 5 µm. **d** The original shape of the nucleus remains recognizable during the expansion process, particularly in the first part of P2 (t_1 to t_2), indicating isomorphic chromatin swelling and not directional transport (Supplementary Movies 13–15). In P1 the nucleus has a lobulated structure, which is maintained (self-similarity) during P2. Finally, the membrane is reached and, for a short period of time, this barrier prevents further expansion until it burst. Scale bar = 5 µm. Live-cell CSLM images

and within 60 min in unstimulated neutrophils (Supplementary Fig. 6b, c). Additionally, sodium azide (NaN_3) was used in this setup as a general inhibitor of metabolic function and, specifically, of metalloproteases[41–43], and MPO was inhibited with 4-aminobenzoic acid hydrazide (4-ABAH)[44,45]. We verified the function of these enzymatic inhibitors by showing that NaN_3 inhibits ROS production in neutrophils immediately after addition for at least 30 min (Supplementary Fig. 6a and 9c) and that 4-ABAH inhibited purified MPO within 1 min and stable within 15 min after PMA activation (Supplementary Fig. 6d). Thus, 4-ABAH directly interferes with PMA-induced NET formation[5]. None of the here-used inhibitors had any measurable effect on NET-production of naïve neutrophils (Fig. 3b), nor did any of them show significant toxicity (Supplementary Fig. 7a). As expected, however, effects of these inhibitors were not exclusive to NET-formation, as 4-ABAH and 2-Deox-Gluc clearly decreased the uptake of FITC-labeled E. coli particles, although NaN_3 showed no effect in this setup (Supplementary Fig. 7b).

When added directly after stimulation all inhibitors significantly reduced NET formation (Fig. 3b). This effect successively decreased when inhibitors were added at later time points. Exposure to NaN_3 after >60 min and to 2-Deox-Gluc or 4-ABAH after >75 min no longer affected the number of decondensed nuclei. This result again implies that P1 depends on energy supply

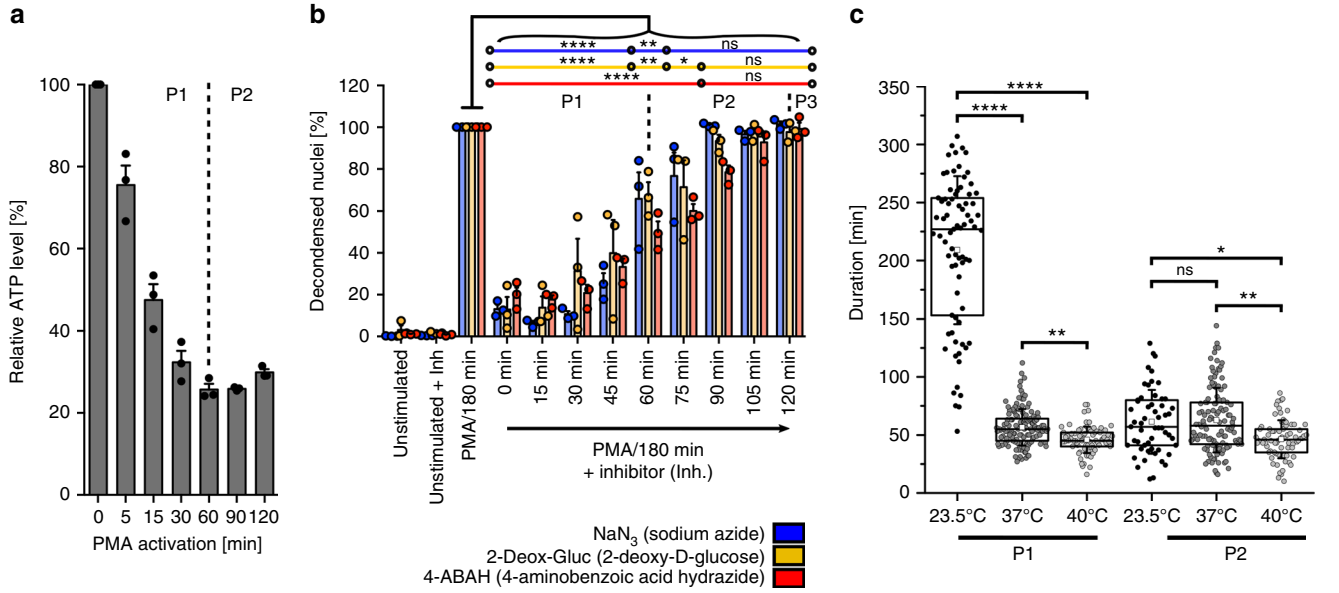

Fig. 3 Active and passive processes during NETosis. **a** ATP levels in stimulated neutrophils decrease during P1 and reach a plateau in P2. Inhibition of glucose metabolism further reduces ATP levels (Supplementary Fig. 6c). $N = 3$. Mean ± SEM. **b** Metabolic inhibitors (sodium azide/3 mM, 2-deoxy-D-glucose/5 mM, 4-aminobenzoic acid hydrazide/100 µM) influence NET formation determined as relative number of decondensed nuclei after 180 min compared to activation with PMA only. All inhibitors decrease NET formation when added in P1, while P2 is not or only slightly affected, indicating a point of no return. $N = 3$ donors. Statistics: two-way ANOVA (Bonferroni's multiple comparisons test; $^{*}p < 0.05$; $^{**}p < 0.01$; $^{****}p < 0.0001$; ns = not significant). Mean ± SEM. **c** Phase duration at different temperatures (23.5, 37, 40 °C). P1 is significantly prolonged at lower temperatures, whereas P2 displays no or marginal temperature dependence. $N = 3$ (23.5, 40 °C). $N = 5$ (37 °C). Statistics: Kruskal-Wallis test (Dunn's multiple comparisons test; $^{*}p < 0.05$; $^{**}p < 0.01$; $^{****}p < 0.0001$; ns = not significant). Life-cell imaging. Boxplots display the 25th and 75th percentile and the horizontal line the median. Hollow squares represent the mean and whiskers the SD

and enzymatic activity, while P2 and P3 do not. So far, NETosis has been generally considered as an active process that requires the aforementioned enzymes. Here, we show that this generalization does not hold true for the complete mechanism.

Another hallmark of enzymatic activity is temperature-dependence. We chose to show the impact of temperature variations on the impact of NETosis as a complementary, inhibitor-free approach to investigate the importance on enzymatic activity. We quantified the duration of the different phases of NETosis at physiological core temperature (37 °C), hypothermia (23.5 °C) and hyperthermia/fever (40 °C). Higher temperatures significantly accelerated P1 whereas P2 showed no or only a slight temperature dependence (Fig. 3c, Supplementary Movie 12), indicating high enzyme activity in P1. If one assumes Arrhenius-like kinetics $\left(k \sim \exp\left(-\frac{E_a}{k_B T}\right)\right)$, the 4.14-fold shortened duration of P1 (227.5 min at 23.5 °C vs. 55.0 min at 37 °C) corresponds to an activation energy of around 80 kJ mol^{-1}, which falls into the range expected for enzyme-catalyzed reactions[46], and again corroborates our hypothesis of a switch from biochemically driven processes to behavior governed by material properties. P3 was not evaluated in the context of temperature-dependency as it is not possible to determine an end-point of P3 after the release of the NET.

Additionally, this result indicates an enzyme activity independent diffusive process in P2 since one expects lower temperature dependence for diffusion. In the first part of P2 (Fig. 1b, 2d, Supplementary Fig. 3a, Supplementary Movies 13–15) the chromatin area A increased linearly with time t and can be interpreted as a 2D diffusion process ($A \approx \langle x^2 \rangle = 4Dt$). The corresponding effective diffusion constant D of 0.0108 µm^2 s^{-1} at 37 °C (Supplementary Fig. 8a) is roughly in agreement with the diffusion of a 2×10^9 DNA sequence of ($D \approx 0.002$ µm^2 s^{-1}, T = 37 °C)[47,48].

Entropic chromatin swelling drives morphological changes. At the beginning of NETosis (P1 in our classification), histones are modified chemically (decrease of positive charge) by enzymes such as PAD4 or NE, which reduces the counterforces that hold the negatively charged DNA/chromatin together[10,49]. A condensed nucleus is under considerable entropic pressure as the radius of gyration of the human genome (length around 2 m) is approximately 150–200 µm[50,51]. Once the counterforces are no longer high enough to balance the entropic pressure, chromatin begins to swell. This time-point corresponds to t_1 (onset of P2) and marks a point of no return.

Another line of evidence pointing to entropic pressure as a relevant factor stems from the observation that small neutrophils rupture faster than larger ones after chromatin filled the whole cell lumen (Fig. 4a). As all cells contain the same amount of chromatin, entropic pressure exerted on the cell membrane is higher if they are smaller. This should lead to earlier rupturing of the membrane. Likewise, large intact neutrophils accumulate during the experiments because smaller ones rupture and release NETs first (Fig. 4b).

To analyze whether the swelling pressure generated during P2 determines if and when the membrane ruptures, we calculated the pressure exerted by chromatin and compared it to the rupture delay time (t_2 to t_3). For that purpose we modified a Navier-Stokes equation-based theory that describes pressure as a function of time t (see Methods[52]):

$$p(t) = \frac{\eta(R(t))}{l_p^2(R(t))} \frac{\mathrm{d}R(t)}{\mathrm{d}t} R(t) \qquad (1)$$

Here η is the viscosity of the chromatin (liquid), $R(t)$ the effective radius of the chromatin area and l_p the chromatin mesh size. STED nanoscopy images of chromatin just before the cells

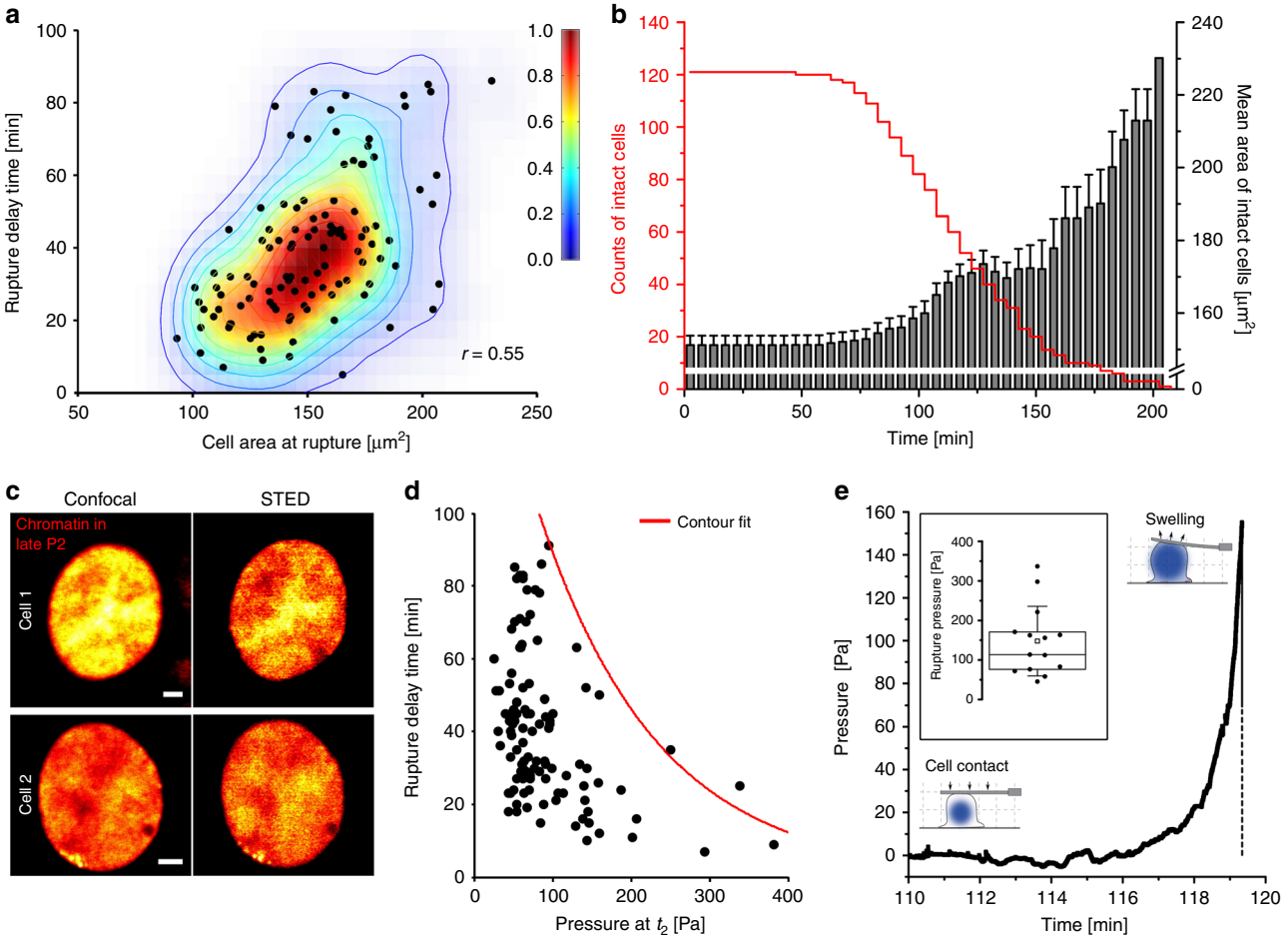

Fig. 4 Entropic swelling of chromatin causes membrane rupture. **a** Correlation between cell area at t_3 (chromatin area at $t_3 \approx$ total cell area at t_3) and time span until membrane rupture occurs following maximal chromatin expansion (t_3- t_2, rupture delay time). Larger cells rupture later than smaller cells. $n =$ 112 cells (only cells of population 1 included, see Supplementary Fig. 3a, b). Fit lines show normalized 2D-probability density function calculated by kernel density estimation (KDE). $N = 5$ donors. **b** Average cell area (at t_3) of remaining/intact cells. The area of intact cells increases from ≈151 to ≈230 µm^2 with time, indicating earlier rupture of small cells. $n = 121$ cells. $N = 5$ donors. Mean ± SEM. **c** Live-cell confocal (left row) and STED (right row) images of chromatin (SiR-DNA) of two neutrophils undergoing NETosis (late P2) show almost uniform distribution of chromatin suggesting a mesh size smaller than the resolution of the microscope (≈120 nm (xy) and ≈150 nm (z), Supplementary Fig. 8b). Scale = 2 µm. **d** Time delay until rupture as a function of the calculated pressure p at t_2. $n = 112$ cells (only cells of population 1 included, see Supplementary Fig. 3a, b). $N = 5$ donors. The contour fit is generated by fitting the maximal data points to an exponential decay curve. **e** Neutrophils undergoing NETosis exert an increasing pressure on a fixed AFM cantilever until they rupture (end point of measurement). Inset: $N = 5$ ($n = 14$ cells). Boxplots display the 25th and 75th percentile and the horizontal line the median. Hollow squares represent the mean and whiskers the SD

ruptured showed no fine structure indicating that the mesh size is below the resolution of this microscope (about ≈120 nm in xy-direction and ≈150 nm in z-direction) (Fig. 4c, Supplementary Fig. 8b, c). Therefore, we assumed that the whole genome (around 2 m DNA) is evenly arranged inside the cell and estimated that l_p to be around 20 nm. Cells exposed to higher pressure ruptured faster than their smaller counterparts (Fig. 4d). The calculated pressure values are in a similar range as pressure values known from osmotic lysis experiments of lipid vesicles[53]. To find out if these calculated pressure values were actually exerted by the cell we measured these forces directly with AFM (Fig. 4e, Supplementary Fig. 8d). A cantilever was positioned in direct contact with the cell and deflected by the rounding cell. This is a known approach to measure rounding forces e.g. during mitosis[54]. The pressure exerted by the cell increased with time and lifted the cantilever until the cell finally ruptured (end point of measurement). The measured pressure values between 100–200 Pa are in the same range as the calculated pressure values from Fig. 4d. Together with the control experiments that show that energy supply (Fig. 3) and the actin cytoskeleton (Fig. 5, below) are not crucial for P2 this result further supports chromatin swelling as the major driving force in P2.

In conclusion, our results show that P1 of NETosis is a biologically active process governed by signaling and enzymatic reactions. In contrast, P2 is mainly passive, based on entropic chromatin swelling and cannot be stopped once it has started. Therefore, the onset of P2 ($t = t_1$) represents a point of no return.

Impact of cytoskeletal rearrangements on NETosis. In addition to the unexpected importance of chromatin dynamics reported this far, the cytoskeleton may also contribute to shape shifts and DNA expulsion. While cytoskeletal components appear to rearrange and F-actin may become degraded during NETosis[4,34], these processes remain poorly understood. Figure 5a shows the F-actin distribution (labeled with SiR-actin) at different time points after PMA-stimulation. During the first 30 min F-actin became more prominent as expected for stimulation with the protein-kinase C activator PMA, which has multiple effects on

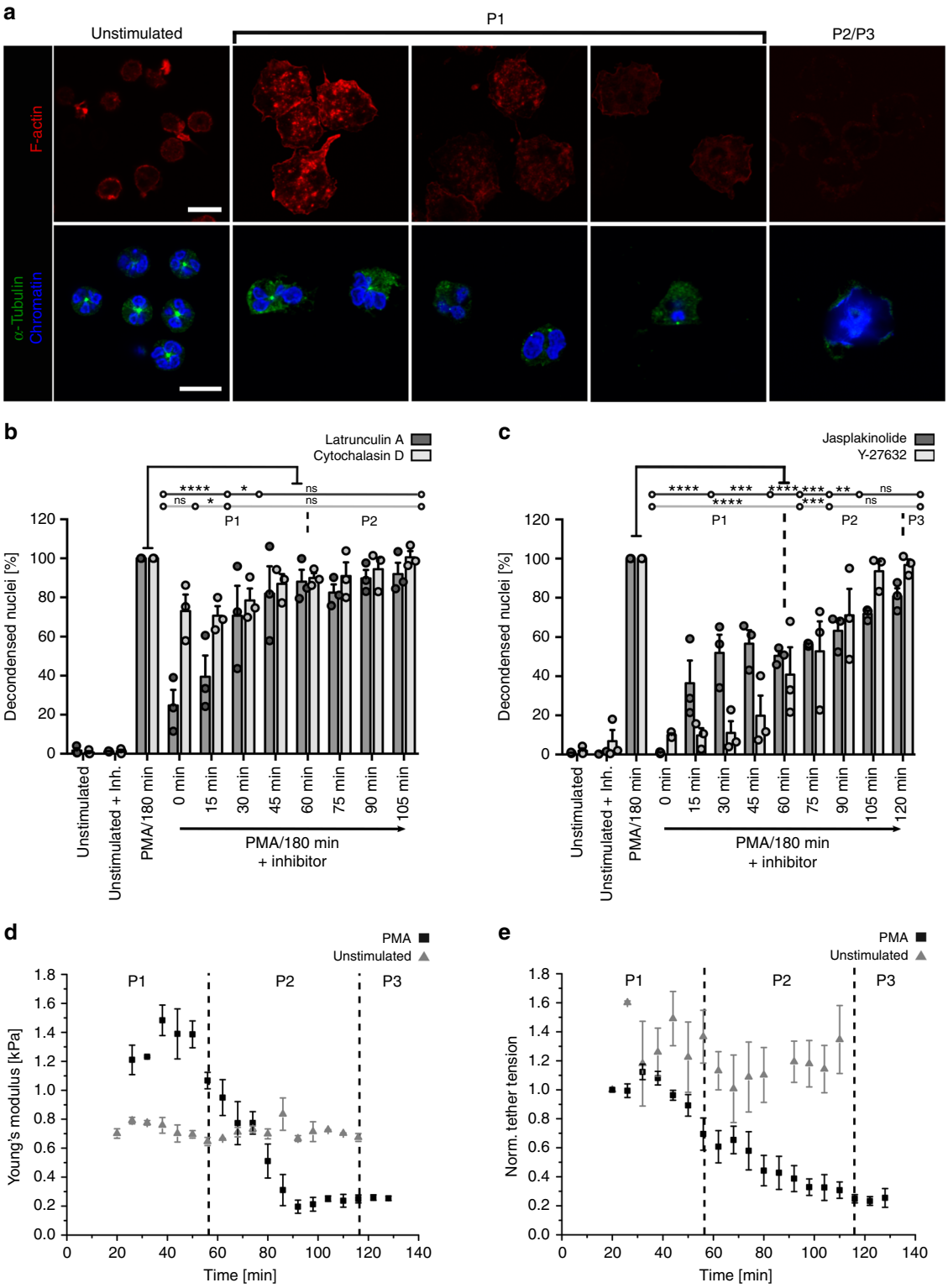

neutrophils, among them the induction of chemotaxis[55]. Then, it diminished and completely disassembled after 90–180 min (see quantification in Supplementary Fig. 9a).

As recently described, α-tubulin is initially organized in filaments originating from the microtubule organization center (MTOC; unstimulated cells)[33]. One could speculate that these MTOCs are involved in active transport of chromatin. However, during phase I after PMA-stimulation, α-tubulin filaments disappeared and were rearranged into dot-like structures, reminiscent of mitotic centrosomes. These were visible until the beginning of chromatin decondensation, namely until the beginning of phase 2 (Fig. 5a). As we did not observe these filaments any more during phase 2, it is unlikely that active chromatin transport along these centrosomes like structures plays a role during the expansion of chromatin.

Additionally, we sought to determine the role of the cytoskeleton through specific inhibition: Jasplakinolide (10 µM, actin stabilization/induction of actin polymerization),

Fig. 5 Rearrangement of the cytoskeleton and evolution of mechanical properties. **a** At the beginning of NETosis F-actin (red) is laterally enriched and localizes in the lamellipodia. α-Tubulin filaments (green) are arranged originating from the microtubule organizing center (MTOC) in unstimulated cells. Within the next hours (during P1) cytoskeletal components disintegrate. Remaining F-actin accumulates at the cell margin and α-tubulin is first rearranged in centrosome-like structures which disappear at the beginning of P2. CLSM images of fixed cells. Activation = PMA (100 nM). Blue = chromatin. Scale = 10 µm. **b**, **c** Inhibition of NET formation with the F-actin polymerization inhibitors Cytochalasin D (100 nM) and Latrunculin A (1 µM), F-actin-stabilizing drug Jasplakinolide (10 µM) and the ROCK-inhibitor Y-27632 (19.2 µM) significantly reduces the formation of NETs (measured as %-relative number of decondensed nuclei after 180 min compared to activation with PMA only) in P1, while P2 depends less or not on F-actin stabilization and ROCK-inhibition. Statistics: two-way ANOVA (Bonferroni's multiple comparisons test; $^{*}p < 0.05$; $^{**}p < 0.01$; $^{***}p < 0.001$; $^{****}p < 0.0001$; ns = not significant). $N = 3$ donors. Mean ± SEM. **d** Normalized tether tension of life neutrophils (measured with AFM) decreases over the entire time course (raw data: >0.35 mN m to <0.07 mN m) of PMA-activated NETosis indicating a loss of cytoskeletal stability. Values of control cells remain stable. $N = 3$. Mean ± SEM. **e** Cell stiffness (Young's modulus) of life neutrophils decreases from >1.5 kPa to <0.3 kPa after stimulation with PMA whereas the stiffness of control cells remains constant. $N = 3$. Mean ± SEM

Cytochalasin D (100 nM, inhibition of actin polymerization), Latrunculin A (1 µM, inhibition of actin polymerization) and Docetaxel (100 nM, inhibition of tubulin depolymerization) were added at different time points after stimulation (with 100 nM, PMA). While Docetaxel exerted no (Supplementary Fig. 9b), Cytochalasin D and Latrunculin A showed a significant reduction of NETosis when added up to 15 min after activation (Fig. 5b). Jasplakinolide inhibited NETosis completely when added from the beginning. The latter effect decreased as NETosis advanced (Fig. 5c). Based on this finding we concluded that reorganization of the cytoskeleton is not only a consequence of NETosis, but also a requirement during the active phase (P1; Fig. 5b, c). Additionally, we manipulated cell motility by inhibiting the rho-associated coiled-coil-containing protein kinase 1 and 2 (ROCK 1/2) signaling pathway using Y-27632 (19.2 µM). Again, we found a strong influence on P1 (Fig. 5c). These results are in good agreement with our results on enzyme activity (Fig. 3b). While it has been shown that cytoskeletal inhibitors may influence the NADPH oxidase[56], we could rule out that these off-target effects were causing the reduction in NETosis, as Jasplakinolide inhibited ROS formation, while Latrunculin A increased it and the Y-27632 and Cytochalasin D had no or only a slight effect on ROS production (Supplementary Fig. 9c). Thus, while effects on ROS production were very heterogeneous, the effect of cytoskeletal inhibition on NET production showed the same pattern for all used inhibitors (Fig. 5b, c). Therefore, we can rule out that the observed effects on NETosis are exclusively mediated by an influence on the NADPH oxidase. None of our cytoskeletal inhibitors produced any significant cytotoxic effect on neutrophils (Supplementary Fig. 7a).

In conclusion, NETosis requires an intact and functional actin cytoskeleton at the beginning of P1 and the reorganization of F-actin is essential to proceed to P2 and P3. Rearrangement of the microtubule apparatus appears to be a marker of the activation of biochemical pathways required for NETosis (namely the activation of cyclin-dependent kinases 6 and 4)[33] and an influence of certain microtubule inhibitors has been postulated by isolated publications[57]. However, in our setup the microtubule apparatus itself appears to be dispensable for NET formation. Taken together, both the actin cytoskeleton of the neutrophils, as well as the microtubule apparatus become dysfunctional as NETosis progresses. Therefore, it is unlikely that the cytoskeleton plays an active role during the final steps of NETosis. Dissolution of these major components, which normally stabilize the cell, likely impairs the cell's mechanical properties, thus helping the final cell membrane rupture.

To test this hypothesis, the cells' mechanical properties were measured by atomic force microscopy (AFM) (Fig. 5d, e, Supplementary Fig. 10, Supplementary Movie 16). Indeed, cells became markedly softer during NETosis, particularly in P2, as evidenced by a decrease of the Young's modulus from $E = 1.5$ to 0.3 kPa (Fig. 5d).

Additionally, retraction curves of individual membrane tethers were analyzed to distinguish the cell's bulk mechanical properties from the mechanical properties of the membrane alone. The membrane tension decreased by 77% (0.35 to 0.07 mN m^{-1}) (Fig. 5e). Although alterations of the plasma membrane are likely to occur in an inflammasome-dependent manner during NETosis[58], such a dramatic decrease cannot be explained by changes of membrane composition only, but must be caused by the disassembly of the actin cortex beneath the membrane[59,60]. The membrane tension T in late P2 corresponds to a membrane pressure $p \approx \frac{2}{R} T \approx 20$ Pa (Young-Laplace equation, radius $R \approx$ µm). The calculated swelling pressure (Fig. 4d) is in the same range indicating that chromatin swelling is sufficient to break the membrane.

Location of membrane rupture. To test the hypothesis that the chromatin swelling pressure determines the membrane breaking point, we correlated swelling speed and anisotropy with the position of the rupture point. Even though swelling itself should be isotropic, the position of the nucleus/lobuli inside the cell varied with respect to the cell boundary. We first looked at chromatin decondensation and calculated the average swelling speed during $t_1 < t < t_2$ (represented by a velocity field, Fig. 6a, Supplementary Fig. 11). Interestingly, in cells in which the nucleus was closer to one side of the cell membrane, the rupture point was usually close to areas of low chromatin movement, e.g., in close proximity to the cell membrane (cell 1–3). In these cases, there was less space for chromatin to expand (higher remaining entropic pressure). If (in the minority of cells) the nucleus was centered in the cell the rupture direction was random (cell 4).

Moreover, cells typically ruptured at the side that experienced the last membrane retraction close to the long axis of the cells before they rounded up (Fig. 6b).

In order to quantify these observations, a rupture point axis was determined by connecting the rupture point A with the center of mass of the respective cell (M). Then, the cells' outlines were fitted with an ellipse and the cell membrane shrinking velocities of both cell sides (A and B) were analyzed along the rupture axis (v_A and v_B) during the last minutes before rupture (30 min ± 16 min) (Fig. 6c). Cells ruptured at the side that experienced significantly more movement after the rounding process started in late P2 ($t > t_2$) (Fig. 6d). Most rupture events occurred close to the previously long axis of the (elliptic) cell (Fig. 6e), thus allowing the prediction of the NET release location.

This analysis of membrane morphology shows that cells become circular before the membrane ruptures on the last moving side close to the previous long axis. Additionally, the position of the nucleus with respect to the membrane determines

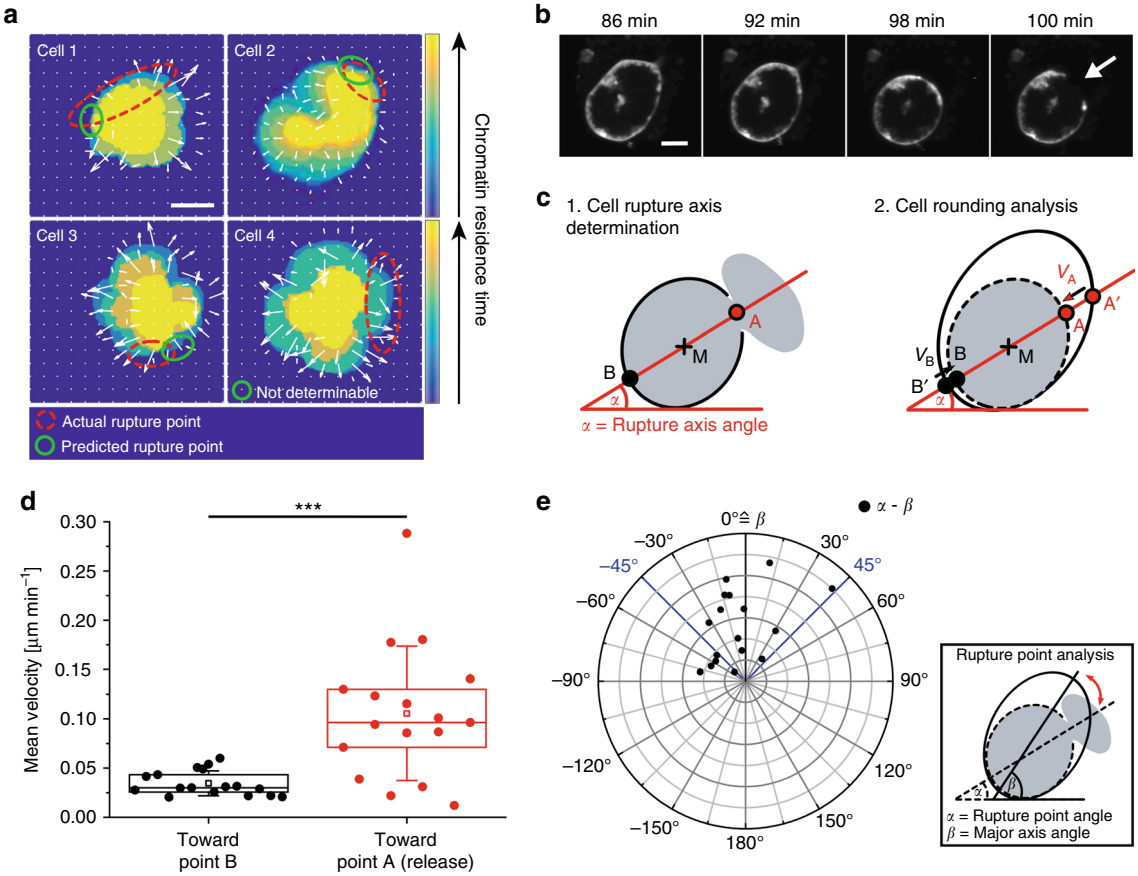

Fig. 6 Predetermination of the membrane rupture point. **a** Velocity plots of chromatin swelling. Changes to darker colors indicate faster movement (shorter residence time) of chromatin. The actual rupture point (red circle) often correlates with areas of slow movement (predicted rupture point, green circle). **b** Live-cell CLSM images of the cell membrane (PKH26 staining) directly before NET release. The cell rounds up and ruptures when maximum circularity is reached ($t = 98$ min). Scale bar = 5 µm. **c** Schematic of the rupture point analysis. Rupture points were analyzed by (1) fitting an ellipse to the cell before it became round and determining the rupture axis between the rupture point A and the center of mass M and (2) determining the retraction speed (v_A and v_B) on both sides of the (previously elliptic) cell (see Methods). **d** Shrinking velocity of the two opposing cell poles (A and B). The neutrophil retracts its membrane with a significantly higher velocity at the future rupture site (A). $n = 17$. $N = 4$ independent experiments. Statistics: Mann–Whitney test, two-tailed (***$p < 0.001$). Boxplots display the 25th and 75th percentile and the horizontal line the median. Hollow squares represent the mean and whiskers the SD. **e** Angle plot shows that the membrane ruptures in proximity of the major axis. α = rupture point angle. β = major axis angle. $n = 17$. $N = 4$ independent experiments

on which side of the cell entropic chromatin pressure becomes higher.

An additional aspect that has not been addressed in detail so far is influence of adhesion in NETosis. We used reflection interference contrast microscopy (RICM) (Supplementary Fig. 4c, d, Supplementary Movies 9–11) to image the interface between cell and substrate and address this question[61,62]. Neutrophils quickly and strongly adhered and left membrane behind, while rounding up. To further test the impact of adhesion we quantified NETosis on differently coated surfaces (Supplementary Fig. 12). Interestingly, on surfaces passivated with poly(L-lysine)-graft-poly(ethylene glycol) (PLL-g-PEG) neutrophils still performed NETosis even though they could not properly adhere (Supplementary Movie 17). This result does not rule out an important role of adhesion in determining the threshold for NETosis especially for different (weaker) activators. However, it shows that once the cell initiated NETosis, additional adhesive cues were not important anymore. Nevertheless, the influence of external factors for the initiation and execution of NETosis, including adhesive cues and surface characteristics like surface stiffness, for example, certainly warrant further investigation in the future.

Discussion

Over the last years, much effort has been put into unraveling the signaling cascades and enzymatic players that are indispensable for NETosis. Here, we provide a comprehensive and unique picture of the complex biophysical aspects that govern the different phases of NETosis using an interdisciplinary approach and innovative imaging methods. We conclude that NETosis is a highly organized process with a first phase (P1) that is governed by biochemical modifications including histone citrullination and phosphorylation of lamins[33] that prepare the cell for later mechanical changes. We show that a point of no return exists after which active processes such as enzymatic activities become secondary and the cells behavior is determined by the characteristics of chromatin (Fig. 7, Supplementary Fig. 13). Morphological changes, as well as rupture/burst of nuclear envelope and cell membrane are driven by entropic swelling of chromatin. At this point, pharmaceutical inhibition of NETosis is no longer possible. These findings may also prove important for other biological processes, such as cell division or other forms of cell death[54,63]. Indeed, it has been shown very recently that broad overlaps exist between NETosis and mitosis from a biochemical

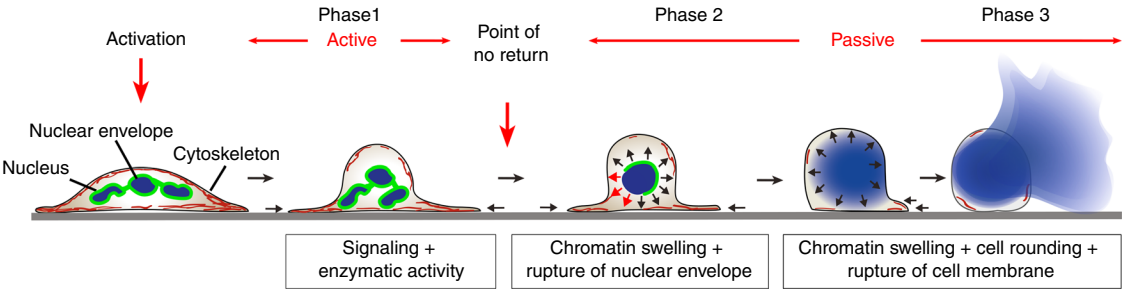

Fig. 7 Biophysical model of NET release NETosis can be divided into three distinct phases (according to chromatin status) that are separated by a point of no return. The major physical driving force for morphological changes and NET release after phase 1 is entropic swelling of chromatin

point of view. It will be worthwhile studying these similarities from a biophysical perspective[33].

Ultimately, cells appear to be more than biochemical factories and complex processes such as NETosis can therefore be driven not only by biochemical signaling but also material properties.

Chromatin is traditionally viewed as a nuclear entity that mainly regulates gene expression. Here, we show that chromatin is much more than a template for information processing but is able to actively conduct biological processes.

Methods

Isolation of human neutrophils. Neutrophils were isolated from human venous blood of healthy donors. The study was approved by the ethics committee of the university medical center goettingen (chairman Prof. Dr. med. Jürger Brockmöller) and fully informed consent of all donors obtained after clearing the possible consequences of the study. The isolation was performed according to previous published standard protocols.[1]

In short, fresh blood was collected with S-Monovettes KE 7.5 ml (Sarstedt). Blood was gently layered in a 1:1 ratio on top of Histopaque 1119 (Sigma-Aldrich) and centrifuged at 1100 × *g* for 21 min. Then, the transparent third and pink fourth layer containing the white blood cells were collected and mixed with HBSS (without Ca^{2+}/Mg^{2+}, Thermo Fisher Scientific). Cells were pelleted by centrifugation for 10 min at 400 × *g*. After discarding the supernatant, the pellet was resuspended in HBSS without Ca^{2+}/Mg^{2+} and layered on top of a phosphate buffered percoll (GE Healthcare) gradient with the concentrations 85, 80, 75, 70, and 65% and centrifuged at 1100 × *g* for 22 min. The accumulated neutrophils were received by collecting half of the 70%, full 75% and half of the 80% layer and washed with HBSS. The remaining cell pellet was resuspended in 1 ml HBSS. Cells were counted and suspended at the required concentration for the following procedures with RPMI 1640 (Lonza) containing 10 mM HEPES (Roth) and 0.5% human serum albumin (HSA) (Sigma-Aldrich). Experiments with lipopolysaccharides (LPS from Pseudomonas aeruginosa serotype 10.22, strain: ATCC 27316, Sigma-Aldrich) or calcium ionophores (CaI, Sigma-Aldrich) were carried out without addition of 0.5% human serum albumin. Cellular identity was confirmed by a cytospin assay (Cytospin 2 Zentrifuge, Shanson) followed by Diff Quick staining (Medion Diagnostics). Cell purity was >95% of isolated cells (without erythrocytes).

Live cell imaging (fluorescence microscopy). Fresh isolated human neutrophils were seeded (4–5 × 10^5 cells per ml) on ibidi treat flow chambers (µ-Slide I 0.8 Luer ibidi Treat, ibidi GmbH) for 30 min (37 °C, 5% CO_2) and stained with 1.62 µM Hoechst 33342 (Sigma-aldrich) for 15 min (37 °C, 5% CO_2). For membrane staining, cells were stained before seeding with 2 µM PKH26 (PKH26-kit, Sigma-aldrich) following the companies' instructions. Cells were activated for NETosis with 100 nM Phorbol-12-myristate-13-acetate (PMA, Sigma-aldrich), 4 µM CaI or 25 µg ml^{-1} LPS. Live cell imaging was performed at 23.5, 37 or 40 °C (ibidi heating system, ibidi GmbH) for 3–5 h with minimized light exposure. Bright field microscopy movies were obtained ×16 magnified (EC Plan-Neofluar Ph1/440331-9901-000, Zeiss) using the camera CoolSNAP ES (Photometrics) and the microscope Axiovert 200 (software: Metamorph 6.3r2., Molecular Devices, Zeiss) with a frame rate of one picture per minute in the blue channel (Filter set 02 shift free/488002-9901-000, Zeiss). For CLSM images an Olympus IX83 inverted microscope (software: Olympus Fluoview Ver.4.2, Olympus) was used and the movies were recorded ×60 magnified (UPlanSApo 1.35 oil, Olympus). Hoechst fluorescence was detected at 405 nm and PKH26 fluorescence at 561 nm. All 2D-movies were obtained with a frame-rate of one picture per 2 min and the 3D-movies with one picture per ten minutes and a z-stack depth of 1 µm per slice. All videos and pictures were further processed with ImageJ (v. 1.46r ad 1.50c4; National Institutes of Health) and MATLAB (v. R2008a/R2014a; The MathWorks, Inc.) as described in the section statistics and data analysis.

Inhibitor experiments. Fresh isolated human neutrophils (10,000 per well) were seeded in 96-glassbottom-well-plates (In vitro scientific) and activated for NETosis with PMA, final concentration 100 nM. Subsequently, the function of cytoskeletal components was inhibited with Cytochalasin D (100 nM, Abcam), Latrunculin A (1 µM, Sigma-Aldrich), Docetaxel (100 nM, Abcam), Jasplakinolide (10 µM, Enzo) or Y-27632 (19.2 µM, Abcam) and enzyme activity inhibited with 2-deoxy-D-glycosis (2- Deox-Gluc, 5 mM, Sigma-aldrich), sodium azide (NaN_3, 3 mM, Merck) or 4-Aminobenzoic acid hydrazide (ABAH, 100 µM, Cayman) at defined time points (0 min, 15 min, 30 min, 45 min, 60 min, 75 min, 90 min, 105 min, and 120 min) after activation. All experiments were performed in triplicates. To stop NET formation, cells were fixed with 2% PFA final concentration (Roth) after 3 h incubation (37 °C, 5% CO_2) and stored over night at 4 °C. The fixed probes were washed 10 min with 1× PBS (Lonza) and chromatin stained with Hoechst at room temperature. After staining, cells were washed with PBS and imaged with the microscope Axiovert 200 (×16 magnification, Zeiss; software: Metamorph 6.3r2, Molecular Devices) and a CoolSNAP ES camera (Photometrics) in the blue channel (Filter set49 DAPI shift free, 488049-9901-000, Zeiss). For each well in total 5-6 images of different regions were collected. For all experiments, the amount of decondensed nuclei, as well as the total cell count was quantified (blinded) with ImageJ. Percentages of decondensed nuclei/NETs were calculated relative to the amount of decondensed nuclei/NETs after stimulation of cells with PMA for 3 h.

ATP measurements. Fresh isolated human neutrophils (10,000 per well in RPMI (10 mM HEPES, 0.5% HSA without phenolred)) were seeded in white 96-well-plates (Greiner bio-one) and activated with PMA in a final concentration of 100 nM for defined time points (5 min, 15 min, 30 min, 60 min, 90 min, and 120 min). After incubation, CellTiter-Glo® Reagent (Promega) was added in a 1:1 ratio and the ATP amount was determined following the company instructions. In short, the mixture was shaken for 2 min to induce cell lysis and incubated for 10 min at room temperature to stabilize the luminescence signal. Subsequently, luminescence was measured (GLOMAX® 96 Microplate Luminometer, Software: GLOMAX 1.9.3, Turner BioSystems) and the ATP levels were calculated relatively to the ATP amount of unstimulated cells incubated for 120 min.

Staining procedures. Fresh isolated human neutrophils (200,000 per well) were seeded on pretreated (99% alcohol) glass cover slips (#1.5) in 24-well plates (Greiner bio-one) and NET formation induced with 100 nM PMA. Cells were then fixed at different time points after NET formation with 2% PFA and stored in PBS over night. The following staining procedure was carried out based on previous published protocols[64]. Briefly, cover slips were gently removed from the 24-well plate and layered upside down on the washing solution (1xPBS). Cells were then permeabilized with a 0.1% TritonX (Merck) containing solution for 10 min at 4 °C, washed and blocked with 5% fetal calf serum (FCS, Merck) or 3% BSA (Lamin B1 staining). Subsequently cells were stained with monoclonal anti-human MPO (IgG, mouse, 1:500) (ab25989, Abcam), monoclonal anti-human α-Tubulin (IgG, rabbit, 1:50) (#2125, Cell Signaling Technology) or polyclonal anti-human lamin B1 (IgG, rabbit, 1:1000) (ab16048, Abcam) as primary antibodies over night (4 °C) and visualized with polyclonal anti-mouse Alexa488 (IgG, goat, 1:1000) (#4408, Cell Signaling Technology) or polyclonal anti-rabbit Alexa488 (IgG, goat, 1:500) (A-11034, ThermoFisher Scientific) as secondary antibodies. In case of staining with SiR-dyes, cells were not permeabilized but directly stained after washing with SiR-Actin (SC001, Spirochrome AG/Tebu-bio) or SiR-DNA (SC007, Spirochrome AG/Tebu-bio) at 3 µM. Then, chromatin was stained with Hoechst if applicable and cover slips were mounted with Faramount Mounting Medium (Dako Agilent Technologies) on microscopy slide. After complete drying and fixation with nail polish, samples were imaged with 40x magnification (Plan-Neofluar 40×/1.30 oil Iris/4440456-0000-000, Zeiss) in a fluorescence microscope (AxioImager M1, Software: AxioVision Rel.4.7, Zeiss) or ×60 magnified with confocal laser scanning microscopy (Olympus IX83 inverted microscope, software: Olympus Fluoview v.4.2).

3D-STED microscopy. In conventional optical microscopy, the resolution is limited by diffraction to about half the wavelength of light ($\lambda/2 \approx 300$ nm) and

about the wavelength ($\lambda \approx 600$ nm) in the lateral and axial direction, respectively. To resolve smaller features samples were stained with SiR-DNA as described in the staining procedure section and were imaged with a super-resolution STED (Stimulated Emission Depletion) microscope[65]. For live cell imaging, cells (10,000 per well) were seeded for 30 min in 10-well CELLview™ glass slides (Greiner Bio-one) in RPMI (10 mM HEPES, 0.5% FCS without phenolred) and activated with 100 nM PMA and stained with 1 µM SiR-DNA. In a canonical STED microscope, the diffraction-limited excitation spot is superimposed with a red-shifted donut-shaped laser beam (STED beam) featuring a zero-intensity at its center. The STED beam has the ability to inhibit fluorescence from excited molecules. The higher the STED intensity, the more efficient this inhibitory effect is. As a consequence, fluorescence is confined to a sub-diffraction sized area. The super-resolution image is recorded by scanning this area across the sample.

To assess information beyond the diffraction limit, experiments were performed with a custom-built 3D-STED microscope. The excitation beam of 640 nm wavelength is emitted from a Picosecond Pulsed Diode Laser Head (LDH-P-C-640B, PicoQuant, Berlin, Germany). As STED light source at 775 nm, sub-nanosecond laser (Katana-08, Onefive GmbH, Zurich, Switzerland) is used. To achieve a super-resolved image in 3D, the Easy3D-STED Module (Abberior Instruments GmbH, Göttingen, Germany) is used: a programmable spatial light modulator (SLM) creates the STED light phase patterns required for 3D STED microscopy. It allowed a lateral (xy) and axial (z) resolution enhancement with only one STED beam instead of two separate STED beams. The relative pulse delay between the excitation laser and the STED laser is set electronically. Laser focusing and fluorescence collection are performed by the same oil immersion objective (UPlanSApo 60 × 1.35 Oil, Olympus Corporation, Tokyo, Japan). An appropriate series of dichroic mirrors and optical filters separates the fluorescent signal from both, the excitation and the STED light, and sends it into the detector. Fluorescence photons are detected by a Single Photon Counting module (SPCM-AQRH-13-FC, Excelitas Technologies Corp., Waltham, MA).

Experiments were run with the software ImSpector (MPI für biophysikalische Chemie, Göttingen, Germany); data analysis was performed with ImageJ (U. S. National Institutes of Health, Bethesda, Maryland, USA, http://imagej.nih.gov/ij/).

Atomic Force Microscopy (AFM). For all AFM-experiments, 60,000 cells (62 cells per mm^2) were seeded on an ibidi-treaded µ-dish (81156, Ibidi) for 30 min. Subsequently, the cells were activated with 100 nM PMA. For imaging, an Olympus IX81 microscope was used and steered with an Olympus CellSense Dimension software (v. 3.15). A custom-made heating system integrated into the dish holder enabled the temperature regulation of the sample ($T = 37$ C°).

For elasticity measurements, a non-conductive silicon nitride tip (MLCT, $f_0 =$ 10–20 kHz, $k = 0.02$ N m^{-1}, Bruker) was directed by a JPK AFM-head system (JPK Instruments 00996, Nanowizard 3), calibrated according to the manufacturer's instructions (Nanowizard 3 user manual) and kept in the medium to equilibrate the temperature. The tip was slowly approached to the cell via force-feedback recognition and positioned above the middle of the cell. In general, the sample was measured over a 20 × 20 µm area with 8 × 8 force curves for each time point and controlled by a JPK SPM Control software (v.5). To prevent plastic deformation a relative set point of 0.5 nN was chosen together with an extension speed of 3 µm s^{-1} and a delay time of 1 s between each force curve measurement resulting in a total iteration time of around 6 min. All force curves were manually reviewed, baseline corrected and the Young's modulus E was calculated using the Hertz fit for pyramidal tip geometries

$$F = \frac{E}{1-\nu^2}\frac{\tan(\alpha)}{\sqrt{2}}\delta^2 \quad (2)$$

with a Poisson's ratio set to $\nu = 0.5$, a face angle of $\alpha = 20°$, the measured force F and the tip-sample distance δ of the force curve. The mean Young's modulus was calculated from the force-curve in the middle of the cell and four direct neighbors to avoid edge effects.

Parallel imaging to verify NETosis and healthiness of the cells were performed on the same system. Here, cells were stained before with 1.62 µM Hoechst (Sigma-Aldrich) and observed with an Orca Flash 2.8 camera (C11440, Hamamatsu) at ×40 magnification (LUCPlan FLN, Olympus). For illumination, an integrated lamp system (cellTIRF-4Line System + IUX-C2, Olympus) was used and filtered by a DAPI filter set (#86-370-OLY, Olympus).

To measure tether tension during NETosis, the baselines of all AFM retraction curves on the cell were analyzed for step like deflection changes that indicate tether formation (sharp increase of cantilever deflection and constant values before and after). All restoring forces were measured with a JPK Data Processing Software (V. spm 5.0.69, JPK Instruments) and stored separately for each frame time t. The membrane tension $T(t)$ was then calculated by using the relation[66–68]

$$T(t) = \frac{F(t)^2}{8B\pi^2} \quad (3)$$

with B representing the bending stiffness of a lipid membrane (set to 3×10^{-12} dyne cm) and $F(t)$ the respective tether force[2]. For each frame, these values were averaged ($n \approx 3$) and each data set was normalized to its first value $T(t_0)$ to enable comparisons between varying base values of control cells.

For pressure measurements, a tipless cantilever (MLCT-O10, f_0 = 10–20 kHz, $k = 0.03$ N m^{-1}, Bruker) was chosen in order to enlarge the contact area of the probed cell. Neutrophils were seeded according to the mentioned protocol, activated with PMA and subsequently incubated for 90 min at 37 °C, 5% CO_2 to ensure unmodified cell properties before cell rupture. Afterwards, cells were placed into the aforementioned setup and the cantilever was manually approached to a single cell using 0.2 µm driving steps of the z-piezo motor until cell contact (deflection increase of the cantilever) could be observed. Henceforth, the height of the z-piezo was set constant and the pushing forces of the swelling cell were passively quantified using the Live Tracker function of the JPK SPM Control software (v.5, JPK Instruments). When the pushing forces reached maximal measurable values of the sensor consecutively, the amount of deflection had to be manually reset by readjusting the alignment mirror (reallocation of laser spot on the sensor). This resulted in a vast decline of the deflection data at certain times (dashed lines in Supplementary Fig. 8d), however an effect on the following process could not be observed. Measurements were continued until a rupture of the cellular membrane occurred which was proven afterwards by both a fast breakdown of the deflection data, as well as propidium iodide stainings (Sigma-Aldrich, $c \approx 1$ µM). To calculate the interior pressure of the cell, a phase contrast image of the respective cell was taken directly after reaching the contact point. With this, the contact area A of the cell could be extracted by thresholding the visible cell area and the result was combined with the force $F(t)$ of the deflection measurements to generate the pressure value $p(t) = F(t)/A$.

Statistics and data analysis. For data analysis Prism 6 for Mac OS X (v. 6.0 h, GraphPad Software, Inc.), origin (OriginPro8, OriginLab Corporation) and MATLAB (v. R2008a/R2014a; The MathWorks, Inc.) were used.

Statistical analysis was performed with Prism 6 for Mac OS X. For all data sets GAUSS distribution was verified with Shapiro-Wilk normality test if applicable and significance proved by t-test or one-/two-way-ANOVA/ Bonferroni's multiple comparisons test (mean ± standard deviation (SD) or standard error of the mean (SEM); $^*p < 0.05$; $^{**}p < 0.01$; $^{***}p < 0.001$; $^{****}p < 0.0001$). For non-Gaussian distributed data sets Mann-Whitney or Kruskal–Wallis/Dunn's multiple comparisons tests ($^*p < 0.05$; $^{**}p < 0.01$; $^{***}p < 0.001$; $^{****}p < 0.0001$) were used.

Time-lapse analysis. To quantify the change of chromatin area and eccentricity over the time course of NETosis an image segmentation script was developed in Matlab (v. 2014a). Live-cell images generated by wide field fluorescence microscopy were used for the quantification of the chromatin area. This area is a projected chromatin area because it is derived from 2D images. CLSM derived time traces were analyzed similarly and are shown for example in Fig. 1b.

For single cells, areas of high contrast (mainly at the edge between stained regions and the background) were carved out, smoothed and filled to generate an outlined image of each object that could be analyzed. Furthermore, total intensity values were normalized to circumvent problems coming from background fluctuations or different staining intensities. From the resulting area-time curves, four characteristic time points were determined manually as shown in Supplementary Fig. 3a: t_1/start of P2: start of first chromatin area increase, t_D: end of uniform/isotropic area increase in P2, t_2: maximal area in P2, t_3/start of P3: second start of increase in chromatin area. Hence, the duration of P1 (activation (0 min) to t_1) and P2 (t_1 to t_3), as well as the diffusion coefficient of the expanding chromatin in P2 (t_1 to t_D) were calculated. For determination of the diffusion coefficient only cells of population 1 ($t_2 \neq t_3$) were used (see Supplementary Fig. 3a).

Quantitative membrane and chromatin analysis (Fig. 6a–d) was based on the same segmentation procedure and extended: For chromatin swelling analysis (Fig. 6a), detected chromatin areas of each frame were binarized first and stacked to produce the shown density plots. Moreover, each frame was divided in a grid of 15 × 15 pixel sized sub-windows and analyzed by measuring the average additional or lost chromatin area per window resulting in a growth/shrinking vector for each of these segments. The final vector plot results from averaging all frame vectors of a respective segment. For membrane analysis (Fig. 6b–d), the position of the rupture point was manually determined from the first frame after membrane burst and then compared with the computed major axis of the fitted cell ellipsoid. Only cells with a clear single rupture point were analyzed.

Pressure calculation. Swelling pressures values shown in Fig. 4d were calculated by using an approach motivated by Mazumder et al.[52] Here, Newtonian properties of the swelling process were assumed and the Stokes-equation was used (effects of inertia were expected to be negligible).

$$\nabla \mathbf{p}(t) = \eta \Delta v(t) \quad (4)$$

In this case, $p(t)$ describes the inherent pressure of the fluid/chromatin network, η is the viscosity of the liquid and $v(t)$ is the velocity field at time point t. The physical problem was simplified in two different ways: First, a radial symmetric force field was assumed ($\nabla \mathbf{p} \approx \frac{p}{R}$) and secondly the resistance was assumed to be dominated by viscous forces at the scale of interstices (pores) in the network, which ultimately leads to $\eta \Delta v(t) \approx \frac{\eta}{l_p^2}\frac{dR}{dt}$ with l_p describing the average mesh size and $R(t)$

the radius of the (chromatin) network. Consequently, it follows

$$p(t) \approx \frac{\eta(R(t))}{l_p^2(R(t))}\frac{\mathrm{d}R(t)}{\mathrm{d}t}R(t). \quad (5)$$

The exact value of $\eta(R(t))$ is unknown. However, in previous studies the viscosity of the nucleus of an eukaryotic cell before expansion was determined to be $\eta_0 = 0.1$ Pa s[52]. It is also known that the viscosity of semiflexible polymer network scales $\eta(R) \sim 1/R^3$ with the overall radius R (correlated to the mesh size)[69]. This relation and η_0 were used to approximate $\eta(R(t))$. Furthermore, to approximate the average mesh size $l_p(R)$, a single DNA strain ($L \approx 2$ m, $d \approx 2.2$ nm) was arranged into a cubic lattice inside a sphere with a radius $R(t)$. $R(t)$ was measured in the time-lapse movies exemplarily shown in Supplementary Movie 2 using $R(t) = \sqrt{A/\pi}$) and $\frac{\mathrm{d}R(t)}{\mathrm{d}t}$ was calculated by fitting the two dimensional diffusion equation $\frac{\mathrm{d}R(t)}{\mathrm{d}t} = \frac{\mathrm{d}\left(\sqrt{4Dt}\right)}{\mathrm{d}t} = \frac{4D}{2\sqrt{4Dt}} = \sqrt{\frac{D}{t}} = \sqrt{\frac{R^2}{4t^2}} = \frac{R}{2t}$ to the chromatin data between $R(t_1)$ to $R(t_D)$ and $R(t_D)$ to $R(t_2)$ and extracting the resulting slope.

Code availability. All Matlab codes used to analyze data are available from the corresponding authors upon request.

Data availability

Data supporting the findings of this manuscript are available from the corresponding authors upon request.

Received: 2 January 2018 Accepted: 11 August 2018
Published online: 14 September 2018

References

1. Mantovani, A., Cassatella, M. A., Costantini, C. & Jaillon, S. Neutrophils in the activation and regulation of innate and adaptive immunity. *Nat. Rev. Immunol.* **11**, 519–531 (2011).
2. Brinkmann, V. et al. Neutrophil extracellular traps kill bacteria. *Science* **303**, 1532–1535 (2004).
3. Brinkmann, V. & Zychlinsky, A. Neutrophil extracellular traps: is immunity the second function of chromatin? *J. Cell. Biol.* **198**, 773–783 (2012).
4. Fuchs, T. A. et al. Novel cell death program leads to neutrophil extracellular traps. *J. Cell. Biol.* **176**, 231–241 (2007).
5. Metzler, K. D. et al. Myeloperoxidase is required for neutrophil extracellular trap formation: implications for innate immunity. *Blood* **117**, 953–959 (2011).
6. von Kockritz-Blickwede, M. et al. Phagocytosis-independent antimicrobial activity of mast cells by means of extracellular trap formation. *Blood* **111**, 3070–3080 (2008).
7. Ueki, S. et al. Eosinophil extracellular DNA trap cell death mediates lytic release of free secretion-competent eosinophil granules in humans. *Blood* **121**, 2074–2083 (2013).
8. Zhang, X., Zhuchenko, O., Kuspa, A. & Soldati, T. Social amoebae trap and kill bacteria by casting DNA nets. *Nat. Commun.* **7**, 10938 (2016).
9. Hawes, M. C. et al. Extracellular DNA: the tip of root defenses? *Plant Sci.* **180**, 741–745 (2011).
10. Papayannopoulos, V., Metzler, K. D., Hakkim, A. & Zychlinsky, A. Neutrophil elastase and myeloperoxidase regulate the formation of neutrophil extracellular traps. *J. Cell. Biol.* **191**, 677–691 (2010).
11. Garcia-Romo, G. S. et al. Netting neutrophils are major inducers of type I IFN production in pediatric systemic lupus erythematosus. *Sci. Transl. Med.* **3**, 73ra20 (2011).
12. Sorensen, O. E. et al. Papillon-Lefevre syndrome patient reveals species-dependent requirements for neutrophil defenses. *J. Clin. Invest.* **124**, 4539–4548 (2014).
13. Martinod, K. et al. PAD4-deficiency does not affect bacteremia in polymicrobial sepsis and ameliorates endotoxemic shock. *Blood* **125**, 1948–1956 (2015).
14. Erpenbeck, L., Schon, M. P. Neutrophil extracellular traps: protagonists of cancer progression? *Oncogene* **36**, 2483 (2016).
15. Brill, A. et al. Neutrophil extracellular traps promote deep vein thrombosis in mice. *J. Thromb. Haemost.* **10**, 136–144 (2012).
16. Savchenko, A. S. et al. VWF-mediated leukocyte recruitment with chromatin decondensation by PAD4 increases myocardial ischemia/reperfusion injury in mice. *Blood* **123**, 141–148 (2014).
17. Kolaczkowska, E. et al. Molecular mechanisms of NET formation and degradation revealed by intravital imaging in the liver vasculature. *Nat. Commun.* **6**, 6673 (2015).
18. Gupta, A. K., Hasler, P., Holzgreve, W., Gebhardt, S. & Hahn, S. Induction of neutrophil extracellular DNA lattices by placental microparticles and IL-8 and their presence in preeclampsia. *Hum. Immunol.* **66**, 1146–1154 (2005).
19. Sur Chowdhury, C. et al. Enhanced neutrophil extracellular trap generation in rheumatoid arthritis: analysis of underlying signal transduction pathways and potential diagnostic utility. *Arthritis Res. Ther.* **16**, R122 (2014).
20. Hoppenbrouwers, T. et al. In vitro induction of NETosis: comprehensive live imaging comparison and systematic review. *PLoS ONE* **12**, e0176472 (2017).
21. Kamoshida, G. et al. Pathogenic Bacterium Acinetobacter baumannii Inhibits the Formation of Neutrophil Extracellular Traps by Suppressing Neutrophil Adhesion. *Front. Immunol.* **9**, 178 (2018).
22. Stavrou, E. X. et al. Factor XII and uPAR upregulate neutrophil functions to influence wound healing. *J. Clin. Invest.* **128**, 944–959 (2018).
23. O'Brien, X. M. & Reichner, J. S. Neutrophil integrins and matrix ligands and NET release. *Front. Immunol.* **7**, 363 (2016).
24. Xu, Z. et al. Interaction of kindlin-3 and beta2-integrins differentially regulates neutrophil recruitment and NET release in mice. *Blood* **126**, 373–377 (2015).
25. Clark, S. R. et al. Platelet TLR4 activates neutrophil extracellular traps to ensnare bacteria in septic blood. *Nat. Med.* **13**, 463–469 (2007).
26. Maugeri, N. et al. Activated platelets present high mobility group box 1 to neutrophils, inducing autophagy and promoting the extrusion of neutrophil extracellular traps. *J. Thromb. Haemost.* **12**, 2074–2088 (2014).
27. Yu, X., Tan, J. & Diamond, S. L. Hemodynamic force triggers rapid NETosis within sterile thrombotic occlusions. *J. Thromb. Haemost.* **16**, 316–329 (2018).
28. Kenny, E. F. et al. Diverse stimuli engage different neutrophil extracellular trap pathways. *eLife* **6**, e24437 (2017).
29. Brinkmann, V., Goosmann, C., Kuhn, L. I. & Zychlinsky, A. Automatic quantification of in vitro NET formation. *Front. Immunol.* **3**, 413 (2012).
30. van der Linden, M., Westerlaken, G. H. A., van der Vlist, M., van Montfrans, J. & Meyaard, L. Differential signalling and kinetics of neutrophil extracellular trap release revealed by quantitative live imaging. *Sci. Rep.* **7**, 6529 (2017).
31. Gupta, S., Chan, D. W., Zaal, K. J. & Kaplan, M. J. A high-throughput real-time imaging technique to quantify NETosis and distinguish mechanisms of cell death in human neutrophils. *J. Immunol.* **200**, 869–879 (2018).
32. Elacqua, J. J., McGregor, A. L. & Lammerding, J. Automated analysis of cell migration and nuclear envelope rupture in confined environments. *PLoS ONE* **13**, e0195664 (2018).
33. Amulic, B. et al. Cell-cycle proteins control production of neutrophil extracellular traps. *Develop. Cell* **43**, 449–462 (2017).
34. Metzler, K. D., Goosmann, C., Lubojemska, A., Zychlinsky, A. & Papayannopoulos, V. A myeloperoxidase-containing complex regulates neutrophil elastase release and actin dynamics during NETosis. *Cell Rep.* **8**, 883–896 (2014).
35. Borregaard, N. & Herlin, T. Energy metabolism of human neutrophils during phagocytosis. *J. Clin. Invest.* **70**, 550–557 (1982).
36. Chacko, B. K. et al. Methods for defining distinct bioenergetic profiles in platelets, lymphocytes, monocytes, and neutrophils, and the oxidative burst from human blood. *Lab. Investig.* **93**, 690–700 (2013).
37. Wick, A. N., Drury, D. R., Nakada, H. I. & Wolfe, J. B. Localization of the primary metabolic block produced by 2-deoxyglucose. *J. Biol. Chem.* **224**, 963–969 (1957).
38. Chen, W. & Gueron, M. The inhibition of bovine heart hexokinase by 2-deoxy-D-glucose-6-phosphate: characterization by 31P NMR and metabolic implications. *Biochimie* **74**, 867–873 (1992).
39. Lane, T. A. & Lamkin, G. E. A reassessment of the energy requirements for neutrophil migration: adenosine triphosphate depletion enhances chemotaxis. *Blood* **64**, 986–993 (1984).
40. Azevedo, E. P. et al. A metabolic shift toward pentose phosphate pathway is necessary for amyloid fibril- and phorbol 12-Myristate 13-Acetate-induced Neutrophil Extracellular Trap (NET) formation. *J. Biol. Chem.* **290**, 22174–22183 (2015).
41. Pitanga, T. N. et al. Neutrophil-derived microparticles induce myeloperoxidase-mediated damage of vascular endothelial cells. *BMC Cell. Biol.* **15**, 21 (2014).
42. Bowler, M. W., Montgomery, M. G., Leslie, A. G., Walker, J. E. How azide inhibits ATP hydrolysis by the F-ATPases. *Proc. Natl Acad. Sci. USA* **103**(23), 8646–8649 (2006).
43. Merrill, G. A., Bretthauer, R., Wright-Hicks, J. & Allen, R. C. Effects of inhibitors on chicken polymorphonuclear leukocyte oxygenation activity measured by use of selective chemiluminigenic substrates. *Comp. Med.* **51**, 16–21 (2001).
44. Kettle, A. J., Gedye, C. A. & Winterbourn, C. C. Mechanism of inactivation of myeloperoxidase by 4-aminobenzoic acid hydrazide. *Biochem. J.* **321**(Pt 2), 503–508 (1997).
45. Kettle, A. J., Gedye, C. A., Hampton, M. B. & Winterbourn, C. C. Inhibition of myeloperoxidase by benzoic acid hydrazides. *Biochem. J.* **308**(Pt 2), 559–563 (1995).
46. Milo, R., Phillips, R. *Cell Biology by the Numbers* (Garland Science, 2016).

47. Prazeres, D. M. F. Prediction of diffusion coefficients of plasmids. *Biotechnol. Bioeng.* **99**, 1040–1044 (2008).
48. Luby-Phelps, K. et al. A novel fluorescence ratiometric method confirms the low solvent viscosity of the cytoplasm. *Biophys. J.* **65**, 236–242 (1993).
49. Wang, Y. et al. Histone hypercitrullination mediates chromatin decondensation and neutrophil extracellular trap formation. *J. Cell. Biol.* **184**, 205–213 (2009).
50. Latulippe, D. R. & Zydney, A. L. Radius of gyration of plasmid DNA isoforms from static light scattering. *Biotechnol. Bioeng.* **107**, 134–142 (2010).
51. Tree, D. R., Muralidhar, A., Doyle, P. S. & Dorfman, K. D. Is DNA a good model polymer? *Macromolecules* **46**, 8369–8382 (2013).
52. Mazumder, A., Roopa, T., Basu, A., Mahadevan, L. & Shivashankar, G. V. Dynamics of chromatin decondensation reveals the structural integrity of a mechanically prestressed nucleus. *Biophys. J.* **95**, 3028–3035 (2008).
53. Koslov, M. M. & Markin, V. S. A theory of osmotic lysis of lipid vesicles. *J. Theor. Biol.* **109**, 17–39 (1984).
54. Stewart, M. P. et al. Hydrostatic pressure and the actomyosin cortex drive mitotic cell rounding. *Nature* **469**, 226–230 (2011).
55. Gabler, W. L., Bullock, W. W. & Creamer, H. R. Phorbol myristate acetate induction of chemotactic migration of human polymorphonuclear neutrophils. *Inflammation* **17**, 521–530 (1993).
56. Bengtsson, T., Orselius, K. & Wettero, J. Role of the actin cytoskeleton during respiratory burst in chemoattractant-stimulated neutrophils. *Cell. Biol. Int.* **30**, 154–163 (2006).
57. Neeli, I., Dwivedi, N., Khan, S. & Radic, M. Regulation of extracellular chromatin release from neutrophils. *J. Innate Immun.* **1**, 194–201 (2009).
58. Chen, K. W. et al. The neutrophil NLRC4 inflammasome selectively promotes IL-1beta maturation without pyroptosis during acute Salmonella challenge. *Cell Rep.* **8**, 570–582 (2014).
59. Pierre, S. & Julie, P. Membrane tension and cytoskeleton organization in cell motility. *J. Phys.* **27**, 273103 (2015).
60. Diz-Muñoz, A., Fletcher, D. A. & Weiner, O. D. Use the force: membrane tension as an organizer of cell shape and motility. *Trends Cell Biol.* **23**, 47–53 (2013).
61. Kruss, S. et al. Adhesion maturation of neutrophils on nanoscopically presented platelet glycoprotein Ibalpha. *ACS Nano* **7**, 9984–9996 (2013).
62. Kruss, S., Erpenbeck, L., Schon, M. P. & Spatz, J. P. Circular, nanostructured and biofunctionalized hydrogel microchannels for dynamic cell adhesion studies. *Lab. Chip.* **12**, 3285–3289 (2012).
63. Fischer-Friedrich, E., Hyman, A. A., Julicher, F., Muller, D. J. & Helenius, J. Quantification of surface tension and internal pressure generated by single mitotic cells. *Sci. Rep.* **4**, 6213 (2014).
64. Brinkmann, V., Laube, B., Abu Abed, U., Goosmann, C., Zychlinsky, A. Neutrophil extracellular traps: how to generate and visualize them. *J. Vis. Exp.* **36**, e1724 (2010).
65. Hell, S. W. & Wichmann, J. Breaking the diffraction resolution limit by stimulated emission: stimulated-emission-depletion fluorescence microscopy. *Opt. Lett.* **19**, 780–782 (1994).
66. Sheetz, M. P. Cell control by membrane-cytoskeleton adhesion. *Nat. Rev. Mol. Cell Biol.* **2**, 392–396 (2001).
67. Waugh, R. E., Song, J., Svetina, S. & Zeks, B. Local and nonlocal curvature elasticity in bilayer membranes by tether formation from lecithin vesicles. *Biophys. J.* **61**, 974–982 (1992).
68. Hochmuth, R. M., Mohandas, N. & Blackshear, P. L. Jr Measurement of the elastic modulus for red cell membrane using a fluid mechanical technique. *Biophys. J.* **13**, 747–762 (1973).
69. Broedersz, C. P. & MacKintosh, F. C. Modeling semiflexible polymer networks. *Rev. Mod. Phys.* **86**, 995–1036 (2014).

Acknowledgements

This project was supported by the state of Lower Saxony (life@nano) and the German Research Foundation (DFG grant KR 4242/4-1 and ER 723/2-1). We acknowledge financial support by the open-access funding program of the German Research Foundation and the publication funds of the University Medical Center (UMG). Part of this work was supported by the Cluster of Excellence and DFG Research Center Nanoscale Microscopy and Molecular Physiology of the Brain (CNMPB). We thank Elisa D'Este and Grazvydas Lukinavicius for input on SiR-Hoechst stainings. We thank Andreas Janshoff and Claudia Steinem for fruitful discussions and support. We are grateful for fruitful discussions about active matter with members of the collaborative research center SFB 937 funded by the DFG.

Author contributions

S.K. and L.E. conceived the study with inputs from M.P.S. E.N. and D.M. performed experiments. E.N., F.R., C.G. and A.E. performed STED microscopy. G.G., A.K.T., J.G. and S.S.S. performed additional staining and inhibitor experiments. E.N., D.M., L.E. and S.K. analyzed data/images. E.N., D.M., L.E., and S.K. wrote the manuscript with inputs from all authors.

Additional information

Supplementary Information accompanies this paper at https://doi.org/10.1038/s41467-018-06263-5.

Competing interests: The authors declare no competing interests.

Reprints and permission information is available online at http://npg.nature.com/reprintsandpermissions/

Publisher's note: Springer Nature remains neutral with regard to jurisdictional claims in published maps and institutional affiliations.

Open Access This article is licensed under a Creative Commons Attribution 4.0 International License, which permits use, sharing, adaptation, distribution and reproduction in any medium or format, as long as you give appropriate credit to the original author(s) and the source, provide a link to the Creative Commons license, and indicate if changes were made. The images or other third party material in this article are included in the article's Creative Commons license, unless indicated otherwise in a credit line to the material. If material is not included in the article's Creative Commons license and your intended use is not permitted by statutory regulation or exceeds the permitted use, you will need to obtain permission directly from the copyright holder. To view a copy of this license, visit http://creativecommons.org/licenses/by/4.0/.

© The Author(s) 2018

2.2 Supplementary information, manuscript I

Supplementary Movies
(All movies can be found as an attachment to this thesis in form of a DVD)

Supp. movie 1: Time-lapse confocal laser scanning microscopy (CLSM) movie of human neutrophils undergoing NETosis stimulated with 100 nM PMA. Cells are stained for chromatin (blue, Hoechst 33342) and membrane (red, PKH26).

Supp. movie 2: Neutrophil during PMA-induced NET formation (example cell in **Fig. 1a** and **1b**).

Supp. movie 3: Time-lapse movie of chromatin decondensation of human neutrophils observed with conventional fluorescence microscopy during PMA-induced NET formation. Chromatin stained by Hoechst 33342.

Supp. movie 4: Example cell 1 of **Supp. movie 3**.

Supp. movie 5: Example cell 2 of **Supp. movie 3**.

Supp. movie 6: Example cell 3 of **Supp. movie 3**.

Supp. movie 7: Time-lapse movie of chromatin decondensation of neutrophils activated to undergo NET formation by PMA (100 nM) (left), LPS (25 µg ml^{-1}, middle) or CaI (4 µM, right), respectively. Chromatin stained by Hoechst 33342.

Supp. movie 8: Time-lapse 3D-CLSM movie of human neutrophils undergoing NETosis stimulated by 100 nM PMA. Cells are stained for chromatin (blue, Hoechst 33342) and membrane (red, PKH26). z-Stack-depth = 1 µm, 10 minutes/ frame.

Supp. movie 9: Reflection interference contrast microscopy (RICM) time-lapse movie on a glass substrate (**Supp. fig. 4c**). Neutrophils are activated with 100 nM PMA.

Supp. movie 10: RICM-time-lapse movie on an ibidi treat substrate (surface equal to CLSM time-lapse movies). Neutrophils are activated with 100 nM PMA.

Supp. movie 11: RICM-time-lapse movie on an ibidi treat substrate coated with Poly-L-lysine (PLL). Neutrophils are activated with 100 nM PMA.

Supp. movie 12: Time-lapse movie of chromatin decondensation of neutrophils activated to undergo NET formation by PMA (100 nM) at 23.5°C (left), 37°C (middle) or 40°C (right), respectively. Chromatin stained by Hoechst 33342.

Supp. movie 13-15: Example cells 1-3 in **Fig. 2d** (cells from **Supp. movie 1**).

Supp. movie 16: Time-lapse movie of a typical height (left) and stiffness map (right) during life cell AFM measurement. The raw data of the marked pixel (force curve) is shown below for each frame.

Supp. movie 17: Time-lapse movie of chromatin decondensation during PMA-induced NET formation on a poly(L-lysine)-graft-poly(ethylene glycol) (PLL-g-PEG) coated ibidi treat substrate (right) in comparison to only ibidi treat (left, conventional fluorescence microscopy). Chromatin stained by Hoechst 33342.

Supplementary figures

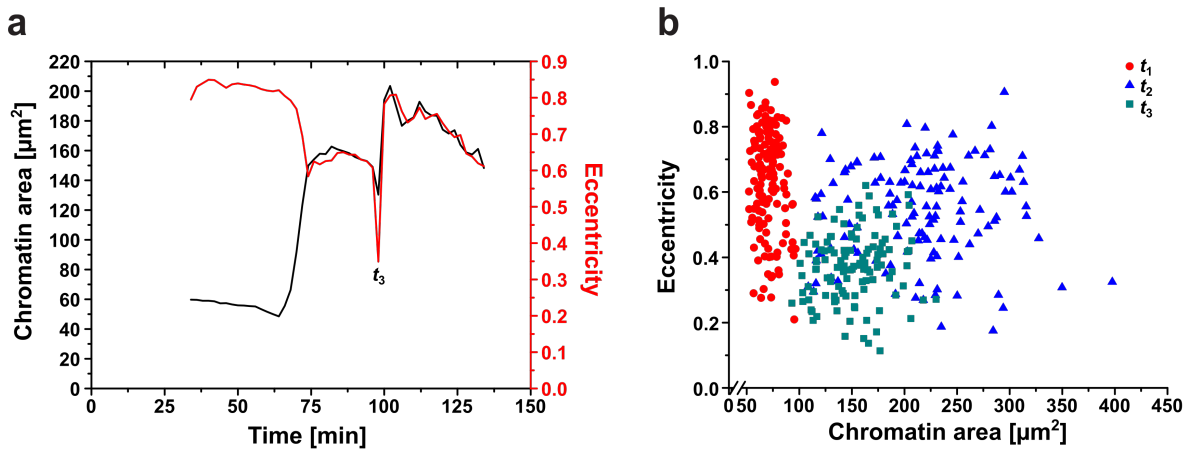

Supplementary fig. 1: Eccentricity of chromatin during NETosis. Chromatin rounds up during Phase 1 and 2 and reaches maximal circularity (minimal eccentricity) exactly before NET release (t_3). **a,** Eccentricity over time displayed for the example cell of **Fig. 1b** (**Supplementary movie 2**). **b,** Comparison of the eccentricity at different time points (t_1, t_2, t_3) for in total 139 cells of five donors.

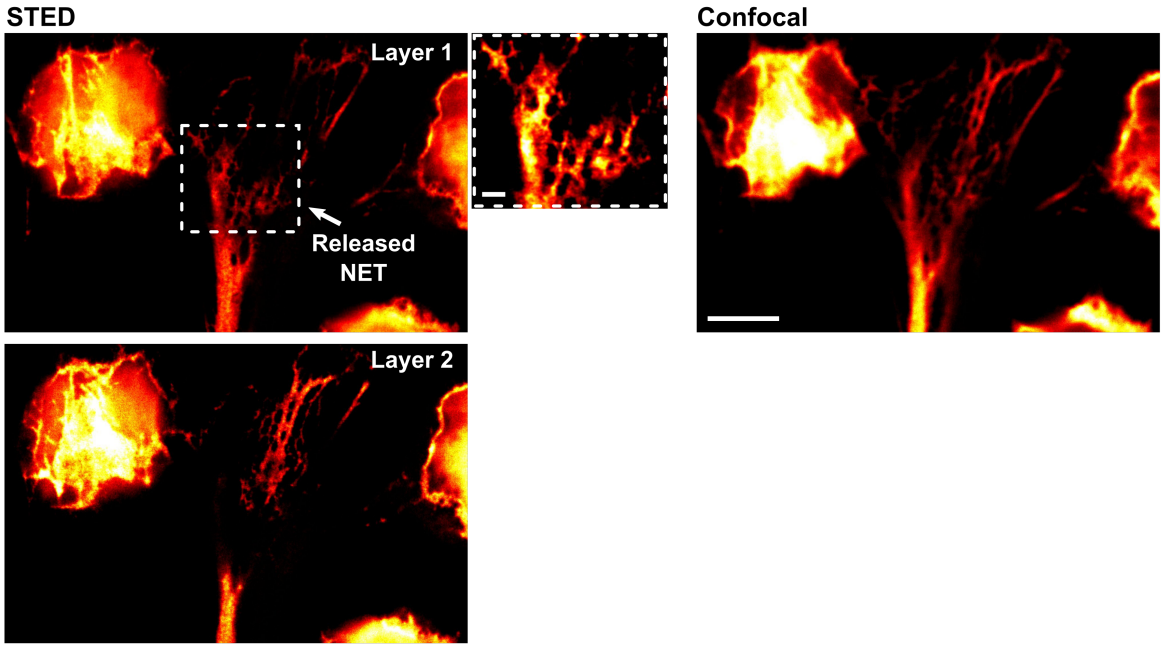

Supplementary fig. 2: STED nanoscopy of NET fine structure. Images of PMA-activated neutrophils (arrow = released NET) in comparison to confocal microscopy. Staining: SiR-DNA on fixed samples. Scale = 5 µm and 1 µm (insert).

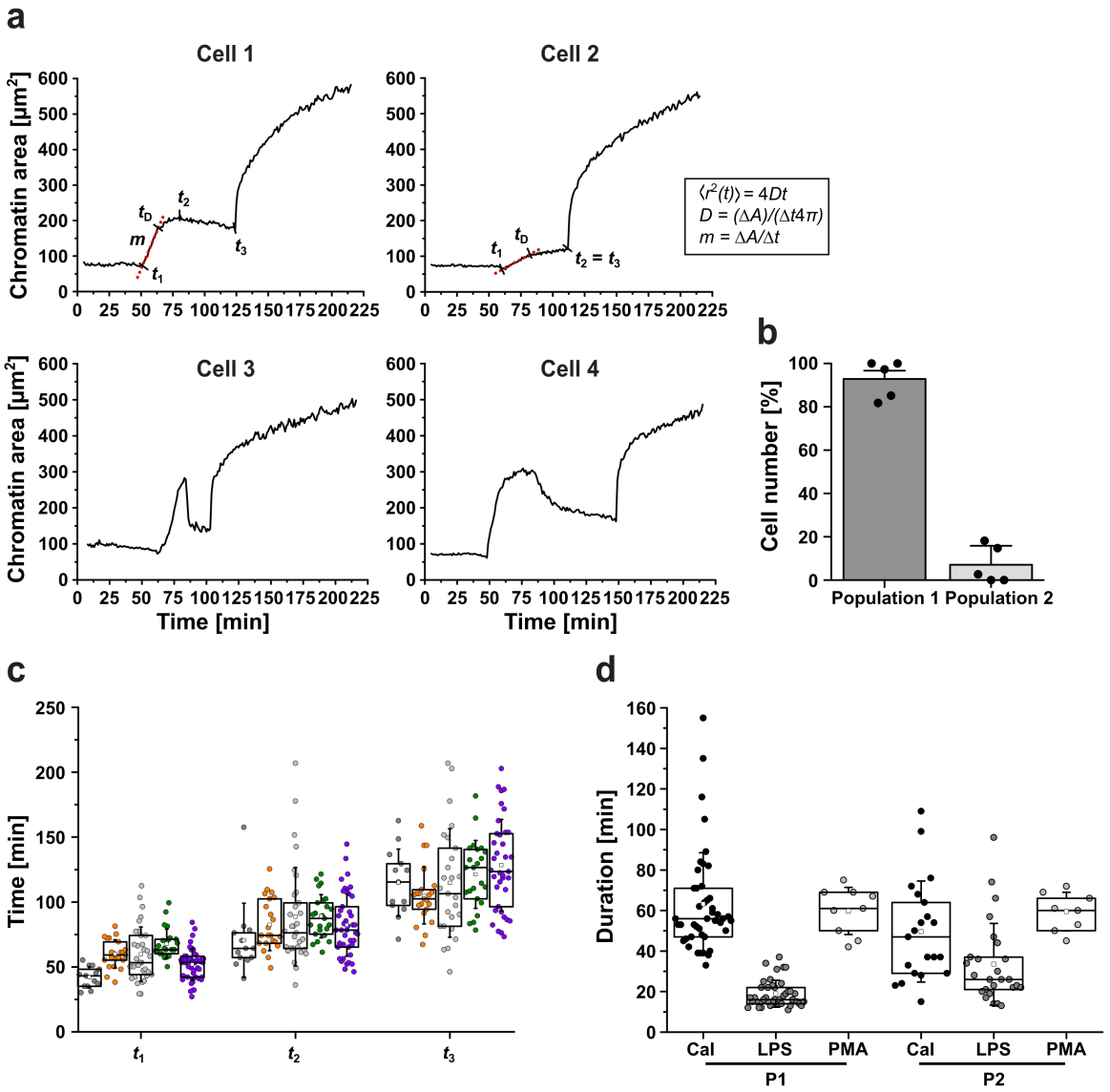

Supplementary fig. 3: Characterization of phases of NETosis. a, b Time course of changes in chromatin area during PMA-induced NETosis displayed for different cells imaged with wide field fluorescence microscopy. Cells can be divided in two different populations based on their chromatin time course. Cells of population 1 show a maximum of chromatin expansion (t_2) in P2. Chromatin of cells of population 2 expands until cell rupture at t_3. t_2 cannot be defined for this population (cell 2). Cell 1, 3 and 4 represent cells of population 1 and cell 2 of population 2. Therefore, only population 1 (> 90 % of cells) has been used to analyze the correlation between cell area at rupture/pressure P at t_2 and the time between t_2 and t_3 (rupture delay time) (**Fig. 4a, d**). The diffusion coefficient shown in **Supplementary fig. S8a** is calculated based on the slope of the linear fit from t_1 to t_D. Mean ± SEM. **c,** Distribution of the time points t_1, t_2 and t_3 of all cells of five individual experiments (summary shown in **Fig. 1c**). Time points were calculated based on time-lapse movies recorded with conventional fluorescence microscopy. N = 5. **d,** Kinetics of NET formation after stimulation with three different stimuli (PMA = 100 nM, LPS = 25 µg ml^{-1}, CaI = 4 µM). Duration of P1 is significantly shortened after stimulation with LPS compared to PMA and CaI, whereas P2 displays only small stimulus dependence. N = 1. Boxplots (**c, d**) display the 25th and 75th percentile with the horizontal line at the median, squares represent the mean and whiskers the SD.

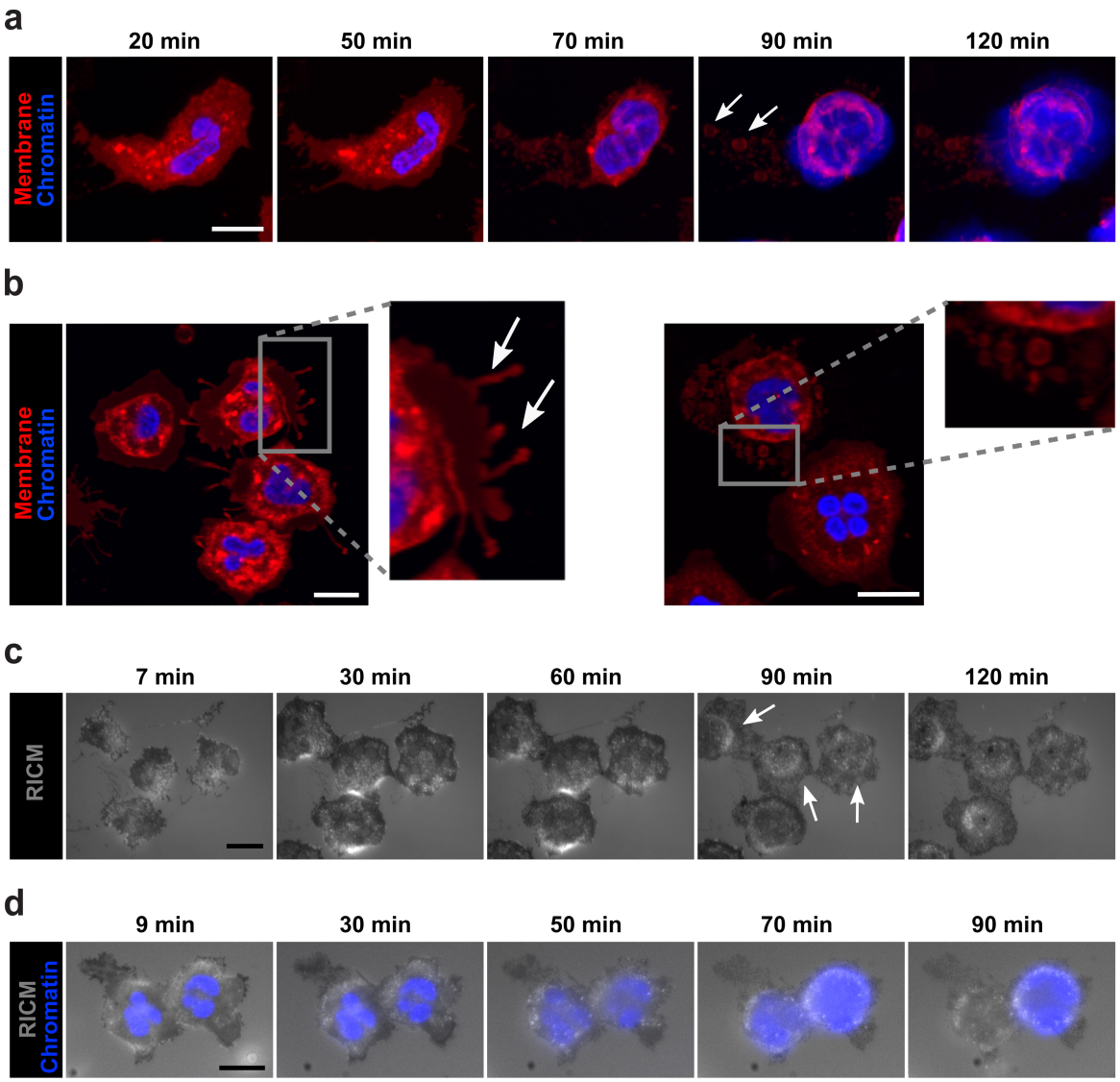

Supplementary fig. 4: Membrane rearrangement during NETosis. a, CLSM images of a human neutrophil undergoing NETosis (blue = Hoechst 33342/DNA, red = PKH26/membrane) observed by 3D-CLSM (see also **Supplementary movie 8**). The cell spreads initially but retracts its cell body leaving membrane behind. Vesicles are formed closely bound to the substrate, probably originating from excess membrane (arrows, t = 90 min). Scale = 10 µm. **b,** Characteristic behavior of the cell membrane during NET formation observed by time-lapse CLSM (blue = DNA, red = membrane). Cells form membrane extensions (arrows) in late P1 (left) and membrane vesicles at the surface during the cell rounding process in P2 (right). Scale = 10 µm. **c,** Representative images of human neutrophils undergoing PMA-induced NET formation recorded with real-time reflection interference contrast microscopy (RICM) on glass. Images allow the label-free analysis of the cell/surface contact area (black = cell closer to the surface, white = further away from the surface). During NETosis, the cells round up, leave membrane closely bound to the substrate behind (arrows, t = 90 min) and expel the NET (see also **Supplementary movie 9)**. Scale = 10 µm. **d,** Overlay of real-time RICM with immunofluorescence (blue = chromatin) to verify NET release (t = 70, 90 min) during time-lapse RICM imaging. Scale = 10 µm.

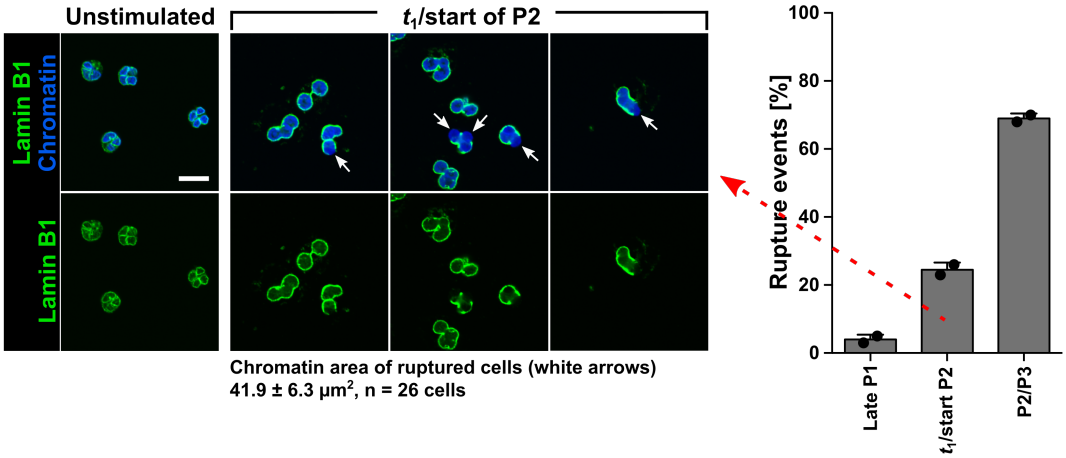

Supplementary fig. 5: Rupture of the nuclear envelope at beginning of P2. Overlay of chromatin (blue) and lamin B1 (green) of unstimulated and NETotic human neutrophil (CLSM, fixed samples). Average chromatin area at rupture point of the surrounding lamin B1 (t_1) is 41.9 ± 6.3 µm^2 (n = 26 cells from two donors) and in good agreement with the chromatin area at t_1 determined during live cell imaging (**Fig. 1a, b**). At this time point, the nuclear envelope rupture events increase (t_1/start P2) until a high rate of rupture events (small whole up to full loss of the Lamin B1 surrounding in P2 and P3). Calculation based on CLSM images of fixed samples. N = 2 donors (100 cells per condition and N). Mean ± SD. Scale = 10 µm.

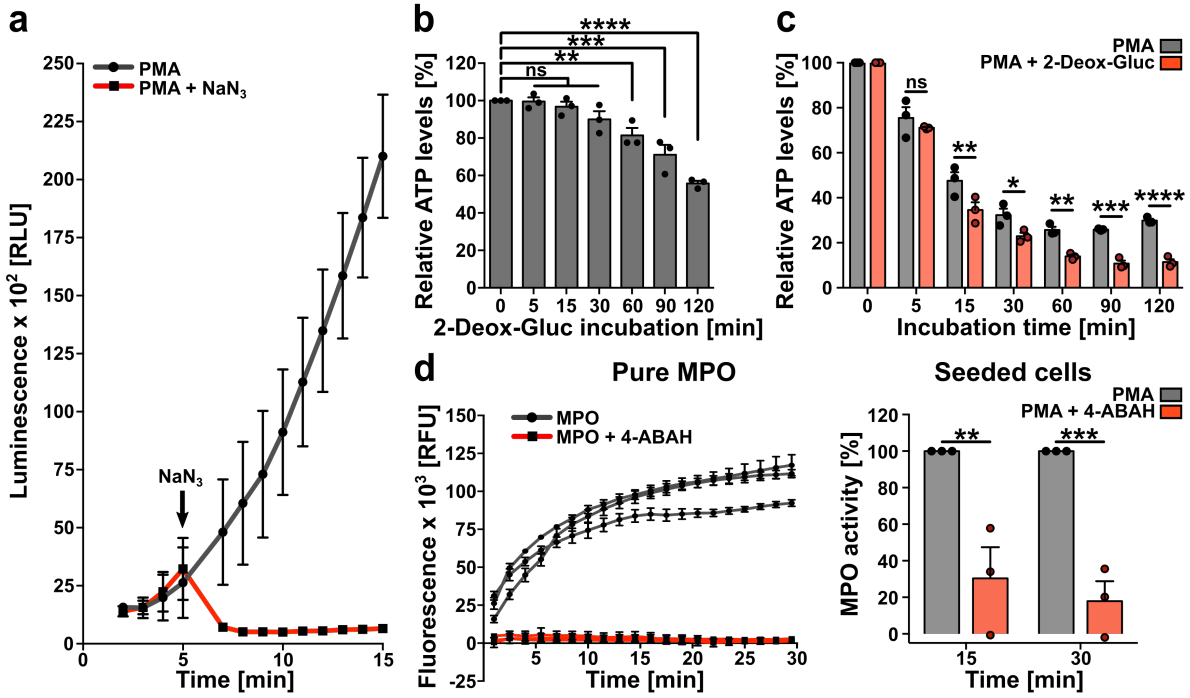

Supplementary fig. 6: Inhibitory effect of NaN_3. 2-Deox-Gluc and 4-ABAH on NETotic cells. **a,** Effect of 3 mM sodium azide (NaN_3) on PMA (100 nM)-induced ROS production of human neutrophils determined by chemiluminescence of luminol. NaN_3 inhibits ROS directly after addition and enables a stable inhibition for at least 30 min, as shown in **Supplementary fig. 9c**. Experimental setup comparable with the setup used for the experiments shown in **Fig. 3b**. N = 1 (triplicates). Mean ± SD. **b**, ATP levels of unstimulated neutrophils after incubation with 5 mM 2-Deoxy-glucose (2-Deox-Gluc) for different time intervals. 2-Deox-Gluc reduces ATP levels already after short incubation and significantly after more than 60 min compared to untreated cells (t = 0 min). Statistics: One-way ANOVA (Bonferroni's multiple comparison test, **p<0.01, ***p < 0.001, ****p < 0.0001). N = 3. Mean ± SEM. **c,** ATP levels of PMA (100 nM)-stimulated neutrophils with and without incubation with 5 mM 2-Deox-Gluc for different time periods. 2-Doxy-Gluc significantly decreases the ATP levels after more than 15 min PMA stimulation compared to exclusive PMA treatment (t = 0 min). PMA stimulation alone

decreases ATP levels by more than 70 %. Experimental setup comparable with the setup used in **Fig. 3b**. Statistics: Two-way ANOVA (Bonferroni's multiple comparisons test, *p < 0.05, **p<0.01, ***p < 0.001, ****p < 0.0001). N = 3. Mean ± SEM. **d,** inhibitory effect of 100 µM 4-aminobenzoic acid hydrazide (4-ABAH) on MPO activity. **left**, 4-ABAH inhibits purified MPO significantly and stable after 1 min for at least 30 min. N = 3. Mean ± SD. **right,** 4-ABAH inhibits PMA (100 nM)-induced MPO activity significantly and stable after 15 min and 30 min cell incubation followed by complete cell lysis for MPO activity measurements. Experimental setup comparable with the setup in **Fig. 3b**. Statistics: Two-way ANOVA (Bonferroni's multiple comparisons test, **p<0.01, ***p < 0.001). N = 3. Mean ± SEM.

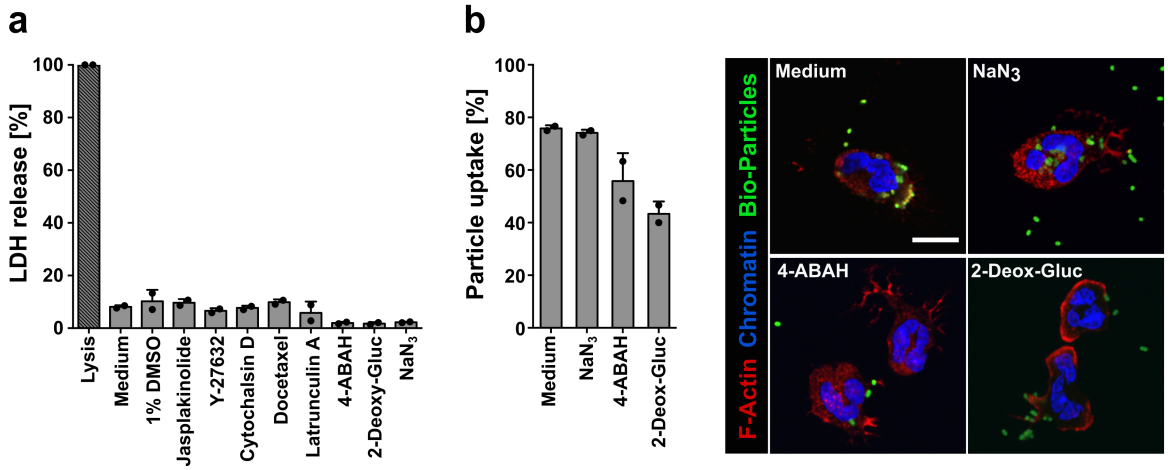

Supplementary fig. 7: Influence of metabolic and cytoskeletal inhibitors on neutrophil function. a, Toxicity of used inhibitors on human neutrophils detected by release of lactatdehydrogenase (LDH) relative to complete cell lysis. All inhibitors were tested for the concentrations used in this study and the maximal incubation time of 3h. All inhibitors show less than 10% cell toxicity, which is below the toxicity of 1% DMSO with 10.2% (maximal solvent concentration in inhibitor studies). N = 2. Mean ± SD. **b,** Effect of NaN_3 (3 mM), 4-ABAH (100 µM) and 2-Deox-Gluc (5 mM) on uptake of FITC-labeled E. coli BioParticles. The particle uptake is not affected by NaN_3, but clearly decreased in presence of 4-ABAH and 2-Deox-Gluc. Calculation based on confocal imaging of fixed samples after incubation with BioParticles for 30 min. Staining: red = F-actin/Phalloidin555, blue = chromatin/Hoechst, green = FITC-labeled E. coli BioParticles. Scale = 10 µm. N = 2 (n = 60 cells per condition and N). Mean ± SD.

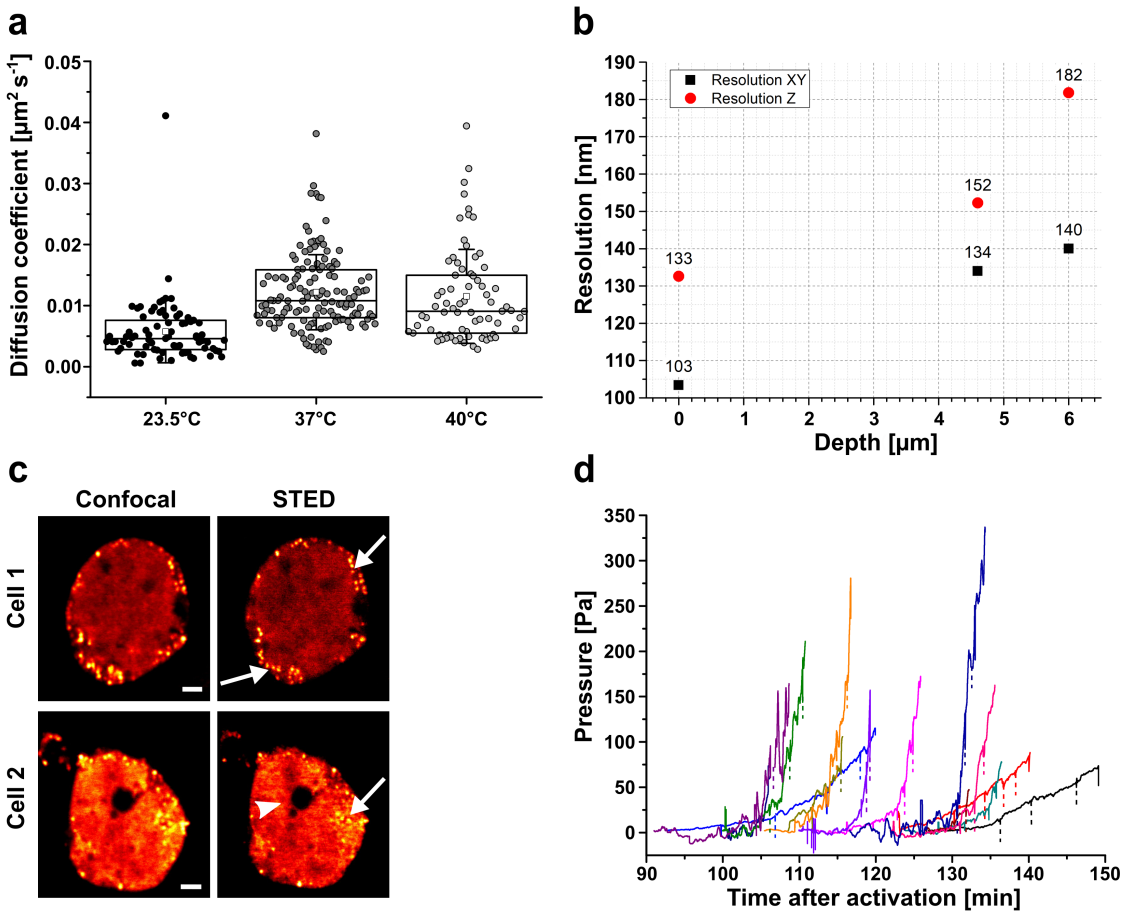

Supplementary fig. 8*:* Properties and consequences of chromatin swelling: a, Effective 2D diffusion coefficient of chromatin expansion in P2 (t_1 to t_D) at different temperatures (Median: 23.5°C = 0.0047 µm^2 s^{-1}, 37°C = 0.0108 µm^2 s^{-1}, 40°C = 0.0091 µm^2) calculated as described in **Supplementary fig. 3a**. N = 3 (23.5°C, 40°C). N = 5 (37°C). Boxplot displays the 25th and 75th percentile, with the horizontal line at the median, squares represent the mean and whiskers SD. **b,** Determination of STED-resolution by measuring the size of calibration beads on living neutrophils. The resolution depends clearly on the distance from the coverslip (depth). **c,** Confocal and STED images of living neutrophils during PMA-induced NET formation (z-direction: around 2-4 µm from the cover slip; cell middle). Chromatin staining: SiR-DNA. Arrow = chromatin dots, mostly appearing close to the surface. Arrowhead = chromatin free areas occurring during the swelling process. Scale = 2 µm. Sometimes in these images small regions of higher intensity (small dots) were observed. It could be chromatin filled vesicles. **d**, Pressure curves measured by tipless cantilever AFM experiments. By getting in contact with a PMA activated cell (at least 90 minutes after activation, 100 nM PMA), the cell starts to push on the cantilever resulting in a deflection of the cantilever. Dividing these forces by the cellular contact area, an internal pressure was estimated (see Methods) that likewise increases until the membrane ruptures (end of the traces). Dashed lines are indicating the time points when the deflection values were reset manually to avoid signal loss of the AFM detector. N = 5 donors (n = 14 cells).

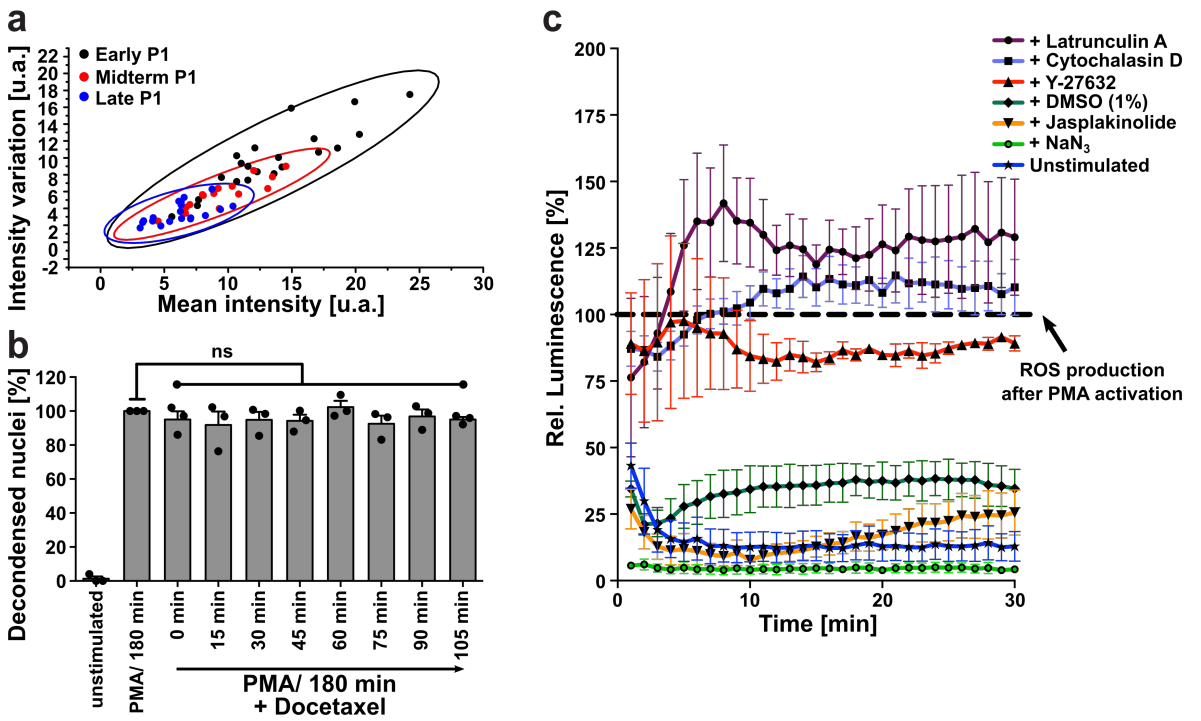

Supplementary fig. 9: Influence of the cytoskeleton: **a,** Quantification of F-Actin disassembly. The mean fluorescence intensity of F-actin decreases with time during NETosis. At the same time the heterogeneity decreases, which is a measure for F-actin structure and not biased by bleaching. Thus, F-actin gets disassembled during NETosis. N = 1 donor, data fitted with 95% confidence ellipse. **b,** NET formation after treatment with Docetaxel (100 nM, inhibition of tubulin depolymerization) at different time points after induction of NETosis with PMA. Docetaxel shows no influence on NET formation (measured as %-relative number decondensed nuclei after 180 min compared to exclusive activation with PMA). n = 3. Mean ± SEM. ns = not significant. Statistics: One-way ANOVA (Bonferroni's multiple comparison test) **c,** Influence of actin cytoskeletal inhibition on PMA (100 nM)-induced ROS production of human neutrophils determined by the chemiluminescence of luminol. Latrunculin A (violet) increases ROS, while Cytochalasin D (violet) and Y-27632 (red) have no or only slight effects on ROS production in the concentrations used for the experiments shown in **Fig. 5b, c**. In contrast, Jasplakinolde (yellow) shows a strong inhibitory effect. As controls, the ROS levels of unstimulated cells (blue), cells after addition of 1% DMSO (dark green, used for Jasplakinolide experiments) and NaN_3 (green) are shown. N = 3. Mean ± SEM.

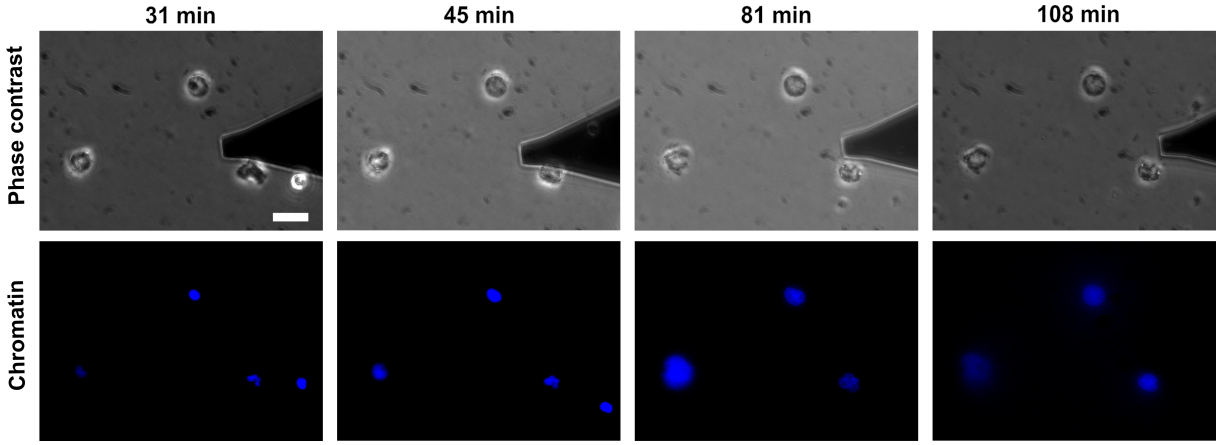

Supplementary fig. 10: Morphology of neutrophils during AFM. Phase contrast and chromatin (blue) images of activated neutrophils during life cell AFM experiments. Within the early stage of NETosis, lobular shape of the nucleus and cell rounding can be observed. After around 40 minutes, DNA decondenses und the cells rupture around t = 80-110 min. No morphological difference between cells probed by AFM and control cells can be observed. Scale = 20 µm.

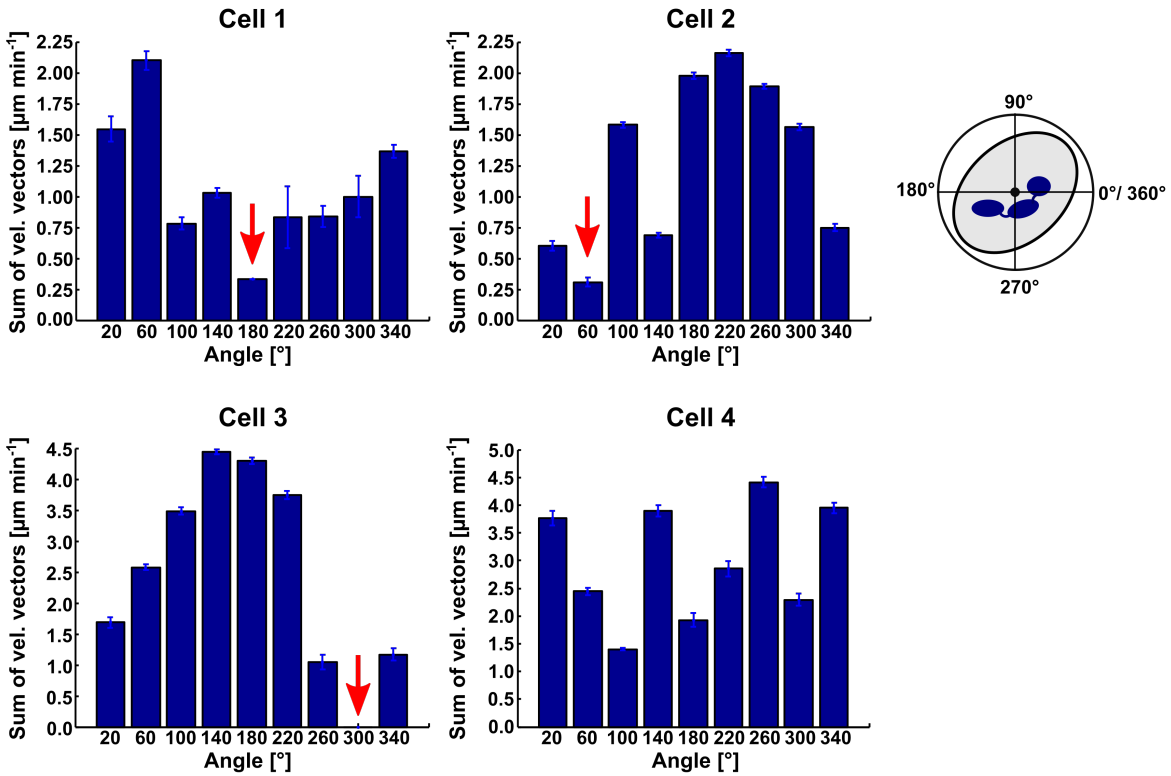

Supplementary fig. 11: **Chromatin swelling directs location of membrane rupture.** Chromatin swelling analysis (data of the cells shown in **Fig. 6a)**. To analyze whether the position of the rupture point correlates with the chromatin swelling behavior, the average swelling velocity and direction was calculated and visualized in a velocity plot (see also Methods). These velocity vectors were sorted (binning angle = 40°) and added up to find regions of different swelling behaviors. Regions of low velocities (red arrow, green circle in **Fig. 6a**) are often in close proximity to the observed rupture point position (red circle in **Fig. 6a**, cell 1-3), whereas no correlation is detectable for uniform swelling processes (cell 4). In this case, the nucleus is centered in the cell. Bar plot show the sum of all velocity vectors within one bin (vector length of all summed up velocity vectors). Error bars display SEM of the aforementioned vectors.

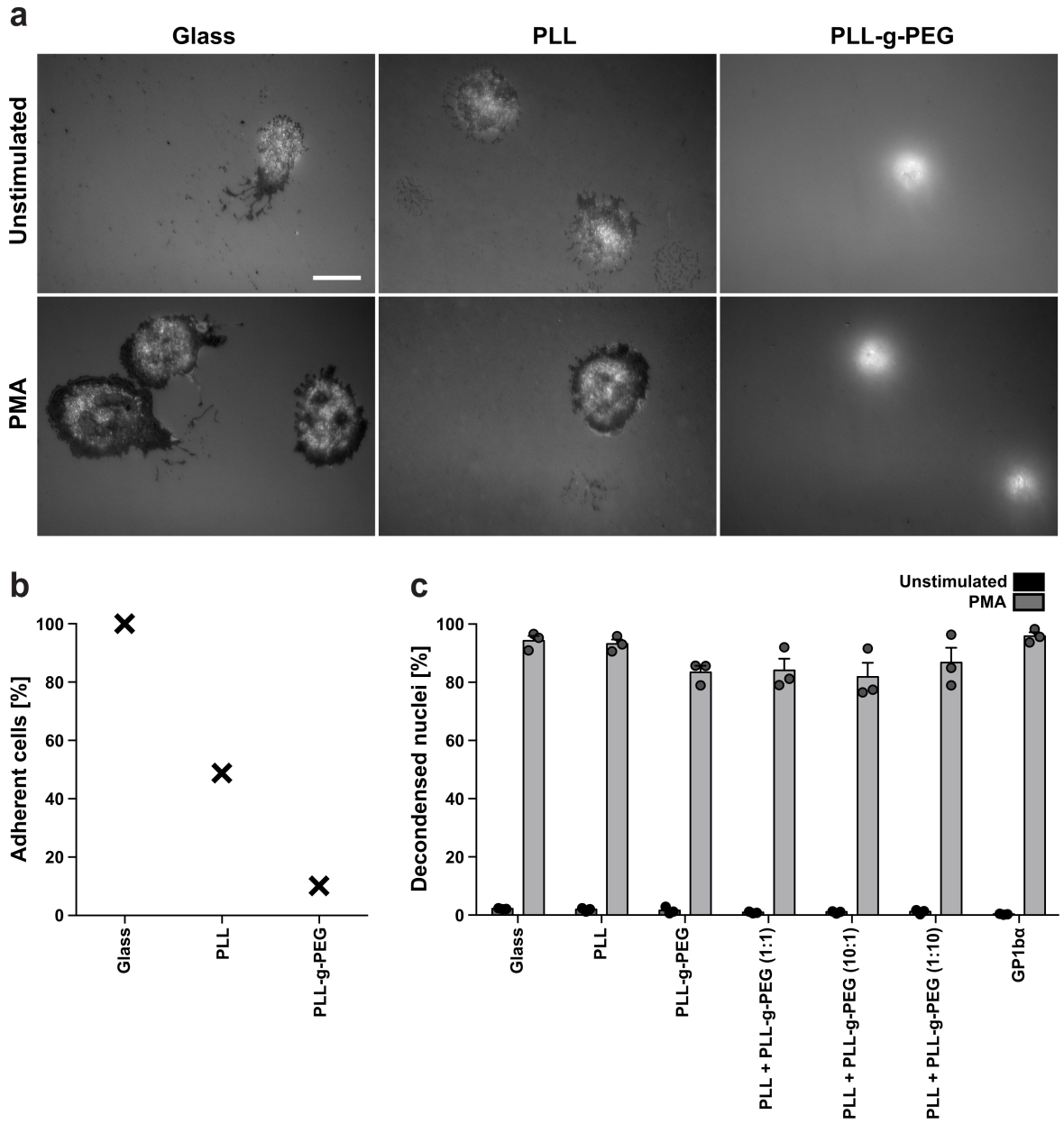

Supplementary fig. 12: PMA-induced NETosis is independent of adhesion. a, RICM images of fixed neutrophils on glass after one-time washing. Images show cells incubated with PMA for 30 min or cells left unstimulated. Cells on PLL-g-PEG (Poly-L-Lysine-grafted-Poly(ethylene glycol)) coated surfaces are barely adherent compared to neutrophils on glass or PLL coating. Scale = 10 µm. **b,** Cell numbers after one-time washing of cells seeded for 30 min on different surfaces. In PLL-g-PEG coated wells only a few cells remain, compared to glass and PLL coating. These cells are still barely adherent as shown in **a**. N = 1. **c,** PMA-induced NETosis (100 nM) performed on different surfaces. The amount of decondensed nuclei is independent of the surface/adhesive properties (surfaces of different passivation level, GPIbα is the ligand of Mac-1 integrin). No washing step was included in this procedure. N = 3. Mean ± SEM.

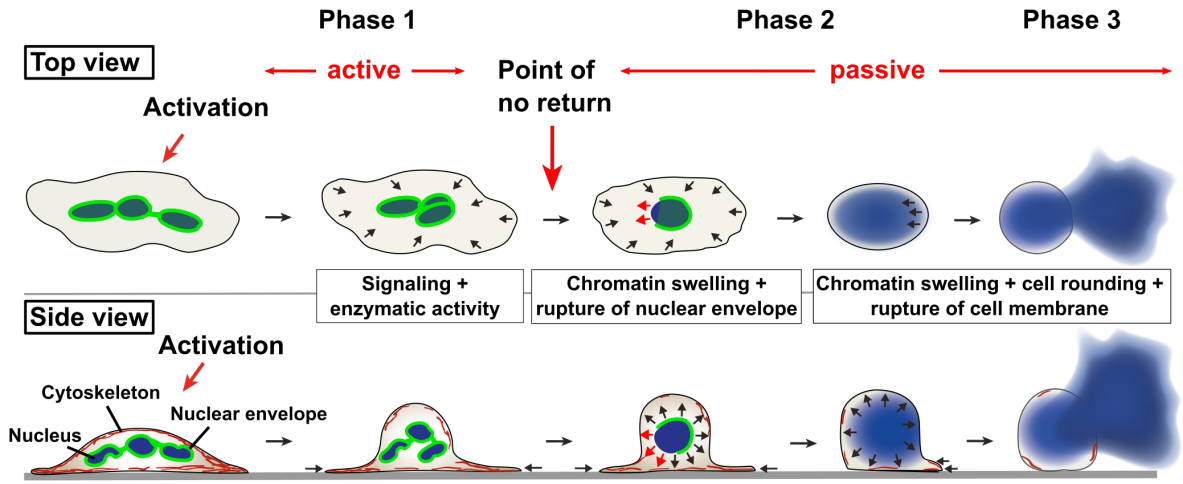

Supplementary fig. 13: Detailed biophysical model of NET formation.

Supplementary Methods

Surface coating

For platelet glycoprotein 1b alpha chain (GP1bα) coating, 96-glassbottom-well-plates were incubated over night with 5 µg ml^{-1} GP1bα (R&G Systems) at 4°C. Then, the wells were washed with 1x PBS followed by blocking with 3% BSA (Roth) for 2 h at 37°C and an additionally washing step.

For Poly-L-lysine hydrobromide (PLL, Sigma-Aldrich) and poly(L-lysine)-graft-poly(ethylene glycol) (PLL-g-PEG, SuSoS AG) coating, 96-glassbottom-well-plates were incubated either with 0.5 mg mL^{-1} PLL in 10 nM HEPES or 0.5 mg mL^{-1} PLL-g-PEG in 10 nM HEPES at room temperature for 45 min. Then solutions were removed and washed one time with culture medium. Further cell experiments were carried out as described below.

Adhesion experiments

Fresh isolated human neutrophils (10 000 per well) were seeded in 96-glassbottom-well-plates directly or wells coated with GP1bα, PLL and/or PLL-g-PEG (0:1, 1:10, 1:1, 10:1, 1:0) as described above. Then, cells were activated for NETosis with PMA in a final concentration of 100 nM for 3h (37 °C, 5% CO_2). All experiments were performed in triplicates. To end NET formation, cells were fixed with 2% PFA final concentration and stored over night at 4°C. The fixed probes were stained with 1.62 µM Hoechst 33342 and the percentage of decondensed nuclei/NETs was analyzed as described in the section Inhibitor Experiments in Methods.

To analyze the adhesion on the different surfaces, 10 000 neutrophils per well were seeded in 96-glassbottom well-plates coated with PLL or PLL-g-PEG or left untreated. The cells were washed one time with 1xPBS after 30 min incubation (37 °C, 5% CO_2) with or without PMA (100 nM). Then, cells were fixed with 2% PFA final concentration. Subsequently, the cells were stained with Hoechst and the amount of remaining cells calculated relatively to the glass sample using ImageJ (six images/well counted in defined regions, counting blinded). Representative RICM images of the fixed samples were recorded in the setup described in the section Reflection Interference Contrast Microscopy (RICM) in Methods.

For time-lapse observations, 4 x 10^5 cell per ml were seeded in an ibidi treat flow chamber coated with PLL-g-PEG and the movie recorded as described in the section Live Cell Imaging" in Methods.

Reflection Interference Contrast Microscopy (RICM)

For RICM, ibidi treated petri dishes (Ibidi GmbH) with a 35 mm radius glass bottom (81158, ibidi) or ibidi treat flow chambers uncoated or coated with PLL were used. 100 000 neutrophils per petri dish or 4 x 10^5 cells per ml per flow chamber were seeded and stained with Hoechst. The microscope setup contained a heating chamber (ibidi heating system, ibidi GmbH) on top of the microscope stage (Axiovert 200, Zeiss) and the temperature was adjusted to 37 C° for all experiments. NETosis was induced by 100 nM PMA. Time-lapse movies were recorded (1 frame per min) 63x magnified (EC Plan-Neofluar Ph3 objective/420481-9911-000, 1.6x Optovar, Zeiss) for both DAPI as well as RICM images. Samples were illuminated by a XCite Series 120Q or HBO 100 (1007-980, Zeiss) lamp together with a respective DAPI (Filter set 02 shift free/488002-9901-000, Zeiss) or RICM filter set (reflector module Pol ACR P&Cfor HBO 100/424924-9901-000, emission filter 416 LP, AHF-Nr.: F76-416/000000-1370-927, Zeiss) and observed with a Zyla SCMOS camera (AndorZyla 5.5) using Micro Manager software (v.1.4) or a CoolSNAP ES camera (Photometrics) using the software Metamorph 6.3r2. (Molecular Devices Inc.). Subsequently, the image contrast was adjusted with ImageJ.

ATP measurements/ 2-Deox-Gluc

Fresh isolated human neutrophils (10 000 per well in RPMI (10 mM HEPES, 0.5% HSA, without phenolred) were seeded in white 96-well-plates and metabolic activity inhibited by adding 5 mM 2-Deox-Gluc for defined time periods at 37°C (5 min, 15 min, 30 min, 60 min, 90 min and 120 min). Simultaneously, cells were activated with PMA in a final concentration of 100 nM or left untreated. After incubation the ATP amount was measured as described in the section ATP measurements in Methods. All experiments were carried out in triplicates and ATP levels were calculated relatively to the ATP amount of unstimulated cells incubated for 120 min without addition of 2-Deox-Gluc.

MPO activity

The activity of MPO was measured with the myeloperoxidase chlorination fluorometric assay kit from Cayman chemical following the company's instructions. To prove the inhibitory effect of 100 µM 4-ABAH on MPO, two different setups were used. First, the effect on purified MPO supplied by the company was studied in presents or absents of 4-ABAH. The activity of MPO was determined by the formation of fluorescein (Thermo Scientific APPLISKAN®, Software: Skanlt RE for Appliskan 2.3, Thermo Fisher Scientific) at 485 nm/535 nm over 29.5 min (frame rate: 1.5 min) at room temperature. All experiments were performed in triplicates. Second, human neutrophils (1 000 000 per well in RPMI (10 mM HEPES, 0.5% HSA)) were seeded in 24-well plates and activated with 100 nM PMA in the presents or absents of 4-ABAH for 15 min or 30 min at 37°C, respectively. After incubation,

the culture medium was removed and cells were washed with 1x PBS. Then, the cells were scraped from the plate and pelleted by 1000 g for 10 min at 4°C. Cell lysis was induced by ultra shall sonication in combination with freeze-thraw cycles. After lysis, cell remnants were removed by centrifugation at 10 000 g for 10 min at 4°C and MPO activity in the supernatant was determined as described above. For all conditions the change in fluorescence signal between 1 min and 29.5 min was determined and the relative MPO activity was calculated between 4-ABAH treated and untreated cells.

Reactive oxygen species (ROS) measurement

Fresh isolated human neutrophils (10 000 per well in HBSS (10 mM HEPES, without phenolred) were seeded in white 96-well-plates (Greiner bio-one) at 37°C. After seeding, luminol (Sigma-Aldrich) was added at a final concentration of 60 µM and actin cytoskeletal components were inhibited by Cytochalasin D (100 nM), Latrunculin A (1 µM), Jasplakinolide (10 µM) or Y-27632 (19.2 µM) respectively. Directly after addition of inhibitors, NETosis was activated with 100 nM PMA and the luminescence was measured (GLOMAX® 96 Microplate Luminometer, Software: GLOMAX 1.9.3, Turner BioSystems) at room temperature (frame rate: 1 min). As controls the change in luminescence signal was recorded for unstimulated cells, cells treated with the maximal solvent concentration of 1% DMSO (used in Japlakinolide studies) and cells which were inhibited with 3 mM NaN_3. All experiments were carried out in triplicates and the luminescence signal was determined relatively to ROS levels after exclusive PMA activation.

For evaluation of NaN_3 activity, cells were seeded (90 000 per well) and activated as described above. NaN_3 (3 mM) was added 5 min after activation with PMA and the change in the luminescence signal was continuously recorded.

Cell toxicity

Cell toxicity of cytoskeletal and metabolic inhibitors was measured by the release of lactatdehydrogenase (LDH) with the CytoTox 96® Non Radioactive Cytotoxicity Assay (Promega) as instructed by the company. By analogy with the assays described in the section Inhibitor Experiments in Methods, 10 000 cells were seeded in plastic 96-well plates (Greiner bio-one) and incubated in RPMI (10 mM HEPES, 0.5% HSA, without phenolred) with Cytochalasin D (100 nM), Latrunculin A (1 µM), Docetaxel (100 nM), Jasplakinolide (10 µM), Y-27632 (19.2 µM), 2-Deox-Gluc (5 mM), NaN_3 (3 mM), 4-ABAH (100 µM), DMSO (1%) or only culture medium for 3 hours at 37°C. The released LDH was measured in the supernatant as described in the assay protocol and cell toxicity was calculated relatively to maximal cell lysis.

Uptake of particles

Fresh isolated human neutrophils (100 000 per well in RPMI (10 mM HEPES, 0.5% HSA) were seeded on pretreated (99% alcohol) glass cover slips (#1.5) in 24-well plates followed by pre-incubation for 30 min with or without 2-Deox-Gluc (5 mM), NaN_3 (3 mM) or 4-ABAH (100 µM), respectively. Then, cells were further incubated with fluorescein-labeled Escherichia

coli (K-12 strain) BioParticles® (0.1 mg ml^{-1}, Vybrant™Phagocytosis Assay Kit (V-6694), Thermo Fisher Scientific) in presents of 2-Deox-Gluc (5 mM), NaN_3 (3 mM) or 4-ABAH (100 µM) and incubated for additionally 30 min. For fixation, 2% PFA final concentration was added and samples then stored after washing with 1x PBS. Cells were stained as described in the section Staining Procedure in Methods for F-actin and chromatin with Phalloidin (PromoFlpur-555P, PromoKine) and Hoechst directly after blocking. For each condition the particle uptake was analyzed manually by 3D confocal laser scanning microscopy (60x magnified, Olympus IX83 inverted microscope, software: Olympus Fluoview v.4.2) and the percentage of particle uptake calculated relatively to the total cell count of 60 cells per condition.

Quantification of fluorescence imaging

For the quantification of Lamin B1 rupture, the rupture of the nuclear envelope was determined for different time points after induction of NETosis with PMA. Therefore, cells were stained for Lamin B1 and Chromatin as described in the section Staining Procedure in Methods and the nuclear envelope rupture was analyzed manually by 3D confocal laser scanning microscopy (60x magnified, Olympus IX83 inverted microscope, software: Olympus Fluoview v.4.2). For each condition the loss of the nuclear envelope (small rupture up to complete loss) was determined for 100 cells and calculated relatively to the total cell count.

Similarly, to quantify the loss of actin within phase 1, CLSM images of stained F-actin areas of fixed cells (exemplarily shown in **Fig. 5a**) where analyzed using the ImageJ thresholding plugin. More precisely, within all pictures, the F-actin area of individual cells were segmented first (Yen thresholding method) and the intensity values of the enclosed actin area was averaged to obtain both, a mean intensity value as well as a number for the intensity variation within the respective area (standard deviation). Both values were plotted to visualize the correlation between the amount and the homogeneity of actin within P1 and a 95% confidence ellipse was drawn.

2.3 Manuscript II

"Serum and Serum Albumin Inhibit *in vitro* Formation of Neutrophil Extracellular Traps (NETs)"

Elsa Neubert[1,2], Susanne N. Senger-Sander[1], Veit S. Manzke[1], Julia Busse[1], Elena Polo[2], Sophie E.F. Scheidmann[1], Michael P. Schön[1,3], Sebastian Kruss[2] and Luise Erpenbeck[1]

These authors contributed equally: Elsa Neubert and Susanne N. Senger-Sander.

[1]Department of Dermatology, Venereology and Allergology, University Medical Center Göttingen, Göttingen, Germany
[2]Institute of Physical Chemistry, University of Göttingen, Göttingen, Germany
[3]Lower Saxony Institute of Occupational Dermatology, University Medical Center Göttingen and University of Osnabrück, Göttingen, Germany

The following paragraph was published in *Frontiers in Immunology*.
DOI: 10.3389/fimmu.2019.00012

Supplementary tables including full lists of supplementary references are available online.
Full link: https://www.frontiersin.org/articles/10.3389/fimmu.2019.00012/full

Received: 22 September 2018
Accepted: 04 January 2019
Published online: 24 January 2019

frontiers in Immunology

ORIGINAL RESEARCH
published: 24 January 2019
doi: 10.3389/fimmu.2019.00012

Serum and Serum Albumin Inhibit *in vitro* Formation of Neutrophil Extracellular Traps (NETs)

Elsa Neubert[1,2†], *Susanne N. Senger-Sander*[1†], *Veit S. Manzke*[1], *Julia Busse*[1], *Elena Polo*[2], *Sophie E. F. Scheidmann*[1], *Michael P. Schön*[1,3], *Sebastian Kruss*[2‡] *and Luise Erpenbeck*[1*‡]

[1] *Department of Dermatology, Venereology and Allergology, University Medical Center Göttingen, Göttingen, Germany,* [2] *Institute of Physical Chemistry, University of Göttingen, Göttingen, Germany,* [3] *Lower Saxony Institute of Occupational Dermatology, University Medical Center Göttingen and University of Osnabrück, Göttingen, Germany*

OPEN ACCESS

Edited by:
Janos G. Filep,
Université de Montréal, Canada

Reviewed by:
Mohib Uddin,
AstraZeneca, Sweden
Luis Enrique Munoz,
Friedrich-Alexander-Universität Erlangen-Nürnberg, Germany

***Correspondence:**
Luise Erpenbeck
luise.erpenbeck@med.uni-goettingen.de

†*These authors have contributed equally to this work*

‡*Sebastian Kruss*
orcid.org/0000-0003-0638-9822
Luise Erpenbeck
orcid.org/0000-0002-6561-472X

Specialty section:
This article was submitted to Molecular Innate Immunity, a section of the journal Frontiers in Immunology

Received: *22 September 2018*
Accepted: *04 January 2019*
Published: *24 January 2019*

Citation:
Neubert E, Senger-Sander SN, Manzke VS, Busse J, Polo E, Scheidmann SEF, Schön MP, Kruss S and Erpenbeck L (2019) Serum and Serum Albumin Inhibit in vitro Formation of Neutrophil Extracellular Traps (NETs). Front. Immunol. 10:12. doi: 10.3389/fimmu.2019.00012

The formation of neutrophil extracellular traps (NETs) is an immune defense mechanism of neutrophilic granulocytes. Moreover, it is also involved in the pathogenesis of autoimmune, inflammatory, and neoplastic diseases. For that reason, the process of NET formation (NETosis) is subject of intense ongoing research. *In vitro* approaches to quantify NET formation are commonly used and involve neutrophil stimulation with various activators such as phorbol 12-myristate 13-acetate (PMA), lipopolysaccharides (LPS), or calcium ionophores (CaI). However, the experimental conditions of these experiments, particularly the media and media supplements employed by different research groups, vary considerably, rendering comparisons of results difficult. Here, we present the first standardized investigation of the influence of different media supplements on NET formation *in vitro.* The addition of heat-inactivated (hi) fetal calf serum (FCS), 0.5% human serum albumin (HSA), or 0.5% bovine serum albumin (BSA) efficiently prevented NET formation of human neutrophils following stimulation with LPS and CaI, but not after stimulation with PMA. Thus, serum components such as HSA, BSA and hiFCS (at concentrations typically found in the literature) inhibit NET formation to different degrees, depending on the NETosis inducer used. In contrast, in murine neutrophils, NETosis was inhibited by FCS and BSA, regardless of the inducer employed. This shows that mouse and human neutrophils have different susceptibilities toward the inhibition of NETosis by albumin or serum components. Furthermore, we provide experimental evidence that albumin inhibits NETosis by scavenging activators such as LPS. We also put our results into the context of media supplements most commonly used in NET research. In experiments with human neutrophils, either FCS (0.5–10%), heat-inactivated (hiFCS, 0.1–10%) or human serum albumin (HSA, 0.05–2%) was commonly added to the medium. For murine neutrophils, serum-free medium was used in most cases for stimulation with LPS and CaI, reflecting the different sensitivities of human and murine neutrophils to media supplements. Thus, the choice of media supplements greatly determines the outcome of experiments on NET-formation, which must be taken into account in NETosis research.

Keywords: neutrophils, neutrophil extracelluar traps, experimental conditions, NET, media, *in vitro* experiments, NETosis

INTRODUCTION

The discovery of neutrophil extracellular traps (NETs) in 2004 (1) marked the beginning of an impressive scientific career of these extracellular DNA meshworks. NETs are expelled by neutrophilic granulocytes under certain (patho) physiological conditions. Different signaling pathways and forms of NET formation have been described in the last years (2, 3). In most studied scenarios, the cells release the NET consisting of decondensed chromatin, decorated with antimicrobial peptides and, most likely, a plethora of cytokines and other proteins. This release occurs after the rupture of the cell membrane into the extracellular space, ultimately leaving the neutrophil to die. This pathway has been called "NETosis" or "suicidal NETosis" (4), in analogy to previously known cell death pathways such as apoptosis and necrosis. In contrast, some publications have also described a faster, different form of NET formation mainly in response to bacteria which leaves the neutrophil alive and functional ("vital NETosis" or "vital NET formation") (5). It remains a matter of debate whether these phenotypes are truly distinct biological processes.

While originally described as a novel immune defense mechanism to trap and kill pathogens like bacterial, fungi and even viruses, it has become increasingly clear that the role of NETs goes far beyond these initial discoveries. Indeed, excessive NET production or a dysregulation of NET clearance have been negatively implicated in an ever growing number of diseases, many of them associated with considerable morbidity and socioeconomic impact such as chronic inflammatory diseases like rheumatoid arthritis (6), systemic lupus erythematosus (7), chronic obstructive pulmonary disease (COPD) (8, 9) and psoriasis (10, 11), ischemia-reperfusion injury after myocardial infarction (12), thrombosis (13), impaired wound healing (14), preeclampsia (15), and cancer (16, 17). Therefore, it is not surprising that publications involving NETs have increased exponentially within the last couple of years and reliable methods to study NET formation are highly desired.

Initially, reports of NETs as contributors to different diseases relied mainly on the *ex vivo* detection of NETs and NET-related proteins by immunofluorescence and immunohistochemistry protocols in affected tissues. More recently, real-time observations of NETs forming *in vivo*, published in several very sophisticated mouse models, has led to great advances of our understanding of NETs and their role in different diseases. Similarly, flow cytometry-based protocols as a means for detecting NETs in blood from mice or humans have facilitated the screening for NET production in full blood under different pathological conditions (18, 19).

Nevertheless, *in vivo* models possess a high level of complexity, which does not allow the assessment of inhibitors and activators of NETosis in a high-throughput fashion and in a well-defined setting. Additionally, observing NETosis on a single-cell level remains very challenging in any *in vivo* setting. For example, testing the isolated influence of different stimuli such as bacterial proteins or inhibitors of certain neutrophilic enzymes on NETosis is hardly feasible *in vivo*; more so, if one aims to determine at which time-point of NETosis these activators or inhibitors play a role (20). Finally, *in vivo* studies (apart from the *ex vivo* assessment of existing NETs in peripheral blood by flow cytometry) are strictly limited to animal models. Currently it is not possible to determine whether neutrophils from patients with certain diseases show a greater propensity for NETosis unless one isolates neutrophils from these patients and stimulates them *ex vivo*. For these reasons, NET research heavily relies on the isolation of fresh neutrophils from donors and their *ex vivo* stimulation. Indeed, as of today, the isolation of neutrophils from patients, healthy donors, or animals followed by an *ex vivo* stimulation of these cells to assess and quantify NET formation is what may be called the gold standard of NET-experiments.

Considering the importance of this method for the whole field of neutrophil biology and the ever-growing number of laboratories performing NET studies, it is alarming to note that experimental conditions under which NETosis experiments are performed vary fundamentally from lab to lab, sometimes from publication to publication in the same group and occasionally even from assay to assay, rendering any comparison of research results nearly impossible. Looney at al. showed early on that the production of NETs by mice depend strongly on exterior influences on the mice. This group was one of the first to perform systematic NETosis experiments, in the context of transfusion-related acute lung injury (TRALI) (21, 22). Relocation of the mouse colony to a housing facility with a stronger barrier and less exposure of the mice to pathogens led to the inability of the group to repeat their own experiments—presumably, neutrophils from the new group of mice were not sufficiently pre-stimulated anymore. Only after exposure of the mice to low amounts of LPS prior to the experiments was the group able to recapitulate their previous results. This very instructive example shows how vulnerable NETosis is to external influences. One would expect neutrophils to be similarly or even more susceptible to variations of experimental conditions. Neutrophils are sensitive to subtle changes in the density and type of surface receptors (23), ranging from different methods of neutrophils isolation (24), type of activator used for the *ex vivo* stimulation of neutrophils [for a comprehensive review on activators of NETosis see also (25)] and kind of culture medium used to incubate neutrophils during NETosis. In human experiments, supplements added to culture media typically vary from no supplement to heat inactivated FCS (0.05 to 10% or 0.1 to 10%) and human serum albumin (HSA; 0.05 to 2 %), yet other supplements such as (heat inactivated) human plasma, (heat inactivated) human serum, and BSA can also be found at variable concentration (**Supplementary Table 1**, **Figure 5**). For murine neutrophils, the most frequently used supplements are FCS and BSA, though some activators of NETosis such as CaI and LPS are largely being studied in serum-free medium. These differences may greatly influence the outcome of NET-experiments, as albumin may bind proteins like lipopolysaccharides (LPS) (26, 27). Furthermore, an effect of supplements on *in vitro* NET formation has been considered from several groups. For instance, an inhibition of NET-formation was seen at very high FCS concentrations under Phorbol-12-myristate-13-acetate (PMA) in a dose-dependent way (4). Another group observed more cells involved in

NET formation in serum-free medium after stimulation with nanoparticles (28), while others reported decreased NET-rates in HSA-containing media and pointed out, that a harmonization of culture conditions is still pending (4, 28, 29). Furthermore, it has been shown that serum-free culture conditions may allow a certain degree of spontaneous NET formation (30). Here, we selected the most commonly used supplements and analyzed the effect of their addition or omission on (suicidal) NETosis in a standardized setup. Additionally, we systematically compared media supplements for *in vitro* NETosis experiments in use in the literature.

MATERIALS AND METHODS

Isolation of Human Neutrophils

Human neutrophils were isolated from venous blood of healthy donors. For all human studies, a pool of 15 healthy donors was available. For all experiments with human neutrophils, blood from at least 3 different donors from this pool was collected to isolate neutrophils. This study was carried out in accordance with the recommendations and with the approval of the Medical Ethics Committee of the University Medical Center Göttingen (UMG), protocol number 29/1/17 with written informed consent from all subjects and in accordance with the Declaration of Helsinki.

The isolation was performed under sterile conditions based on previously published protocols (31) using gradient centrifugation. In brief, fresh blood of healthy donors was collected in S-Monovettes EDTA (7.5 ml, Sarstedt) and immediately layered in a ratio of 1 to 1 on top of Histopaque 1119 (Sigma Aldrich). After centrifugation and washing with HBSS (without Ca^{2+}/Mg^{2+}) (Lonza) cells were separated a second time on a gradient consisting of 65, 70, 75, 80, and 85% of 10:1 diluted Percoll (GE Healthcare). Then, cells were washed and resuspended in 1 ml HBSS without Ca^{2+}/Mg^{2+}. Cellular identity and a purity of the isolated cells of >95% was confirmed by cytospin (Cytospin 2 Zentrifuge, Shanson) followed by Diff Quick staining (Medion Diagnostics).

Isolation of Mouse Neutrophils

Mouse neutrophils were isolated from 6 to 10-week-old wild type C57BL/6J mice (male and female mice, equally distributed between groups). The blood was collected from the retroorbital venous plexus under full anesthesia with isoflurane and collected into the 15 mM EDTA (Gibco) containing BSA/PBS-solution. The isolation was performed according to previously published standard protocols (32, 33). After centrifugation, the cells were layered on top of a 10:1-diluted percoll gradient consisting of 78, 69, and 52% layers in PBS. Afterwards, erythrocytes were lysed with deionized water followed by a washing-step. Then, cells were resuspended in HBSS and cellular identity as well as purity >95% were confirmed as described above.

Stimulation Assay

Freshly isolated human or murine neutrophils were counted and suspended in RPMI 1640 (Lonza) containing 10 mM HEPES (Roth) (RPMI/HEPES) and 0.5% HSA (Sigma-Aldrich), 0.5%/1%/2% FCS (Biochrom GmbH, Merck Millipore) or 0.5% BSA (Roth), respectively. FCS was heat inactivated at 56°C (Thermostat plus, Eppendorf, Hamburg) for 30 min before use. 10,000 cells per well were seeded in 96-glassbottom-well-plates (*in vitro* scientific) for 30 min (37°C, 5% CO_2) and stimulated to undergo NET formation with either LPS from *Pseudomonas aeruginosa* (Sigma-Aldrich) at 10, 25, or 100 μg/ml, CaI (Sigma-Aldrich) at 4 μM, or PMA (Sigma-Aldrich) at 100 nM. After an incubation time of 3 h, cells were fixed with 2% PFA (Roth) to end NET formation and stored over night at 4°C. The fixed samples were washed with PBS (Sigma-Aldrich) and stained with 1.62 μM Hoechst (Sigma-Aldrich) for 15 min at room temperature. After staining, cells were washed and imaged by fluorescence microscopy (Axiovert 200, Zeiss; software: Metamorph 6.3r2., Molecular Devices) with the camera CoolSNAP ES (Photometrics). For each well, in total 5–6 images of clearly defined regions were obtained blinded in an automated fashion. For all experiments, the number of decondensed nuclei and the total cell counts were assessed using ImageJ (https://imagej.nih.gov/ij/download.html) and the percentage of decondensed nuclei/ NETs calculated by Excel (version: 14.3.0; Microsoft corporation).

Immunofluorescence Staining

Human neutrophils were isolated, seeded (200,000/well) in 24-well plates on glass coverslips and activated to undergo NET formation as described above. After fixation with 2 % PFA (Roth) over night, cells were permeabilized 0.1 % TritonX (Merck) and incubated with 5 % FCS (Biochrom) to block unspecific antibody binding. Subsequently, cells were stained using monoclonal anti-human MPO (IgG, mouse) as primary antibody (Abcam, ab25989, 1:500) and polyclonal anti-mouse Alexa 555 (IgG, goat) as secondary antibody (Life technologies, A21422, 1:2000). Neutrophil DNA was stained with 1.62 μM Hoechst (Sigma-Aldrich) as described above. After the staining procedure, cells were stored protected from light at 4°C. Representative confocal fluorescence images were obtained with the olympus IX83 inverted microscope (software: Olympus Fluoview Ver.4.2, Olympus) and recorded 60x magnified (UPlanSApo 1.35 oil, Olympus). All pictures were recorded at equal exposure times for MPO to ensure comparability.

Neutrophil Elastase NET Assays

1×10^6 human neutrophils in RMPI/HEPES with or without 0.5% HSA were seeded in 24-well-plates and stimulated with LPS from *Pseudomonas aeruginosa* (100 μg/ml), CaI (4 μM) or PMA (100 nM) for 2–3 h at 37°C. Measurement of neutrophil elastase (NE) bound to extracellular neutrophil chromatin was carried out with the NETosis assays kit (Cayman) according to the company's instructions. In short, NETs were washed after stimulation to remove unbound NE, chromatin was decomposed by DNase and subsequently the activity of NE was measured in the supernatant by formation of the 4-nitroaniline product from a NE-substrate (N-methoxysuccinyl-Ala-Ala-Pro-Val p-nitroanilide). Absorption of the resulting product was measured at 405 nm (Thermo Scientific APPLISKAN® Software: Skanlt RE for Appliskan 2.3, Thermo Fisher Scientific). All measurements were carried out in duplicates.

Anisotropy Measurements

Fluorescence anisotropy measurements were performed with a Fluoromax-4 spectrofluorometer (Horiba Scientific). All fluorescence emission spectra were recorded with excitation at 280 nm for BSA and 295 nm for HSA using excitation and emission slit widths of 5 nm. Emission detection wavelength was set at $\lambda_{em} = 344$ nm for BSA and $\lambda_{em} = 350$ nm for HSA, integration time was 1 s and detection steps were 1 nm. The cuvette used was a QS high precision cell (10x2 m; Hellma Analytics). First, anisotropy of 0.005% BSA, or 0.005% HSA was monitored for 500 s. Then, 10, 25, or 100 μg/ml LPS from pseudomonas aeruginosa were added to 0.005% BSA or 0.005% HSA for another 500 s. The system was allowed to reach equilibrium for 50 s.

Calcium Measurements

Calcium concentrations in presents or absence of 0.5% HSA were determined in the medical laboratory of the University Medical Center Göttingen using standard protocols.

Systematic Literature Review

For the literature review the online data base PubMed was used with the search terms "Neutrophil extracellular trap," "NETosis" and "Neutrophil + NET" up to 1st of March 2018. We included 460 human and 108 murine *in vitro* NET studies published after 2004 with full access to the PDF and written in English. Reviews and exclusive *in vivo* studies were excluded. Moreover, we included only studies performed on murine or human neutrophils, not on other cell types, co-cultures, transfected cells or cell lines. This study required unequivocal primary information on the used medium and the performed stimulation method to be included in this work (**Supplementary Figure 1**). For comparison of spontaneous NET formation in serum-free culture conditions, we analyzed all human *in vitro* NET studies performed with neutrophils from healthy donors in media without addition of solvents or stimuli that reported relative spontaneous NETosis rates (29 out of 255 publications).

Statistics and Data Analysis

All statistics were calculated with GraphPad Prism (Version 6.0, GraphPad Software Inc.). Significance was tested using standard two-way-ANOVA with Bonferroni's multiple comparisons test (ns, not significant; $^{*}p < 0.05$, $^{**}p < 0.01$, $^{***}p < 0.001$, $^{****}p < 0.0001$), after testing for normal distribution, where applicable. Fluorescence images were processed with ImageJ.46r (National Institutes of Health) and all cell counts obtained using the Plugin "Cell Counter".

RESULTS

Albumin and Serum Inhibit CaI- and LPS-, but Not PMA-Induced NETosis in Human Neutrophils

In the first series of experiments, we determined whether the different medium supplements have an influence on NET formation *in vitro*. To this end, we tested the frequently used supplements BSA, HSA and (hi)FCS at different concentrations on human neutrophils, taking into account the most commonly used concentrations in the literature (**Supplementary Table 1**). Firstly, we added FCS which had been heat-inactivated at 56°C (56°C hiFCS) to avoid side effects and degradation by serum nucleases, which is the most commonly applied manner of heat-inactivation. In 2009, von Köckritz-Blickwede et al. reported that even 56°C hiFCS may still contain heat-stable nucleases and recommended the use of FCS inactivated at 70°C (34). Nonetheless, we did not observe any difference in NETosis studied in 70°C hiFCS compared to 56°C hiFCS on the results in our setup (data not shown) and therefore decided for the more frequently used 56°C hiFCS for this study. We stimulated freshly isolated human neutrophils with CaI at 4 μM, PMA at 100 nM and LPS at 10 μg/ml, 25 μg/ml and 100 μg/ml to assess whether neutrophils stimulated by different inducers of NETosis would react differently to the media supplements (**Figure 1**). The identity of NETs was confirmed by co-staining of DNA and the neutrophil marker myeloperoxidase (MPO) (**Figure 2**) as well as release of neutrophil elastase (NE)-containing extracellular DNA (**Supplementary Figure 2**). The decondensed DNA of neutrophils having undergone NETosis in supplement-free RPMI/ HEPES clearly colocalized with MPO in confocal microscopy images after stimulation with CaI, PMA, or LPS. Furthermore, the NE-based NETosis assay showed the release of DNA-bound NE into the extracellular space after stimulation with the aforementioned stimuli, thus corroborating the induction of NETs in our experimental system.

We found that addition of BSA 0.5% as well as HSA 0.5% to RPMI/ HEPES significantly inhibited spontaneous NETosis and completely abolished NET formation mediated by CaI and LPS at 10, 25, and 100 μg/ml, whereas stimulation in pure RPMI/ HEPES led to a robust induction of NETs (**Figures 1A,B**). Interestingly, stimulation of neutrophils by 100 nM PMA was not influenced by either BSA or HSA (**Figures 1A,B**). In line with these observations, the release of DNA-bound NE after stimulation with CaI or LPS (100 μg/ml) was inhibited by addition of 0.5% HSA, but was not reduced in response to PMA (**Supplementary Figure 2**). Similarly, addition of hiFCS led to a dose-dependent decrease of CaI-induced NET formation but did not inhibit PMA-mediated NETosis (**Figure 1C**). Moreover, the addition of hiFCS significantly inhibited LPS-induced NETosis in a manner dependent on the concentration of both LPS and hiFCS itself. When 10 μg/ml LPS were used for the induction of NETosis, 0.5% hiFCS were sufficient to reduce NET formation dramatically from 95 to 5%. When 100 μg/ml LPS were employed, a significant reduction of NETosis to 22% could only be reached by adding 2% hiFCS (**Figure 1C**).

Murine and Human Neutrophils React Differently to Media Supplements

As many studies addressing NETosis are being conducted with murine neutrophils (**Supplementary Table 2**), we also sought to study whether media supplements such as FCS or BSA would influence murine NETosis in a similar way as described above for human neutrophils. Again, the three well established

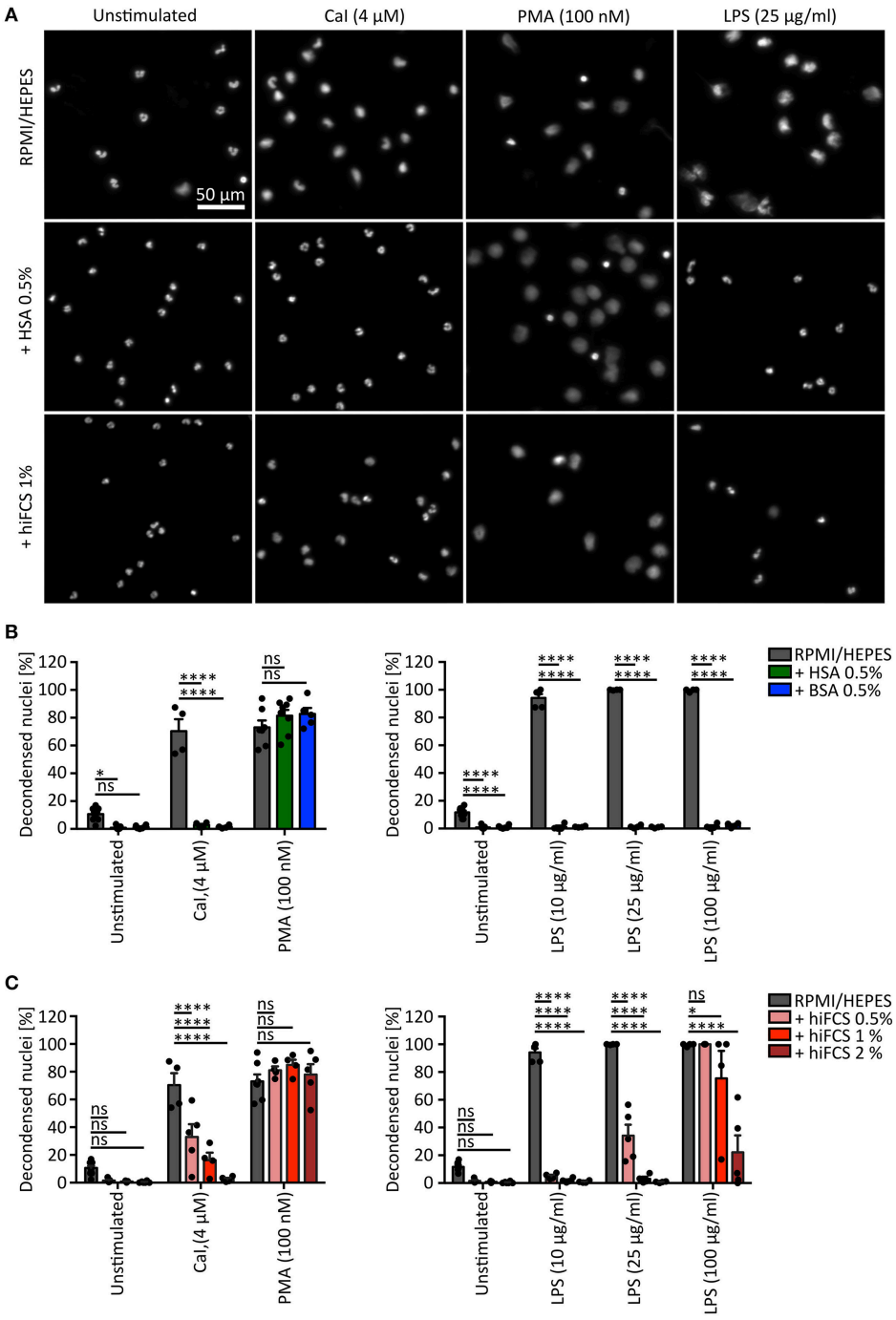

FIGURE 1 | Influence of serum and serum albumin supplements on NET formation of human neutrophils. **(A)** Representative fluorescence images of human neutrophils (chromatin stained by Hoechst) after stimulation with Cal (4 µM), PMA (100 nM), or LPS (25 µg/ml) for 180 min, respectively. NET formation of neutrophils was studied in RPMI 1,640 with 10 mM HEPES (RPMI/HEPES), RPMI/ HEPES + 0.5% human serum albumin (HSA) or + 1% heat inactivated (56°C) fetal calf serum (hiFCS). Chromatin decondensation induced by PMA is clearly visible with all three culture conditions, while LPS or Cal only cause NET formation in BSA- and HSA-free RPMI/HEPES. Scale = 50 µm. **(B)** Neutrophils were stimulated to undergo NET formation with Cal (4 µM), PMA (100 nM) or LPS (10, 25, or 100 µg/ml), respectively. Both, HSA and BSA inhibit Cal and LPS-induced formation of NETs (determined as percentage of decondensed nuclei/NETs of total neutrophils). NETosis stimulated by PMA is independent of serum albumin addition. Error bars = mean ± SEM. ns, not significant. $^{*}p < 0.05$, $^{****}p < 0.0001$. $N = 4–9$ [pool = 15 donors, 6–9 (unstimulated), 4 (Cal, 25 and 100 µg/ml LPS), 4–5 (10 µg/ml LPS), 5–8 (PMA)]. Two-way-ANOVA, Bonferroni's multiple comparisons test. **(C)** NET formation of neutrophils stimulated in RPMI/ HEPES supplemented with 0.5, 1, or 2% heat inactivated (56°C) fetal calf serum (hiFCS). Addition of hiFCS to RPMI/ HEPES decreases the percentage of decondensed nuclei/NETs after stimulation by Cal or LPS in a dose-dependent manner. PMA-induced NET formation occurs independently of FCS addition. Error bars = mean ± SEM. ns, not significant. $^{*}p < 0.05$. $^{****}p < 0.0001$. $N = 3–8$ [pool = 15 donors, 5–8 (unstimulated), 3–5 (100 µg/ml LPS), 4–5 (PMA, Cal, 10 and 25 µg/ml LPS)]. Two-way-ANOVA, Bonferroni's multiple comparisons test.

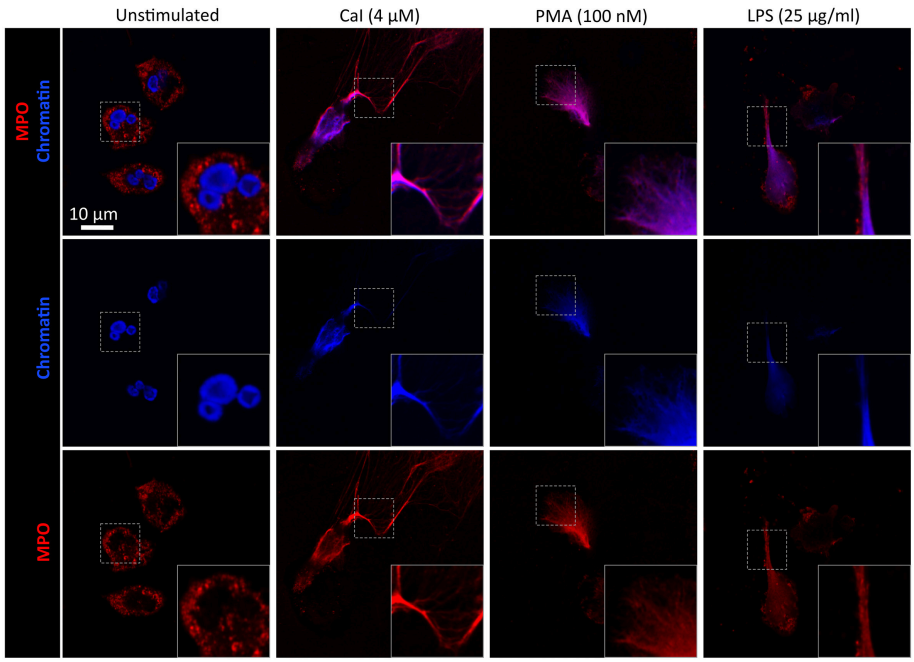

FIGURE 2 | Extracellular NETotic DNA is rich in MPO. Representative fluorescence images of NETs induced by CaI (4 μM), PMA (100 nM), or LPS (25 μg/ml) activated in supplement-free RPMI/HEPES. The images show a clear colocalization of MPO (red) with the extracellular DNA-fibers (blue) of released NETs. Scale = 10 μm.

NET-inducers, CaI, PMA and LPS were used (**Figure 3**). This question was especially interesting in light of the fact that murine studies typically forego the addition of media supplements for selected stimuli as CaI and LPS, whereas human studies more often include either albumin or serum in the media (see also **Figures 5**, **6**). While CaI was able to induce a strong response, causing almost 100% of neutrophils to undergo NETosis, PMA (at 100 nM) induced NETosis only in 28% of the neutrophils, which is in line with published results from the literature (4). Interestingly, the addition of 0.5% BSA or 2% 56°C hiFCS to RPMI/ HEPES was able to significantly inhibit both CaI- and PMA-induced NET-formation, contrary to what we had observed for human neutrophils. Similar results have been published for PMA-induced NETosis of murine neutrophils after the addition of hiFCS (4). For LPS from *Pseudomonas aeruginosa*, a minimum concentration of 25 μg/ml was needed to induce significant NET formation in murine neutrophils (23%) even without addition of media supplements. In general, LPS-induced NET formation was lower compared to that of human neutrophils at the same LPS concentration (**Figure 3**). However, similar to human neutrophils, addition of 0.5% BSA, or 2% hiFCS sufficed to completely inhibit LPS-induced NETosis.

Human and Bovine Serum Albumin Bind LPS From *Pseudomonas aeruginosa*

As bovine and human albumin diminished NET-formation in most tested scenarios, we hypothesized that albumin, as part of its action in our setup, may bind part of the activators and thus lower their biologically active concentration. Indeed, it has already been shown that CaI binds to albumin (35, 36) and it appears likely that a similar mechanism exists for PMA.

To test the hypothesis that direct binding of activators to albumin diminishes NETosis, we performed fluorescence anisotropy measurements to quantify binding of LPS to albumin as an example of such an interaction. Fluorescence anisotropy measurements are a quantitative and standardized method to determine interactions between proteins and binding partners in solution (**Figure 4**). Solubilized albumin performs a certain rotational movement, which results in the emission of a fluorescence signal when the solution is excited by polarized light. The binding of molecules such as LPS to BSA or HSA causes this rotational diffusion to slow, which results in a measurable increase of fluorescence anisotropy. We used a concentration of 0.005% BSA (**Figure 4A**) or 0.005% HSA (**Figure 4B**), respectively, in our experimental system and added LPS at concentrations between 10 and 50 μg/ml. We found a dose-dependent increase of anisotropy with LPS, indicating that both BSA and HSA do indeed bind LPS. Even at concentrations of HSA and BSA that were lower than those used in our NETosis experiments, a clear binding between partners could be observed, which would be higher at higher HSA/BSA concentrations. Consequently, the presence of albumins in the medium, even at low concentrations, lowers the effective concentration of LPS, which explains the inhibiting effect in our *in vitro* setup. Due to the small size of PMA and CaI similar measurements could not be performed but it is likely that there is a similar binding as albumins are known to bind many different molecules (37–39), among them CaI, as indicated above (35, 36).

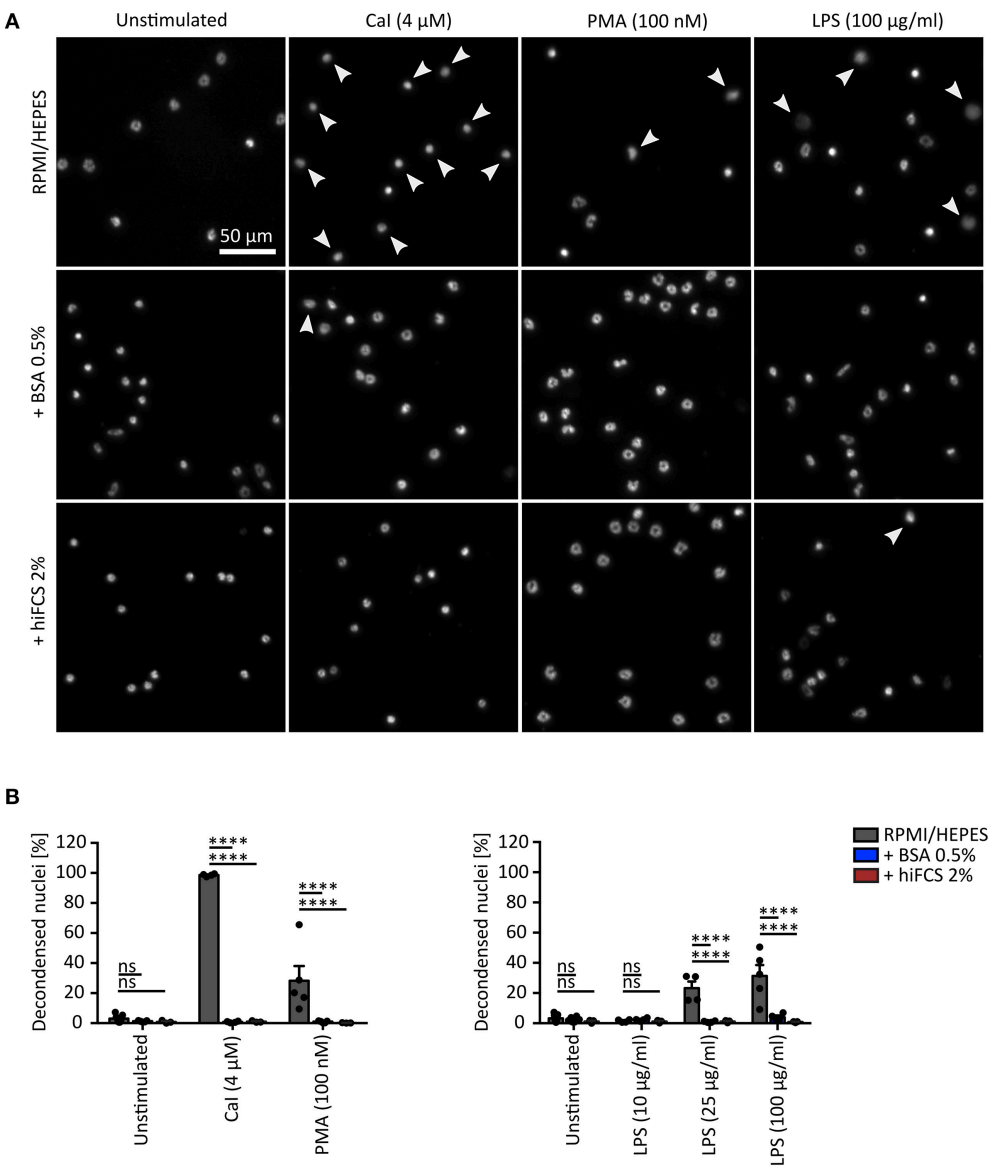

FIGURE 3 | Influence of serum and serum albumin supplements on NET formation of murine neutrophils. **(A)** Representative fluorescence images of nuclei of murine neutrophils (Hoechst) after stimulation with CaI (4 µM), PMA (100 nM) or LPS (25 µg/ml) for 180 min, respectively. NET formation of neutrophils was studied in RPMI/ HEPES without supplements and RPMI/ HEPES supplemented with 0.5% BSA or 2% hiFCS, as indicated. Chromatin decondensation is only inducible in RPMI/ HEPES (white arrow heads). Scale = 50 µm. **(B)** Percentage of decondensed nuclei/ NETs after stimulation with PMA (100 nM), CaI (4 µM), or LPS (10, 25, or 100 µg/ml) for 180 min. Murine neutrophils were studied in RPMI/ HEPES and RPMI/ HEPES supplemented with 0.5% BSA or 2% hiFCS. Addition of 0.5% BSA or 2% hiFCS to RPMI/ HEPES, inhibits chromatin decondensation induced by PMA, CaI and LPS completely. Error bars = mean ± SEM. ns = not significant. $^{****}p < 0.0001$. $N = 3$–13 mice [3–13 (unstimulated), 3–5 (100 µg/ml LPS), 3–4 (CaI, 10 and 25 µg/ml LPS), 3–5 (PMA)]. two-way-ANOVA, Bonferroni's multiple comparisons test.

Media Supplements Reveal Functional Differences Between Human and Mouse Neutrophils

We conducted a systematic literature research regarding human and mouse experiments studying NETosis *ex vivo/in vitro* to assess which supplements were commonly used by other groups working in the NETosis field (**Supplementary Figure 1**). Media supplements in studies dealing with human neutrophils (460 publications total) ranged from no supplement to FCS (0.05% to 10%), hiFCS (0.1 to 10%), human plasma (HP, 3 to 100%), hiHP (2 to 5%), human serum (HS, 0.2 to 100%), hiHS (0.1 to 100%) and serum albumin (HSA, 0.05 to 2%; BSA, 0.1 to 2%) (**Supplementary Table 1).** *Ex vivo* studies with murine neutrophils (108 publications) were carried out in media without supplements or medium supplemented with FCS (0.5 to 10%), hiFCS (0.1 to 10%), mouse serum (MS, 1 to 100%), BSA (0.1–2%) or in medium with HSA and bovine growth serum (BGS, 2%) (**Supplementary Table 2**).

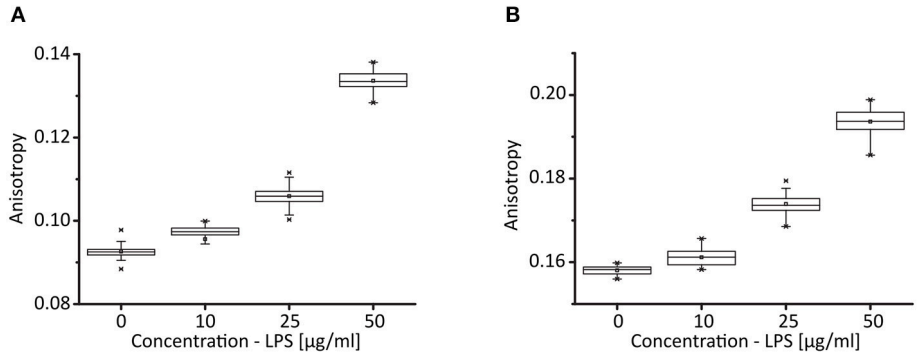

FIGURE 4 | Binding of LPS to serum albumins. Box plots represent fluorescence anisotropy values for **(A)**, bovine serum albumin (0.005%) and **(B)**, human serum albumin (0.005%) after addition of LPS from Pseudomonas aeruginosa at 10, 25, or 50 µg/ml, as indicated. The anisotropy of albumin increases with higher LPS concentrations. For each concentration, the average anisotropy value (monitored for 500s) between two LPS additions is shown. Box plots show 25 and 75 percentiles with the midline as median, the square as arithmetic middle and crosses as 99%/1% values. Whiskers include all data points within the 1.5 interquartile range. $N = 1$.

Approximately half of the experiments in human (51 %) and mouse (56 %) neutrophils were performed without any supplement (**Figures 5A**, **6A**) and the other half with very heterogeneous supplements. Additionally, even within the group that refrained from using media supplements, experimental conditions were overall quite diverse, as different basal media and different stimuli were used (see **Supplementary Tables 1, 2**).

As it is possible that the choice of media supplements is influenced by the activator of NETosis, we also plotted our extracted data into five groups according to the "major" NETosis stimulants (PMA, LPS, ionophores/ionomycin, pathogens, and cytokines/chemokines). Indeed, after this selection, certain activator-specific characteristics became apparent, such as the fact that for LPS, used in human studies, more than half of the publications forewent the use of media supplements, while in the publications using Ionophores or pathogens this approach was less common. Interestingly, studies using pathogens or cytokines and chemokines as inducers of NETosis generally showed the highest use of human plasma at different concentrations (**Figure 5B**).

In mice, the specific differences between experiments performed with different inhibitors were even more striking. While the use of PMA and pathogens led to a heterogeneous picture relatively similar to that seen with human neutrophils, LPS and ionophores were rarely or not at all employed in media-containing supplements (**Figure 6B**).

These striking differences led us to propose that media supplements might differentially influence different activators of NETosis and might lead to different results in human or mouse neutrophils. We would like to emphasize that in this analysis we did not differentiate between "vital" and "suicidal" NETosis and that we did not assess whether an assay successfully caused NET release or not. We included all manuscripts which clearly stated to study *in vitro* NETosis. Nonetheless, several of the included publications reported problems or failure to achieve a robust activation especially in media supplemented with serum or serum albumin. For instance, Wang et al. did not observe NETosis of TNFα-primed mouse neutrophils after stimulation with 100 ng/ml LPS in media containing 0.5% BSA and Papayannopoulos et al. clearly showed that peritoneal mouse neutrophils did not respond to PMA (100 nM) in media supplemented with 10 % FCS (40, 41). In *ex vivo* studies with human neutrophils several groups reported no or only a slight response to LPS in FCS containing media (Hoppenbrouwers et al.: 10% FCS, 5 µg/ml LPS; Barquero-Calvo et al.: 1% FCS, 0.7–100 µg/ml LPS; Hoffmann et al.: 2% FCS, 300 ng/ml LPS; Zhu et al.: 4% hiFCS, around 10% activation with 100 ng/ml LPS) or BSA (Ohbuchi et al.: 1% BSA, 10 ng−1 µg/ml LPS) (25, 29, 42–44) and Clark et al. did not observe any activation after stimulating human neutrophils with 5 µg/ml LPS in the presence of 10% plasma (45). As the publication of negative data is relatively rare, it is reasonable to assume the omission of media supplements in over half of the publications here analyzed indirectly reflects the difficulties of neutrophil stimulation in media containing albumin or serum supplements, at least for certain stimuli. In any case, the starting conditions of different studies are very divergent, which makes the publications in the field virtually impossible to compare, thus potentially diminishing the scientific significance and making the overall picture difficult to interpret.

DISCUSSION

NETosis and NET-related topics are currently intensely investigated topics with the number of publications steadily rising for the last couple of years. Despite the attention that the process of NETosis has attracted since its first publication in 2004 (1), little effort has been put into the standardization of experimental conditions for *in vitro* experiments. We are therefore advocating a consensus to define the experimental conditions as uniformly as possible in order to be able to better compare the results of different groups and better define important biological processes.

Previous sporadic publications had addressed the question of different culture media and media supplements such as FCS in an arbitrary manner (29), some of them hinting that indeed the addition of such components might greatly influence the

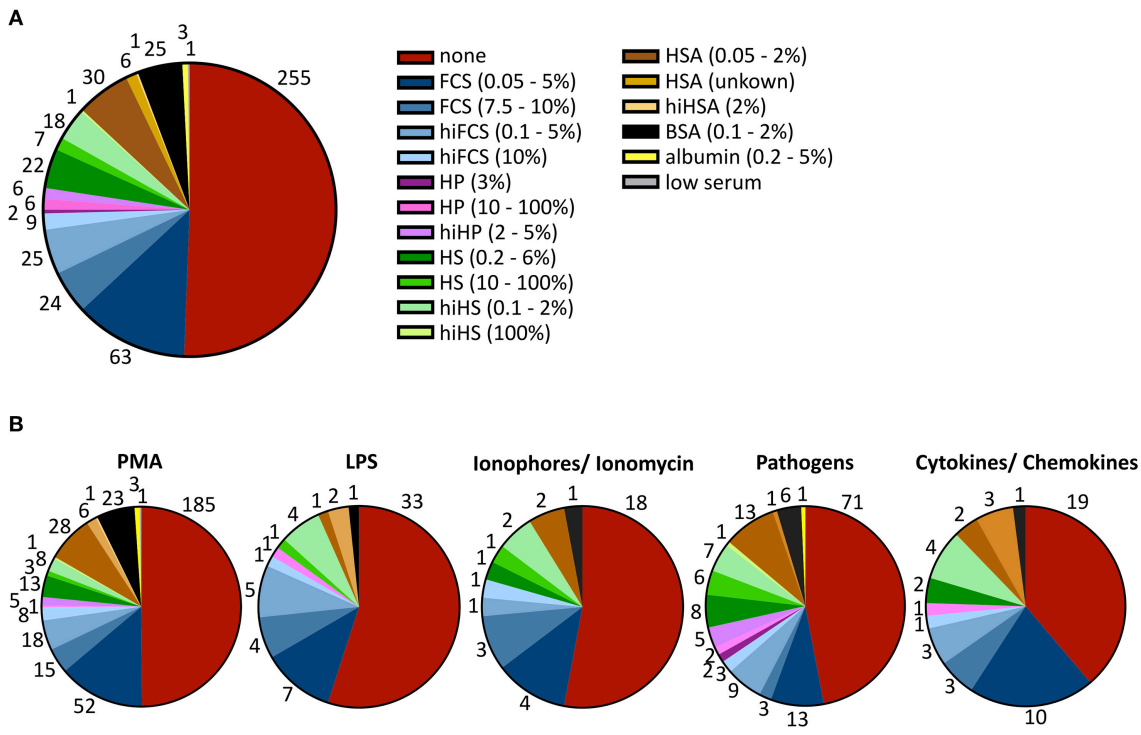

FIGURE 5 | Heterogeneity in media supplements for human *in vitro* NETosis studies. Pie charts of serum, plasma, or serum albumin supplements used in human *in vitro* NETosis studies, as indicated (numbers represent the absolute numbers of publications using a certain supplement while the slices represent percentages of all considered publications). **(A)** chart for all stimuli combined (all publications were counted once). **(B)** charts for PMA, Ionophore/ Ionomycin, LPS, pathogen and cytokines/chemokines, respectively. Publications were counted for multiple activator-specific pie charts if more than one NET-activator was used. $N = 460$ publications up to the 1st of March 2018.

outcome of NETosis experiments (4, 28–30). For this reason, we systematically tested the popular media supplements BSA, HSA and hiFCS and compared the effect of their addition to NETosis experiments without supplements. We used three of the currently best-established and most-used inducers of NET-formation, CaI, PMA, and LPS isolated from *Pseudomonas aeruginosa*. We chose these three activators because their mechanism of NET-induction has been well studied and they are known to involve different signaling cascades (46). Other popular inducers of NETosis include CXCL8 (IL-8) (15), reactive oxygen species such as H_2O_2 (4), activated platelets (47), microcrystals (48), *Aspergillus fumigatus* and *Candida albicans* hyphae (49) as well as live bacteria (1) [for a comprehensive review on activators of NETosis please see (25)].

We found that in media without albumin or serum components, CaI, PMA and LPS at all tested concentrations induced a strong and reproducible NET-formation in human neutrophils. On the other hand, spontaneous NETosis rates were relatively high in serum-free and serum-low conditions with a mean of 10.6% NET-rates. The increase of spontaneous NETosis rates in serum-free media is in line with results that have been reported in the literature (**Supplementary Figure 3**) (30).

The addition of BSA or HSA at 0.5% (which is at the lower range of concentrations used in the literature) led to an almost complete inhibition of NETosis induced by CaI or LPS. Thus, the experimental system appeared to be highly vulnerable to the influence of these media components. Astonishingly, PMA-induced NETosis remained unaffected by the addition of albumin (**Figures 1A,B**). Similarly, PMA-induced NETosis was not inhibited by any of the three tested concentrations of hiFCS (**Figures 1A,C**). This is in line with a plethora of publications that show robust induction of NETosis of human neutrophils by PMA in media containing albumin or serum components (14, 31, 50). We cannot exclude an inhibitory effect of FCS on PMA-induced NETosis at very high FCS concentrations, as has been shown by Fuchs et al. who used up to 20% FCS to inhibit NETosis (4), however we refrained from reproducing this setup as such high FCS concentrations are rarely used in the literature.

In contrast, CaI-induced and LPS-induced NETosis were inhibited not only by BSA or HSA, as discussed above, but also by hiFCS. Again, this corroborates previously published data which has described LPS as a poor and unreliable inducer of NETosis when using media complemented with FCS or BSA (25, 29, 42–44, 51). It is interesting to note that for human neutrophils, which are often cultured in media containing either

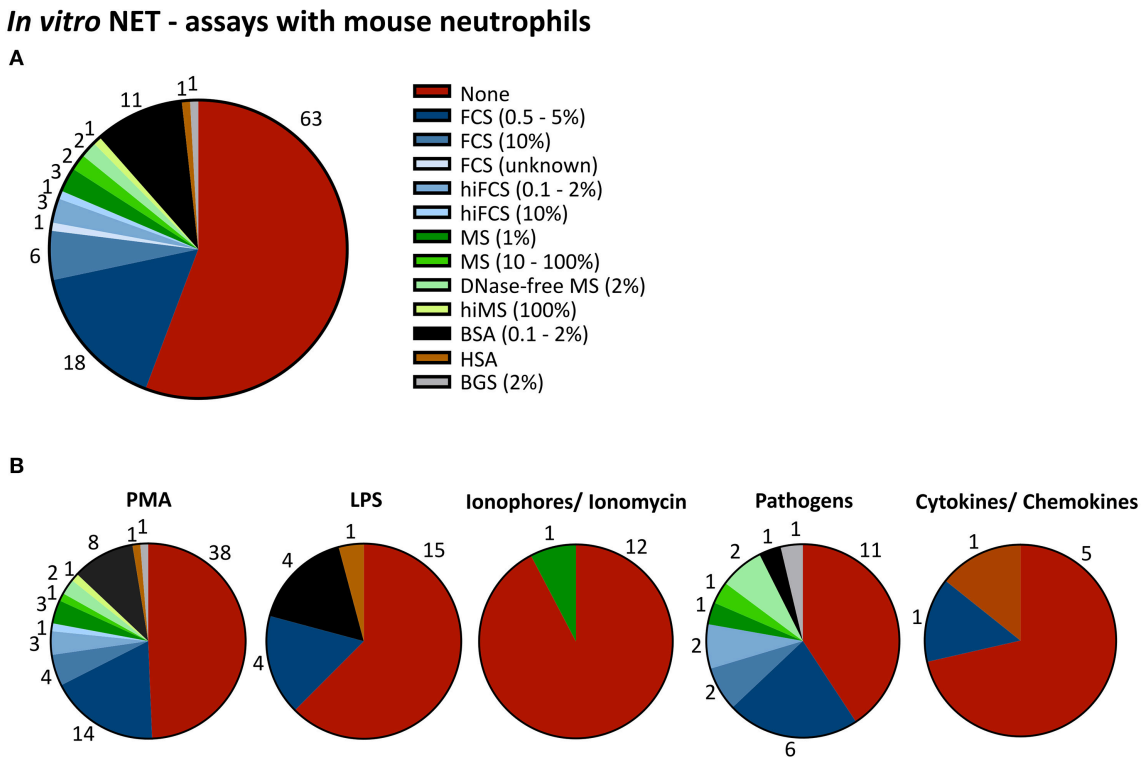

FIGURE 6 | Heterogeneity in media supplements for murine *in vitro* NETosis studies. Pie charts of serum, plasma, or serum albumin supplements used in murine *in vitro* NETosis studies, as indicated (numbers represent the absolute numbers of publications using a certain supplement while the slices represent percentages of all considered publication). **(A)** chart for all stimuli combined. **(B)** charts for PMA, Ionophore/ Ionomycin, LPS, pathogen, and cytokines/chemokines, respectively. Publications were counted for multiple activator-specific pie charts if more than one NET-activator was used. *N* = 108 publications up to the 1st of March 2018.

albumin or serum components, LPS is used as an inducer of NETosis more rarely than in mouse studies, which are carried out without media supplements in the majority of cases (52). This becomes especially obvious in publications using both human and mouse neutrophils (14, 53). On the other hand, many human studies which do employ LPS as an inducer use serum-free media (54–57) (see also **Supplementary Table 1**). The reason for these observations may be that LPS, even at high concentrations, fails to adequately activate neutrophils to produce NETs in the presence of BSA, HSA or hiFCS (**Figure 1C**). A possible explanation for this phenomenon is a strong binding of LPS by large proteins such as albumin (**Figure 4**) and, very likely, also by other serum components. Additionally, NETosis induction by LPS relies heavily on integrin receptors such as MAC-1 (58) and this outside-in signaling may be influenced by the addition of large proteins and certainly also of serum components which contain a mixture of active components that can engage integrin receptors. In contrast, PMA is a direct activator of protein kinase C (PKC) (59), a vital and relatively far downstream step in most pathways leading to NETosis. Therefore, outside-in signaling could be expected to be less crucial during the activation cascade, at least for human neutrophils.

However, it is important to bear in mind that the isolation and stimulation of neutrophils *ex vivo* is a complex process, which depends on many factors apart from the used media and media supplements. It is likely that the method of neutrophil isolation, activation as well as the predisposition of the donor will also influence whether stimulation of neutrophils is successful or not. To minimize side-effects of the isolation method such as pre-activation of the used neutrophils, we decided to employ well characterized density gradient methods for neutrophil isolation (14, 33). Gradient-based isolation technics are one of the most commonly used methods in NETosis-studies. Compared to isolation by polymorphprep^{TM} or combinations with lysis of erythrocytes, pure gradients reveal comparably low spontaneous NET formation, as reported in the literature and corroborated in our own results (**Supplementary Figure 3**). Furthermore, the used anticoagulant can significantly influence pre-activation, calcium levels, and number of obtained neutrophils (60). For instance, heparin anticoagulation can influence the expression of adhesion molecules (61). For this reason, we have employed EDTA as an anticoagulant in this study (60).

Additionally, for LPS also the bacterial source has a significant impact on the success of stimulation and concentrations needed for this assay (62). Therefore, it is not surprising that concentrations of LPS used for *ex vivo* studies differ widely and, in some cases, LPS-induced NETosis occurred even in media containing albumin or serum components (63–65) or occasionally revealed only low NET-rates in supplement-free media (66, 67).

For mouse neutrophils, PMA-induced NETosis was, surprisingly, strongly inhibited by addition of 0.5% BSA and 2% hiFCS. In general, mouse neutrophils appear to be harder to activate than human neutrophils, they require higher threshold concentrations for LPS and produce less NETs upon PMA activation. One may speculate that mouse neutrophils may need a higher concentration of PMA to reach the same threshold of activation and that a minimal scavenging of available PMA or a certain unspecific "stabilizing effect" of BSA/HSA would thus affect murine NETosis more profoundly than it would for human cells. This would be in line with the data shown by Fuchs et al. (4) for the inhibitory effects of high concentrations of FCS (up to 20%) on PMA-activated human neutrophils: If human neutrophils required much lower concentrations of PMA to still perform NETosis, then a considerable "scavenging" effect of the activator would be of consequence only at high FCS concentrations.

Another possible explanation that must be taken into account for the differences seen between inductors of NETosis in response to media supplements is a possible influence on extracellular calcium levels. Calcium has been shown to be bound by albumin (68, 69) and appears to be essential for NETosis activation by PMA and, to a lesser extent, for CaI (46, 70). However, in our experimental setup we could not observe a significant influence of HSA on calcium levels (**Supplementary Figure 4**) and doubling of calcium-concentration (to 0.8 mM) did not reverse the inhibitory effect of HSA in our hands (data not shown).

Concerning the differences seen between PMA-induced NETosis in humans and mice, it must be taken into account that PMA-induced NETosis in mice may in part rely on different biochemical pathways in these two different species. For example, for murine neutrophils an involvement of enzymes such as PAD4 has been reported previously (71), whereas the involvement of PAD4 in PMA-induced human NETosis is still under discussion (46, 72). A similar observation, namely that decondensation of chromatin and NETosis in human neutrophils depends on PAD4 function to a lesser extent, was reported for *Staphylococcus* (73). In the context of different human diseases, a number of endogenous and receptor-mediated, inflammatory pathways have been identified that may lead to and regulate NET formation. For instance, in COPD the chemokine IL-8 (CXCL-8) and signaling through the CXCR2 receptor are thought to be involved in the disease (74) and in lupus nephritis, NET formation is thought to be regulated by engagement of the uniquely human FcγRIIA by soluble immune complexes (75). It remains to be explored how these pathways differ in humans and mice and how environmental conditions may influence them.

The effect of media supplements on NETosis experiments is most likely a complex one, however one may speculate that a great part of this effect is brought about by binding of the activators to albumin or to other serum proteins. In fact, for LPS and CaI binding to albumin has already been reported, and we here confirm and exemplify the binding of LPS to albumin by fluorescence anisotropy measurements. Indeed, binding of toxic and immune-activating substances like LPS or chemoattractants is likely a mechanism to protect the host from an overactive immune system and dysregulated NETosis, which has been shown to have deleterious effects (76–78). Additionally, serum even contains active DNases which are able to degrade already released NETs, which also shows that the composition of the environment in which neutrophils become activated are part of an immune regulation to limit excess inflammation (79).

On the other hand, serum condition in the tissue to which neutrophils are recruited in case of an inflammation to fight pathogens might be different from those of the blood, i.e., serum composition in the blood is arguably different from that in solid tissues. It is thus likely that, in part, a different grade of inhibition of neutrophil function under different conditions directs neutrophil behavior and orchestrates immune responses (30).

Our experimental results are indirectly reflected in the literature of experiments studying NETosis. While generally there is a plethora of different experimental conditions being employed in the field, it is striking to note the differences between human and mouse experiments and particularly in the experimental conditions used when LPS or CaI are employed as activators. Here, the vast majority of all publications refrained from adding any culture supplements, which is in line with our observation that CaI- and LPS-induced NETosis are very strongly inhibited by albumin.

Thus, the choice of media supplements greatly determines the outcome of *in vitro* experiments on NET-formation, which must be considered when planning and comparing NET-studies. Studies using different media settings may not be comparable and in general the question must be asked to which extent experiments omitting media supplements are actually recapitulating the natural function of neutrophils and NETs. On the other side, *in vivo* compartments are also different and differ in concentrations of chemokines, adhesion receptors, and other cells. Therefore, the questions we addressed in this paper is not restricted to *in vitro* experiments but also highly relevant for the assessment of *in vivo* experiments.

A standardization of protocols for NET experiments would allow for a better comparison between results from different groups.

AUTHOR CONTRIBUTIONS

EN and SS-S performed most experiments, co-wrote the paper, and designed the study together with LE. VM, JB, and SS performed experiments and analyzed data. EP provided the anisotropy data, supervised by SK. SK and MS provided crucial technical and scientific input and helped design the study. LE designed and supervised all experiments and co-wrote the paper. All authors critically proofread and edited the manuscript.

ACKNOWLEDGMENTS

LE was funded by the DDG/ADF Clinician Scientist fellowship, the DFG (ER723/2-1) and the Heidenreich von Siebold Programm of the UMG. SK acknowledges support by the DFG (Kr 4242/4-1), life@nano (MWK Niedersachsen) and the cluster

of excellence CNMPB. We thank Stefan Erdelt for his very important input. We thank Ivan Bogeski and Hedwig Stanisz-Bogeski for helpful input concerning calcium measurements. And we thank the department of medical statistics in Göttingen for advice on the systematic review.

SUPPLEMENTARY MATERIAL

The Supplementary Material for this article can be found online at: https://www.frontiersin.org/articles/10.3389/fimmu.2019.00012/full#supplementary-material

REFERENCES

1. Brinkmann V, Reichard U, Goosmann C, Fauler B, Uhlemann Y, Weiss DS, et al. Neutrophil extracellular traps kill bacteria. *Science* (2004) 303:1532–5. doi: 10.1126/science.1092385
2. Yousefi S, Simon HU. NETosis – does it really represent nature's "suicide bomber"? *Front Immunol.* (2016) 7:328. doi: 10.3389/fimmu.2016.00328
3. Papayannopoulos V. Neutrophil extracellular traps in immunity and disease. *Nat Rev Immunol.* (2018) 18:134–47. doi: 10.1038/nri.2017.105
4. Fuchs TA, Abed U, Goosmann C, Hurwitz R, Schulze I, Wahn V, et al. Novel cell death program leads to neutrophil extracellular traps. *J Cell Biol.* (2007) 176:231–41. doi: 10.1083/jcb.200606027
5. Pilsczek FH, Salina D, Poon KK, Fahey C, Yipp BG, Sibley CD, et al. A novel mechanism of rapid nuclear neutrophil extracellular trap formation in response to *Staphylococcus aureus*. *J Immunol.* (2010) 185:7413–25. doi: 10.4049/jimmunol.1000675
6. Sur Chowdhury C, Giaglis S, Walker UA, Buser A, Hahn S, Hasler P. Enhanced neutrophil extracellular trap generation in rheumatoid arthritis: analysis of underlying signal transduction pathways and potential diagnostic utility. *Arthritis Res Ther.* (2014) 16:R122. doi: 10.1186/ar4579
7. Leffler J, Gullstrand B, Jonsen A, Nilsson JA, Martin M, Blom AM, et al. Degradation of neutrophil extracellular traps co-varies with disease activity in patients with systemic lupus erythematosus. *Arthritis Res Ther*. (2013) 15:R84. doi: 10.1186/ar4264
8. Grabcanovic-Musija F, Obermayer A, Stoiber W, Krautgartner WD, Steinbacher P, Winterberg N, et al. Neutrophil extracellular trap (NET) formation characterises stable and exacerbated COPD and correlates with airflow limitation. *Respir Res*. (2015) 16:59. doi: 10.1186/s12931-015-0221-7
9. Pedersen F, Marwitz S, Holz O, Kirsten A, Bahmer T, Waschki B, et al. Neutrophil extracellular trap formation and extracellular DNA in sputum of stable COPD patients. *Respir Med*. (2015) 109:1360–2. doi: 10.1016/j.rmed.2015.08.008
10. Hu SC, Yu HS, Yen FL, Lin CL, Chen GS, Lan CC. Neutrophil extracellular trap formation is increased in psoriasis and induces human beta-defensin-2 production in epidermal keratinocytes. *Sci Rep*. (2016) 6:31119. doi: 10.1038/srep31119
11. Schön MP, Erpenbeck L. The interleukin-23/interleukin-17 axis links adaptive and innate immunity in psoriasis. *Front Immunol.* (2018) 9:1323. doi: 10.3389/fimmu.2018.01323
12. Savchenko AS, Borissoff JI, Martinod K, De Meyer SF, Gallant M, Erpenbeck L, et al. VWF-mediated leukocyte recruitment with chromatin decondensation by PAD4 increases myocardial ischemia/reperfusion injury in mice. *Blood* (2014) 123:141–8. doi: 10.1182/blood-2013-07-514992
13. Brill A, Fuchs TA, Savchenko AS, Thomas GM, Martinod K, De Meyer SF, et al. Neutrophil extracellular traps promote deep vein thrombosis in mice. *J Thromb Haemost.* (2012) 10:136–44. doi: 10.1111/j.1538-7836.2011.04544.x
14. Wong SL, Demers M, Martinod K, Gallant M, Wang Y, Goldfine AB, et al. Diabetes primes neutrophils to undergo NETosis, which impairs wound healing. *Nat Med.* (2015) 21:815–9. doi: 10.1038/nm.3887
15. Gupta AK, Hasler P, Holzgreve W, Gebhardt S, Hahn S. Induction of neutrophil extracellular DNA lattices by placental microparticles and IL-8 and their presence in preeclampsia. *Hum Immunol*. (2005) 66:1146–54. doi: 10.1016/j.humimm.2005.11.003
16. Cools-Lartigue J, Spicer J, McDonald B, Gowing S, Chow S, Giannias B, et al. Neutrophil extracellular traps sequester circulating tumor cells and promote metastasis. *J Clin Invest*. (2013). doi: 10.1172/jci67484
17. Erpenbeck L, Schön MP. Neutrophil extracellular traps: protagonists of cancer progression? *Oncogene* (2017) 36:2483–90. doi: 10.1038/onc.2016.406
18. Gavillet M, Martinod K, Renella R, Harris C, Shapiro NI, Wagner DD, et al. Flow cytometric assay for direct quantification of neutrophil extracellular traps in blood samples. *Am J Hematol*. (2015) 90:1155–8. doi: 10.1002/ajh.24185
19. Masuda S, Shimizu S, Matsuo J, Nishibata Y, Kusunoki Y, Hattanda F, et al. Measurement of NET formation *in vitro* and *in vivo* by flow cytometry. *Cytometry* (2017) 91:822–9. doi: 10.1002/cyto.a.23169
20. Neubert EMD, Rocca F, Kwaczala-Tessmann A, Grandke J, Senger-Sander S, Geisler C, et al. (2018). Chromatin swelling drives neutrophil extracellular trap release. *Nature Commun.* (2018) 9:3767. doi: 10.1038/s41467-018-06263-5
21. Looney MR, Nguyen JX, Hu Y, Van Ziffle JA, Lowell CA, Matthay MA. Platelet depletion and aspirin treatment protect mice in a two-event model of transfusion-related acute lung injury. *J Clin Invest*. (2009) 119:3450–61. doi: 10.1172/JCI38432
22. Gilliss BM, Looney MR. Experimental models of transfusion-related acute lung injury. *Transfus Med Rev*. (2011) 25:1–11. doi: 10.1016/j.tmrv.2010.08.002
23. Kruss S, Erpenbeck L, Schon MP, Spatz JP. Circular, nanostructured and biofunctionalized hydrogel microchannels for dynamic cell adhesion studies. *Lab Chip* (2012) 12:3285–9. doi: 10.1039/c2lc40611j
24. Kruss S, Erpenbeck L, Amschler K, Mundinger TA, Boehm H, Helms HJ, et al. Adhesion maturation of neutrophils on nanoscopically presented platelet glycoprotein Ibalpha. *ACS Nano* (2013) 7:9984–96. doi: 10.1021/nn403923h
25. Hoppenbrouwers T, Autar ASA, Sultan AR, Abraham TE, van Cappellen WA, Houtsmuller AB, et al. *in vitro* induction of NETosis: comprehensive live imaging comparison and systematic review. *PLoS ONE* (2017) 12:e0176472. doi: 10.1371/journal.pone.0176472
26. David SA, Balaram P, Mathan VI. Characterization of the interaction of lipid A and lipopolysaccharide with human serum albumin: implications for an endotoxin carrier function for albumin. *J Endot Res.* (1995) 2:99–106. doi: 10.1177/096805199500200204
27. de Haas CJ, van Leeuwen HJ, Verhoef J, van Kessel KP, van Strijp JA. Analysis of lipopolysaccharide (LPS)-binding characteristics of serum components using gel filtration of FITC-labeled LPS. *J Immunol Methods* (2000) 242:79–89. doi: 10.1016/S0022-1759(00)00207-6
28. Bartneck M, Keul HA, Zwadlo-Klarwasser G, Groll J. Phagocytosis independent extracellular nanoparticle clearance by human immune cells. *Nano Lett*. (2010) 10:59–63. doi: 10.1021/nl902830x
29. Hoffmann JH, Schaekel K, Gaiser MR, Enk AH, Hadaschik EN. Interindividual variation of NETosis in healthy donors: introduction and application of a refined method for extracellular trap quantification. *Exp Dermatol*. (2016) 25:895–900. doi: 10.1111/exd.13125
30. Kamoshida G, Kikuchi-Ueda T, Nishida S, Tansho-Nagakawa S, Kikuchi H, Ubagai T, et al. Spontaneous formation of neutrophil extracellular traps in serum-free culture conditions. *FEBS Open Bio* (2017) 7:877–86. doi: 10.1002/2211-5463.12222
31. Brinkmann V, Laube B, Abu Abed U, Goosmann C, Zychlinsky A. Neutrophil extracellular traps: how to generate and visualize them. *J Vis Exp.* (2010) 36:1724. doi: 10.3791/1724
32. Martinod K, Witsch T, Erpenbeck L, Savchenko A, Hayashi H, Cherpokova D, et al. Peptidylarginine deiminase 4 promotes age-related organ fibrosis. *J Exp Med.* (2017) 214:439–58. doi: 10.1084/jem.20160530
33. Demers M, Krause DS, Schatzberg D, Martinod K, Voorhees JR, Fuchs TA, et al. Cancers predispose neutrophils to release extracellular DNA traps that contribute to cancer-associated thrombosis. *Proc Natl Acad Sci USA*. (2012) 109:13076–81. doi: 10.1073/pnas.1200419109
34. von Kockritz-Blickwede M, Chow OA, Nizet V. Fetal calf serum contains heat-stable nucleases that degrade neutrophil extracellular traps. *Blood* (2009) 114:5245–6. doi: 10.1182/blood-2009-08-240713.

35. Feinstein MB, Fraser C. Human platelet secretion and aggregation induced by calcium ionophores. Inhibition by PGE1 and dibutyryl cyclic AMP. *J Gen Physiol*. (1975) 66:561–81.
36. Hoffman T, Lizzio EF. Albumin in monocyte function assays. Differential stimulation of superoxide or arachidonate release by calcium ionophores. *J Immunol Methods* (1988) 112:9–14.
37. He XM, Carter DC. Atomic structure and chemistry of human serum albumin. *Nature* (1992) 358:209–15. doi: 10.1038/358209a0
38. Zsila F, Bikadi Z, Malik D, Hari P, Pechan I, Berces A, et al. Evaluation of drug-human serum albumin binding interactions with support vector machine aided online automated docking. *Bioinformatics* (2011) 27:1806–13. doi: 10.1093/bioinformatics/btr284
39. Zhivkova ZD. Studies on drug-human serum albumin binding: the current state of the matter. *Curr Pharm Des*. (2015) 21:1817–30. doi: 10.2174/1381612821666150302113710
40. Papayannopoulos V, Metzler KD, Hakkim A, Zychlinsky A. Neutrophil elastase and myeloperoxidase regulate the formation of neutrophil extracellular traps. *J Cell Biol*. (2010) 191:677–91. doi: 10.1083/jcb.201006052
41. Wang Y, Wang W, Wang N, Tall AR, Tabas I. Mitochondrial oxidative stress promotes atherosclerosis and neutrophil extracellular traps in aged mice. *Arterioscler Thromb Vasc Biol*. (2017) 37:e99–107. doi: 10.1161/atvbaha.117.309580
42. Barquero-Calvo E, Mora-Cartin R, Arce-Gorvel V, de Diego JL, Chacon-Diaz C, Chaves-Olarte E, et al. Brucella abortus induces the premature death of human neutrophils through the action of its lipopolysaccharide. *PLoS Pathog*. (2015) 11:e1004853. doi: 10.1371/journal.ppat.1004853
43. Ohbuchi A, Kono M, Kitagawa K, Takenokuchi M, Imoto S, Saigo K. Quantitative analysis of hemin-induced neutrophil extracellular trap formation and effects of hydrogen peroxide on this phenomenon. *Biochem Biophys Rep*. (2017) 11:147–53. doi: 10.1016/j.bbrep.2017.07.009
44. Zhu L, Liu L, Zhang Y, Pu L, Liu J, Li X, et al. High level of neutrophil extracellular traps correlates with poor prognosis of severe influenza a infection. *J Infect Dis*. (2018) 217:428–37. doi: 10.1093/infdis/jix475
45. Clark SR, Ma AC, Tavener SA, McDonald B, Goodarzi Z, Kelly MM, et al. Platelet TLR4 activates neutrophil extracellular traps to ensnare bacteria in septic blood. *Nat Med*. (2007) 13:463–9. doi: 10.1038/nm1565
46. Kenny EF, Herzig A, Kruger R, Muth A, Mondal S, Thompson PR, et al. Diverse stimuli engage different neutrophil extracellular trap pathways. *Elife* (2017) 6:e24437. doi: 10.7554/eLife.24437
47. Caudrillier A, Kessenbrock K, Gilliss BM, Nguyen JX, Marques MB, Monestier M, et al. Platelets induce neutrophil extracellular traps in transfusion-related acute lung injury. *J Clin Invest*. (2012) 122:2661–71. doi: 10.1172/jci61303
48. Li Y, Cao X, Liu Y, Zhao Y, Herrmann M. Neutrophil extracellular traps formation and aggregation orchestrate induction and resolution of sterile crystal-mediated inflammation. *Front Immunol*. (2018) 9:1559. doi: 10.3389/fimmu.2018.01559
49. Branzk N, Lubojemska A, Hardison SE, Wang Q, Gutierrez MG, Brown GD, et al. Neutrophils sense microbe size and selectively release neutrophil extracellular traps in response to large pathogens. *Nat Immunol*. (2014) 15:1017–25. doi: 10.1038/ni.2987
50. Metzler KD, Goosmann C, Lubojemska A, Zychlinsky A, Papayannopoulos V. A myeloperoxidase-containing complex regulates neutrophil elastase release and actin dynamics during NETosis. *Cell Rep*. (2014) 8:883–96. doi: 10.1016/j.celrep.2014.06.044
51. Shimomura Y, Suga M, Kuriyama N, Nakamura T, Sakai T, Kato Y, et al. Recombinant human thrombomodulin inhibits neutrophil extracellular trap formation *in vitro*. *J Intensive Care* (2016) 4:48. doi: 10.1186/s40560-016-0177-9
52. Li P, Li M, Lindberg MR, Kennett MJ, Xiong N, Wang Y. PAD4 is essential for antibacterial innate immunity mediated by neutrophil extracellular traps. *J Exp Med*. (2010) 207:1853–62. doi: 10.1084/jem.20100239
53. Farley K, Stolley JM, Zhao P, Cooley J, Remold-O'Donnell E. A serpinB1 regulatory mechanism is essential for restricting neutrophil extracellular trap generation. *J Immunol*. (2012) 189:4574–81. doi: 10.4049/jimmunol.1201167
54. Liu CL, Tangsombatvisit S, Rosenberg JM, Mandelbaum G, Gillespie EC, Gozani OP, et al. Specific post-translational histone modifications of neutrophil extracellular traps as immunogens and potential targets of lupus autoantibodies. *Arthr Res Ther*. (2012) 14:R25–25. doi: 10.1186/ar3707
55. McInturff AM, Cody MJ, Elliott EA, Glenn JW, Rowley JW, Rondina MT, et al. Mammalian target of rapamycin regulates neutrophil extracellular trap formation via induction of hypoxia-inducible factor 1 alpha. *Blood* (2012) 120:3118–25. doi: 10.1182/blood-2012-01-405993
56. Khan MA, Palaniyar N. Transcriptional firing helps to drive NETosis. *Sci Rep*. (2017) 7:41749. doi: 10.1038/srep41749
57. Nadesalingam A, Chen JHK, Farahvash A, Khan MA. Hypertonic saline suppresses NADPH oxidase-dependent neutrophil extracellular trap formation and promotes apoptosis. *Front Immunol*. (2018) 9:359. doi: 10.3389/fimmu.2018.00359
58. Neeli I, Dwivedi N, Khan S, Radic M. Regulation of extracellular chromatin release from neutrophils. *J Innate Immun*. (2009) 1:194–201. doi: 10.1159/000206974
59. Blumberg PM. Protein kinase C as the receptor for the phorbol ester tumor promoters: sixth Rhoads memorial award lecture. *Cancer Res*. (1988) 48:1–8.
60. Freitas M, Porto G, Lima JL, Fernandes E. Isolation and activation of human neutrophils *in vitro*. The importance of the anticoagulant used during blood collection. *Clin Biochem* (2008) 41:570–5. doi: 10.1016/j.clinbiochem.2007.12.021
61. El Habbal MH, Smith L, Elliott MJ, Strobel S. Effect of heparin anticoagulation on neutrophil adhesion molecules and release of IL8: C3 is not essential. *Cardiovasc Res*. (1995) 30:676–81.
62. Pieterse E, Rother N, Yanginlar C, Hilbrands LB, van der Vlag J. Neutrophils discriminate between lipopolysaccharides of different bacterial sources and selectively release neutrophil extracellular traps. *Front Immunol*. (2016) 7:484. doi: 10.3389/fimmu.2016.00484
63. Joshi MB, Lad A, Bharath Prasad AS, Balakrishnan A, Ramachandra L, Satyamoorthy K. High glucose modulates IL-6 mediated immune homeostasis through impeding neutrophil extracellular trap formation. *FEBS Lett*. (2013) 587:2241–6. doi: 10.1016/j.febslet.2013.05.053
64. Van Avondt K, van der Linden M, Naccache PH, Egan DA, Meyaard L. Signal inhibitory receptor on leukocytes-1 limits the formation of neutrophil extracellular traps, but preserves intracellular bacterial killing. *J Immunol*. (2016) 196:3686–94. doi: 10.4049/jimmunol.1501650
65. Mor-Vaknin N, Saha A, Legendre M, Carmona-Rivera C, Amin MA, Rabquer BJ, et al. DEK-targeting DNA aptamers as therapeutics for inflammatory arthritis. *Nat Commun*. (2017) 8:14252. doi: 10.1038/ncomms14252
66. Hazeldine J, Harris P, Chapple IL, Grant M, Greenwood H, Livesey A, et al. Impaired neutrophil extracellular trap formation: a novel defect in the innate immune system of aged individuals. *Aging Cell* (2014) 13:690–8. doi: 10.1111/acel.12222
67. Richardson JJR, Hendrickse C, Gao-Smith F, Thickett DR. Characterization of systemic neutrophil function in patients undergoing colorectal cancer resection. *J Surg Res*. (2017) 220:410–418.e411. doi: 10.1016/j.jss.2017.07.036
68. Besarab A, DeGuzman A, Swanson JW. Effect of albumin and free calcium concentrations on calcium binding *in vitro*. *J Clin Pathol*. (1981) 34:1361–7.
69. Guillaume YC, Guinchard C, Berthelot A. Affinity chromatography study of magnesium and calcium binding to human serum albumin: pH and temperature variations. *Talanta* (2000) 53:561–9.
70. Gupta AK, Giaglis S, Hasler P, Hahn S. Efficient neutrophil extracellular trap induction requires mobilization of both intracellular and extracellular calcium pools and is modulated by cyclosporine A. *PLoS ONE* (2014) 9:e97088. doi: 10.1371/journal.pone.0097088
71. Knight JS, Subramanian V, O'Dell AA, Yalavarthi S, Zhao W, Smith CK, et al. Peptidylarginine deiminase inhibition disrupts NET formation and protects against kidney, skin and vascular disease in lupus-prone MRL/lpr mice. *Ann Rheum Dis*. (2015) 74:2199–206. doi: 10.1136/annrheumdis-2014-205365
72. Tatsiy O, McDonald PP. Physiological stimuli induce PAD4-dependent, ROS-independent NETosis, with early and late events controlled by discrete signaling pathways. *Front Immunol*. (2018) 9:2036. doi: 10.3389/fimmu.2018.02036
73. Lewis HD, Liddle J, Coote JE, Atkinson SJ, Barker MD, Bax BD, et al. Inhibition of PAD4 activity is sufficient to disrupt mouse and human NET formation. *Nat Chem Biol*. (2015) 11:189–91. doi: 10.1038/nchembio.1735
74. Pedersen F, Waschki B, Marwitz S, Goldmann T, Kirsten A, Malmgren A, et al. Neutrophil extracellular trap formation is regulated by CXCR2 in COPD neutrophils. *Eur Respir J*. (2018) 51:1700970. doi: 10.1183/13993003.00970-2017

75. Chen K, Nishi H, Travers R, Tsuboi N, Martinod K, Wagner DD, et al. Endocytosis of soluble immune complexes leads to their clearance by FcgammaRIIIB but induces neutrophil extracellular traps via FcgammaRIIA *in vivo*. *Blood* (2012) 120:4421–31. doi: 10.1182/blood-2011-12-401133
76. Villanueva E, Yalavarthi S, Berthier CC, Hodgin JB, Khandpur R, Lin AM, et al. Netting neutrophils induce endothelial damage, infiltrate tissues, and expose immunostimulatory molecules in systemic lupus erythematosus. *J Immunol*. (2011) 187:538–52. doi: 10.4049/jimmunol.1100450
77. Saffarzadeh M, Juenemann C, Queisser MA, Lochnit G, Barreto G, Galuska SP, et al. Neutrophil extracellular traps directly induce epithelial and endothelial cell death: a predominant role of histones. *PLoS ONE* (2012) 7:e32366. doi: 10.1371/journal.pone.0032366
78. Radic M, Marion TN. Neutrophil extracellular chromatin traps connect innate immune response to autoimmunity. *Semin Immunopathol*. (2013) 35:465–80. doi: 10.1007/s00281-013-0376-6
79. Meng W, Paunel-Gorgulu A, Flohe S, Witte I, Schadel-Hopfner M, Windolf J, et al. Deoxyribonuclease is a potential counter regulator of aberrant neutrophil extracellular traps formation after major trauma. *Mediators Inflamm*. (2012) 2012:149560. doi: 10.1155/2012/149560

Conflict of Interest Statement: The authors declare that the research was conducted in the absence of any commercial or financial relationships that could be construed as a potential conflict of interest.

Copyright © 2019 Neubert, Senger-Sander, Manzke, Busse, Polo, Scheidmann, Schön, Kruss and Erpenbeck. This is an open-access article distributed under the terms of the Creative Commons Attribution License (CC BY). The use, distribution or reproduction in other forums is permitted, provided the original author(s) and the copyright owner(s) are credited and that the original publication in this journal is cited, in accordance with accepted academic practice. No use, distribution or reproduction is permitted which does not comply with these terms.

2.4 Supplementary information, manuscript II

Supplementary tables

Supplementary tables including full lists of supplementary references are available online.
Full link: https://www.frontiersin.org/articles/10.3389/fimmu.2019.00012/full

Supplementary figures

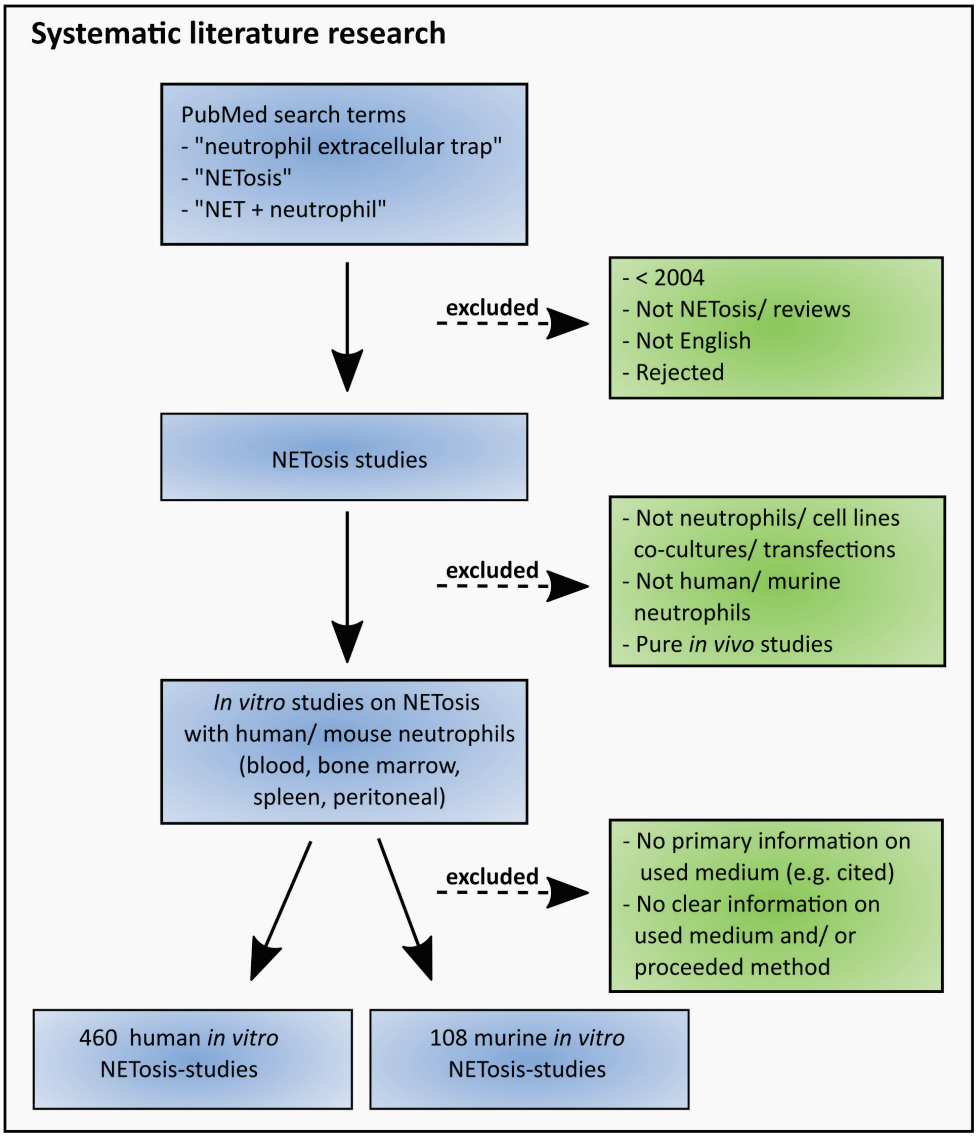

Supplementary figure 1: Literature research.

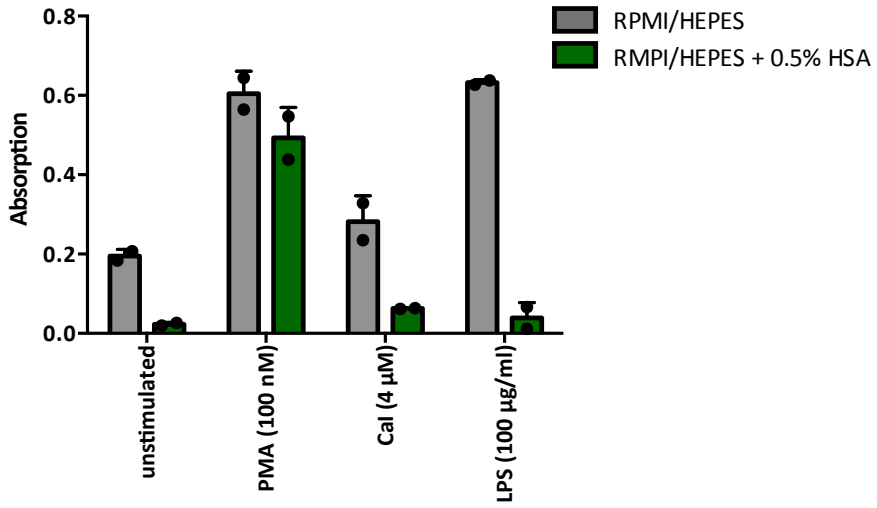

Supplementary figure 2: Neutrophil elastase (NE) is released together with extracellular DNA after stimulation. DNA-bound NE was measured after stimulation of human neutrophils by PMA (100 nM, 3h), CaI (4 µM, 2h) or LPS (100 µg/ml, 3h) in RPMI/HEPES with and without HSA. Neutrophils release DNA-bound NE in response to all stimuli. In media containing 0.5% HSA the release is clearly decreased after LPS and CaI stimulation, but appears stable in response to PMA. Error bars = mean ± SD. N = 2.

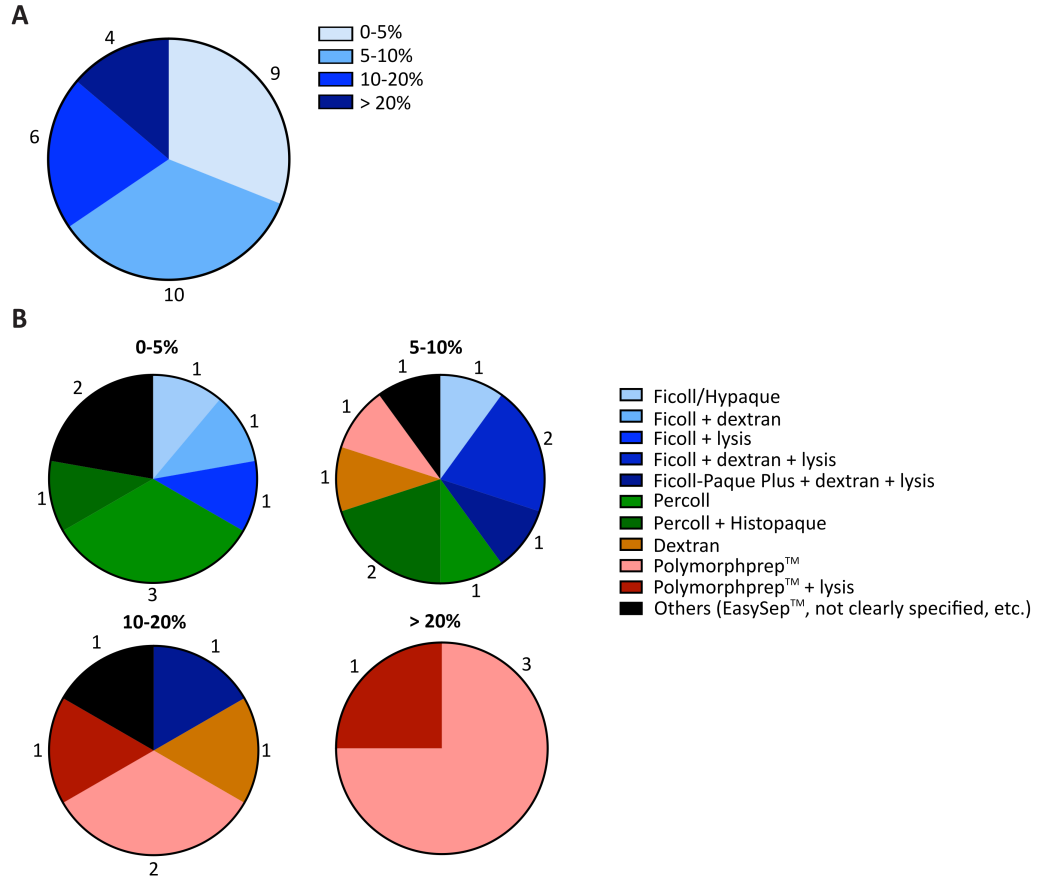

Supplementary figure 3: Spontaneous NETosis in literature. (A) Percent of spontaneous NET formation in publications using serum- and albumin-free culture conditions. NETosis without further stimulation of isolated human neutrophils range between 0% and more than 20% NETotic cells. N = 29 publications with clear displayed percentage of NETs (out of all 255 publication without serum-supplements). **(B)** Spontaneous NET formation depending on neutrophil isolation technique. In literature neutrophils isolated by Polymorphprep™ show a higher tendency for spontaneous NET formation than neutrophils isolated by density-gradient techniques.

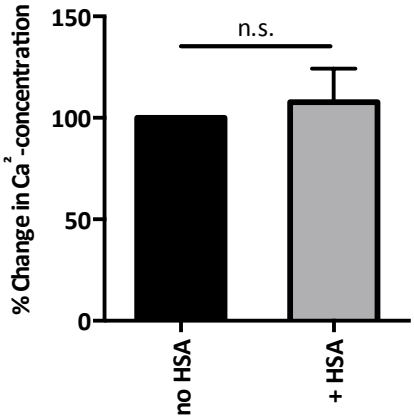

Supplementary figure 4: HSA does not influence calcium concentrations. The concentration of calcium in PBS does not significantly change in presence or absence of 0.5% HSA. Statistic: two-tailed t test. ns = not significant. N = 3. Error = SD.

2.5 Manuscript III

"Blue and Long-wave Ultraviolet Light Induce *in vitro* Neutrophil Extracellular Trap Formation"

Elsa Neubert[1,2*], Katharina M. Bach[1*], Julia Busse[1], Ivan Bogeski[3], Michael P. Schön[1,5], Sebastian Kruss[2,4] and Luise Erpenbeck[1+]

These authors contributed equally: Elsa Neubert and Katharina M. Bach.

[1]Department of Dermatology, Venereology and Allergology, University Medical Center Göttingen, Göttingen, Germany
[2]Institute of Physical Chemistry, Göttingen University, Göttingen, Germany
[3]Department of Cardiovascular Physiology, University Medical Center Göttingen, Göttingen, Germany
[4]Center for Nanoscale Microscopy and Molecular Physiology of the Brain (CNMPB), Göttingen, Germany
[5]Lower Saxony Institute of Occupational Dermatology, University Medical Center Göttingen, Germany

The following paragraph is prepared for submission to *Frontiers in Immunology*.

Key points:

Ultraviolet A (UVA) and blue light induce NET formation in a neutrophil elastase- and myeloperoxidase-dependent fashion. Riboflavin acts as a photosensitizer that generates extracellular ROS. This process may contribute to light-sensitivity in autoimmune diseases like systemic lupus erythematosus.

Abstract

Neutrophil Extracellular Traps (NETs) are produced by neutrophilic granulocytes and consist of decondensed chromatin decorated with antimicrobial peptides. They defend the organism against intruders and are released upon various stimuli including pathogens, mediators of inflammation or chemical triggers. NET formation is also involved in inflammatory, cardiovascular, malignant diseases and autoimmune disorders like rheumatoid arthritis, psoriasis or systemic lupus erythematosus (SLE). In many autoimmune diseases like SLE or dermatomyositis, light of the ultraviolet-visible (UV-VIS) spectrum is well known to trigger and aggravate disease severity. However, the underlying connection between NET formation, light exposure and disease exacerbation remains enigmatic.
Therefore, we studied the effect of UVA (375 nm), blue (470 nm) and green (565 nm) light on NETosis in human neutrophils *ex vivo*. Our results show a dose- and wavelength-dependent induction of NETosis. Light-induced NETosis depended on the generation of extracellular ROS in response to riboflavin excitation and subsequent reaction with substrates like tryptophan. This process required both neutrophil elastase (NE) and myeloperoxidase (MPO) activation. These findings suggest that NET formation as a response to light could be the hitherto missing link between elevated susceptibility to NET formation in autoimmune patients and photosensitivity for example in SLE and dermatomyositis patients. This novel connection could provide a clue for a deeper understanding of light-sensitive diseases in general and for the development of new pharmacological strategies to avoid disease exacerbation upon light exposure.

Introduction

Neutrophilic granulocytes (hereafter referred to as neutrophils) are able to expel fibril networks of decondensed chromatin, decorated with a variety of antimicrobial substances, in a process termed neutrophil extracellular trap (NET) formation or NETosis [1]. Initially, NETosis was seen as an immune defense strategy against intruding pathogens, distinct from phagocytosis and the release of cytotoxic substances [2]. Apart from their role in the defense within the innate immune system, the dysregulation of NETosis appears to be involved in the pathology of various diseases [3] such as rheumatoid arthritis [4], systemic lupus erythematosus (SLE) [5], psoriasis [6, 7], thrombosis [8], atherosclerosis [9] and cancer [10]. The activation mechanisms and underlying cascades of NETosis depend highly on the particular stimulus [11, 12]. Additionally, neutrophils are very sensitive to environmental

cues that affect for example adhesion [13, 14]. Therefore, factors that govern adhesion such as substrate stiffness or other environmental factors such as the presence of serum proteins, affect NETosis [15, 16]. In most scenarios, the cell undergoes a characteristic sequence of morphological changes during NETosis including chromatin decondensation, cytoskeleton degradation, cell rounding and softening, which ultimately lead to NET expulsion and cell death ('suicidal' NETosis) [2, 17]. Initially, active enzyme-dependent mechanisms dominate these processes ('first phase' of NETosis). For instance, the initiation of chromatin decondensation often involves the release of neutrophil elastase (NE) and myeloperoxidase (MPO) from the neutrophil granules and subsequent translocation to the nucleus [18, 19]. After start of chromatin decondensation, which represents the point of no return in NETosis, further progression until the NET release is mainly driven by the material properties of the NETotic cell such as the entropic swelling of its chromatin ('second phase') [17] .

Interestingly, a connection between dysregulated NET formation and the production of autoantibodies against NET components has been implicated in several diseases including SLE, rheumatoid arthritis and small-vessel vasculitis [20, 21]. Mechanistically, NET formation often relies on the activity of peptidylarginine deiminase 4 (PAD4), which travels to the nucleus and citrullinates histones contributing to chromatin decondensation [22-27]. This hypercitrullination has been linked to the development of autoantigens against citrullinated histones for instance in the pathogenesis of rheumatoid arthritis [28]. Strikingly, a defect in the clearance of NETs (for example through impaired DNase activity or increased NET formation) appears to be directly associated with the development of autoimmune diseases, which has become especially evident in the pathogenesis of systemic lupus erythematosus [29]. The latter, as well as other autoimmune disorders such as dermatomyositis, can be triggered and/or aggravated by light. Interestingly, although for systemic lupus erythematosus both the increased propensity for NET formation as well as the marked light sensitivity is well documented [30-32], the connection between these two phenomena has not been yet thoroughly investigated.

Electromagnetic radiation of wavelengths above ultraviolet C (UVC) light passes the ozone layer of the stratosphere and is therefore able to reach the human skin [33]. Once there, the light intensity is modified by reflection, absorption and scattering [34]. The penetration depth of the light into the human skin increases with higher wavelengths, while the energy decreases [35, 36]. This connection could lead to a 'window' in which light, whose energy is sufficient to initiate certain biological processes, penetrates into skin layers in which susceptible cells occur. The actual penetration of each wavelength depends strongly on the specific skin composition, as well as body region, age, gender, skin type, pigmentation and therefore ethnicity.
High-energy UV light causes severe skin damage. This has been linked not only to photodermatoses but also to phototoxic and photoallergic reactions, skin cancer and photoaging [37, 38]. Many of these reactions are mediated by highly reactive radicals and/or reactive oxygen species (ROS) originating from the excitation of photosensitive substances

[39]. Prominent examples are flavin-based molecules originating from riboflavin (also knows as vitamin B2). After excitation, flavins can react with biological substrates such as DNA, proteins, lipids and aromatic amino acids (tryptophan and tyrosine) and forms a variety of photo-adducts [40]. Under physiological conditions, these reactions are kept in balance by antioxidants, but can be strongly dysregulated in the context of diseases and after persistent exposure to UV light. Furthermore, light has immunomodulatory activities and affects cell functions within the skin [41-43]. For instance, irradiation with UVB light recruits neutrophils into upper layers of the skin and has been linked to photoaging [38, 46]. Furthermore, increased apoptosis rates of neutrophils occur upon direct irradiation with high doses of UVB or UVC light [44, 45]. UVC light can also induce a unique form of NOX-independent NETosis (named apoNETosis) [44]. However, the physiological relevance of this observation is questionable, as UVC light does not reach the earth's surface at all and even if it did, it would not penetrate human skin in large amounts. Direct contact with neutrophils is therefore precluded. In consequence, the connection between NET formation and light in a physiologically relevant setting is still elusive. Thus, a deeper understanding of direct effects of light on immune cells could greatly add to our understanding of light-induced or -aggravated diseases and facilitate the development of therapeutic strategies.
Here, we show that neutrophils release NETs *ex vivo* in response to UVA/blue light in a ROS- and NE/MPO-dependent manner. This process depends on the excitation of the photosensitive substance riboflavin and subsequent generation of extracellular ROS. Thus, these results provide a link between NET formation and direct effects of UVA and blue light on neutrophils.

Material and Methods

Isolation of neutrophils

All experiments with human neutrophils were approved by the Ethics Committee of the University Medical Center (UMG) Göttingen (protocol number: 29/1/17). Neutrophils were isolated from fresh venous blood of healthy donors. Beforehand, all donors were fully informed about possible risks, and their informed consent was obtained in writing, consent could be withdrawn at any time during the study. Blood was collected in S-Monovettes EDTA (7.5 ml, Sarstedt), and neutrophils were isolated according to previously published protocols based on histopaque 1119 (Sigma Aldrich) as well as percoll (GE Healthcare) density gradients [17, 47]. Neutrophils were resuspended in $HBSS^{-Ca2+/Mg2+}$ and further diluted in the desired medium as described in the appropriate methods sections and figure legends. Purity of the cell preparation was > 95% as assessed by cytospin (Cytospin 2 centrifuge, Shanson) and Diff Quick staining (Medion, Diagnostics).

Irradiation of neutrophils with LED light

Neutrophils were suspended in either Roswell Park Memorial Institute (RPMI) comp. (RPMI without phenol red (Gibco) + 0.5% heat-inactivated (at 56°C) fetal calf serum (hiFCS, Biochrom GmbH, Merck Millipore)) +/- 10 mM HEPES (Roth) or Hank's balanced salt solution

(HBSS) comp. ($HBSS^{+Ca2+/Mg2+}$ without phenol red (Lonza) containing 0.5% hiFCS and glucose (AppliChem) equalized to RPMI). If applicable, these media were supplemented with 0.2 or 2 mg/l riboflavin (Sigma-Aldrich) and 1 mM tryptophan (Sigma-Aldrich) as indicated in the figure captions. Cells were seeded at 10,000 cells per well in CELLviewTH black glass-10-well-slides (Greiner bio-one) and left to settle for 30 minutes (37°C, 5% CO_2). Afterward, the appropriate medium (volume equal to PMA stimulation) was added and cells were irradiated with the indicated LED-light at 37°C (ibidi heating system). Cells were irradiated in the heating chamber from below with LEDs of 375 nm (ultraviolet light, M375L3 Mounted LED, Thorlabs GmbH), 470 nm (blue light, M470L3 Mounted LED, Thorlabs GmbH) or 565 nm (green light, M565L3 Mounted LED, Thorlabs GmbH), which were attached to an uncoated convex lens (PLANO-CONVEX LA1131, f = 50.0 mm, uncoated, Thorlabs GmbH) and a T-cube LED Driver (Thorlabs GmbH). For evaluation of light dose-dependent effects, cells were irradiated with cumulative doses of 3.5 J/cm^2, 18 J/cm^2, 35 J/cm^2 and 70 J/cm^2 at 375 nm or 21 J/cm^2, 54 J/cm^2, 107 J/cm^2 and 214 J/cm^2 at 470 nm. The light doses were calculated with respect to the actual power of the LED as measured with the PM12-122 Compact USB Power Meter (Thorlabs GmbH), taking into account the actual distance between the light source and the cells as well as the light transmission through the CELLviewTH glass-10-well-slides according to the manufacturer's specifications. For experiments with equal light energy or photon flux, the light-doses or duration of exposure, respectively, were adjusted for 470 nm and 565 nm, the reference value was irradiation with 70 J/cm^2 at 375 nm. Exclusive treatment with the indicated medium without irradiation was used as negative control and activation with 100 nM PMA (Sigma Aldrich) as positive control. Before, during and after activation with light or PMA the cells were carefully shielded from other light sources. After the activation, the cells were incubated for 3 hours, and NETosis was stopped by fixing the cells in 2% paraformaldehyde (PFA, Roth). Before further staining, the cells were kept at 4°C.

Inhibitor experiments

For inhibition experiments, cells were isolated, settled in RPMIcomp. supplemented with 10 mM HEPES and activated as described above. Inhibitors or ROS scavengers were added at least 20 minutes (in case of MitoTEMPO 1h) before cell irradiation with 70 J/cm^2 of 375 nm or 214 J/cm^2 of 470 nm, at 37°C. For an additional control experiment, Trolox and catalase/SOD were separately added after irradiation. The cells were then incubated for an additional 3 hours in the presence of the inhibitors to allow for NET formation and fixed by 2 % PFA. Pure medium or 100 nM PMA without irradiation were used as negative and positive controls, respectively. The following inhibitors and ROS scavengers were used in this study: GW-311616A hydrochloride (iNE, Axon Medchem) at 5 µM, 4-aminobenzoic acid hydrazide (4-ABAH, Cayman chemicals) at 100 µM, z-VAD-FMK (Promega) at 20 µM, necrostatin-1 (Nec-1, Enzo) at 50 µM, Y-27632-dihydrochloride (Abcam) at 20 µM, Cl-amidine (Merck Millipore) at 200 µM, MitoTEMPO (Sigma-Aldrich) at 5 µM, diphenyleneiodonium chloride (DPI, Sigma-Aldrich) at 1 µM, Trolox (Sigma-Aldrich) at 50 µM, and a mixture of catalase (filtered, Worthington) and superoxide dismutase (SOD, Sigma Aldrich/Merck) at 2,000 U/ml and 50 U/ml, respectively.

NET quantification

To investigate levels of NETosis, cells were washed two times with PBS (Sigma-Aldrich) and, subsequently, neutrophil DNA was stained with 1.62 µM Hoechst 33342 (Thermo Fisher Scientific) for 15 minutes. After staining, the cells were stored in PBS for further analysis. For blinded quantification, six microscopic fluorescence images (16x) were obtained in a standardized manner (Axiovert 200 equipped with EC Plan-Neofluar Ph1 and DAPI filter Set 49, Zeiss, software: Metamorph 6.3r2., Molecular Devices or Micro Manager 1.4) using the camera CoolSNAP ES (Photometrics). The number of decondensed vs. condensed nuclei was counted in these images using ImageJ 1.46r (National Institutes of Health), and the relative number of decondensed nuclei/expelled NETs was determined as percentage of total cells ('NETosis rate') according to previously published studies [17, 48]. Relative NETosis rates were calculated for the inhibitor experiments vs. experiments without inhibitor.

Live cell imaging/discontinuous irradiation of neutrophils

Neutrophils ($5x10^6$ per ml in RPMI + 0.5% HSA + 10 mM HEPES) were seeded in ibidi channel slides (µ-Slide $I^{0.6}$ Luer, ibidi) and stained with 1.62 µM Hoechst at 37°C for 10 min. Cells were irradiation with broad-spectrum UVA light (300-400 nm) for 3 min using the DAPI filter Set 49, and NET formation was observed in real time for 3.5 hours with a frame rate of one picture (Uniblitz stutter driver, model VCM-D1, Visitron Systems) per minute and 15 ms exposure time. Images were recorded at 16x magnification. To exclude toxic effects by photo-activation of Hoechst, a control experiment was performed without DNA staining during live cell imaging. In this case, NET rates were determined by Hoechst staining directly after 3.5 hours. Images in the center of the light beam and in non-irradiated areas were obtained in a standardized pattern and in a blinded manner, and NETosis rates determined as described above. The representative combined panorama image in **figure 1** was obtained with the Plugin MosaicJ for ImageJ [49].

Immunofluorescence staining

To prove co-localization of MPO with decondensed chromatin as a marker for NETosis, activated cells were analyzed by immunofluorescence according to previously published protocols [17]. For the staining, the primary monoclonal anti-human antibody against myeloperoxidase (IgG1, mouse, clone:2C7, ab25989, 1:1000, Abcam) and the polyclonal anti-mouse Alexa488 secondary antibody (IgG, goat, 1:1000, #4408, Cell Signaling Technology) were used. Directly before mounting with fluorescence mounting medium (Dako), DNA was stained with Hoechst. Co-localization of MPO and DNA was imaged at 40x magnification (Plan-Neofluar 40x/1,30 Oil, Zeiss) by fluorescence microscopy (Axiovert 200, Zeiss; software: Metamorph 6.3r2., Molecular Devices).

ROS Detection/AmplexRed assay

Cells were seeded at 10,000 cells per well in RPMIcomp. + 10 mM HEPES, HBSScomp. or HBSScomp. + 2 mg/l riboflavin + 1 mM tryptophan and activated at 70 J/cm^2 of 375 nm light. After activation, 5 µl-samples of the supernatant were taken at defined time points (0, 10,

20, 30, or 40 min) close to the slide bottom for reactive oxygen species (ROS) detection. As controls, cells in all three media were either left without irradiation, only media was irradiated or cells were treated with 100 nM PMA without irradiation. The obtained samples were diluted in a black 96-well-plate (BRANDplates, BRAND GMBH) with PBS containing 50 µM of AmplexRed reagent (Thermo Fisher Scientific), a highly sensitive probe for H_2O_2, and 0.5 U/ml horseradish peroxidase (HRP, Sigma-Aldrich/Merck). Additionally, 10 U/ml SOD (Sigma Aldrich/Merck) were added, to ensure complete detection of ROS by transformation of superoxide radicals to H_2O_2. During the sample collection, cells were gently rocked to ensure equal distribution of ROS. For all samples, the fluorescence intensities of the formed resorufin were measured with the microplate reader Clario Star (software 5.40.R3, BMG labtech), and the results were processed with the software MARS (version 3.32, BMG labtech). Absolute H_2O_2 concentrations were determined *via* calibration with H_2O_2 (Roth) in HBSScomp. After ROS detection, cells were further incubated for a total of 3 hours before terminating the activity with 2% PFA, and relative NET amounts were determined.

Light absorption by riboflavin

The absorbance spectrum of riboflavin (Sigma-Aldrich) was obtained in PBS against PBS alone with the UV-VIS-NIR spectrometer (JASCO V-670, Spectra Manager Software) using a 10 mm-path cuvette.

Statistics

Statistical analysis was performed using GraphPad Prism (version 6.0 for Mac, GraphPad Software Inc.). If applicable, GAUSS distribution was confirmed by the Shapiro-Wilk normality test. Significance was assessed by a one-way or a two-way ANOVA/Bonferroni's multiple comparisons test with *p<0.05, **p<0.01, ***p<0.001, ****p<0.0001. Error = mean± standard error of the mean (SEM) or standard deviation (SD), as indicated.

Results

UVA and blue light induce NETosis dose-dependently

To investigate whether UVA light is sufficient to activate NETosis, freshly isolated human neutrophils were irradiated for 3 minutes with physiologically relevant broad-spectrum UVA light in a standard microscopy setup (wavelengths 300-400 nm, approx. 60 J/cm^2). Morphological changes of the nuclei were recorded using Hoechst staining over 3.5 hours in real-time (**Supplementary movie**). Neutrophilic chromatin readily decondensed over time, rounded up and finally formed cloud-like structures of decondensed chromatin 1-2 hours after exposure to light. This characteristic rearrangement of chromatin is consistent with previously published live-cell studies of NETosis [17, 50-52] and morphologically similar to PMA-induced NETosis (100 nM) observed in the same setup [17]. Interestingly, this dramatic effect was restricted to the light-exposed area and did not occur in unexposed areas (> 1500 µm from the light center) (**Figure 1**). In addition, the effect was reproducible with neutrophils from different donors (**Supplementary figure 1**). To exclude light-induced

cytotoxic effects of the Hoechst chromatin staining, neutrophils were stained after the full incubation period of 3.5 hours (**Figure 1).**

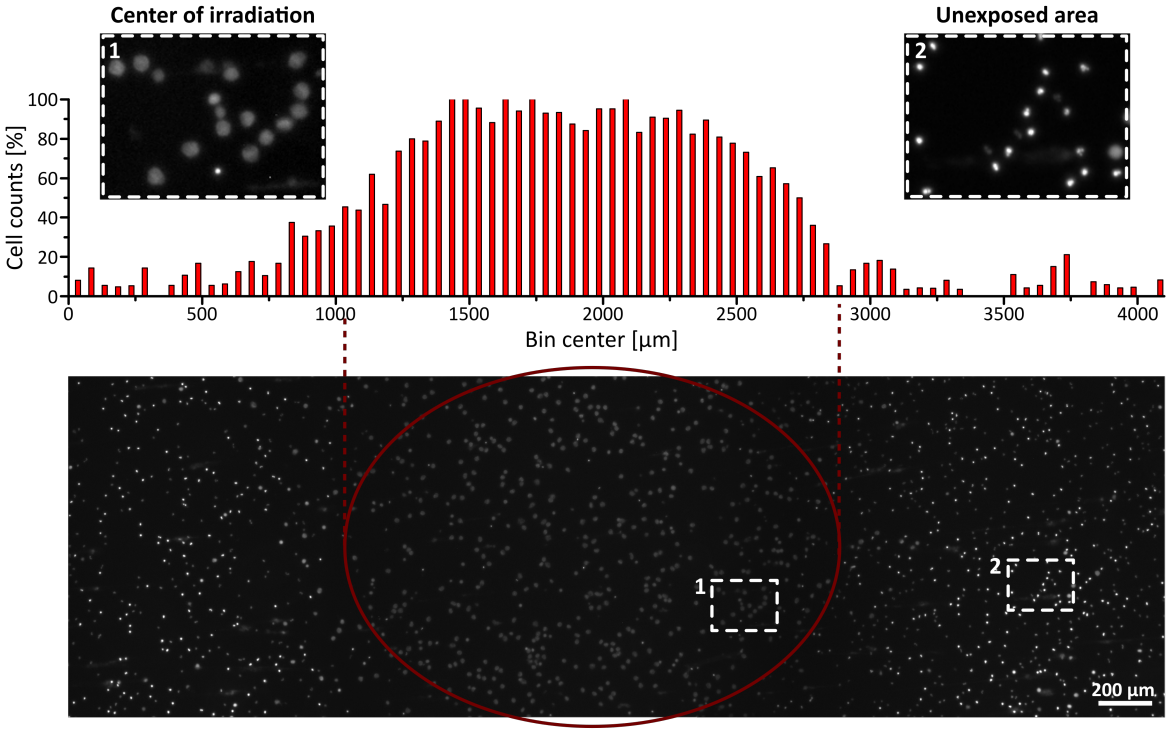

Figure 1: UVA light-induced, locally restricted decondensation of chromatin. UVA light (300-400 nm, approx. 60 J/cm^2) leads to chromatin decondensation. This effect is locally restricted to the area of irradiation. Irradiation: 3 minutes to induce NET formation + intermitted during live-cell imaging (3.5 hours; frame rate: 1 image/min) (see s**upplementary movie**). Chromatin was stained (Hoechst) after full light exposure to exclude light-induced cytotoxicity by the dye.

For the initial experiments in **figure 1,** broad-spectrum UVA (300-400 nm) light was used, and cells were observed over 3.5 hours with a combination of continuous (cell activation) and intermittent light exposure (live-cell imaging). Therefore, to verify the obtained results in a controlled fashion, we established a precisely defined LED-light-based setup and irradiated the cells from below with light of distinct wavelengths and doses (**Figure 2**). Cells were exposed to 3.4 J/cm^2, 18 J/cm^2, 35 J/cm^2 or 70 J/cm^2 of UVA light (375 nm) and 21 J/cm^2, 54 J/cm^2, 107 J/cm^2 or 214 J/cm^2 of visible blue light (470 nm). Light-induced chromatin decondensation was dose-dependent and started with significant rates of NETosis at 70 J/cm^2 for 375 nm and at 107 J/cm^2 for 470 nm, respectively (**Figure 2A/B**). For both tested wavelengths, the decondensed chromatin colocalized with MPO, a typical feature of NET formation (**Figure 2C**).

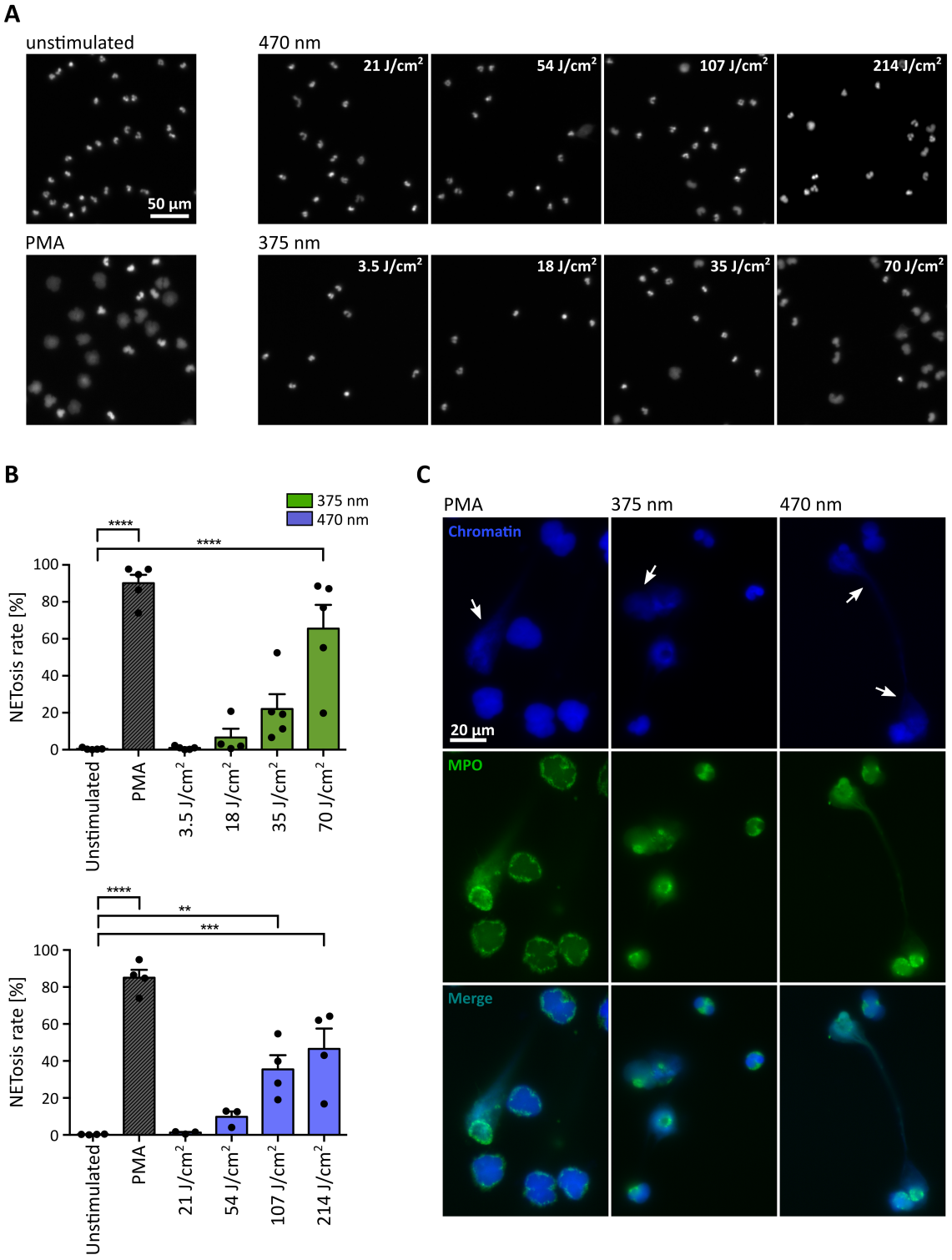

Figure 2: UVA and blue light induce the formation of NETs in a dose-dependent manner. (**A**) Representative fluorescence images of neutrophils exposed to different doses of LED-light (375 nm (3.4 J/cm^2, 18 J/cm^2, 35 J/cm^2 and 70 J/cm^2) or 470 nm (21 J/cm^2, 54 J/cm^2, 107 J/cm^2 and 214 J/cm^2)). Decondensation of chromatin, stained by Hoechst, clearly increases with duration of light exposure and shows a similar morphology as seen after activation with 100 nM PMA. (**B**) NET rates significantly increase for both tested LEDs with light doses. Statistics: one-way-ANOVA with Bonferroni's multiple comparisons test (tested against unstimulated cells). **p < 0.01, ***p < 0.001, ****p < 0.0001. N = 3-5 independent experiments. Error bars = SEM. (**C**) Decondensed chromatin (blue/Hoechst, arrows) after irradiation colocalizes with MPO (green/alexa488) for both tested wavelengths, similar to PMA-induced NETosis. Cells were fixed before performing microscopy. Cells were kept in RPMIcomp. + 10 mM HEPES.

Light-induced NETosis depends on MPO and NE

One of the hallmarks of NET formation is the strong dependency on enzyme activity, especially in the first phase of NETosis, enabling histone modification and, consequently, chromatin decondensation [17]. The involved enzymes can vary among different stimuli. In most cases, the activation of granular enzymes such as NE and MPO or members of the PAD family, particularly PAD4, are indispensable. Therefore, we inhibited the activity of various enzymes known to be involved in chromatin decondensation or required for associated signaling cascades of well-described activators of NETosis.

For both tested wavelengths a significant reduction of NETosis was observed in the presence of the MPO-inhibitor 4-aminobenzoic acid hydrazide (4-ABAH, 100 µM) [53] or the NE-inhibitor GW-311616A (iNE, 5 µM) [54] (**Figure 3A/B**). Both inhibitors efficiently blocked the decondensation of chromatin (**Figure 3A**), thus indicating that decondensation in light-induced NETosis depended on MPO and NE activity as reported for PMA-induced NETosis [18, 19]. Additionally, inhibition of PAD activity by Cl-amidine (200 µM) [55] reduced NET formation after irradiation with light of both wavelengths by around 25-50%. This effect reached significance for irradiation with blue light (470 nm-LED; **Figure 3B**). Therefore, it is likely that the activity of PAD enzymes can enhance light-induced NETosis by modifying proteins, particularly histones by citrullination [22, 23, 56]. Dependency on Rho-associated coil kinase 1 and 2 (ROCK 1/2) activity, which is implicated in cytoskeleton regulation, has only recently been linked to PMA-induced NETosis [17]. Nonetheless, irradiation of neutrophils in the presence of Y-27632 (20 µM) blocking the ATP binding site of ROCK 1/2 [57], showed no effect on NETosis rates in response to light (**Figure 3B**). It is important to note that inhibitors were still functional after irradiation with UVA light as demonstrated in PMA-induced NET formation (**Supplementary figure 2A**).

In order to exclude that the observed effects are associated with neutrophil apoptosis or necroptosis, the involvement of caspases and the receptor-interacting protein kinase (RIPK) 1/3-mixed lineage kinase domain-like protein (MLKL)-necroptosis-pathway after UVA irradiation was investigated. Toward this end, cells were irradiated in the presence of the pan-caspase inhibitor z-VAD-FMK (20 µM) [58] and the RIP1 kinase inhibitor necrostatin-1 (Nec-1, 50 µM) [59], respectively. Indeed, the involvement of apoptotic or necroptotic pathways was not detected (**Supplementary figure 2B**).

Altogether, these findings suggest that UVA and blue light induce NETosis in an MPO- and NE-dependent manner. This process can be supported by PAD enzymes and appears to be independent of caspases and RIPK1 activity.

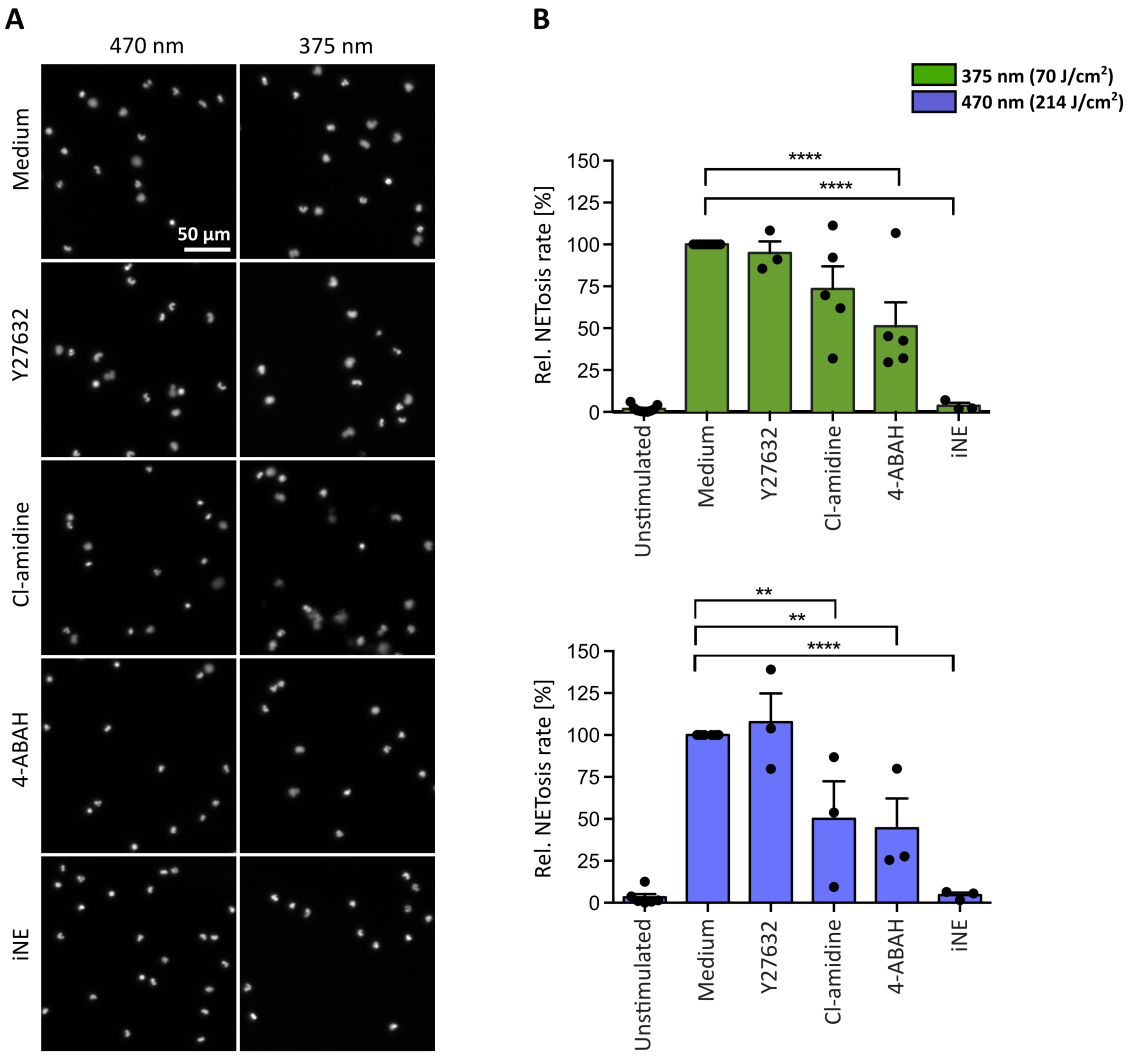

Figure 3: Neutrophil elastase (NE) and myeloperoxidase (MPO) are indispensable for light-induced NETosis. (**A**) Representative images of neutrophil nuclei stained by Hoechst after exposure to UVA (70 J/cm^2 of 375 nm) or blue light (214 J/cm^2 of 470 nm) in the presence of specific inhibitors. NETosis is clearly reduced upon inhibition of MPO (4-ABAH, 100 µM), NE (GW-311616A, iNE, 5 µM) and, to a lower extent, of PAD enzymes (Cl-amidine, 200 µM). However, neutrophils were still able to undergo NETosis in the presence of ROCK 1/2 inhibition by Y-27632 (20 µM). (**B**) Quantification of NETosis rates after irradiation with LED-light of 375 nm or 470 nm, respectively, in the presence of Y-27632, Cl-amidine, 4-ABAH or iNE. The inhibition of MPO and NE significantly reduces light-induced NET formation. Inhibition of PAD-enzymes decrease NET rates induced by LED-light of 375 nm, but significantly inhibited NET formation induced by light of 470 nm. However, NETosis appears independent of ROCK 1/2 activity. Statistics: one-way-ANOVA with Bonferroni's multiple comparisons test (tested against activation in medium). **p < 0.01, ****p < 0.0001. N = 3-6 independent experiments. Error bars = SEM. Cells were kept in RPMIcomp. + 10 mM HEPES.

Light-induced NETosis is mediated by riboflavin excitation and subsequent ROS generation

The penetration of light through the human skin depends strongly on the wavelength. Approximately 10-15% of UVA light and 40-50% of blue light can pass the epidermis and reach deeper layers [35, 36]. In principle, light of higher wavelengths penetrates deeper into the skin [36]. To evaluate whether light of higher wavelengths is also sufficient to induce NET formation, we irradiated neutrophils with light up to 700 nm (565 nm LED; green light), of

which more than 60% reach the dermis and in part, even the subcutaneous tissue [35]. To make comparisons possible, cells were irradiated with the same light energy (**Figure 4A**) and the same photon flux for each wavelength (**Figure 4B**). The calculations were based on 70 J/cm^2 375 nm-LED light. Interestingly, at the same energy and same photon flux, neutrophils did not undergo NETosis after exposure to green light, whereas irradiation with UVA or blue light revealed robust NETosis (**Figure 4A/B**).

Several substances, which are present at high concentrations in human skin, can absorb light in the UV-VIS region and were reported to enhance light-mediated tissue damage. One of the most prominent and well-documented photosensitizer is riboflavin [40, 60]. Riboflavin is present in tissues with permanent light exposure such as skin and eyes (3 mg/kg and 1.7 mg/kg dry matter, respectively [40]) and has multiple essential biological functions. Most prominently, it acts in flavoprotein-dependent processes as a precursor for FAD and FMN [60, 61]. Photosensitizing mechanisms of riboflavin are based on the absorption of UVA and blue light with maxima at 373 nm and 445 nm as confirmed within this study in line with previously published data [62] (**Figure 4C**). Riboflavin is excited to a stable triplet-state *via* a short-lived singlet-state. The excited triplet-state can directly react with oxygen (type II photoreaction) or with reactive substrates (type I photoreaction) to radicals or radical anions. These radicals can then further react with molecular oxygen to hydrogen peroxide (H_2O_2) or hydroxyl anions via superoxide anion radicals [40, 63, 64] (for a potential type I photoreaction with tryptophan see **Supplementary figure 3**). Importantly, riboflavin is present in the culture medium RPMI at 0.2 mg/l and was previously linked to an increased phototoxicity in culture media in *in vitro* studies. Such reactions were observed for instance in combination with the culture buffer 4-(2-hydroxyethyl)-1-piperazineethanesulfonic acid (HEPES) [65] or amino acids like tryptophan and tyrosine supplemented to RPMI [66].

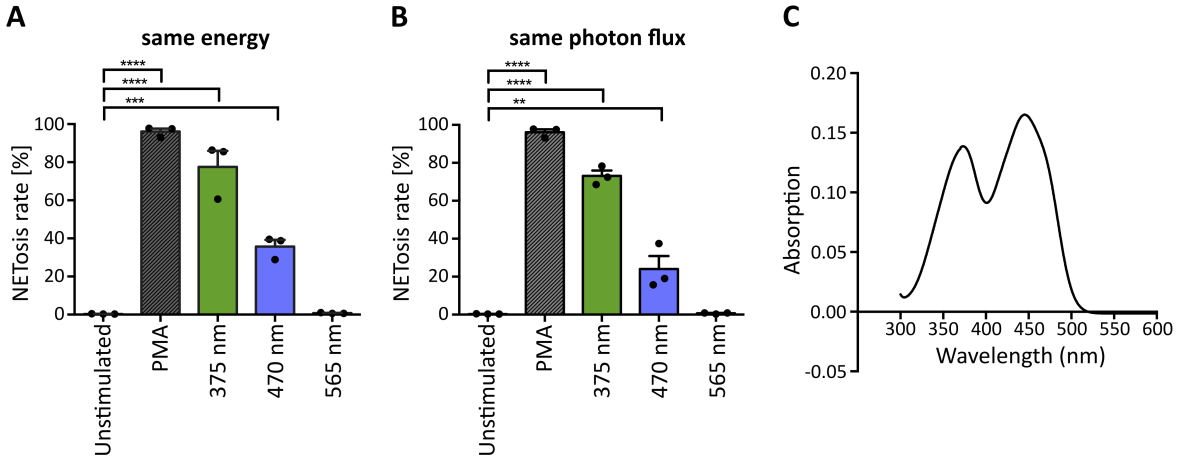

Figure 4: Wavelength-dependency of NET formation correlates with light absorption by riboflavin. UVA and blue light significantly induce NET formation at (**A**) the same energy and (**B**) the same photon flux, whereas green light (565 nm) does not induce NETosis under either condition. Cells were kept in RPMIcomp. + 10 mM HEPES. Statistics: one-way-ANOVA with Bonferroni's multiple comparisons test (tested against unstimulated cells). **p < 0.01, ***p < 0.001, ****p < 0.0001. N = 3 independent experiments. Error bars = SEM. (**C**) Riboflavin absorbs light in the UVA/blue light region with maxima at 373 nm and 445 nm. At 375 nm, the absorption is slightly higher (0.138), than at 470 nm (0.130).

Given the wavelength-dependency of NETosis, the absorption spectra of riboflavin (**Figure 4**) and the fact that H_2O_2 as a ROS can induce NETosis [2, 67-69], it appeared likely that the observed light-induced NETosis was mediated by the excitation of riboflavin and subsequent ROS production. To test this hypothesis, we first scavenged ROS by the cell-permeable vitamin E derivate Trolox at a concentration of 50 µM [70]. Indeed, scavenging ROS with Trolox significantly reduced NET formation in response to UVA irradiation (**Figure 5A**). To further analyze this mechanism in detail, extra- and intracellular ROS generation were addressed separately. Extracellular ROS was scavenged by a mixture of catalase and superoxide dismutase (SOD) (2,000 U/ml and 50 U/ml, respectively) [71, 72], NADPH oxidase-derived ROS was blocked by diphenyleneiodonium chloride (DPI, 1 µM) [73] and mitochondrial-derived ROS was inhibited by MitoTEMPO (5 µM) [74]. While the inhibition of intracellular ROS generation showed no effect on the obtained NETosis rates, scavenging extracellular ROS by catalase and SOD abrogated NETosis completely (**Figure 5A**). This result strongly supported the hypothesis that extracellular substrate-mediated production of ROS facilitated light-induced NETosis. Furthermore, the addition of the catalase-SOD-mixture after the irradiation was still fully sufficient to inhibit NETosis (**Supplementary figure 4C**) excluding that side products of catalase or SOD themselves after UVA irradiation were responsible for the observed effect.

In a second step, we studied the mechanism of extracellular ROS generation in greater depth. As described above, aromatic amino acids such as tryptophan can react with excited riboflavin/flavoproteins. As essential components of proteins, these amino acids are frequently expressed in human skin and can, therefore, contribute to ROS formation triggered by riboflavin excitation. To precisely evaluate the contribution of tryptophan to NET formation, neutrophils were irradiated in the culture buffer HBSS containing 0.5% FCS (HBSScomp.) supplemented with 0.2 mg/l or 2 mg/l riboflavin, a reasonable physiological range of riboflavin within human skin [40], in the presence or absence of 1 mM tryptophan. Indeed, in comparison to non-irradiated cells, UVA light exposure resulted in marked NETosis in the presence of both riboflavin and tryptophan. This effect was increased with the higher riboflavin concentration. In contrast, no NET formation was observed in pure HBSScomp. or in buffer supplemented exclusively with riboflavin (**Figure 5B**). These results strongly support the hypothesis that riboflavin mediated NET formation increases in the presence of additional substrates like tryptophan. Interestingly, a similar effect was observed for HEPES-buffer in RPMIcomp. NET rates markedly increased in the presence of HEPES, the standard medium condition used for this study, compared to RPMIcomp. without HEPES (**Supplementary figure 4A**).

To confirm this hypothesis, extracellular ROS levels were measured after irradiation in the above-described solutions based on an AmplexRed assay. In line with the observed NET rates (**Figure 5B**), irradiation with UVA light led to dramatically increased extracellular ROS levels in both RPMIcomp. + HEPES as well as HBSScomp. + riboflavin (2 mg/l) + tryptophan (**Figure 5C**). Sole irradiation of these two media compositions consistently resulted in stable ROS levels of 60 µM to 100 µM. In contrast, irradiation of supplement-free HBSScomp. as well as culturing of cells in media without irradiation did not lead to ROS production. As a

control, extracellular ROS levels were determined after activation with 100 nM PMA. As expected, low levels of extracellular ROS were observable after PMA treatment, which increased over time (**Figure 5C**) [71]. Importantly, in this experimental setup, we obtained NET rates comparable to the rates displayed in **figure 5B** after UVA irradiation of cells in RPMIcomp. + HEPES or HBSScomp. + riboflavin (2 mg/l) + tryptophan (**Supplementary figure 4B**). Overall, these results support the hypothesis that ROS-mediated UVA/blue light-induced NET formation is a consequence of riboflavin excitation. Excited riboflavin most likely reacts with biological substrates such as tryptophan, which further react and release ROS [40, 66, 75-77].

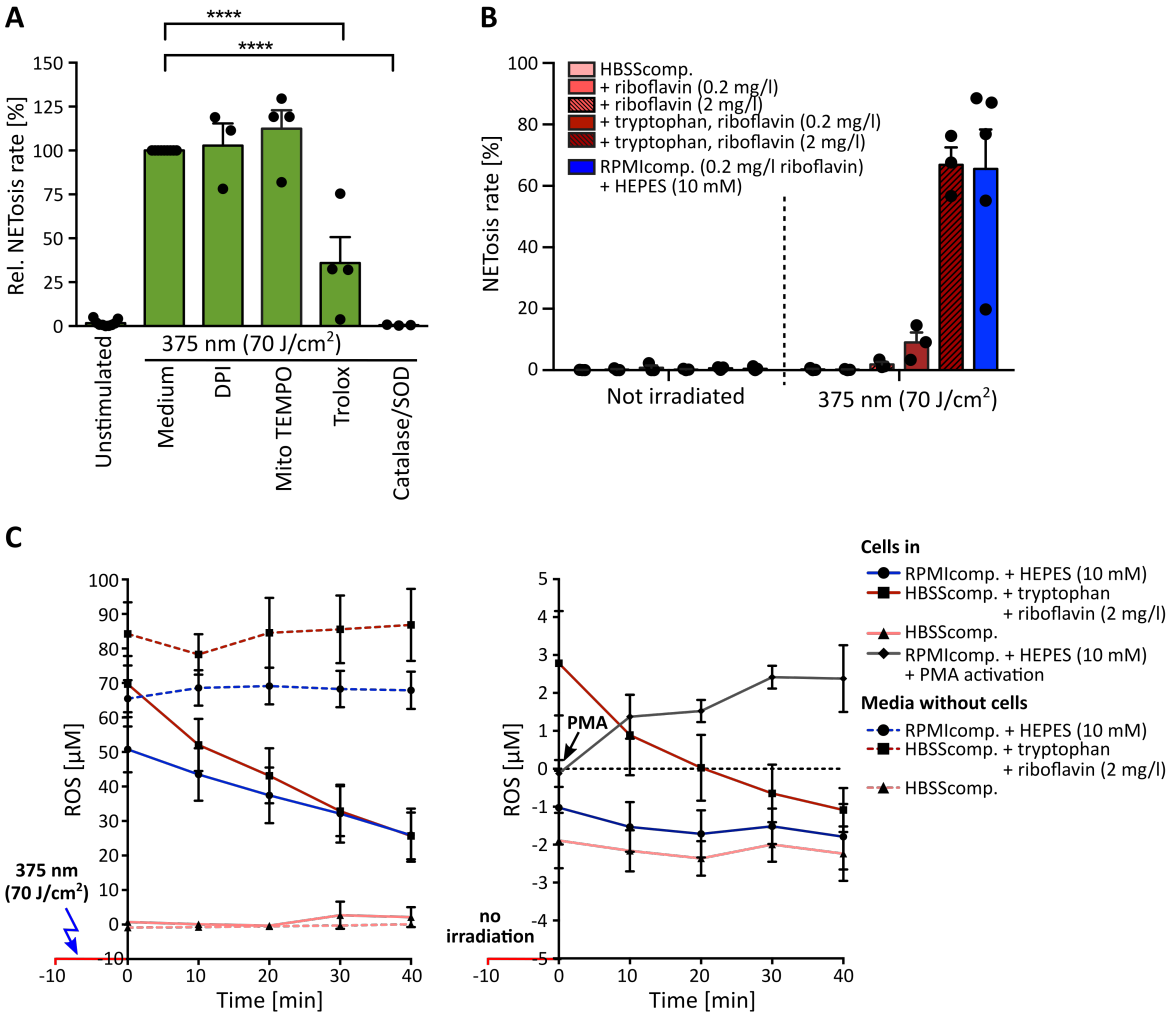

Figure 5: Light-induced NETosis depends on extracellular reactive oxygen species (ROS) generation. (**A**) Light-induced NETosis is significantly inhibited by the ROS scavenger Trolox (50 µM) and by exclusively scavenging external ROS by a combination of catalase/SOD (2 000 U/ml and 50 U/ml). NETosis appears to be independent of intracellular ROS production by NADPH oxidase, as shown by inhibition of DPI (1 µM) or mitochondrial ROS, which were inhibited by MitoTEMPO (5 µM). Cells were kept in RPMIcomp. + 10 mM HEPES. Statistics: one-way-ANOVA with Bonferroni's multiple comparisons test (tested against activation in medium). ****p < 0.0001. N = 3-4 independent experiments. Error bars = SEM. (**B**) 70 J/cm^2 of 375 nm light clearly induces NET formation in HBSScomp. + of riboflavin (2 mg/l) + tryptophan (1 mM). The obtained NET rates are comparable with NETosis induced in RPMIcomp. (containing 0.2 mg/l riboflavin) + 10 mM HEPES. In contrast, irradiation in HBSScomp. alone or supplemented only with riboflavin (0.2 or 2 mg/l) does not lead to NET formation.. N = 3-5 independent experiments. (**C**) Irradiation of HBSScomp. + 2 mg/l riboflavin + 1 mM tryptophan (dashed red

line, symbol ■) or RPMIcomp. (0.2 mg/l riboflavin) + 10 mM HEPES (dashed blue line, symbol ●) induces stable extracellular ROS levels between 60 and 100 µM, as detected by AmplexRed. Similar ROS levels are measurable after irradiation of neutrophils in these two media (left graph). In the presence of cells, ROS levels are continuously reduced over 40 min to around 20 to 40 µM (solid red line, symbol ■ and solid blue line, symbol ●). In HBSScomp. without riboflavin and tryptophan, neither direct irradiation (dashed light red line, symbol ▲) nor irradiation in the presence of neutrophils (solid light red line, symbol ▲) causes any increase in ROS levels (left graph). Without irradiation (right graph), ROS levels are stable in all three tested media at background values. After stimulation with 100 nM PMA (solid grey line, symbol ◆) extracellular ROS increase within 40 min up to 1.5 to 3 µM. N = 3-4 independent experiments. Error bars = SEM. Left graph: with irradiation (70 J/cm^2 of 375 nm). Right graph: without irradiation.

Discussion

UVA and blue light penetrate into human skin and especially the energy-rich UV light can cause severe tissue injury *via* immunological and inflammatory effects [43]. Both UVA and blue light from the sun reach the earth's surface and penetrate into the human epidermis. Although it has been shown that *in vitro* irradiation of neutrophils with UVB [45] or UVC light [78] can cause cell death and exposure to UVA light can enhance ROS production [79], the influence of light on NET formation remained largely enigmatic. We have discovered that light of the UVA or blue spectrum is able to induce the release of NETs. The formation of NETs in this scenario depends on extracellular ROS, which are generated through the excitation of riboflavin in conjunction with substrates such as tryptophan. During the 'classical' NETosis cascade, NE and MPO are typically released from neutrophil granules and translocate to the nucleus where they promote chromatin decondensation. According to our findings, light-induced NET formation also depends on MPO and NE. Additionally, inhibition of PAD activity by Cl-amidine during irradiation with UVA or blue light clearly showed reduction in NET formation especially after exposure to light of 470 nm wavelength. Therefore, the citrullination of histones most likely contributes to decondensation of chromatin in this setting. Altogether, these results imply that this novel light-mediated NET formation culminates in the initiation of the 'classical' pathway of suicidal NETosis by engaging the enzymes MPO, NE and PAD4 (**Figure 6**), as extensively described for different stimuli throughout the last years [12].

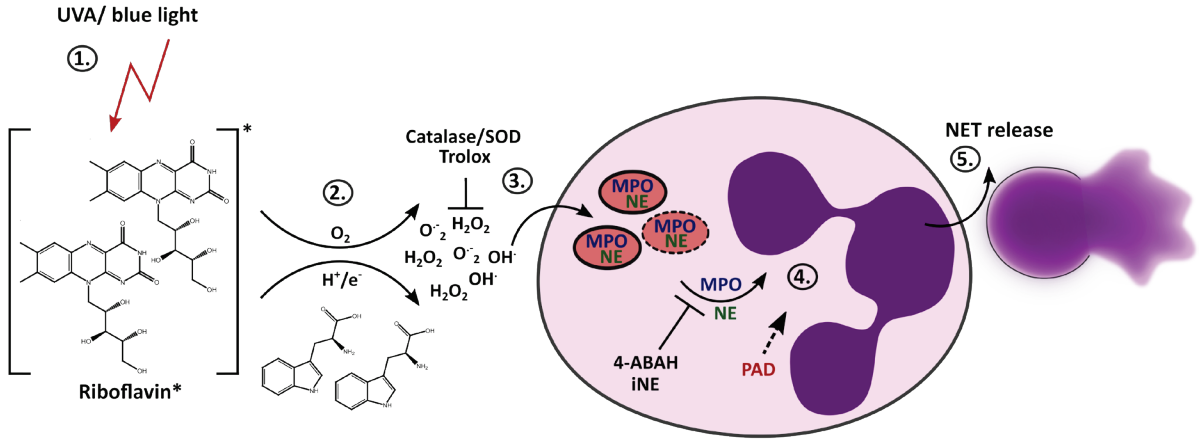

Figure 6: Proposed mechanism of light-induced NETosis. 1. Riboflavin absorbs UVA and blue light and is excited to the triplet state. 2. Tryptophan or other substrates (e.g., HEPES-buffer, tyrosine) transfer electrons or protons to triplet-riboflavin, which leads to ROS production. 3. Extracellular ROS generation (e.g., H_2O_2/ OH^- or $O^{\cdot-}_2$) by excited riboflavin in the presence of reactive substrates is required for further progression of NET formation. Extracellular ROS can be scavenged by Trolox or catalase/SOD. 4. Extracellular ROS activates the translocation of granular enzymes like NE and MPO to the nucleus, which leads to the decondensation of chromatin. The activation of NE and MPO is mandatory for chromatin decondensation and can be inhibited by 4-ABAH and iNE. Citrullination by PAD enzymes can presumably enhance decondensation. 5. After full decondensation, cells release the NET.

Interestingly, in response to near infrared (980 nm) laser light, a ROS-dependent form of NET formation has been reported recently [80], which was shown to involve autophagy signaling. In spite of the fact that NETs have been shown to impair wound healing [48], this laser light-mediated NET formation was suggested to be particularly relevant in the context of photobiostimulation with 980 nm diode lasers used to improve wound healing [80]. However, the exact mode of action of the laser light remains unclear.
In a different study, UVC light was reported to trigger apoptosis and/or NOX-independent suicidal NETosis in a dose-dependent manner [44]. Highly energetic UVC light had triggered NETosis dependent on mitochondrial ROS and p38 MAPK activation. Additionally, certain biochemical features of apoptosis such as caspase-3 activation accompanied UVC-dependent NETosis. Therefore, the authors termed this new NETosis pathway 'ApoNETosis' [44]. Of note, one must bear in mind that naturally occurring UVC light is almost completely absorbed by the ozone-layer [33] and thus does not reach the human skin. Moreover, while artificial light sources are able to generate UVC light, this would not be expected to penetrate in high amounts across the stratum corneum of the skin. Thus, the physiological relevance of UVC light in the context of NETosis remains disputable. Nevertheless, there may be some relevance for *ex vivo* neutrophil studies.

In contrast to the above-discussed reports, our study focused on the physiologically relevant and naturally occurring light spectra. Therefore, it is difficult to compare the mechanism unraveled by us with UVC-induced ApoNETosis. Nevertheless, the mechanism described here is also NOX-independent, similarly to 'ApoNETosis'. However, UVA or blue light-induced NETosis does not involve mitochondrial ROS production, but clearly depends on MPO and NE

activation (**Figure 3 and Figure 5A**). The release of NE from the azurosome depends on MPO activity and NADPH-dependent H_2O_2-generation [18]. In this study, we detected a high extracellular light-induced ROS-production in riboflavin-containing media, which was stable for over 40 min after irradiation (**Figure 5C**). This result indicates that riboflavin excitation together with reactive substrates induces high levels of stable ROS species like H_2O_2 [81]. H_2O_2 can easily diffuse into the cell and directly activate the release of serine proteases from the neutrophilic granules. Thus, in NETosis induced by extracellular ROS, additional production of H_2O_2 *via* NADPH-oxidase would not be required, which explains our observation that light-induced NETosis was independent of NADPH.
Importantly, the production of H_2O_2 in these media (especially RPMI + HEPES) and the subsequent release of NETs has to be considered for live cell imaging of neutrophils, especially when working with light of the blue or UVA spectrum. Choosing media without light-sensitive substances would avoid light-induced, ROS-mediated NETosis *ex vivo*.

Typically, in non-inflamed skin, neutrophils closest to the skin surface are found within the superficial arterio-venous plexus of the papillary dermis [82]. The transmission of light depends on the local skin composition, but one can estimate that 10-15% of UVA light and 40-50% of blue light reach the upper papillary dermis [35, 36].
In our study, we observed NET formation after irradiation of neutrophils starting with 18 J/cm^2 of 375 nm and 54 J/cm^2 of 470 nm LED-light (**Figure 2**). This dose corresponds to around 40 hours (375 nm) or 9 hours (470 nm LED spectrum) sun exposure at the specific wavelength, respectively. However, under real-life conditions one must consider the complex spectrum of sunlight, which is not limited to single wavelengths, as well as factors such as the thickness of the local ozone-layer, location on earth, weather, irradiation angle, level above the sea as well as time of day and season will affect those numbers [33]. Nonetheless, UVA and blue light-induced NET formation may play a more important role in pathological situations of skin. For example, this mechanism could be of great importance in individuals with a generally heightened propensity for light-induced NET formation but also in conditions where neutrophils are present in higher layers of the skin.

In healthy skin, ROS levels are closely regulated by enzymatic and non-enzymatic antioxidants like glutathione-peroxidase and catalase, vitamin C and vitamin E. As human skin contains significant amounts of riboflavin, ROS generation by excitation of riboflavin and subsequent reaction with active substrates (e.g. in a type I photoreaction) including aromatic amino acids is very likely [40, 66, 75-77]. Nonetheless, the antioxidants systems mentioned above balance out these reactions under normal circumstances. In the context of diseases, this complex antioxidant system can be dysregulated or exhausted. For instance, extensive or continuous exposure of sunlight causes increased ROS levels with associated inflammation and tissue damage, even in healthy individuals [83]. This ROS-associated oxidative tissue damage is mostly mediated by the deeper-penetrating UVA portion of the spectrum.

Interestingly, increased redox stress has been documented in autoimmune disorders [84]. For instance, SLE appears to be frequently associated with high oxidative stress indicated by decrease in antioxidant systems, general increased ROS levels as well as elevated antibodies against oxidatively modified proteins [85]. In fact, neutrophils from SLE patients reveal higher oxidative burst [86] with decreased intracellular antioxidant systems [87], what makes them less resistant towards extracellular ROS generation.
Additionally, neutrophils of patients suffering from psoriasis and SLE were reported to be generally primed for NETosis [4, 88][89] and NETosis is clearly involved in the pathogenesis of many chronic inflammatory and autoimmune diseases [21]. For example, autoantigens against NET components were detected in SLE [90]. Furthermore, impaired clearance of NETs has been described in the pathogenesis of systemic lupus, leading to an accumulation of potential autoantigens in the form of NET components [29].
Most likely both conditions - ROS imbalance and an increased propensity for NET formation - will add to one another and result in a ROS-mediated inflammatory loop. To what extent NETosis induced by light contributes to this cycle, has to be investigated within *in vivo* studies.

Several autoimmune diseases, most prominently the above-mentioned systemic and cutaneous lupus erythematosus as well as dermatomyositis, show severe photosensitivity. Patients suffering from lupus, whether acute, subacute or chronic, develop new cutaneous lesions after sun exposure. Even an exacerbation of systemic symptoms like fatigue or joint pain has been well documented after light-exposure [30]. Nevertheless, the exact pathophysiological mechanism has not been unraveled yet and involves a differential interplay between different light-induced effects [30].
Most likely, the abnormal response of lupus patients to light is not a monocausal one but given the importance of NETs in this disease and other autoimmune disorders it appears likely that a connection between light exposure and NET formation is an important factor. The question of whether neutrophils of lupus and dermatomyositis patients are *per se* more prone to light-induced NETosis and whether these reactions can be prevented warrant further translational studies. In this context, also the question as to what extent light-induced NETs are targets for autoantibody formation remains a highly interesting one.

Altogether, it is important to bear in mind that, according to our calculations, NET formation in response to moderate doses of light is most likely not a frequent event and that in healthy individuals NETs are usually rapidly cleared by DNases and subsequent phagocytosis [91, 92]. Thus, it is unlikely that exposure to modest doses of sunlight in healthy individuals will lead to a profound inflammatory reaction.

On the other hand, light-mediated, ROS-dependent NETosis may also be instrumentalized in a clinical setting to help fight bacteria in bacterial keratitis, as a recent study has impressively shown. Here, the combination of UVA light with riboflavin was used in the ‘photochemical’ therapy of bacterial keratitis due to its bactericidal effect [93]. Furthermore, one may

speculate whether at least a part of the effect of photodynamic therapy (PDT), can be explained by NET generation. Visible light irradiation, especially of the red but also blue light spectrum is used in combination with photosensitizers such as aminolevulinic acid (ALA) or methyl aminolevulinate (MAL) in the therapy of basal cell carcinomas, Bowen's disease and actinic keratosis (*carcinoma in situ*) [94]. This therapy is based on the excitation of the photosensitizer porphyrin originating from ALA or MAL and subsequent ROS generation similar to what we have reported in this study for riboflavin. Therefore, the highly interesting question remains whether NETosis can be activated by ROS generation also in this therapeutic context.

In conclusion, we show that UV-Vis light causes ROS-dependent NET formation, which most likely bears great clinical relevance for important diseases such as systemic lupus erythematosus and dermatomyositis.

Acknowledgments

This project was supported by the state of Lower Saxony (life@nano) and the German Research Foundation (DFG grant KR 4242/4-1 and ER 723/2-1). LE was further funded by the DDG/ADF Clinician Scientist fellowship and the Heidenreich von Siebold Programm of the UMG Göttingen. We thank Zhang Xin for technical support with ROS-measurements. We thank Hedwig Stanisz-Bogeski, Andreas Janshoff and Claudia Steinem for fruitful discussions and support.

Author contributions

EN and KMB performed most experiments, co-wrote the paper and designed the study together with LE. LE supervised the project. JB provided selected data sets. SK, MS and IB provided crucial scientific input as well as technical support. All authors proofread and edited the final manuscript.

Conflict of Interest Disclosures

All authors declare no conflicts of interest.

References

1. Brinkmann, V., et al., *Neutrophil extracellular traps kill bacteria.* Science, 2004. **303**: p. 1532-1535.
2. Fuchs, T.A., et al., *Novel cell death program leads to neutrophil extracellular traps.* J Cell Biol, 2007. **176**(2): p. 231-41.
3. Sollberger, G., D.O. Tilley, and A. Zychlinsky, *Neutrophil Extracellular Traps: The Biology of Chromatin Externalization.* Dev Cell, 2018. **44**(5): p. 542-553.
4. Sur Chowdhury, C., et al., *Enhanced neutrophil extracellular trap generation in rheumatoid arthritis: analysis of underlying signal transduction pathways and potential diagnostic utility.* Arthritis Res Ther, 2014. **16**(3): p. R122.

5. Leffler, J., et al., *Degradation of neutrophil extracellular traps co-varies with disease activity in patients with systemic lupus erythematosus.* Arthritis Res Ther, 2013. **15**(4): p. R84.
6. Hu, S.C., et al., *Neutrophil extracellular trap formation is increased in psoriasis and induces human beta-defensin-2 production in epidermal keratinocytes.* Sci Rep, 2016. **6**: p. 31119.
7. Schön, M.P. and L. Erpenbeck, *The Interleukin-23/Interleukin-17 Axis Links Adaptive and Innate Immunity in Psoriasis.* Frontiers in immunology, 2018. **9**: p. 1323-1323.
8. Jimenez-Alcazar, M., et al., *Host DNases prevent vascular occlusion by neutrophil extracellular traps.* Science, 2017. **358**(6367): p. 1202-1206.
9. Warnatsch, A., et al., *Inflammation. Neutrophil extracellular traps license macrophages for cytokine production in atherosclerosis.* Science, 2015. **349**(6245): p. 316-20.
10. Erpenbeck, L. and M.P. Schön, *Neutrophil extracellular traps: protagonists of cancer progression?* Oncogene, 2016.
11. Kenny, E.F., et al., *Diverse stimuli engage different neutrophil extracellular trap pathways.* 2017. **6**.
12. Papayannopoulos, V., *Neutrophil extracellular traps in immunity and disease.* Nat Rev Immunol, 2018. **18**(2): p. 134-147.
13. Kruss, S., et al., *Circular, nanostructured and biofunctionalized hydrogel microchannels for dynamic cell adhesion studies.* Lab Chip, 2012. **12**(18): p. 3285-9.
14. Kruss, S., et al., *Adhesion Maturation of Neutrophils on Nanoscopically Presented Platelet Glycoprotein Ibα.* ACS Nano, 2013. **7**(11): p. 9984-9996.
15. Neubert, E., et al., *Serum and Serum Albumin Inhibit in vitro Formation of Neutrophil Extracellular Traps (NETs).* Front Immunol, 2019. **10**: p. 12.
16. Erpenbeck, L., et al., *Effect of Adhesion and Substrate Elasticity on Neutrophil Extracellular Trap Formation.* bioRxiv, 2019: p. 508366.
17. Neubert, E., et al., *Chromatin swelling drives neutrophil extracellular trap release.* Nature Communications, 2018. **9**(1): p. 3767.
18. Metzler, K.D., et al., *A myeloperoxidase-containing complex regulates neutrophil elastase release and actin dynamics during NETosis.* Cell Rep, 2014. **8**(3): p. 883-96.
19. Papayannopoulos, V., et al., *Neutrophil elastase and myeloperoxidase regulate the formation of neutrophil extracellular traps.* J Cell Biol, 2010. **191**(3): p. 677-91.
20. Radic, M. and T.N. Marion, *Neutrophil extracellular chromatin traps connect innate immune response to autoimmunity.* Semin Immunopathol, 2013. **35**(4): p. 465-80.
21. Lee, K.H., et al., *Neutrophil extracellular traps (NETs) in autoimmune diseases: A comprehensive review.* Autoimmun Rev, 2017. **16**(11): p. 1160-1173.
22. Nakashima, K., T. Hagiwara, and M. Yamada, *Nuclear localization of peptidylarginine deiminase V and histone deimination in granulocytes.* J Biol Chem, 2002. **277**(51): p. 49562-8.
23. Leshner, M., et al., *PAD4 mediated histone hypercitrullination induces heterochromatin decondensation and chromatin unfolding to form neutrophil extracellular trap-like structures.* Front Immunol, 2012. **3**: p. 307.
24. Hosseinzadeh, A., et al., *Nicotine induces neutrophil extracellular traps.* J Leukoc Biol, 2016. **100**(5): p. 1105-1112.
25. Neeli, I., S.N. Khan, and M. Radic, *Histone Deimination As a Response to Inflammatory Stimuli in Neutrophils.* The Journal of Immunology, 2008. **180**(3): p. 1895-1902.

26. Tatsiy, O. and P.P. McDonald, *Physiological Stimuli Induce PAD4-Dependent, ROS-Independent NETosis, With Early and Late Events Controlled by Discrete Signaling Pathways.* Front Immunol, 2018. **9**: p. 2036.
27. Lewis, H.D., et al., *Inhibition of PAD4 activity is sufficient to disrupt mouse and human NET formation.* Nat Chem Biol, 2015. **11**(3): p. 189-91.
28. Khandpur, R., et al., *NETs are a source of citrullinated autoantigens and stimulate inflammatory responses in rheumatoid arthritis.* Science translational medicine, 2013. **5**(178): p. 178ra40-178ra40.
29. Hakkim, A., et al., *Impairment of neutrophil extracellular trap degradation is associated with lupus nephritis.* Proc Natl Acad Sci U S A, 2010. **107**(21): p. 9813-8.
30. Kim, A. and B.F. Chong, *Photosensitivity in cutaneous lupus erythematosus.* Photodermatology, photoimmunology & photomedicine, 2013. **29**(1): p. 4-11.
31. Lood, C., et al., *Neutrophil extracellular traps enriched in oxidized mitochondrial DNA are interferogenic and contribute to lupus-like disease.* Nat Med, 2016. **22**(2): p. 146-53.
32. Garcia-Romo, G.S., et al., *Netting neutrophils are major inducers of type I IFN production in pediatric systemic lupus erythematosus.* Sci Transl Med, 2011. **3**(73): p. 73ra20.
33. Gueymard, C.A., D. Myers, and K. Emery, *Proposed reference irradiance spectra for solar energy systems testing.* Solar Energy, 2002. **73**(6): p. 443-467.
34. Anderson, R.R., J. Hu, and J.A. Parrish, *Optical radiation transfer in the human skin and applications in in vivo remittance spectroscopy.* Marks R., Payne P.A. (eds) Symposium Bioengineering and the Skin, 1981.
35. Svobodova, A. and J. Vostalova, *Solar radiation induced skin damage: review of protective and preventive options.* Int J Radiat Biol, 2010. **86**(12): p. 999-1030.
36. Anderson, R.R. and J.A. Parrish, *The optics of human skin.* J Invest Dermatol, 1981. **77**(1): p. 13-9.
37. D'Orazio, J., et al., *UV radiation and the skin.* International journal of molecular sciences, 2013. **14**(6): p. 12222-12248.
38. Rijken, F., R.C. Kiekens, and P.L. Bruijnzeel, *Skin-infiltrating neutrophils following exposure to solar-simulated radiation could play an important role in photoageing of human skin.* Br J Dermatol, 2005. **152**(2): p. 321-8.
39. Pattison, D.I. and M.J. Davies, *Actions of ultraviolet light on cellular structures.* EXS, 2006(96): p. 131-57.
40. Cardoso, D.R., S.H. Libardi, and L.H. Skibsted, *Riboflavin as a photosensitizer. Effects on human health and food quality.* Food Funct, 2012. **3**(5): p. 487-502.
41. Cooper, K.D., *Cell-mediated immunosuppressive mechanisms induced by UV radiation.* Photochem Photobiol, 1996. **63**(4): p. 400-6.
42. Aubin, F., *Mechanisms involved in ultraviolet light-induced immunosuppression.* Eur J Dermatol, 2003. **13**(6): p. 515-23.
43. Clydesdale, G.J., G.W. Dandie, and H.K. Muller, *Ultraviolet light induced injury: immunological and inflammatory effects.* Immunol Cell Biol, 2001. **79**(6): p. 547-68.
44. Azzouz, D., et al., *Two-in-one: UV radiation simultaneously induces apoptosis and NETosis.* Cell Death Discov, 2018. **4**: p. 51.
45. Sweeney, J.F., et al., *Ultraviolet irradiation accelerates apoptosis in human polymorphonuclear leukocytes: protection by LPS and GM-CSF.* J Leukoc Biol, 1997. **62**(4): p. 517-23.

46. Lee, P.L., H. van Weelden, and P.L. Bruijnzeel, *Neutrophil infiltration in normal human skin after exposure to different ultraviolet radiation sources.* Photochem Photobiol, 2008. **84**(6): p. 1528-34.
47. Brinkmann, V., et al., *Neutrophil extracellular traps: how to generate and visualize them.* J Vis Exp, 2010(36).
48. Wong, S.L., et al., *Diabetes primes neutrophils to undergo NETosis, which impairs wound healing.* Nat Med, 2015. **21**(7): p. 815-9.
49. Thevenaz, P. and M. Unser, *User-friendly semiautomated assembly of accurate image mosaics in microscopy.* Microsc Res Tech, 2007. **70**(2): p. 135-46.
50. Gupta, S., et al., *A High-Throughput Real-Time Imaging Technique To Quantify NETosis and Distinguish Mechanisms of Cell Death in Human Neutrophils.* The Journal of Immunology, 2017.
51. van der Linden, M., et al., *Differential Signalling and Kinetics of Neutrophil Extracellular Trap Release Revealed by Quantitative Live Imaging.* Sci Rep, 2017. **7**(1): p. 6529.
52. Brinkmann, V., et al., *Automatic quantification of in vitro NET formation.* Front Immunol, 2012. **3**: p. 413.
53. Kettle, A.J., C.A. Gedye, and C.C. Winterbourn, *Mechanism of inactivation of myeloperoxidase by 4-aminobenzoic acid hydrazide.* Biochemical Journal, 1997. **321**(Pt 2): p. 503-508.
54. Macdonald, S.J., et al., *The discovery of a potent, intracellular, orally bioavailable, long duration inhibitor of human neutrophil elastase--GW311616A a development candidate.* Bioorg Med Chem Lett, 2001. **11**(7): p. 895-8.
55. Luo, Y., et al., *Inhibitors and inactivators of protein arginine deiminase 4: functional and structural characterization.* Biochemistry, 2006. **45**(39): p. 11727-36.
56. Wang, Y., et al., *Human PAD4 regulates histone arginine methylation levels via demethylimination.* Science, 2004. **306**(5694): p. 279-83.
57. Narumiya, S., T. Ishizaki, and M. Uehata, *Use and properties of ROCK-specific inhibitor Y-27632.* Methods Enzymol, 2000. **325**: p. 273-84.
58. Slee, E.A., et al., *Benzyloxycarbonyl-Val-Ala-Asp (OMe) fluoromethylketone (Z-VAD.FMK) inhibits apoptosis by blocking the processing of CPP32.* Biochem J, 1996. **315 (Pt 1)**: p. 21-4.
59. Degterev, A., et al., *Identification of RIP1 kinase as a specific cellular target of necrostatins.* Nat Chem Biol, 2008. **4**(5): p. 313-21.
60. Pinto, J. and R. Rivlin, *Riboflavin (Vitamin B2).* Handbook of Vitamins, 5th Edition, 2013: p. 191-266.
61. Powers, H.J., *Riboflavin (vitamin B-2) and health.* Am J Clin Nutr, 2003. **77**(6): p. 1352-60.
62. Gore, D.M., et al., *Two-photon fluorescence microscopy of corneal riboflavin absorption.* Invest Ophthalmol Vis Sci, 2014. **55**(4): p. 2476-81.
63. Martin, C.B., et al., *The Reaction of Triplet Flavin with Indole. A Study of the Cascade of Reactive Intermediates Using Density Functional Theory and Time Resolved Infrared Spectroscopy.* Journal of the American Chemical Society, 2002. **124**(24): p. 7226-7234.
64. Heelis, P.F., *The photophysical and photochemical properties of flavins (isoalloxazines).* Chemical Society Reviews, 1982. **11**(1): p. 15-39.

65. Keynes, R.G., C. Griffiths, and J. Garthwaite, *Superoxide-dependent consumption of nitric oxide in biological media may confound in vitro experiments.* Biochem J, 2003. **369**(Pt 2): p. 399-406.
66. Wang, R.J. and B.R. Nixon, *Identification of hydrogen peroxide as a photoproduct toxic to human cells in tissue-culture medium irradiated with "daylight" fluorescent light.* In Vitro, 1978. **14**(8): p. 715-22.
67. Behnen, M., et al., *Extracellular Acidification Inhibits the ROS-Dependent Formation of Neutrophil Extracellular Traps.* Front Immunol, 2017. **8**: p. 184.
68. Nadesalingam, A., et al., *Hypertonic Saline Suppresses NADPH Oxidase-Dependent Neutrophil Extracellular Trap Formation and Promotes Apoptosis.* Front Immunol, 2018. **9**: p. 359.
69. Zawrotniak, M., A. Kozik, and M. Rapala-Kozik, *Selected mucolytic, anti-inflammatory and cardiovascular drugs change the ability of neutrophils to form extracellular traps (NETs).* Acta Biochim Pol, 2015. **62**(3): p. 465-73.
70. Hamad, I., et al., *Intracellular scavenging activity of Trolox (6-hydroxy-2,5,7,8-tetramethylchromane-2-carboxylic acid) in the fission yeast, Schizosaccharomyces pombe.* Journal of natural science, biology, and medicine, 2010. **1**(1): p. 16-21.
71. Bjornsdottir, H., et al., *Neutrophil NET formation is regulated from the inside by myeloperoxidase-processed reactive oxygen species.* Free Radic Biol Med, 2015. **89**: p. 1024-35.
72. Jancinova, V., et al., *The combined luminol/isoluminol chemiluminescence method for differentiating between extracellular and intracellular oxidant production by neutrophils.* Redox Rep, 2006. **11**(3): p. 110-6.
73. Ellis, J.A., S.J. Mayer, and O.T. Jones, *The effect of the NADPH oxidase inhibitor diphenyleneiodonium on aerobic and anaerobic microbicidal activities of human neutrophils.* The Biochemical journal, 1988. **251**(3): p. 887-891.
74. Bordt, E.A. and B.M. Polster, *NADPH oxidase- and mitochondria-derived reactive oxygen species in proinflammatory microglial activation: a bipartisan affair?* Free Radic Biol Med, 2014. **76**: p. 34-46.
75. Silva, E., et al., *Riboflavin-sensitized photoprocesses of tryptophan.* J Photochem Photobiol B, 1994. **23**(1): p. 43-8.
76. Shen, L. and H.F. Ji, *A theoretical study on the quenching mechanisms of triplet state riboflavin by tryptophan and tyrosine.* J Photochem Photobiol B, 2008. **92**(1): p. 10-2.
77. Martin, C.B., et al., *The reaction of triplet flavin with indole. A study of the cascade of reactive intermediates using density functional theory and time resolved infrared spectroscopy.* J Am Chem Soc, 2002. **124**(24): p. 7226-34.
78. Frasch, S.C., et al., *p38 mitogen-activated protein kinase-dependent and -independent intracellular signal transduction pathways leading to apoptosis in human neutrophils.* J Biol Chem, 1998. **273**(14): p. 8389-97.
79. Li, C., et al., *Ultraviolet light A irradiation induces immunosuppression associated with the generation of reactive oxygen species in human neutrophils.* Journal of Innovative Optical Health Sciences, 2016. **09**(01): p. 1650001.
80. Migliario, M., et al., *Near infrared laser irradiation induces NETosis via oxidative stress and autophagy.* Lasers Med Sci, 2018. **33**(9): p. 1919-1924.
81. Mahns, A., et al., *Irradiation of cells with ultraviolet-A (320-400 nm) in the presence of cell culture medium elicits biological effects due to extracellular generation of hydrogen peroxide.* Free Radic Res, 2003. **37**(4): p. 391-7.

82. Swerlick, R.A., *The structure and function of the cutaneous vasculature.* J Dermatol, 1997. **24**(11): p. 734-8.
83. Wagener, F.A.D.T.G., C.E. Carels, and D.M.S. Lundvig, *Targeting the redox balance in inflammatory skin conditions.* International journal of molecular sciences, 2013. **14**(5): p. 9126-9167.
84. Glennon-Alty, L., et al., *Neutrophils and redox stress in the pathogenesis of autoimmune disease.* Free Radic Biol Med, 2018. **125**: p. 25-35.
85. Shah, D., et al., *Oxidative stress and its biomarkers in systemic lupus erythematosus.* Journal of Biomedical Science, 2014. **21**(1): p. 23-23.
86. Perazzio, S.F., et al., *Increased neutrophil oxidative burst metabolism in systemic lupus erythematosus.* Lupus, 2012. **21**(14): p. 1543-51.
87. Li, K.J., et al., *Deranged bioenergetics and defective redox capacity in T lymphocytes and neutrophils are related to cellular dysfunction and increased oxidative stress in patients with active systemic lupus erythematosus.* Clin Dev Immunol, 2012. **2012**: p. 548516.
88. Hu, S.C.-S., et al., *Neutrophil extracellular trap formation is increased in psoriasis and induces human β-defensin-2 production in epidermal keratinocytes.* Scientific Reports, 2016. **6**: p. 31119.
89. Villanueva, E., et al., *Netting neutrophils induce endothelial damage, infiltrate tissues, and expose immunostimulatory molecules in systemic lupus erythematosus.* J Immunol, 2011. **187**(1): p. 538-52.
90. Carmona-Rivera, C. and M.J. Kaplan, *Detection of SLE antigens in neutrophil extracellular traps (NETs).* Methods Mol Biol, 2014. **1134**: p. 151-61.
91. Kolaczkowska, E., et al., *Molecular mechanisms of NET formation and degradation revealed by intravital imaging in the liver vasculature.* Nat Commun, 2015. **6**: p. 6673.
92. Farrera, C. and B. Fadeel, *Macrophage clearance of neutrophil extracellular traps is a silent process.* J Immunol, 2013. **191**(5): p. 2647-56.
93. Makdoumi, K., et al., *UVA-riboflavin photochemical therapy of bacterial keratitis: a pilot study.* Graefes Arch Clin Exp Ophthalmol, 2012. **250**(1): p. 95-102.
94. Wan, M.T. and J.Y. Lin, *Current evidence and applications of photodynamic therapy in dermatology.* Clinical, cosmetic and investigational dermatology, 2014. **7**: p. 145-163.

2.6 Supplementary information, manuscript III

Supplementary movie

(The movie can be found as an attachment to this thesis in form of a DVD)

Changes of the nuclear morphology of human neutrophil granulocytes during UVA-induced NETosis. Staining: Hoechst.

Supplementary figures

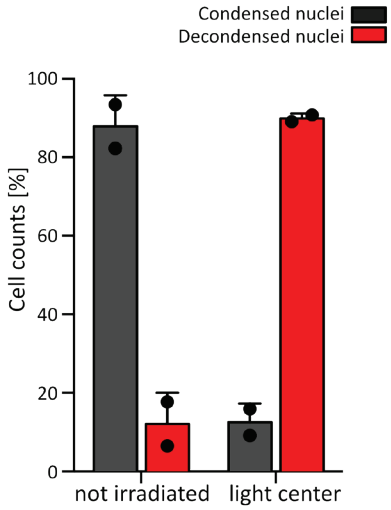

Supplementary figure 1: Quantification of locally-restricted light-induced NETosis. NETosis rates are 60-70% higher in the center of light exposure compared to non-illuminated areas (> 1500 µm distance from light center). Cells were kept in RPMIcomp. + 10 mM HEPES. N = 2 donor. Error = SD.

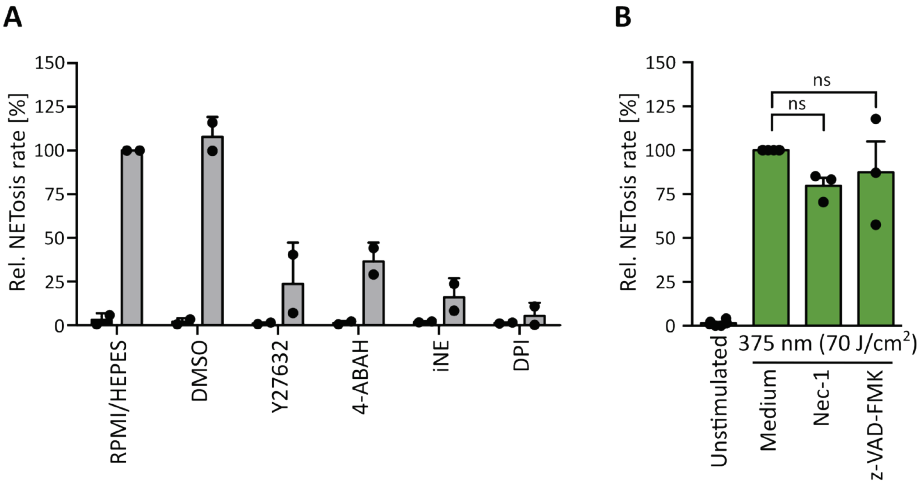

Supplementary figure 2: Functionality of inhibitors and exclusion of other cell death pathways. (**A**) NETosis in response to PMA (100 nM) is inhibited by 4-ABAH (100 µM), iNE (5 µM), DPI (1 µM) and Y-27632 (20 µM), even after inhibitors were treated with 70 J/cm^2 of 375 nm, ruling out that inhibitor function was altered by light exposure. Induction of NETosis by PMA is not altered upon the addition of DMSO (solvent for inhibitors) in the highest used concentration (1%). Cells were kept in RPMIcomp. + 10 mM HEPES. N = 2. Error = SD. (**B**) Light-induced NETosis (70 J/cm^2 of 375 nm) occurs independently of nec-1 (RPI1 kinase inhibitor) and z-VAD-FMK (pan-caspase inhibitor). Statistics: one-way-ANOVA with Bonferroni's multiple comparisons test. ns = not significant. Cells were kept in RPMIcomp. + 10 mM HEPES. N = 3. Error = SEM.

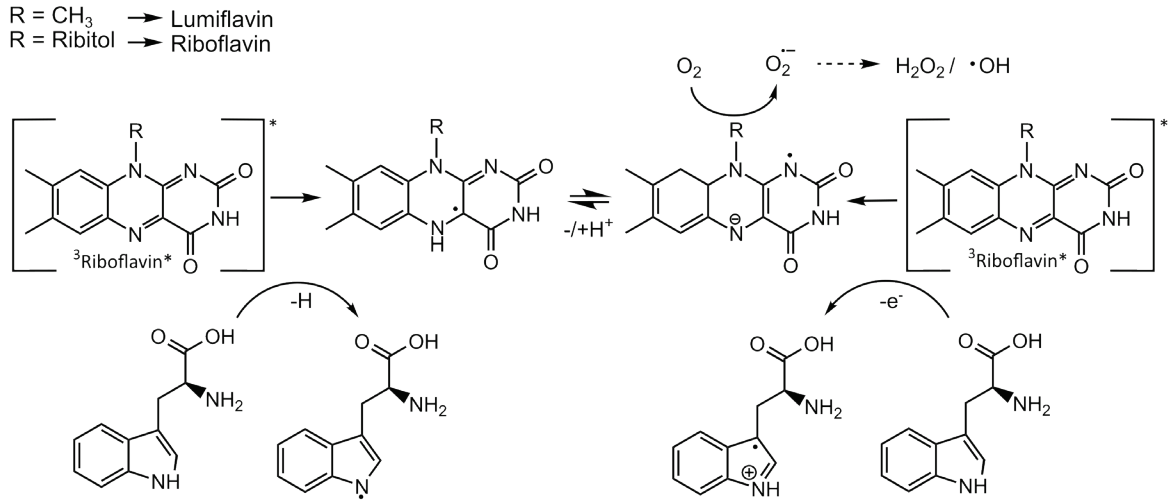

Supplementary figure 3: Reaction of triplet-riboflavin with tryptophan. Tryptophan can transfer an electron or a proton to excited triplet-riboflavin (type I photoreaction). This intermediate can further react with molecular oxygen and thus generate ROS. Riboflavin is transferred back to the ground state. This schema is based on previous published reactions between riboflavin and tryptophan **[1-4]**.

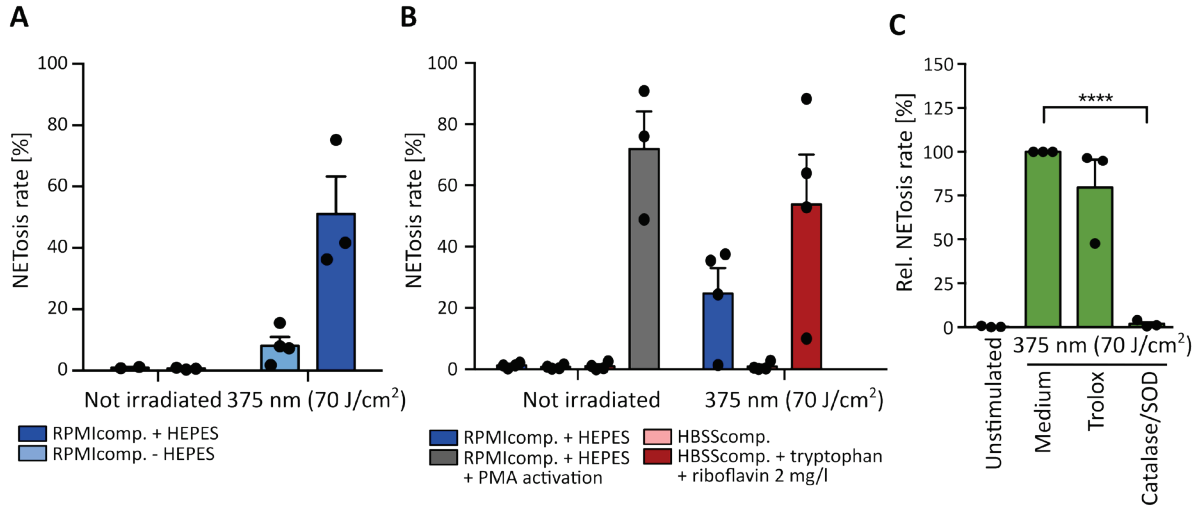

Supplementary figure 4: Light-induced NETosis is dependent on extracellular ROS. (**A**) NET rates in response to light of 375 nm 70 J/cm^2 are enhanced in the presence of the culture buffer HEPES (10 mM). N = 3-4. Error = SEM. (**B**) During AmplexRed measurements NETosis is stably induced by PMA (100 nM) and light. N = 3-4. Error = SEM. (**C**) Catalase/SOD significantly inhibits NETosis and Trolox clearly reduces NET rates, when added after full illumination with 70 J/cm^2 of 375 nm. Cells were kept in RPMIcomp. + 10 mM HEPES. N = 3. Error = SEM. Statistics: one-way-ANOVA with Bonferroni's multiple comparisons test. ****p < 0.0001.

References

1. Silva, E., et al., *Riboflavin-sensitized photoprocesses of tryptophan.* J Photochem Photobiol B, 1994. **23**(1): p. 43-8.
2. Shen, L. and H.F. Ji, *A theoretical study on the quenching mechanisms of triplet state riboflavin by tryptophan and tyrosine.* J Photochem Photobiol B, 2008. **92**(1): p. 10-2.
3. Martin, C.B., et al., *The reaction of triplet flavin with indole. A study of the cascade of reactive intermediates using density functional theory and time resolved infrared spectroscopy.* J Am Chem Soc, 2002. **124**(24): p. 7226-34.
4. Cardoso, D.R., S.H. Libardi, and L.H. Skibsted, *Riboflavin as a photosensitizer. Effects on human health and food quality.* Food Funct, 2012. **3**(5): p. 487-502.

CHAPTER 3 **- Summary**

3.1 Summary - Manuscript I

„Chromatin Swelling Drives Neutrophil Extracellular Trap Release“
(Nature Communications, 2018)

Detailed real-time observations on single human neutrophils conducted within this study, led to the conclusion that NETosis occurs in three distinct phases (P1-P3). These phases were reproducible among different donors as well as with frequently used NET-inductors such as PMA, calcium ionophore (CaI) and LPS. The first phase (P1) depended strongly on temperature and enzyme activity as verified by time-resolved inhibition of energy generation and MPO activity. Within this phase, the cell consumed substantial amounts of ATP, started to rearrange membranes and degraded the cytoskeleton. During this process, the cell softened and decreased its membrane tension. The chromatin within the neutrophil nucleus remained condensed in P1. The second phase (P2) was characterized by chromatin decondensation and was mostly independent of enzymatic activity and temperature variation. Consequently, the main driving force of P2 was the entropic swelling of chromatin. The onset of P2, the start of chromatin decondensation, was interestingly also accompanied by the rupture of the nuclear envelope as determined by lamin B fluorescence staining. After this time-point, NETosis could not be inhibited any more. Therefore, the onset of P2 in NETosis marks a point of no return. After complete chromatin decondensation, cytoskeleton degradation and cell rounding, the cell membrane ruptured and released the NET (P3). The point of cytoplasmic membrane rupture was biomechanically pre-determined by the position of the nucleus within the cell as well as plasma membrane dynamics during NETosis. In summary, NETosis consists of an active first phase and a second phase driven by material properties, which are separated by a clear point of no return. These results present a detailed insight into the exact regulation of NETosis and demonstrate how material properties can drive the complex behavior of cells.

CONTRIBUTION:
General: Experimental design together with all authors; main parts of the manuscript with Sebastian Kruss, Luise Erpenbeck and Daniel Meyer (D.M.); figure arrangement; co-supervision of Susanne N. Senger-Sander and Anja Kwaczala-Tessmann, who both contributed with selected data sets.
Data generation and analysis: Figures: Fig. 1a-e; Fig. 2a/d; Fig. 2c (imaging); Fig. 3; Fig. 4b; Fig. 4a/d (all raw data; data analysis by D.M.); Fig. 4c (sample preparation); Fig. 5a (F-actin); Fig. 5b (Latrunculin A); Fig. 5c (Jasplakinolide); Fig. 6a-e (all raw data; data analysis together with D.M.) and Fig. 7 (together with D.M.). Supplementary figures: Supp. fig. 1; Supp. fig. 2 (sample preparation); Supp. fig. 3; Supp. fig. 4a/b; Supp. fig. 4d (together with D.M.); Supp. fig. 5; Supp. fig. 6; Supp. fig. 7; Supp. fig. 8a; Supp. fig. 8b/c (sample preparation); Supp. fig. 9a (all raw data, data analysis by D.M.); Supp. fig. 9c; Supp. fig. 11 (all raw data, data analysis by D.M.) and Supp. fig. 13 (together with D.M.). Supplementary movies: movie 1-8; movie 12-15 and movie 17. Analysis by customized Matlab code of D.M.: Fig. 1b-e; Fig. 3c; Fig. 4a/b/d; Supp. fig. 1; Supp. fig. 3 and Supp. fig. 8a.

3.2 Summary - Manuscript II

"Serum and Serum Albumin Inhibit *in vitro* Formation of Neutrophil Extracellular Traps (NETs)"
(Frontiers in Immunology, 2019)

As the composition of cell culture media can massively alter the results of *in vitro* cell studies, the effect of serum supplement in culture media on NETosis was analyzed *in vitro*. A complementary systematic literature search was also conducted. *In vitro* NETosis induced by PMA, calcium ionophore (CaI) or LPS depended strongly on supplementation of serum or serum albumin to culture media. In serum-free media, all tested stimuli activated NETosis as verified by colocalization of extracellular DNA with MPO and release of active NE-DNA-complexes. The addition of serum albumin (HSA, BSA), however, significantly inhibited CaI- and LPS-induced NETosis of human neutrophils. The same effect occurred in media supplemented with heat-inactivated fetal calf serum (hiFCS). This pronounced inhibitory effect of serum supplements could be mediated by activator binding effects, as shown for LPS and albumin by fluorescence anisotropy measurements. Remarkably, these supplements did not affect PMA-induced NETosis of human neutrophils. However, in assays with murine cells, which in general showed lower NETosis rates, serum and serum albumin were sufficient to inhibit NETosis in response to all three stimuli. This observation emphasizes the variability of NETosis in different species.

These results are of particular interest regarding the considerable variation in serum and serum albumin supplements used for *in vitro* NETosis studies in the literature, as shown in a comprehensive literature search. Interestingly, the choice of supplement varies according to the applied NET inducer reflecting our experimental results.

The experimental data together with the literature research corroborate the importance for the standardization of culture conditions used in *in vitro* NET assays in order to obtain comparable results. It also allows speculations about the remarkable susceptibility of NETosis by small variations of the neutrophil environment and therefore regulation of NETosis *in vivo*.

CONTRIBUTION:

General: Experimental design together with all authors; main parts of the manuscript together with Luise Erpenbeck and Susanne N. Senger-Sander (SN. S-S.); complete data plotting, statistics and figure arrangement; co-supervision of SN. S-S. (who provided the literature research and contributed to the data set of Fig. 1).

Data generation and analysis: Figures: Fig. 1 (main raw data except one selected data set by SN. S-S.); Fig. 2; Fig. 3 (main raw data, except stimulation with PMA and LPS (10 and 25 µg/ml) in RPMI/HEPES (Veit S. Manzke) and one selected data set by Sophie E.F. Scheidmann). Supplementary figures: Supp. fig. 1; Supp. fig. 2. and Supp. fig. 4. Literature research: co-supervision of SN. S-S. (who provided complete data set) and independent verification of all data.

3.3 Summary - Manuscript III

"Blue and Long-wave Ultraviolet Light Induce *in vitro* Neutrophil Extracellular Trap Formation"

(Prepared for submission to Frontiers in Immunology)

The effect of UV-Vis light on *in vitro* NET formation is the main focus of the third manuscript. Neutrophils, freshly isolated from healthy human donors, released NETs in response to UVA and blue light. The identity of these NETs was verified by colocalization of MPO with extracellular decondensed chromatin. NE and MPO regulated this novel pathway of 'suicidal' NET formation (NETosis) supported by PAD activity. There was no involvement of necroptotic, apoptotic or RHO/ROCK-related pathways as verified by RIPK1, pan-caspase and ROCK1/2 inhibition.

Interestingly, light-induced NETosis could be activated in a locally restricted fashion and depended strongly on light doses and wavelength. While UVA and blue light (375 nm and 470 nm LEDs) revealed high NET rates, green light (565 nm LED) failed to induce NETosis. This wavelength-dependency was reproducible for equal light energy and photon flux and correlated with the absorption spectrum of the photosensitive substance riboflavin (vitamin B2). In contrast to several previously described NETosis pathways, light-induced NETosis took place independently of mitochondrial ROS production or NADPH oxidase activation but required extracellular ROS generation. The formation of ROS was triggered by riboflavin excitation in combination with sensitizing substances such as tryptophan or HEPES buffer present in culture media.

Since riboflavin and tryptophan are present at high concentrations in human skin and UVA as well as blue light can penetrate the epidermis in significant amounts, light-induced NETosis could be relevant for skin light-sensitivity. Particularly a contribution to disease onset and exacerbation of autoimmune disorders is conceivable, especially in the context of the frequently documented dysregulation of NETosis, high ROS imbalance and increased light sensitivity in these disorders. Therefore, a more profound understanding of NETosis in response to UV-Vis light can shed light into this still enigmatic correlation.

CONTRIBUTION:

General: Experimental design together with all authors; manuscript draft; final manuscript together with Luise Erpenbeck and Katharina M. Bach (KM. B.); complete data plotting, statistics and figure arrangement; co-supervision of KM. B (who provided a main data sets for this study).

Data generation and analysis: Figures: Fig. 1; selective data for Fig. 3 (N = 4-5 for Cl-amidine and 4-ABAH at 375 nm); Fig. 4c; Fig. 5 (except ROS measurements in RPMIcomp. + HEPES (KM. B.)) and Fig. 6. Supplementary data: Supp. fig. 1; Supp. fig. 2a (analysis), Supp. fig 2b; Supp. fig. 3; Supp. fig. 4 and Supp. movie.

CHAPTER 4 **- Discussion and outlook**

Many studies investigating NETosis focus on the identification of specific players in the multiple NET pathways in physiological and pathological contexts [193, 212, 214]. These experiments are essential in order to understand the signaling, which underlies NETosis and can profoundly accelerate the development of new therapeutic strategies of NET-associated disorders. Most of them are carried out in mouse models or *in vitro* with isolated human neutrophils. However, the outcome of these experiments can vary among different species (**manuscript II**), donors [225] or even when using the same stimulus (*e.g.*, LPS stimulation [212, 225, 277], **manuscript II**)**.** The central question remains, why a certain stimulus does sometimes fail to induce stable NETosis rates, and therefore, how onset and progression of NETosis are regulated for a specific stimulus. In addition, the question arises what these observations tell us about *in vivo* processes and their involvement in underlying pathologies as discussed in **manuscript II and III**.

The detailed biophysical analysis of NET formation presented in **manuscript I** is of particular interest to address these questions. The three distinct phases of NETosis, differentially orchestrated by different driving forces, provide a valuable tool to analyze which specific influencing factor acts as a modulator, accelerator or inhibitor during NET formation. The following paragraphs will address the questions of how NETosis is actively modified and regulated within the first phase (P1) (**paragraph 4.1**), what factors possibly alter the entropic chromatin swelling in the second phase (P2) (**paragraph 4.2**) and how these results can be implicated in therapeutically strategies of NET-associated diseases (**paragraph 4.3 and 4.4**).

4.1 Active modulation of NETosis dynamics

4.1.1 Variations in NETosis activation

As discussed in **manuscript I**, NETosis has three distinct phases, of which only the first phase (P1) depends on active enzyme-driven processes. NETosis also relies immensely on external factors. Whether a specific activator induces NETosis can depend on access of the stimulus to its target, pre-activation of the cell or requirement for co-stimulation. For instance, as shown in **manuscript II**, even a small amount of serum or serum albumin within culture media can effectively inhibit NET formation of human and mouse neutrophils (**manuscript II, Fig. 1** and **3**). It is reasonable to assume that these interactions are mainly due to the binding of the activator to serum proteins [361, 362] as discussed in **manuscript II** and verified for the binding of LPS to serum albumin (**manuscript II**, **Fig. 4**). Besides direct activator binding, other mechanisms are also conceivable to explain the obtained results. The serum proteins studied in **manuscript II** can attach to the cell surface or assay substrate and thereby restrict the access of the stimulus to its receptors or intervene with cell adhesion. Indeed, serum, as well as serum albumin, can strongly decrease the spreading area of cells as shown for neutrophils on human serum albumin (HSA)-coated surfaces [363] or hamster kidney cells in serum-containing media [364]. This observation is of particular interest for stimuli, which require preceding adhesion for NET formation. One prominent example is LPS, a frequently

used NET stimulus known for its inconsistent activation in *in vitro* NET assays. NETosis induced by LPS depends on Mac-1 activation as demonstrated by inhibition of the integrin subunit α_M (CD11b) [281]. In a current study, we were able to corroborate these findings. Induction of NETosis with LPS directly correlated with the spreading area of neutrophils on their substrate (*Erpenbeck, Gruhn et al.*, preprint uploaded to bioRxiv [365], data not shown). These experiments were performed by using different substrate stiffnesses (indicated by the Young's (E) modulus) together with collagen I- or fibronectin coatings. Interestingly, the spreading area of neutrophils after LPS stimulation not only correlated with NET rates but also with increasing substrate stiffness [365]. These observations together with the data obtained in **manuscript II** highlight once more how the cells' environment can alter the onset of *in vitro* NETosis and how important standardized assays are for the comparability of *in vitro* experiments as well as their transferability to *in vivo* conditions. For instance, distinct tissues reveal different amounts of serum albumin [366], adhesion molecule expression [66] and stiffness [367].

Based on these considerations, it is not surprising that activation with stimuli which do not require receptor-mediated signaling, like PMA, are more stable against modifications of environmental parameters. The same applies for neutrophil adhesion. PMA-induced NETosis progresses mainly independently of Mac-1-mediated adhesion [368] and is functional even in suspended neutrophils derived from patients with leukocyte adhesion deficiency 1 (LAD1; deficiency in the β_2-integrin) [369] and on passivated surfaces (**manuscript I, Supp. fig. 12**), which severely limit neutrophil adhesion. In direct comparison, PMA-induced NETosis progressed independently of surface passivation, but NETosis was completely impaired in response to LPS [365]. Therefore, the differential requirement of adhesion for NET formation represents an additional explanation for the results presented in **manuscript II**, namely fully functional PMA-induced NETosis of human neutrophils in serum or serum albumin supplemented media in contrast to LPS (**manuscript II, Fig. 1**). However, as also reported by *Fuchs et al.*, high serum concentrations (5-20% hiFCS) are sufficient to decrease PMA-induced NETosis even in human neutrophils [98]. One can, therefore, assume that serum proteins still reduce the active PMA concentration or act through other, as yet unidentified, pathways. This provides an additional explanation for the apparent inhibition of PMA-induced NETosis by serum proteins observed for mouse neutrophils (**manuscript II, Fig. 3**), especially since NET stimulation of murine cells is weak either way.

Apart from direct alteration of NETosis, neutrophils can exhibit an activated or primed phenotype, e.g. in infections and chronic diseases. For instance, neutrophils isolated from patients with diabetes or SLE are more prone to NETosis, presumably owing to their lower activation level for the onset of P1 [69, 70]. *In vitro*, neutrophil priming was frequently considered for different cytokines such as TNFα, which enabled NETosis after IL-8 or LPS activation [76]. Similar mechanisms are conceivable for light-induced NETosis (**manuscript III**) *in vivo***.** It is unlikely that neutrophils in tissues respond to light with high NET rates under physiological circumstances. However, under pathophysiological conditions, priming of neutrophils possibly decreases the activation level for NETosis particularly in combination with a pathological infiltration of neutrophils into the skin. Additionally, ROS

induction by light-sensitive substances (**manuscript III, Fig. 5**) can possibly act additively within the cell and therefore enhance NET rates. Since H_2O_2 reacts downstream of NADPH oxidase activation within the signaling cascade of ROS-dependent NETosis, it is conceivable that the increasing H_2O_2 levels not only facilitate or enhance NETosis but also shorten the time of the first phase/P1 and hence accelerate the formation of NETs.

4.1.2 Active modulation of NETosis progression

After stimulation, the progression of NETosis depends on the induction of a specific signaling cascade. Indeed, the duration of P1 varies for different stimuli (**manuscript I, Supp. fig. 3**). Not surprisingly and extensively discussed in **manuscript I**, general alterations of active processes such as temperature variation and energy depletion can profoundly alter the duration of P1 or even entirely abrogate NET formation (**manuscript I, Fig. 3**). In line with this, even small variations of the neutrophils' surrounding can interfere with the progression of NETosis. A prominent example is an increase in extracellular pH towards alkaline conditions. In three independent studies, alkaline pH was correlated with enhanced NOX-dependent as well as NOX-independent NETosis. The increased NET rates were linked to enhanced ROS generation (NOX-dependent and NOX-independent), histone 4 cleavage and PAD4-mediated citrullination [370-372]. Therefore, changes in the surrounding conditions not only interfere with the onset of NETosis as discussed in **paragraph 4.1.1** (see also **manuscript II**), they can also directly alter NET progression; an essential observation for studying NETosis *in vitro* and *in vivo*.

Specific inhibition of NET-associated enzymes in P1 prevents the further progression of NETosis whereas P2 is not affected as studied by time-resolved MPO inhibition in **manuscript I** (**Fig. 3**). Simultaneously to our study (**manuscript I**), *Tatsiy et al.* reported a model, which included active modulation of early and late events in NETosis. For all tested inhibitors, they observed a clear inhibition from the beginning on, which became negligible for most inhibitors within the first hour. This observation is in perfect agreement with our data. However, for selected substances, they obtained a sufficient reduction of NOX-dependent NET formation at time-points up to 120 min [224], which would match with our P2. At a first glance, this observation is contradictory to our model. However, the authors use significantly different experimental conditions, which can massively alter the onset and progression of NETosis as already discussed above. Additionally, the quantification of NETosis by extracellular DNA release (PlaNET dye) used in this study, does not allow to draw conclusions regarding chromatin state of the analyzed cells and therefore on how many cells reached the point of no return after 120 min in their setting.

Interestingly, although cells initially spread on the surface (**manuscript I, Fig. 1** and **2**), adhesion is no prerequisite for PMA-induced NETosis in our model. In contrast, during P1, the cell retracts its body to allow cell rounding and free chromatin swelling within the cell. One can postulate that the functionality of this cell body retraction is required for the progression of NETosis. In this context, *Uotila et al.* analyzed the involvement of filamin A [373]. Filamin A is an actin cross-linker [374] involved in uropod retraction of neutrophils [375] and inhibits integrin-dependent cell adhesion [376]. Although neutrophils show regular

surface expression of integrins, knockout of filamin A enhanced integrin-mediated adhesion and subsequently decreased NETosis in response to LPS and PMA in mice [373]. In agreement with the diminished NETosis rates, enhanced integrin activity was correlated with a decrease of neutrophil elastase (NE) production [373]. Therefore, *Uotila et al.* suggested that enhanced integrin β_2 activity has a negative impact on NETosis [373]. They also proposed a more mechanistic function of filamin A in NET formation because of its actin cross-linking activity and involvement in uropod retraction. Indeed, filamin A depletion may interfere with cell rounding and softening which is, based on our results, a requirement for NET formation within P1. Interestingly, the retraction of the cell membrane from the substrate (**manuscript I, Fig. 2, Supp. fig. 4** and **Supp. movies 1/2/8/9**) is accompanied by significant degradation of the cytoskeleton and stabilization of actin filamentation by jasplakinolide inhibits NETosis persistently and significantly until early P2. In contrast, interaction of actin filament formation with cytochalasin D or latrunculin A can only diminish NETosis in the first half of P1 (**manuscript I, Fig. 5**). Thus, a functional cytoskeleton seems to be required for early events of NETosis such as translocation of proteins within the cell and most likely active uropod retraction, but the degradation of actin appears to be indispensable for later events such as translocation of NE into the nucleus [228] and further cell softening. Consequently, the cell gets biomechanically prepared for membrane rearrangement, rounding, chromatin decondensation and rupture in P2.

4.2 Chromatin swelling – a new function of chromatin?

For a long time, neutrophils were considered as terminally differentiated cells with a unique nuclear structure allowing them to squeeze through tissues. With the discovery of NETosis, entirely new properties of neutrophil nuclei became interesting. The striking finding that these cells can actively initiate chromatin reorganization such as decondensation by mixing of eu- and heterochromatin, the hallmark of NET formation [98], challenged the idea of an exclusively 'passive' neutrophil nucleus [92]. Additionally, NETosis contributes to pathogen defense and immune response in physiological as well as pathophysiological conditions. This was postulated to be "*the second function of chromatin*" [377]. With the findings presented in **manuscript I**, we add a 'third' until now undescribed function of chromatin. After initiation of chromatin decondensation at the point of no return, the swelling of the chromatin polymer appears to be the main driving force for nuclear and plasma membrane rupture. This observation paves the way for new concepts of how cells can use material properties to facilitate complex biological processes**.**

4.2.1 Entropic swelling bursts the nuclear envelope

Besides containing the genetic information of chromosomes, the cell nucleus is a very dynamic organelle. Its morphology can vary from cell type to cell type with pronounced associations with cell functions and gene expression. In addition, it is flexible, depending on the cell environment and cell activity [95]. From a biomechanical point of view, the nucleus can undergo several major changes as in migration and cell division [116, 378]. As already

pointed out, the neutrophil nucleus has to allow massive structural alterations to squeeze through the endothelium into the tissue. The description of NETosis adds several new requirements for its architecture.

The neutrophil nucleus is not only characterized by its eponymous lobulated shape, but also by a unique composition of its envelope. These characteristics develop during granulopoiesis and comprise the lack in lamin A/C and proteins of the LINC complex, decreased lamin B levels as well as markedly increased LBR. These changes most likely contribute to the remarkable flexibility of neutrophils for instance during migration [94, 133]. Interestingly, the absence of lamin A/C does not only mediate overall flexibility but also causes a lack of lamin A/C-binding to chromatin [379] and makes the cell softer and less resistant as shown in migration studies [380]. Together with the decreased expression of the tethering LINC complex [119], it possibly allows the chromatin to redistribute more easily and faster as recently discussed by *Manley et al.* [94, 237, 381]. Additionally, the rapid re- and-decondensation of chromatin in neutrophils reported under hypotonic conditions supported this hypothesis [100]. As a consequence, the nuclear envelope is overall more fragile. This makes neutrophils evolutionarily prepared for profound reorganizations and most likely allows the fast chromatin remodeling observed in the first phase of NETosis (P1). Subsequently, it prepares the following chromatin decondensation in P2 (**manuscript I, Fig. 1** and **2**). It is likely that the nuclear envelope increases its "*susceptibility to chromatin-exerted pressure*" [94]. Interestingly, murine neutrophils and HL-60 model cells contain more lamins and, at the same time, appear less fragile [99, 382]. It is therefore likely that these cells are less predisposed for chromatin remodeling as well as nuclear envelope rupture, which may lead to a delayed onset of P2. Indeed, stimulation of murine neutrophils yielded lower NET rates than human neutrophils, as repeatedly reported [383] and verified in **manuscript II** (**Fig. 1** *vs*. **Fig. 3**)**.** It would be interesting to study this phenomenon in more detail in our phase model to clarify whether NETosis in murine neutrophils shows a prolonged P1 and therefore reaches the point of no return later, or whether mice generally have lower NET rates for other reasons.

In their review, *Manley et al.* also correlated the lack in lamin A/C with the short life-span of neutrophils, as the lack of lamin A/C renders the nucleus less protected and more prone to cell death [384] and DNA damage [385, 386]. This is of particular interest for aging neutrophils, which show an activated, pro-inflammatory phenotype [71, 73] including higher NET rates [387]. It is possible that DNA alterations can prime chromatin decondensation and facilitate the onset of chromatin swelling. In addition, NE from aging neutrophils can be released more easily from granules, cleave gasdermin D and induce lytic cell death by pore-formation in membranes [388], a mechanism which was only recently implicated in NETosis. This could affect the integrity of membranes and thereby prime the cells for NETosis.

In contrast, neutrophils from older hosts display impaired NETosis [76, 77]. Interestingly, alterations in lamin proteins were previously described for different cell types of aging hosts [389, 390]. Whether neutrophils also show these changes in lamin expression, such as increase in lamin A/C levels, and whether these alterations correlate with impaired NETosis due to aggravated envelope rupture, remains to be investigated.

In addition to its unique composition, the nuclear envelope can become modified further during NET formation, for instance by phosphorylation of the remaining lamin A/C [235]. Based on our phase model (**manuscript I**), it is expected that these modifications take place predominantly in the first and active phase of NETosis (P1) (**manuscript I, Fig. 3**). Whether this particular alteration has a functional implication in the subsequent envelope rupture or whether it is a by-stander product of the mitosis pathway is unclear. However, it is likely that the nuclear envelope undergoes even more profound changes than anticipated. For instance, it was postulated that the passive or active decrease/down-regulation of LBR, the most crucial tethering molecule in the neutrophil nuclear envelope, supports delobulation and decreases heterochromatin detachment from the nuclear membrane [94]. Similar mechanisms are likely to take place during P1. LBR decrease could mainly support chromatin remodeling and the onset of chromatin swelling. Nonetheless, this hypothesis requires further investigation especially in neutrophils from mice lacking LBR [391] or time-resolved observations of the nuclear envelope proteins correlated with the state of chromatin decondensation in human neutrophils.

In two independent studies, *Fuchs et al.* and *Amulic et al.,* postulated nuclear membrane dissolution during NETosis into vesicles [98, 235]. As already discussed in **manuscript I**, this process coincides with time-points of our P2, clearly after the start of chromatin decondensation. At which stage of NETosis the nuclear membrane actually starts to disintegrate was not further addressed in these two publications. In our study, we observed the rupture of the lamina (lamin B1) significantly earlier, exactly with the onset of P2 (t_1) (**manuscript I, Fig. 2**). Together with our real-time observations, which show an impressive increase in chromatin area directly after t_1, it is very likely that the generated entropic pressure of the swelling chromatin is sufficient to burst at least the nuclear lamina and literally ‘free’ the chromatin to swell further within the cytoplasm. Whether this corresponds with the burst of the nuclear membrane, or whether the membrane is already significantly weakened beforehand and starts to dissolve already within P1, however, is not clear. Potential mechanisms of membrane weakening include gasdermin D-induced pore formation [229, 230] and alterations of the supporting cytoskeleton [228]. Most likely, the membrane is prepared by specific modifications for rupture by the expanding chromatin. These considerations are even more important given that the release of ETs is not restricted to human neutrophils, but rather represents a highly conserved process among different species, cells and organisms. Therefore, the fluidity of chromatin within the neutrophil nucleus and the unique composition of its nuclear envelope might prime neutrophils, especially human neutrophils, to undergo NETosis. However, this is most likely not the only underlying mechanism. It is expected that cells either undergo a conserved program to prepare the nuclear envelope for rupture by swelling chromatin, or the entropic chromatin swelling itself, enabled by degradation and modification of DNA and histones, is sufficient to ‘burst’ the nuclear envelope regardless of its predisposition. Further live-cell observations, however, are needed to correlate the state of chromatin remodeling in the first phase with the exact composition of the nuclear envelope. Likewise, studies on isolated nuclei from

different species could clarify how much pressure is generated by the swelling chromatin and whether this pressure suffices to burst the nuclear envelope of nuclei from all species.

4.2.2 Modulation of chromatin swelling

Each stimulus induces a specific time-course for NETosis depending on the underlying signaling cascade with its own onset for chromatin swelling [277]. Interestingly, the appearance of the released NET itself can also differ from stimulus to stimulus [277]. It is likely that the kind of chromatin modification in the first phase, which differs markedly between NOX-dependent and NOX-independent NETosis, is responsible for these variances. Thereby, the different enzymes contributing to chromatin decondensation can alter the polymer structure and therefore influence chromatin swelling in P2. Obviously, this will not hinder chromatin swelling itself, but it can provide an explanation for the slight variations observed in P2 duration in response to different stimuli (**manuscript I, Supp. fig. 3**).
It is conceivable that general changes in extracellular conditions, such as fluid osmolarity, also modulate chromatin swelling properties. For instance, hyperosmolar stress can enhance NETosis [392]. How this is biophysically regulated, however, remains unexplored.
Moreover, neutrophils are capable of actively stabilizing the swelling chromatin during NET formation, for instance by cross-linking of proteins through MPO-generated HOCl [393]. This observation also explains, at least in part, the ordered structure of the released NET and possibly allows the NET to stay intact during release. It may also facilitate the directed attack on pathogens. The question remains, what effect such alterations can have on the generated pressure and swelling behavior of the polymer itself. This is especially interesting, given that modification of the chromatin polymer structure could, thereby, influence internal structures to modulate passive energy-independent processes.
Bearing in mind that the proteome of NETs can change dramatically in response to different stimuli [245, 246], the question of whether newly generated enzymes can modify NETosis is also important. In this context, inhibition of translation and transcription do not influence NETosis in response to several stimuli tested in murine and human neutrophils [214, 394]. Thus, NETosis seems to proceed independently of newly synthesized proteins. However, with regard to the diverse NET-proteome, it is possible that neutrophils are still able to generate proteins in the first phase of NETosis. The high energy levels required for protein generation [395] could be an additional explanation for the massive decrease in ATP levels within the first 15-30 minutes of NET formation (**manuscript I, Fig. 3**).
However, a conflicting study of *Khan et al*., clearly showed dependency on transcription particularly on the promoter melting step in response to PMA, Ionomycin and LPS [396]. To explain this observation, the authors came up with a model in which promoter melting carries out an aberrant function, the support of chromatin decondensation. They termed this process "*transcriptional firing*". Interestingly, for all stimuli, the number of released NETs increased over time independently of promoter melting inhibition [396]. With regard to our phase classification, it is therefore possible that inhibition of "*transcriptional firing*" only delays NETosis. It either prolongs P1 and delays the point of no return or prolongs P2 due to alterations of the polymer structure.

Besides promoter melting, other mechanisms, which are involved in gene regulation such as histone modifications [106], were reported to have aberrant functions in NETosis. For instance, PAD4 activity with subsequent histone citrullination was frequently implicated in chromatin decondensation during NETosis. Furthermore, inhibition of chromatin deacetylation [397] or methylation [398] have been associated with increased decondensation. These mechanisms are exciting, but require further biophysical investigations with a focus on the altered chromatin structure. It is evident that several cell functions can exert until now underestimated roles, which can result in dramatic cell alterations such as NETosis.

4.2.3 Pressure of entropic chromatin swelling bursts plasma membranes

Similar to the nuclear membrane, the plasma membrane also undergoes profound changes during NETosis (**manuscript I**). Even before chromatin decondensation, the cytoskeleton degrades, the membrane rounds up and the cell height increases (**manuscript I, Fig. 2**). After full decondensation, the plasma membrane ruptures at a point predetermined by chromatin position and membrane behavior (**manuscript I, Fig. 6**). The plasma membrane was thought to become permeabilized by gasdermin D-induced pores [230]. Nonetheless, from the results of *Sollberger et al.* it is not possible to ultimately answer the question whether these pores are located only in the plasma membrane, in all membranes or whether gasdermin D is even secondarily pushed to the plasma membrane by the swelling chromatin. However, in their study, *Sollberger et al.* pointed out that gasdermin D-cleavage and the resulting pores are required for PMA-induced NET formation. Interestingly and perfectly in line with our phase model, they observed that once the cell has reached the step of chromatin decondensation (point of no return), it always lyses after the same period of time [230].
We also observed the generation of small membrane vesicles during NETosis, which remained on the substrate surface after cell retraction during cell rounding. Thereby, the cells possibly reduce excess membrane and therefore facilitate the final membrane rupture (**manuscript I, Fig. 2, Supp. fig. 4** and **Supp. movies 1/2/8/9**). Since we were also able to rule out that PMA-induced NETosis is dependent on adhesion (**manuscript I, Supp. fig. 12**), vesicle formation might not be required for NETosis. Furthermore, it has to be clarified whether these vesicles are also formed on physiological substrates. Nonetheless, reduction of excess membrane might facilitate NETosis and provide a reasonable explanation for the accelerated NETosis in aged neutrophils. However, this hypothesis requires further investigation, particularly in live-cell and in *in vivo* settings.
In this context, it would be of considerable interest to investigate how changes in membrane lipid composition alter the time-course of NETosis, especially the duration of P2. For cholesterol, an implication in NET release was already documented. Interestingly, depletion of cholesterol clearly enhanced NETosis [399, 400].

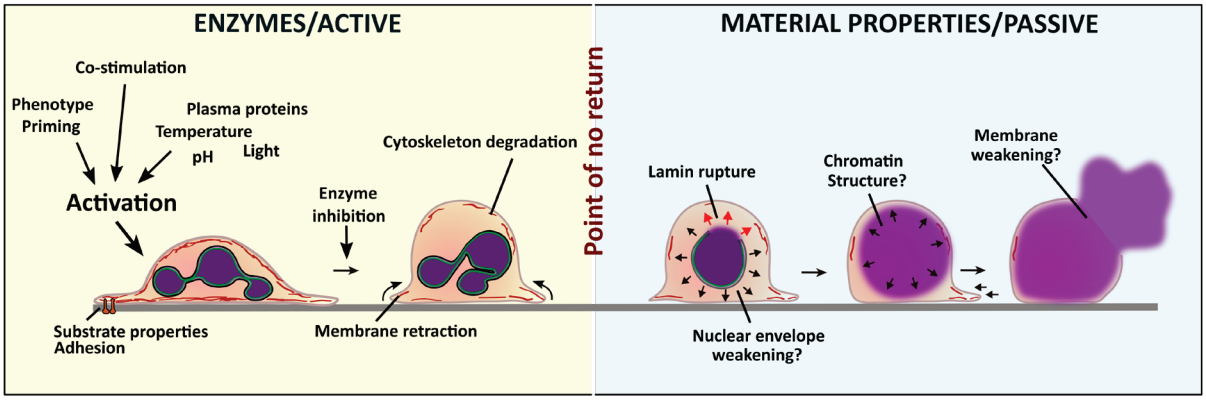

Figure 9: Model of NET formation and regulation. The active, first phase of NETosis depends on enzyme activity. Within this phase, NETosis can be inhibited or attenuated by several external factors as well as active biological signaling processes and enzymatic activity. Additionally, the cell reorganizes its membranes, rounds up and degrades the cytoskeleton. With the start of chromatin decondensation, NETosis reaches a point of no return. Thereafter, NETosis is driven by material properties, above all entropic chromatin swelling. The progression of this second phase can be modified by, for instance, membrane predisposition and chromatin polymer structure. *Neubert et al. in preparation.*

In summary, all these alterations including cytoskeleton degradation, DNA modification, histone degradation, remodeling of the cell body as well as modification of nuclear and plasma membrane, indicate that neutrophils actively prepare themselves in the first energy-dependent phase of NETosis for the passive entropic swelling of chromatin in the second phase. Therefore, the cell can actively remodel its cell body to make use of material properties of its interior. This observation expands the toolbox of cells by a very interesting feature, which is, bearing in mind the broad distribution of ET formation among various species, most likely not restricted to neutrophils or even to the process of ETosis. The transferability of this concept to other dramatic morphological changes in biology has to be investigated in further studies.

4.3 Implementation of the NETosis phase model in therapies

With increasing implications in pathological conditions, NETosis is also of growing interest as a pharmaceutical target. Thereby, researchers mostly rely on knockout mouse models and *ex vivo* stimulation assays with isolated neutrophils. In this context, the inhibition/deletion of key enzymes involved in NET signaling such as PAD4, NE, MPO or NADPH oxidase are unavoidable. These models are indispensable to understand the underlying signaling cascades. However, they have the widely known limitation to only partially reflect *in vivo* conditions in humans. Obviously, this is of interest for NET assays, bearing in mind the pronounced dependency of NETosis on external factors, different stimuli as well as on the neutrophil species (human *vs.* murine) (**manuscript II**, **paragraph 4.1** and **4.2**). Additionally, several enzymes implicated in NETosis have multiple functions. For instance, knockout of NADPH oxidase inhibits NETosis. The afflicted mice, however, can suffer from severe infections due to decreased overall immune defense [297].

With the phase model presented in **manuscript I**, we added another important factor, which has to be considered when exploring NET-related therapeutic approaches: NET formation is only partially regulated by enzymatic activity. Therefore, if cells already passed the point of

no return, the progression of NET formation cannot be stopped anymore. This observation restricts the window of pharmacological intervention by direct inhibition of NET-associated enzymes but highlights the importance of considering other strategies. However, it has to be considered that neutrophils occur at different stages of NET formation within the tissue. Therefore, a combination of 'alternative' strategies with active inhibition of NET-associated enzymes represents a very promising approach.

Among these 'alternative' strategies, the clearance of NETs by DNase is perhaps the most widely used one. DNase treatment was tested in several *in vitro* and *in vivo* studies with good results, especially in chronic inflammation [227]. Interestingly, DNase treatment was already established as inhaled medication in cystic fibrosis therapy (Dornase alpha/Pulmozyme®, approval 1994) long before the formation of NETs was implicated in the pathogenesis of this disorder [246]. However, the treatment with DNase also holds risks and is not the ultimate solution for all NET-associated diseases [192]. As shown by *Kolaczkowska et al.*, NETs are only incompletely cleared by DNase treatment and leave active enzymes behind, which can cause severe tissue damage. This observation has to be considered in NET therapy [256]. To decrease the damage by cytotoxic NET-proteins a different concept of clearance was proposed: the neutralization of these mostly cationic proteins. This strategy revealed good results in a model of sepsis. In this study, the non-anticoagulant form of heparin could neutralize cytotoxic histones and improve survival in mice [401]. A combination of protein neutralization with DNase treatment could be an interesting approach in tissue to address locally restricted NETosis and avoid further damage by reactive proteins.

However, it would also be beneficial to directly interfere with the passive phase (P2) (**manuscript I**) and delay or inhibit NET release in pathological conditions. Here, the most reasonable concepts include the stabilization of the plasma membrane by, for instance, alteration of membrane lipid composition or cross-linking of the chromatin polymer within the cell to stop chromatin swelling. Both concepts would 'freeze' NET formation to some extent and possibly allow subsequent clearance by phagocytosis. Importantly, this could allow a silent clearance of NETotic cells in comparison to DNase treatment. Nonetheless, several questions remain before such concepts can be tested *in vivo*, among them, which substances specifically target neutrophils and intercalate into the membrane or penetrate through the membrane to the chromatin polymer. It also has to be clarified whether NETotic cells express specific 'eat-me'-signals at the surface, which would induce subsequent phagocytosis even without membrane rupture. To give one example, the typical 'eat-me'-signal of apoptotic neutrophils, phosphatidylserine, is only visible for NETotic cells after membrane rupture [98].

It is also conceivable to use the pronounced susceptibility of NETosis towards external factors for its intervention. For instance, accurate regulation of osmolarity, plasma protein concentration, temperature, ROS scavenging and pH could decrease NETosis [370, 392] (**all manuscripts**) and possibly improve the effect of specific inhibitors of NET-associated proteins in combined dosage forms. One straightforward target for such combinations is the

superficial dysregulation of NETosis such as on the surface of the cornea as suggested in the therapy of ophthalmic diseases [392].

The precise targeting of NETosis in tissues, however, appears to be far more complex. The increasing knowledge of different neutrophil phenotypes and recruitment pathways in specific tissues [14, 35, 402] also expands the options in NETosis targeting. Specific inhibition of neutrophil recruitment into the affected organ could contribute to a more precise intervention of NET-associated diseases compared to an overall inhibition of NETosis. In this context, it is important to investigate further whether NET formation is necessarily associated with attenuated migration, especially after the point of no return or whether neutrophils are still able to migrate even after successful activation.

4.4 Relevance of light-induced NETosis *in vivo*

As extensively discussed in **manuscript III**, *in vitro* ROS-mediated light-induced NETosis is a starting point to further investigate the role of neutrophils and NETosis in light-sensitive skin diseases. Therefore, NET formation has to be verified within the tissue of patients suffering from photodermatoses. Controlled irradiation of human skin with light of defined wavelengths and subsequent collection of skin sections would be most suitable to clarify the contribution of each modality. However, with regard to the exclusivity of these samples, precise dose-monitored irradiation in model mouse could mainly support our understanding of light-induced NETosis *in vivo*.

Along with these studies, it is essential to clarify the involvement of PAD4 activity in light-induced NET formation. This is of particular interest regarding the high antigen levels directed against citrullinated proteins in many autoimmune disorders. In the inhibitor studies of **manuscript III**, we observed decreased NET rates after pan-PAD inhibition with Cl-amidine (**Fig. 3**). Based on these results, at least, a contribution of PAD enzymes to the observed chromatin decondensation is likely. However, further studies are required to investigate the exact role of PAD4 by specific inhibitor studies [403], with isolated neutrophils as well as verification of citrullinated proteins in skin sections and mouse models. For the latter, it is essential to differentiate between general improvement of symptoms, decrease in citrullinated proteins, and NET formation, as PAD inhibition does not selectively block NETosis. PAD4 also restricts general protein citrullination and contributes to the anti-inflammatory response. Additionally, all results obtained in mouse models have to be precisely verified and validated in human tissue, as the involvement of PAD4 in NET formation in different species is a matter of ongoing debate [214, 224, 403, 404].

Neutrophils from patients with autoimmune disorders were also frequently reported to be primed for NETosis (discussion of **manuscript III**). Whether this also applies particularly for light-induced NETosis, can be clarified by controlled irradiation of neutrophils from patients in comparison to healthy controls. However, the questions remain whether neutrophil priming can reduce the threshold for NETosis in response to light and whether this effect is attributable to a particular neutrophil phenotype, for instance LDGs of patients with SLE.

The results of **manuscript III** also indicate that light-induced NET formation in our setup is mediated by extracellular ROS formation (**Fig. 5**). Since several light sensitive autoimmune disorders show a pronounced ROS imbalance (see also discussion of **manuscript III**), it would be interesting to study the possible correlation between these two. Therefore, the redox capacity within the skin has to be correlated with the individual NETosis rate after light irradiation, conceptually similar to a recent study from *Inoue et al.*, which correlates redox imbalance in blood with NET-associated lung metastasis [405]. Subsequently, if a correlation between these two characteristics exists, the application of ROS scavengers in mice model could serve as a proof of principle to target light-induced NETosis. Importantly, a beneficial effect of ROS scavenging was already described in NETosis targeting in autoimmune diseases [37].

Apart from its relevance in disease progression, light-induced ROS generation with subsequent NET release could also be important in therapeutic settings (see discussion of **manuscript III**). Induction of cell death by ROS generation after excitation of blue light-sensitive porphyrin- or flavin-based photosensitizers is involved in the photodynamic therapy (PDT) of basal cell carcinoma, Bowen's disease and actinic keratosis (*carcinoma in situ*) and has been linked to bactericidal effects in bacterial keratitis or acne. Whether NETosis is involved in these settings has to be addressed in separate *in vivo* studies. However, based on our current understanding and the data presented in **manuscript III**, it appears likely that NETs play a role in this process.

Parts of the introduction and discussion including figures are prepared for the submission to a peer-reviewed journal in form of a review on the driving forces in NET formation.

References

1. Murphy, K., et al., *Janeway's immunobiology. 8th ed.* New York: Garland Science, 2012.
2. Netea, M.G., et al., *Trained immunity: A program of innate immune memory in health and disease.* Science, 2016. **352**(6284).
3. Netea, M.G., J. Quintin, and J.W. van der Meer, *Trained immunity: a memory for innate host defense.* Cell Host Microbe, 2011. **9**(5): p. 355-61.
4. Jenne, C.N., S. Liao, and B. Singh, *Neutrophils: multitasking first responders of immunity and tissue homeostasis.* Cell Tissue Res, 2018. **371**(3): p. 395-397.
5. Brinkmann, V., et al., *Neutrophil extracellular traps kill bacteria.* Science, 2004. **303**: p. 1532-1535.
6. Lahoz-Beneytez, J., et al., *Human neutrophil kinetics: modeling of stable isotope labeling data supports short blood neutrophil half-lives.* Blood, 2016. **127**(26): p. 3431-8.
7. Colotta, F., et al., *Modulation of granulocyte survival and programmed cell death by cytokines and bacterial products.* Blood, 1992. **80**(8): p. 2012-20.
8. Pillay, J., et al., *In vivo labeling with 2H2O reveals a human neutrophil lifespan of 5.4 days.* Blood, 2010. **116**(4): p. 625-7.
9. Tofts, P.S., et al., *Doubts concerning the recently reported human neutrophil lifespan of 5.4 days.* Blood, 2011. **117**(22): p. 6050-6052.
10. Malcolm, K.C., et al., *Microarray analysis of lipopolysaccharide-treated human neutrophils.* Am J Physiol Lung Cell Mol Physiol, 2003. **284**(4): p. L663-70.
11. Zhang, X., et al., *Gene expression in mature neutrophils: early responses to inflammatory stimuli.* J Leukoc Biol, 2004. **75**(2): p. 358-72.
12. Tsukahara, Y., et al., *Gene expression in human neutrophils during activation and priming by bacterial lipopolysaccharide.* J Cell Biochem, 2003. **89**(4): p. 848-61.
13. Scapini, P. and M.A. Cassatella, *Social networking of human neutrophils within the immune system.* Blood, 2014. **124**(5): p. 710-9.
14. Nauseef, W.M. and N. Borregaard, *Neutrophils at work.* Nature Immunology, 2014. **15**: p. 602.
15. Rosales, C., *Neutrophil: A Cell with Many Roles in Inflammation or Several Cell Types?* Front Physiol, 2018. **9**: p. 113.
16. Hong, C.W., *Current Understanding in Neutrophil Differentiation and Heterogeneity.* Immune Netw, 2017. **17**(5): p. 298-306.
17. Costa, S., et al., *Recent advances on the crosstalk between neutrophils and B or T lymphocytes.* Immunology, 2019. **156**(1): p. 23-32.
18. Leliefeld, P.H.C., L. Koenderman, and J. Pillay, *How Neutrophils Shape Adaptive Immune Responses.* Frontiers in immunology, 2015. **6**: p. 471-471.
19. Hampton, H.R. and T. Chtanova, *The lymph node neutrophil.* Semin Immunol, 2016. **28**(2): p. 129-36.
20. Lin, A. and K. Lore, *Granulocytes: New Members of the Antigen-Presenting Cell Family.* Front Immunol, 2017. **8**: p. 1781.
21. Fanger, N.A., et al., *Activation of human T cells by major histocompatability complex class II expressing neutrophils: proliferation in the presence of superantigen, but not tetanus toxoid.* Blood, 1997. **89**(11): p. 4128-35.

22. Sandilands, G.P., et al., *Major histocompatibility complex class II (DR) antigen and costimulatory molecules on in vitro and in vivo activated human polymorphonuclear neutrophils.* Immunology, 2006. **119**(4): p. 562-571.
23. Radsak, M., et al., *Polymorphonuclear neutrophils as accessory cells for T-cell activation: major histocompatibility complex class II restricted antigen-dependent induction of T-cell proliferation.* Immunology, 2000. **101**(4): p. 521-30.
24. Beauvillain, C., et al., *CCR7 is involved in the migration of neutrophils to lymph nodes.* Blood, 2011. **117**(4): p. 1196-204.
25. Liang, F., et al., *Vaccine priming is restricted to draining lymph nodes and controlled by adjuvant-mediated antigen uptake.* Sci Transl Med, 2017. **9**(393).
26. Beauvillain, C., et al., *Neutrophils efficiently cross-prime naive T cells in vivo.* Blood, 2007. **110**(8): p. 2965-73.
27. Duffy, D., et al., *Neutrophils transport antigen from the dermis to the bone marrow, initiating a source of memory CD8+ T cells.* Immunity, 2012. **37**(5): p. 917-29.
28. Hufford, M.M., et al., *Influenza-infected neutrophils within the infected lungs act as antigen presenting cells for anti-viral CD8(+) T cells.* PLoS One, 2012. **7**(10): p. e46581.
29. Scapini, P., F. Bazzoni, and M.A. Cassatella, *Regulation of B-cell-activating factor (BAFF)/B lymphocyte stimulator (BLyS) expression in human neutrophils.* Immunol Lett, 2008. **116**(1): p. 1-6.
30. Puga, I., et al., *B cell–helper neutrophils stimulate the diversification and production of immunoglobulin in the marginal zone of the spleen.* Nature Immunology, 2011. **13**: p. 170.
31. Breedveld, A., et al., *Granulocytes as modulators of dendritic cell function.* J Leukoc Biol, 2017. **102**(4): p. 1003-1016.
32. Prame Kumar, K., A.J. Nicholls, and C.H.Y. Wong, *Partners in crime: neutrophils and monocytes/macrophages in inflammation and disease.* Cell Tissue Res, 2018. **371**(3): p. 551-565.
33. Blomgran, R. and J.D. Ernst, *Lung neutrophils facilitate activation of naive antigen-specific CD4+ T cells during Mycobacterium tuberculosis infection.* J Immunol, 2011. **186**(12): p. 7110-9.
34. Jaeger, B.N., et al., *Neutrophil depletion impairs natural killer cell maturation, function, and homeostasis.* J Exp Med, 2012. **209**(3): p. 565-80.
35. Soehnlein, O., et al., *Neutrophils as protagonists and targets in chronic inflammation.* Nat Rev Immunol, 2017. **17**(4): p. 248-261.
36. Mortaz, E., et al., *Update on Neutrophil Function in Severe Inflammation.* Frontiers in immunology, 2018. **9**: p. 2171-2171.
37. Gupta, S. and M.J. Kaplan, *The role of neutrophils and NETosis in autoimmune and renal diseases.* Nat Rev Nephrol, 2016.
38. Uribe-Querol, E. and C. Rosales, *Neutrophils in Cancer: Two Sides of the Same Coin.* Journal of immunology research, 2015. **2015**: p. 983698-983698.
39. Amulic, B., et al., *Neutrophil function: from mechanisms to disease.* Annu Rev Immunol, 2012. **30**: p. 459-89.
40. Dancey, J.T., et al., *Neutrophil kinetics in man.* J Clin Invest, 1976. **58**(3): p. 705-15.
41. Ehrlich, P. and F. Himmelweit, *Collected papers of Paul Ehrlich: in four volumes including a complete bibliography.* Pergamon Press, 1956. **1**: p. 666.
42. Zucker-Franklin, D., *Electron microscopic studies of human granulocytes: structural variations related to function.* Semin Hematol, 1968. **5**(2): p. 109-33.

43. Zucker-Franklin, D., *Physiological and pathological variations in the ultrastructure of neutrophils and monocytes.* Clin Haematol, 1975. **4**(3): p. 485-508.
44. Rorvig, S., et al., *Ficolin-1 is present in a highly mobilizable subset of human neutrophil granules and associates with the cell surface after stimulation with fMLP.* J Leukoc Biol, 2009. **86**(6): p. 1439-49.
45. Cowland, J.B. and N. Borregaard, *Granulopoiesis and granules of human neutrophils.* Immunol Rev, 2016. **273**(1): p. 11-28.
46. Bainton, D.F., J.L. Ullyot, and M.G. Farquhar, *The development of neutrophilic polymorphonuclear leukocytes in human bone marrow.* The Journal of experimental medicine, 1971. **134**(4): p. 907-934.
47. Perie, L., et al., *The Branching Point in Erythro-Myeloid Differentiation.* Cell, 2015. **163**(7): p. 1655-62.
48. Notta, F., et al., *Distinct routes of lineage development reshape the human blood hierarchy across ontogeny.* Science, 2016. **351**(6269): p. aab2116.
49. Gorgens, A., et al., *Revision of the human hematopoietic tree: granulocyte subtypes derive from distinct hematopoietic lineages.* Cell Rep, 2013. **3**(5): p. 1539-52.
50. Rorvig, S., et al., *Proteome profiling of human neutrophil granule subsets, secretory vesicles, and cell membrane: correlation with transcriptome profiling of neutrophil precursors.* J Leukoc Biol, 2013. **94**(4): p. 711-21.
51. Cowland, J.B. and N. Borregaard, *The individual regulation of granule protein mRNA levels during neutrophil maturation explains the heterogeneity of neutrophil granules.* J Leukoc Biol, 1999. **66**(6): p. 989-95.
52. Borregaard, N., et al., *Biosynthesis of granule proteins in normal human bone marrow cells. Gelatinase is a marker of terminal neutrophil differentiation.* Blood, 1995. **85**(3): p. 812-7.
53. Mora-Jensen, H., et al., *Technical advance: immunophenotypical characterization of human neutrophil differentiation.* J Leukoc Biol, 2011. **90**(3): p. 629-34.
54. Sugiyama, T., et al., *Maintenance of the hematopoietic stem cell pool by CXCL12-CXCR4 chemokine signaling in bone marrow stromal cell niches.* Immunity, 2006. **25**(6): p. 977-88.
55. Kunisaki, Y., et al., *Arteriolar niches maintain haematopoietic stem cell quiescence.* Nature, 2013. **502**: p. 637.
56. Kim, H.K., et al., *G-CSF down-regulation of CXCR4 expression identified as a mechanism for mobilization of myeloid cells.* Blood, 2006. **108**(3): p. 812-20.
57. Semerad, C.L., et al., *G-CSF potently inhibits osteoblast activity and CXCL12 mRNA expression in the bone marrow.* Blood, 2005. **106**(9): p. 3020-3027.
58. Köhler, A., et al., *G-CSF-mediated thrombopoietin release triggers neutrophil motility and mobilization from bone marrow via induction of Cxcr2 ligands.* Blood, 2011. **117**(16): p. 4349-57.
59. Eash, K.J., et al., *CXCR2 and CXCR4 antagonistically regulate neutrophil trafficking from murine bone marrow.* J Clin Invest, 2010. **120**(7): p. 2423-31.
60. Laan, M., et al., *Neutrophil recruitment by human IL-17 via C-X-C chemokine release in the airways.* J Immunol, 1999. **162**(4): p. 2347-52.
61. Jones, C.E. and K. Chan, *Interleukin-17 stimulates the expression of interleukin-8, growth-related oncogene-alpha, and granulocyte-colony-stimulating factor by human airway epithelial cells.* Am J Respir Cell Mol Biol, 2002. **26**(6): p. 748-53.
62. Pelletier, M., et al., *Evidence for a cross-talk between human neutrophils and Th17 cells.* Blood, 2010. **115**(2): p. 335-343.

63. Boettcher, S., et al., *Endothelial cells translate pathogen signals into G-CSF-driven emergency granulopoiesis.* Blood, 2014. **124**(9): p. 1393-403.
64. Manz, M.G. and S. Boettcher, *Emergency granulopoiesis.* Nature Reviews Immunology, 2014. **14**: p. 302.
65. Stark, M.A., et al., *Phagocytosis of apoptotic neutrophils regulates granulopoiesis via IL-23 and IL-17.* Immunity, 2005. **22**(3): p. 285-94.
66. Kolaczkowska, E. and P. Kubes, *Neutrophil recruitment and function in health and inflammation.* Nat Rev Immunol, 2013. **13**(3): p. 159-75.
67. Gallin, J.I., *Human neutrophil heterogeneity exists, but is it meaningful?* Blood, 1984. **63**(5): p. 977-83.
68. El-Benna, J., et al., *Priming of the neutrophil respiratory burst: role in host defense and inflammation.* Immunol Rev, 2016. **273**(1): p. 180-93.
69. Wong, S.L., et al., *Diabetes primes neutrophils to undergo NETosis, which impairs wound healing.* Nat Med, 2015. **21**(7): p. 815-9.
70. Garcia-Romo, G.S., et al., *Netting neutrophils are major inducers of type I IFN production in pediatric systemic lupus erythematosus.* Sci Transl Med, 2011. **3**(73): p. 73ra20.
71. Casanova-Acebes, M., et al., *Rhythmic modulation of the hematopoietic niche through neutrophil clearance.* Cell, 2013. **153**(5): p. 1025-35.
72. Adrover, J.M., J.A. Nicolas-Avila, and A. Hidalgo, *Aging: A Temporal Dimension for Neutrophils.* Trends Immunol, 2016. **37**(5): p. 334-345.
73. Zhang, D., et al., *Neutrophil ageing is regulated by the microbiome.* Nature, 2015. **525**: p. 528.
74. Alves-Filho, J.C., F. Spiller, and F.Q. Cunha, *Neutrophil paralysis in sepsis.* Shock, 2010. **34 Suppl 1**: p. 15-21.
75. Tsuda, Y., et al., *Three different neutrophil subsets exhibited in mice with different susceptibilities to infection by methicillin-resistant Staphylococcus aureus.* Immunity, 2004. **21**(2): p. 215-26.
76. Hazeldine, J., et al., *Impaired neutrophil extracellular trap formation: a novel defect in the innate immune system of aged individuals.* Aging cell, 2014. **13**(4): p. 690-698.
77. Tseng, C.W., et al., *Innate immune dysfunctions in aged mice facilitate the systemic dissemination of methicillin-resistant S. aureus.* PLoS One, 2012. **7**(7): p. e41454.
78. Sapey, E., et al., *Phosphoinositide 3-kinase inhibition restores neutrophil accuracy in the elderly: toward targeted treatments for immunosenescence.* Blood, 2014. **123**(2): p. 239-48.
79. Qian, F., et al., *Reduced bioenergetics and toll-like receptor 1 function in human polymorphonuclear leukocytes in aging.* Aging (Albany NY), 2014. **6**(2): p. 131-9.
80. Tseng, C.W. and G.Y. Liu, *Expanding roles of neutrophils in aging hosts.* Curr Opin Immunol, 2014. **29**: p. 43-8.
81. Gorlino, C.V., et al., *Neutrophils exhibit differential requirements for homing molecules in their lymphatic and blood trafficking into draining lymph nodes.* J Immunol, 2014. **193**(4): p. 1966-74.
82. Massena, S., et al., *Identification and characterization of VEGF-A-responsive neutrophils expressing CD49d, VEGFR1, and CXCR4 in mice and humans.* Blood, 2015. **126**(17): p. 2016-26.
83. Silvestre-Roig, C., A. Hidalgo, and O. Soehnlein, *Neutrophil heterogeneity: implications for homeostasis and pathogenesis.* Blood, 2016. **127**(18): p. 2173-81.

84. Hacbarth, E. and A. Kajdacsy-Balla, *Low density neutrophils in patients with systemic lupus erythematosus, rheumatoid arthritis, and acute rheumatic fever.* Arthritis Rheum, 1986. **29**(11): p. 1334-42.
85. Denny, M.F., et al., *A distinct subset of proinflammatory neutrophils isolated from patients with systemic lupus erythematosus induces vascular damage and synthesizes type I IFNs.* J Immunol, 2010. **184**(6): p. 3284-97.
86. Lood, C., et al., *Neutrophil extracellular traps enriched in oxidized mitochondrial DNA are interferogenic and contribute to lupus-like disease.* Nat Med, 2016. **22**(2): p. 146-153.
87. Villanueva, E., et al., *Netting neutrophils induce endothelial damage, infiltrate tissues, and expose immunostimulatory molecules in systemic lupus erythematosus.* J Immunol, 2011. **187**(1): p. 538-52.
88. Darcy, C.J., et al., *Neutrophils with myeloid derived suppressor function deplete arginine and constrain T cell function in septic shock patients.* Crit Care, 2014. **18**(4): p. R163.
89. Mishalian, I., Z. Granot, and Z.G. Fridlender, *The diversity of circulating neutrophils in cancer.* Immunobiology, 2017. **222**(1): p. 82-88.
90. Condamine, T., et al., *Lectin-type oxidized LDL receptor-1 distinguishes population of human polymorphonuclear myeloid-derived suppressor cells in cancer patients.* Sci Immunol, 2016. **1**(2).
91. Sagiv, J.Y., S. Voels, and Z. Granot, *Isolation and Characterization of Low- vs. High-Density Neutrophils in Cancer.* Methods Mol Biol, 2016. **1458**: p. 179-93.
92. Carvalho, L.O., et al., *The Neutrophil Nucleus and Its Role in Neutrophilic Function.* J Cell Biochem, 2015. **116**(9): p. 1831-6.
93. Vestweber, D., *How leukocytes cross the vascular endothelium.* Nat Rev Immunol, 2015. **15**(11): p. 692-704.
94. Manley, H.R., M.C. Keightley, and G.J. Lieschke, *The Neutrophil Nucleus: An Important Influence on Neutrophil Migration and Function.* Frontiers in Immunology, 2018. **9**: p. 2867.
95. Skinner, B.M. and E.E. Johnson, *Nuclear morphologies: their diversity and functional relevance.* Chromosoma, 2017. **126**(2): p. 195-212.
96. Sanchez, J.A. and L.J. Wangh, *New insights into the mechanisms of nuclear segmentation in human neutrophils.* J Cell Biochem, 1999. **73**(1): p. 1-10.
97. Campbell, M.S., M.A. Lovell, and G.J. Gorbsky, *Stability of nuclear segments in human neutrophils and evidence against a role for microfilaments or microtubules in their genesis during differentiation of HL60 myelocytes.* J Leukoc Biol, 1995. **58**(6): p. 659-66.
98. Fuchs, T.A., et al., *Novel cell death program leads to neutrophil extracellular traps.* J Cell Biol, 2007. **176**(2): p. 231-41.
99. Olins, D.E. and A.L. Olins, *Granulocyte heterochromatin: defining the epigenome.* BMC Cell Biol, 2005. **6**: p. 39.
100. Hubner, B., et al., *Remodeling of nuclear landscapes during human myelopoietic cell differentiation maintains co-aligned active and inactive nuclear compartments.* Epigenetics Chromatin, 2015. **8**: p. 47.
101. Richmond, T.J. and C.A. Davey, *The structure of DNA in the nucleosome core.* Nature, 2003. **423**(6936): p. 145-50.
102. Schalch, T., et al., *X-ray structure of a tetranucleosome and its implications for the chromatin fibre.* Nature, 2005. **436**(7047): p. 138-41.

103. Luger, K., et al., *Crystal structure of the nucleosome core particle at 2.8 A resolution.* Nature, 1997. **389**(6648): p. 251-60.
104. Horn, P.J. and C.L. Peterson, *Molecular biology. Chromatin higher order folding--wrapping up transcription.* Science, 2002. **297**(5588): p. 1824-7.
105. Zhu, Y., et al., *Comprehensive characterization of neutrophil genome topology.* Genes Dev, 2017. **31**(2): p. 141-153.
106. Kouzarides, T., *Chromatin modifications and their function.* Cell, 2007. **128**(4): p. 693-705.
107. Li, B., M. Carey, and J.L. Workman, *The role of chromatin during transcription.* Cell, 2007. **128**(4): p. 707-19.
108. Callan, H.G. and S.G. Tomlin, *Experimental studies on amphibian oocyte nuclei. I. Investigation of the structure of the nuclear membrane by means of the electron microscope.* Proc R Soc Lond B Biol Sci, 1950. **137**(888): p. 367-78.
109. Beck, M. and E. Hurt, *The nuclear pore complex: understanding its function through structural insight.* Nat Rev Mol Cell Biol, 2017. **18**(2): p. 73-89.
110. de Leeuw, R., Y. Gruenbaum, and O. Medalia, *Nuclear Lamins: Thin Filaments with Major Functions.* Trends Cell Biol, 2018. **28**(1): p. 34-45.
111. Shimi, T., et al., *Structural organization of nuclear lamins A, C, B1, and B2 revealed by superresolution microscopy.* Molecular biology of the cell, 2015. **26**(22): p. 4075-4086.
112. Gerace, L., A. Blum, and G. Blobel, *Immunocytochemical localization of the major polypeptides of the nuclear pore complex-lamina fraction. Interphase and mitotic distribution.* J Cell Biol, 1978. **79**(2 Pt 1): p. 546-66.
113. Guelen, L., et al., *Domain organization of human chromosomes revealed by mapping of nuclear lamina interactions.* Nature, 2008. **453**(7197): p. 948-51.
114. Crisp, M., et al., *Coupling of the nucleus and cytoplasm: role of the LINC complex.* J Cell Biol, 2006. **172**(1): p. 41-53.
115. Sosa, B.A., U. Kutay, and T.U. Schwartz, *Structural insights into LINC complexes.* Curr Opin Struct Biol, 2013. **23**(2): p. 285-91.
116. Ungricht, R. and U. Kutay, *Mechanisms and functions of nuclear envelope remodelling.* Nat Rev Mol Cell Biol, 2017. **18**(4): p. 229-245.
117. Dahl, K.N., A.J. Ribeiro, and J. Lammerding, *Nuclear shape, mechanics, and mechanotransduction.* Circ Res, 2008. **102**(11): p. 1307-18.
118. Yabuki, M., et al., *Role of nuclear lamins in nuclear segmentation of human neutrophils.* Physiol Chem Phys Med NMR, 1999. **31**(2): p. 77-84.
119. Olins, A.L., et al., *The LINC-less granulocyte nucleus.* Eur J Cell Biol, 2009. **88**(4): p. 203-14.
120. Davidson, P.M., et al., *Design of a microfluidic device to quantify dynamic intra-nuclear deformation during cell migration through confining environments.* Integr Biol (Camb), 2015. **7**(12): p. 1534-46.
121. Broers, J.L., et al., *Decreased mechanical stiffness in LMNA-/- cells is caused by defective nucleo-cytoskeletal integrity: implications for the development of laminopathies.* Hum Mol Genet, 2004. **13**(21): p. 2567-80.
122. Lammerding, J., et al., *Lamin A/C deficiency causes defective nuclear mechanics and mechanotransduction.* J Clin Invest, 2004. **113**(3): p. 370-8.
123. Olins, A.L. and D.E. Olins, *Cytoskeletal influences on nuclear shape in granulocytic HL-60 cells.* BMC Cell Biol, 2004. **5**: p. 30.

124. Gruenbaum, Y., et al., *The nuclear lamina comes of age.* Nat Rev Mol Cell Biol, 2005. **6**(1): p. 21-31.
125. Olins, A.L., et al., *Lamin B receptor: multi-tasking at the nuclear envelope.* Nucleus, 2010. **1**(1): p. 53-70.
126. Nikolakaki, E., I. Mylonis, and T. Giannakouros, *Lamin B Receptor: Interplay between Structure, Function and Localization.* Cells, 2017. **6**(3).
127. Park, B.H., J. Dolen, and B. Snyder, *Defective chemotactic migration of polymorphonuclear leukocytes in Pelger-Huet anomaly.* Proc Soc Exp Biol Med, 1977. **155**(1): p. 51-4.
128. Hoffmann, K., et al., *Mutations in the gene encoding the lamin B receptor produce an altered nuclear morphology in granulocytes (Pelger-Huet anomaly).* Nat Genet, 2002. **31**(4): p. 410-4.
129. Hoffmann, K., et al., *The granulocyte nucleus and lamin B receptor: avoiding the ovoid.* Chromosoma, 2007. **116**(3): p. 227-35.
130. Sanchez, J.A., R.J. Karni, and L.J. Wangh, *Fluorescent in situ hybridization (FISH) analysis of the relationship between chromosome location and nuclear morphology in human neutrophils.* Chromosoma, 1997. **106**(3): p. 168-77.
131. Olins, A.L. and D.E. Olins, *The mechanism of granulocyte nuclear shape determination: possible involvement of the centrosome.* Eur J Cell Biol, 2005. **84**(2-3): p. 181-8.
132. Feng, D., et al., *Neutrophils emigrate from venules by a transendothelial cell pathway in response to FMLP.* J Exp Med, 1998. **187**(6): p. 903-15.
133. Salvermoser, M., et al., *Nuclear Deformation During Neutrophil Migration at Sites of Inflammation.* Frontiers in immunology, 2018. **9**: p. 2680-2680.
134. Hoang, A.N., et al., *Measuring neutrophil speed and directionality during chemotaxis, directly from a droplet of whole blood.* Technology (Singap World Sci), 2013. **1**(1): p. 49.
135. Nathan, C., *Points of control in inflammation.* Nature, 2002. **420**: p. 846.
136. Zarbock, A., et al., *Leukocyte ligands for endothelial selectins: specialized glycoconjugates that mediate rolling and signaling under flow.* Blood, 2011. **118**(26): p. 6743-51.
137. Ramachandran, V., et al., *Dynamic alterations of membrane tethers stabilize leukocyte rolling on P-selectin.* Proc Natl Acad Sci U S A, 2004. **101**(37): p. 13519-24.
138. Sundd, P., et al., *'Slings' enable neutrophil rolling at high shear.* Nature, 2012. **488**(7411): p. 399-403.
139. Massena, S., et al., *A chemotactic gradient sequestered on endothelial heparan sulfate induces directional intraluminal crawling of neutrophils.* Blood, 2010. **116**(11): p. 1924-31.
140. Phillipson, M., et al., *Intraluminal crawling of neutrophils to emigration sites: a molecularly distinct process from adhesion in the recruitment cascade.* J Exp Med, 2006. **203**(12): p. 2569-75.
141. Garrido-Urbani, S., et al., *Vascular and epithelial junctions: a barrier for leucocyte migration.* Biochemical Society Transactions, 2008. **36**(2): p. 203-211.
142. Heit, B., et al., *An intracellular signaling hierarchy determines direction of migration in opposing chemotactic gradients.* The Journal of cell biology, 2002. **159**(1): p. 91-102.

143. McDonald, B., et al., *Kupffer cells and activation of endothelial TLR4 coordinate neutrophil adhesion within liver sinusoids during endotoxemia.* American Journal of Physiology-Gastrointestinal and Liver Physiology, 2013. **305**(11): p. G797-G806.
144. Lammermann, T., et al., *Neutrophil swarms require LTB4 and integrins at sites of cell death in vivo.* Nature, 2013. **498**(7454): p. 371-5.
145. Lominadze, G., et al., *Proteomic analysis of human neutrophil granules.* Mol Cell Proteomics, 2005. **4**(10): p. 1503-21.
146. Uriarte, S.M., et al., *Comparison of proteins expressed on secretory vesicle membranes and plasma membranes of human neutrophils.* J Immunol, 2008. **180**(8): p. 5575-81.
147. Schön, M.P., S.M. Broekaert, and L. Erpenbeck, *Sexy again: the renaissance of neutrophils in psoriasis.* Exp Dermatol, 2017. **26**(4): p. 305-311.
148. Yin, C. and B. Heit, *Armed for destruction: formation, function and trafficking of neutrophil granules.* Cell Tissue Res, 2018. **371**(3): p. 455-471.
149. Borregaard, N., et al., *Stimulus-dependent secretion of plasma proteins from human neutrophils.* J Clin Invest, 1992. **90**(1): p. 86-96.
150. Borregaard, N., L.J. Miller, and T.A. Springer, *Chemoattractant-regulated mobilization of a novel intracellular compartment in human neutrophils.* Science, 1987. **237**(4819): p. 1204-6.
151. Sengelov, H., et al., *Mobilization of granules and secretory vesicles during in vivo exudation of human neutrophils.* J Immunol, 1995. **154**(8): p. 4157-65.
152. Schaff, U.Y., et al., *Calcium flux in neutrophils synchronizes beta2 integrin adhesive and signaling events that guide inflammatory recruitment.* Ann Biomed Eng, 2008. **36**(4): p. 632-46.
153. Sengelov, H., L. Kjeldsen, and N. Borregaard, *Control of exocytosis in early neutrophil activation.* J Immunol, 1993. **150**(4): p. 1535-43.
154. Sengeløv, H., et al., *Subcellular localization and dynamics of Mac-1 (alpha m beta 2) in human neutrophils.* The Journal of clinical investigation, 1993. **92**(3): p. 1467-1476.
155. Sengelov, H., et al., *Subcellular localization and translocation of the receptor for N-formylmethionyl-leucyl-phenylalanine in human neutrophils.* Biochem J, 1994. **299 (Pt 2)**: p. 473-9.
156. Wei, C., et al., *Calcium flickers steer cell migration.* Nature, 2008. **457**: p. 901.
157. Hoffstein, S.T., R.S. Friedman, and G. Weissmann, *Degranulation, membrane addition, and shape change during chemotactic factor-induced aggregation of human neutrophils.* The Journal of Cell Biology, 1982. **95**(1): p. 234-241.
158. Leffell, M.S. and J.K. Spitznagel, *Intracellular and extracellular degranulation of human polymorphonuclear azurophil and specific granules induced by immune complexes.* Infection and immunity, 1974. **10**(6): p. 1241-1249.
159. Jog, N.R., et al., *The actin cytoskeleton regulates exocytosis of all neutrophil granule subsets.* Am J Physiol Cell Physiol, 2007. **292**(5): p. C1690-700.
160. Tapper, H., W. Furuya, and S. Grinstein, *Localized exocytosis of primary (lysosomal) granules during phagocytosis: role of Ca2+-dependent tyrosine phosphorylation and microtubules.* J Immunol, 2002. **168**(10): p. 5287-96.
161. Munafo, D.B., et al., *Rab27a is a key component of the secretory machinery of azurophilic granules in granulocytes.* Biochem J, 2007. **402**(2): p. 229-39.
162. Elstak, E.D., et al., *The munc13-4-rab27 complex is specifically required for tethering secretory lysosomes at the plasma membrane.* Blood, 2011. **118**(6): p. 1570-8.

163. Nordenfelt, P., et al., *Different requirements for early and late phases of azurophilic granule-phagosome fusion.* Traffic, 2009. **10**(12): p. 1881-93.
164. Freeman, S.A., et al., *Integrins Form an Expanding Diffusional Barrier that Coordinates Phagocytosis.* Cell, 2016. **164**(1-2): p. 128-140.
165. Fällman, M., R. Andersson, and T. Andersson, *Signaling properties of CR3 (CD11b/CD18) and CR1 (CD35) in relation to phagocytosis of complement-opsonized particles.* J Immunol, 1993. **151**(1): p. 330-8.
166. Abram, C.L. and C.A. Lowell, *Convergence of immunoreceptor and integrin signaling.* Immunol Rev, 2007. **218**: p. 29-44.
167. Metchnikoff, E. and F.G. Binnie, *Immunity in Infective Diseases*. 1905: University Press.
168. Nordenfelt, P. and H. Tapper, *Phagosome dynamics during phagocytosis by neutrophils.* J Leukoc Biol, 2011. **90**(2): p. 271-84.
169. Segal, A.W., J. Dorling, and S. Coade, *Kinetics of fusion of the cytoplasmic granules with phagocytic vacuoles in human polymorphonuclear leukocytes. Biochemical and morphological studies.* J Cell Biol, 1980. **85**(1): p. 42-59.
170. Tapper, H., *The secretion of preformed granules by macrophages and neutrophils.* J Leukoc Biol, 1996. **59**(5): p. 613-22.
171. Nguyen, G.T., E.R. Green, and J. Mecsas, *Neutrophils to the ROScue: Mechanisms of NADPH Oxidase Activation and Bacterial Resistance.* Front Cell Infect Microbiol, 2017. **7**: p. 373.
172. Nauseef, W.M., et al., *Assembly of the neutrophil respiratory burst oxidase. Protein kinase C promotes cytoskeletal and membrane association of cytosolic oxidase components.* J Biol Chem, 1991. **266**(9): p. 5911-7.
173. Harbecke, O., et al., *Desensitization of the fMLP-induced NADPH-oxidase response in human neutrophils is lacking in okadaic acid-treated cells.* J Leukoc Biol, 1997. **61**(6): p. 753-8.
174. Dahlgren, C. and A. Karlsson, *Respiratory burst in human neutrophils.* J Immunol Methods, 1999. **232**(1-2): p. 3-14.
175. Hampton, M.B., A.J. Kettle, and C.C. Winterbourn, *Inside the neutrophil phagosome: oxidants, myeloperoxidase, and bacterial killing.* Blood, 1998. **92**(9): p. 3007-17.
176. Manfredi, A.A., et al., *The Neutrophil's Choice: Phagocytose vs Make Neutrophil Extracellular Traps.* Front Immunol, 2018. **9**: p. 288.
177. Branzk, N., et al., *Neutrophils sense microbe size and selectively release neutrophil extracellular traps in response to large pathogens.* Nat Immunol, 2014. **15**(11): p. 1017-25.
178. Dalli, J., et al., *Heterogeneity in neutrophil microparticles reveals distinct proteome and functional properties.* Mol Cell Proteomics, 2013. **12**(8): p. 2205-19.
179. Timár, C.I., et al., *Antibacterial effect of microvesicles released from human neutrophilic granulocytes.* Blood, 2013. **121**(3): p. 510-518.
180. Hess, C., et al., *Ectosomes released by human neutrophils are specialized functional units.* J Immunol, 1999. **163**(8): p. 4564-73.
181. Mesri, M. and D.C. Altieri, *Leukocyte microparticles stimulate endothelial cell cytokine release and tissue factor induction in a JNK1 signaling pathway.* J Biol Chem, 1999. **274**(33): p. 23111-8.
182. Dalli, J., et al., *Annexin 1 mediates the rapid anti-inflammatory effects of neutrophil-derived microparticles.* Blood, 2008. **112**(6): p. 2512-9.

183. Eken, C., et al., *Ectosomes of polymorphonuclear neutrophils activate multiple signaling pathways in macrophages.* Immunobiology, 2013. **218**(3): p. 382-92.
184. Christenson, K., et al., *In vivo-transmigrated human neutrophils are resistant to antiapoptotic stimulation.* J Leukoc Biol, 2011. **90**(6): p. 1055-63.
185. Kennedy, A.D. and F.R. DeLeo, *Neutrophil apoptosis and the resolution of infection.* Immunologic Research, 2009. **43**(1): p. 25-61.
186. Poon, I.K.H., et al., *Apoptotic cell clearance: basic biology and therapeutic potential.* Nature Reviews Immunology, 2014. **14**: p. 166.
187. Manfredi, A.A., et al., *Instructive influences of phagocytic clearance of dying cells on neutrophil extracellular trap generation.* Clinical and experimental immunology, 2015. **179**(1): p. 24-29.
188. Takei, H., et al., *Rapid killing of human neutrophils by the potent activator phorbol 12-myristate 13-acetate (PMA) accompanied by changes different from typical apoptosis or necrosis.* J Leukoc Biol, 1996. **59**(2): p. 229-40.
189. Brinkmann, V., et al., *Neutrophil extracellular traps kill bacteria.* Science, 2004. **303**(5663): p. 1532-5.
190. Steinberg, B.E. and S. Grinstein, *Unconventional roles of the NADPH oxidase: signaling, ion homeostasis, and cell death.* Sci STKE, 2007. **2007**(379): p. pe11.
191. Brinkmann, V., *Neutrophil Extracellular Traps in the Second Decade.* J Innate Immun, 2018: p. 1-8.
192. Papayannopoulos, V., *Neutrophil extracellular traps in immunity and disease.* Nat Rev Immunol, 2018. **18**(2): p. 134-147.
193. Sollberger, G., D.O. Tilley, and A. Zychlinsky, *Neutrophil Extracellular Traps: The Biology of Chromatin Externalization.* Dev Cell, 2018. **44**(5): p. 542-553.
194. Goldmann, O. and E. Medina, *The expanding world of extracellular traps: not only neutrophils but much more.* Front Immunol, 2012. **3**: p. 420.
195. Pertiwi, K.R., et al., *Extracellular traps derived from macrophages, mast cells, eosinophils and neutrophils are generated in a time-dependent manner during atherothrombosis.* J Pathol, 2018.
196. Wong, K.W. and W.R. Jacobs, Jr., *Mycobacterium tuberculosis exploits human interferon gamma to stimulate macrophage extracellular trap formation and necrosis.* J Infect Dis, 2013. **208**(1): p. 109-19.
197. Doster, R.S., et al., *Macrophage Extracellular Traps: A Scoping Review.* J Innate Immun, 2018. **10**(1): p. 3-13.
198. Yousefi, S., et al., *Catapult-like release of mitochondrial DNA by eosinophils contributes to antibacterial defense.* Nat Med, 2008. **14**: p. 949-953.
199. Mukherjee, M., P. Lacy, and S. Ueki, *Eosinophil Extracellular Traps and Inflammatory Pathologies-Untangling the Web!* Front Immunol, 2018. **9**: p. 2763.
200. von Kockritz-Blickwede, M., et al., *Phagocytosis-independent antimicrobial activity of mast cells by means of extracellular trap formation.* Blood, 2008. **111**: p. 3070-3080.
201. Wei, Z., et al., *Canine Neutrophil Extracellular Traps Release Induced by the Apicomplexan Parasite Neospora caninum In Vitro.* Frontiers in immunology, 2016. **7**: p. 436-436.
202. Wardini, A.B., et al., *Characterization of neutrophil extracellular traps in cats naturally infected with feline leukemia virus.* J Gen Virol, 2010. **91**(Pt 1): p. 259-64.
203. Villagra-Blanco, R., et al., *Bovine Polymorphonuclear Neutrophils Cast Neutrophil Extracellular Traps against the Abortive Parasite Neospora caninum.* Front Immunol, 2017. **8**: p. 606.

204. Pisanu, S., et al., *Neutrophil extracellular traps in sheep mastitis.* Veterinary research, 2015. **46**(1): p. 59-59.
205. Pijanowski, L., et al., *Carp neutrophilic granulocytes form extracellular traps via ROS-dependent and independent pathways.* Fish Shellfish Immunol, 2013. **34**(5): p. 1244-52.
206. Chuammitri, P., et al., *Chicken heterophil extracellular traps (HETs): novel defense mechanism of chicken heterophils.* Vet Immunol Immunopathol, 2009. **129**(1-2): p. 126-31.
207. Ng, T.H., et al., *Shrimp hemocytes release extracellular traps that kill bacteria.* Dev Comp Immunol, 2013. **41**(4): p. 644-51.
208. Poirier, A.C., et al., *Antimicrobial histones and DNA traps in invertebrate immunity: evidences in Crassostrea gigas.* J Biol Chem, 2014. **289**(36): p. 24821-31.
209. Zhang, X., et al., *Social amoebae trap and kill bacteria by casting DNA nets.* Nat Commun, 2016. **7**: p. 10938.
210. Homa, J., W. Ortmann, and E. Kolaczkowska, *Conservative Mechanisms of Extracellular Trap Formation by Annelida Eisenia andrei: Serine Protease Activity Requirement.* PLoS One, 2016. **11**(7): p. e0159031.
211. Wen, F., et al., *Extracellular DNA is required for root tip resistance to fungal infection.* Plant Physiol, 2009. **151**(2): p. 820-9.
212. Hoppenbrouwers, T., et al., *In vitro induction of NETosis: Comprehensive live imaging comparison and systematic review.* 2017. **12**(5): p. e0176472.
213. van der Linden, M., et al., *Differential Signalling and Kinetics of Neutrophil Extracellular Trap Release Revealed by Quantitative Live Imaging.* Sci Rep, 2017. **7**(1): p. 6529.
214. Kenny, E.F., et al., *Diverse stimuli engage different neutrophil extracellular trap pathways.* 2017. **6**.
215. Saitoh, T., et al., *Neutrophil extracellular traps mediate a host defense response to human immunodeficiency virus-1.* Cell Host Microbe, 2012. **12**(1): p. 109-16.
216. Yost, C.C., et al., *Neonatal NET-inhibitory factor and related peptides inhibit neutrophil extracellular trap formation.* The Journal of clinical investigation, 2016. **126**(10): p. 3783-3798.
217. Metzler, K.D., et al., *Myeloperoxidase is required for neutrophil extracellular trap formation: implications for innate immunity.* Blood, 2011. **117**(3): p. 953-9.
218. Papayannopoulos, V., et al., *Neutrophil elastase and myeloperoxidase regulate the formation of neutrophil extracellular traps.* J Cell Biol, 2010. **191**(3): p. 677-91.
219. Abi Abdallah, D.S., et al., *Toxoplasma gondii triggers release of human and mouse neutrophil extracellular traps.* Infect Immun, 2012. **80**(2): p. 768-77.
220. Guimaraes-Costa, A.B., et al., *Leishmania amazonensis promastigotes induce and are killed by neutrophil extracellular traps.* Proc Natl Acad Sci U S A, 2009. **106**(16): p. 6748-53.
221. Avila, E.E., et al., *Entamoeba histolytica Trophozoites and Lipopeptidophosphoglycan Trigger Human Neutrophil Extracellular Traps.* PLoS One, 2016. **11**(7): p. e0158979.
222. Rossaint, J., et al., *Synchronized integrin engagement and chemokine activation is crucial in neutrophil extracellular trap-mediated sterile inflammation.* Blood, 2014. **123**(16): p. 2573-84.
223. Martinelli, S., et al., *Induction of genes mediating interferon-dependent extracellular trap formation during neutrophil differentiation.* J Biol Chem, 2004. **279**: p. 44123-44132.

224. Tatsiy, O. and P.P. McDonald, *Physiological Stimuli Induce PAD4-Dependent, ROS-Independent NETosis, With Early and Late Events Controlled by Discrete Signaling Pathways.* Front Immunol, 2018. **9**: p. 2036.
225. Hoffmann, J.H., et al., *Interindividual variation of NETosis in healthy donors: introduction and application of a refined method for extracellular trap quantification.* Exp Dermatol, 2016. **25**(11): p. 895-900.
226. Schauer, C., et al., *Aggregated neutrophil extracellular traps limit inflammation by degrading cytokines and chemokines.* Nat Med, 2014. **20**(5): p. 511-7.
227. Warnatsch, A., et al., *Inflammation. Neutrophil extracellular traps license macrophages for cytokine production in atherosclerosis.* Science, 2015. **349**(6245): p. 316-20.
228. Metzler, K.D., et al., *A myeloperoxidase-containing complex regulates neutrophil elastase release and actin dynamics during NETosis.* Cell Rep, 2014. **8**(3): p. 883-96.
229. Chen, K.W., et al., *Noncanonical inflammasome signaling elicits gasdermin D-dependent neutrophil extracellular traps.* Sci Immunol, 2018. **3**(26).
230. Sollberger, G., et al., *Gasdermin D plays a vital role in the generation of neutrophil extracellular traps.* Sci Immunol, 2018. **3**(26).
231. Remijsen, Q., et al., *Neutrophil extracellular trap cell death requires both autophagy and superoxide generation.* Cell Res, 2011. **21**(2): p. 290-304.
232. Tang, S., et al., *Neutrophil extracellular trap formation is associated with autophagy-related signalling in ANCA-associated vasculitis.* Clin Exp Immunol, 2015. **180**(3): p. 408-18.
233. Schreiber, A., et al., *Necroptosis controls NET generation and mediates complement activation, endothelial damage, and autoimmune vasculitis.* Proceedings of the National Academy of Sciences, 2017.
234. Desai, J., et al., *PMA and crystal-induced neutrophil extracellular trap formation involves RIPK1-RIPK3-MLKL signaling.* Eur J Immunol, 2016. **46**(1): p. 223-9.
235. Amulic, B., et al., *Cell-Cycle Proteins Control Production of Neutrophil Extracellular Traps.* Developmental Cell.
236. Yipp, B.G. and P. Kubes, *NETosis: how vital is it?* Blood, 2013. **122**(16): p. 2784-94.
237. Pilsczek, F.H., et al., *A Novel Mechanism of Rapid Nuclear Neutrophil Extracellular Trap Formation in Response to Staphylococcus aureus.* Journal of Immunology, 2010. **185**(12): p. 7413-7425.
238. Yipp, B.G., et al., *Infection-induced NETosis is a dynamic process involving neutrophil multitasking in vivo.* Nat Med, 2012. **18**(9): p. 1386-1393.
239. Yousefi, S., et al., *Viable neutrophils release mitochondrial DNA to form neutrophil extracellular traps.* Cell Death Differ, 2009. **16**(11): p. 1438-1444.
240. Desai, J., et al., *Matters of life and death. How neutrophils die or survive along NET release and is "NETosis" = necroptosis?* Cell Mol Life Sci, 2016.
241. Konig, M.F. and F. Andrade, *A Critical Reappraisal of Neutrophil Extracellular Traps and NETosis Mimics Based on Differential Requirements for Protein Citrullination.* Front Immunol, 2016. **7**: p. 461.
242. Munoz, L.E., et al., *Missing in action-The meaning of cell death in tissue damage and inflammation.* Immunol Rev, 2017. **280**(1): p. 26-40.
243. Urban, C.F., et al., *Neutrophil extracellular traps contain calprotectin, a cytosolic protein complex involved in host defense against Candida albicans.* PLoS Pathog, 2009. **5**(10): p. e1000639.

244. O'Donoghue, A.J., et al., *Global substrate profiling of proteases in human neutrophil extracellular traps reveals consensus motif predominantly contributed by elastase.* PLoS One, 2013. **8**(9): p. e75141.
245. Khandpur, R., et al., *NETs are a source of citrullinated autoantigens and stimulate inflammatory responses in rheumatoid arthritis.* Sci Transl Med, 2013. **5**(178): p. 178ra40.
246. Dwyer, M., et al., *Cystic fibrosis sputum DNA has NETosis characteristics and neutrophil extracellular trap release is regulated by macrophage migration-inhibitory factor.* J Innate Immun, 2014. **6**(6): p. 765-79.
247. Kim, H.S., et al., *cDNA cloning and characterization of buforin I, an antimicrobial peptide: a cleavage product of histone H2A.* Biochem Biophys Res Commun, 1996. **229**(2): p. 381-7.
248. Hirsch, J.G., *Bactericidal action of histone.* The Journal of experimental medicine, 1958. **108**(6): p. 925-944.
249. Thomas, M.P., et al., *Leukocyte protease binding to nucleic acids promotes nuclear localization and cleavage of nucleic acid binding proteins.* J Immunol, 2014. **192**(11): p. 5390-7.
250. Dubois, A.V., et al., *Influence of DNA on the activities and inhibition of neutrophil serine proteases in cystic fibrosis sputum.* Am J Respir Cell Mol Biol, 2012. **47**(1): p. 80-6.
251. Lauth, X., et al., *M1 protein allows Group A streptococcal survival in phagocyte extracellular traps through cathelicidin inhibition.* Journal of innate immunity, 2009. **1**(3): p. 202-214.
252. Halverson, T.W., et al., *DNA is an antimicrobial component of neutrophil extracellular traps.* PLoS Pathog, 2015. **11**(1): p. e1004593.
253. von Kockritz-Blickwede, M., S. Blodkamp, and V. Nizet, *Interaction of Bacterial Exotoxins with Neutrophil Extracellular Traps: Impact for the Infected Host.* Front Microbiol, 2016. **7**: p. 402.
254. Urban, C.F., et al., *Neutrophil extracellular traps capture and kill Candida albicans yeast and hyphal forms.* Cell Microbiol, 2006. **8**(4): p. 668-76.
255. Saffarzadeh, M., et al., *Neutrophil Extracellular Traps Directly Induce Epithelial and Endothelial Cell Death: A Predominant Role of Histones.* PLOS ONE, 2012. **7**(2): p. e32366.
256. Kolaczkowska, E., et al., *Molecular mechanisms of NET formation and degradation revealed by intravital imaging in the liver vasculature.* Nat Commun, 2015. **6**: p. 6673.
257. Farrera, C. and B. Fadeel, *Macrophage clearance of neutrophil extracellular traps is a silent process.* J Immunol, 2013. **191**(5): p. 2647-56.
258. Thammavongsa, V., D.M. Missiakas, and O. Schneewind, *Staphylococcus aureus degrades neutrophil extracellular traps to promote immune cell death.* Science, 2013. **342**(6160): p. 863-6.
259. Berends, E.T., et al., *Nuclease expression by Staphylococcus aureus facilitates escape from neutrophil extracellular traps.* J Innate Immun, 2010. **2**(6): p. 576-86.
260. Beiter, K., et al., *An endonuclease allows Streptococcus pneumoniae to escape from neutrophil extracellular traps.* Curr Biol, 2006. **16**(4): p. 401-7.
261. Buchanan, J.T., et al., *DNase expression allows the pathogen group A Streptococcus to escape killing in neutrophil extracellular traps.* Curr Biol, 2006. **16**(4): p. 396-400.

262. Wartha, F., et al., *Capsule and D-alanylated lipoteichoic acids protect Streptococcus pneumoniae against neutrophil extracellular traps.* Cell Microbiol, 2007. **9**(5): p. 1162-71.
263. Zinkernagel, A.S., et al., *The IL-8 protease SpyCEP/ScpC of group A Streptococcus promotes resistance to neutrophil killing.* Cell Host Microbe, 2008. **4**(2): p. 170-8.
264. Eby, J.C., M.C. Gray, and E.L. Hewlett, *Cyclic AMP-mediated suppression of neutrophil extracellular trap formation and apoptosis by the Bordetella pertussis adenylate cyclase toxin.* Infect Immun, 2014. **82**(12): p. 5256-69.
265. Kamoshida, G., et al., *Pathogenic Bacterium Acinetobacter baumannii Inhibits the Formation of Neutrophil Extracellular Traps by Suppressing Neutrophil Adhesion.* Frontiers in immunology, 2018. **9**: p. 178-178.
266. Hakkim, A., et al., *Activation of the Raf-MEK-ERK pathway is required for neutrophil extracellular trap formation.* Nat Chem Biol, 2011. **7**(2): p. 75-7.
267. Sorensen, O.E., et al., *Papillon-Lefevre syndrome patient reveals species-dependent requirements for neutrophil defenses.* J Clin Invest, 2014. **124**(10): p. 4539-48.
268. Keshari, R.S., et al., *Reactive oxygen species-induced activation of ERK and p38 MAPK mediates PMA-induced NETs release from human neutrophils.* J Cell Biochem, 2013. **114**(3): p. 532-40.
269. Douda, D.N., et al., *Akt is essential to induce NADPH-dependent NETosis and to switch the neutrophil death to apoptosis.* Blood, 2014. **123**(4): p. 597-600.
270. Nakashima, K., T. Hagiwara, and M. Yamada, *Nuclear localization of peptidylarginine deiminase V and histone deimination in granulocytes.* J Biol Chem, 2002. **277**(51): p. 49562-8.
271. Wang, Y., et al., *Human PAD4 regulates histone arginine methylation levels via demethylimination.* Science, 2004. **306**(5694): p. 279-83.
272. Vossenaar, E.R., et al., *Expression and activity of citrullinating peptidylarginine deiminase enzymes in monocytes and macrophages.* Ann Rheum Dis, 2004. **63**(4): p. 373-81.
273. Dwivedi, N. and M. Radic, *Citrullination of autoantigens implicates NETosis in the induction of autoimmunity.* Ann Rheum Dis, 2014. **73**(3): p. 483-91.
274. Mor-Vaknin, N., et al., *DEK-targeting DNA aptamers as therapeutics for inflammatory arthritis.* Nat Commun, 2017. **8**: p. 14252.
275. Douda, D.N., et al., *SK3 channel and mitochondrial ROS mediate NADPH oxidase-independent NETosis induced by calcium influx.* Proc Natl Acad Sci U S A, 2015. **112**(9): p. 2817-22.
276. Parker, H., et al., *Requirements for NADPH oxidase and myeloperoxidase in neutrophil extracellular trap formation differ depending on the stimulus.* J Leukoc Biol, 2012. **92**(4): p. 841-9.
277. de Bont, C.M., et al., *Stimulus-dependent chromatin dynamics, citrullination, calcium signalling and ROS production during NET formation.* Biochim Biophys Acta Mol Cell Res, 2018. **1865**(11 Pt A): p. 1621-1629.
278. Neeli, I., S.N. Khan, and M. Radic, *Histone Deimination As a Response to Inflammatory Stimuli in Neutrophils.* The Journal of Immunology, 2008. **180**(3): p. 1895-1902.
279. Neeli, I. and M. Radic, *Opposition between PKC isoforms regulates histone deimination and neutrophil extracellular chromatin release.* Front Immunol, 2013. **4**: p. 38.

280. Pieterse, E., et al., *Neutrophils Discriminate between Lipopolysaccharides of Different Bacterial Sources and Selectively Release Neutrophil Extracellular Traps.* Front Immunol, 2016. **7**: p. 484.
281. Neeli, I., et al., *Regulation of extracellular chromatin release from neutrophils.* J Innate Immun, 2009. **1**(3): p. 194-201.
282. Khan, M.A., et al., *JNK Activation Turns on LPS- and Gram-Negative Bacteria-Induced NADPH Oxidase-Dependent Suicidal NETosis.* Scientific Reports, 2017. **7**(1): p. 3409.
283. Yao, W., et al., *ONO-5046 suppresses reactive oxidative species-associated formation of neutrophil extracellular traps.* Life Sci, 2018.
284. Leshner, M., et al., *PAD4 mediated histone hypercitrullination induces heterochromatin decondensation and chromatin unfolding to form neutrophil extracellular trap-like structures.* Front Immunol, 2012. **3**: p. 307.
285. Verschure, P.J., et al., *In vivo HP1 targeting causes large-scale chromatin condensation and enhanced histone lysine methylation.* Mol Cell Biol, 2005. **25**(11): p. 4552-64.
286. Popova, E.Y., et al., *Epigenetic heterochromatin markers distinguish terminally differentiated leukocytes from incompletely differentiated leukemia cells in human blood.* Exp Hematol, 2006. **34**(4): p. 453-62.
287. Majewski, P., et al., *Inhibitors of Serine Proteases in Regulating the Production and Function of Neutrophil Extracellular Traps.* Front Immunol, 2016. **7**: p. 261.
288. Sallenave, J.-M., et al., *Secretory leukocyte proteinase inhibitor is a major leukocyte elastase inhibitor in human neutrophils*. Vol. 61. 1997. 695-702.
289. Cooley, J., et al., *The serpin MNEI inhibits elastase-like and chymotrypsin-like serine proteases through efficient reactions at two active sites.* Biochemistry, 2001. **40**(51): p. 15762-70.
290. Benarafa, C., et al., *Characterization of four murine homologs of the human ov-serpin monocyte neutrophil elastase inhibitor MNEI (SERPINB1).* J Biol Chem, 2002. **277**(44): p. 42028-33.
291. Jacobsen, L.C., et al., *The secretory leukocyte protease inhibitor (SLPI) and the secondary granule protein lactoferrin are synthesized in myelocytes, colocalize in subcellular fractions of neutrophils, and are coreleased by activated neutrophils.* J Leukoc Biol, 2008. **83**(5): p. 1155-64.
292. Farley, K., et al., *A serpinB1 regulatory mechanism is essential for restricting neutrophil extracellular trap generation.* Journal of immunology (Baltimore, Md. : 1950), 2012. **189**(9): p. 4574-4581.
293. Zabieglo, K., et al., *The inhibitory effect of secretory leukocyte protease inhibitor (SLPI) on formation of neutrophil extracellular traps.* J Leukoc Biol, 2015. **98**(1): p. 99-106.
294. Liu, X., et al., *Inflammasome-activated gasdermin D causes pyroptosis by forming membrane pores.* Nature, 2016. **535**(7610): p. 153-8.
295. Kaplan, M.J. and M. Radic, *Neutrophil extracellular traps: double-edged swords of innate immunity.* J Immunol, 2012. **189**(6): p. 2689-95.
296. Klebanoff, S.J., et al., *Myeloperoxidase: a front-line defender against phagocytosed microorganisms.* J Leukoc Biol, 2013. **93**(2): p. 185-98.
297. Jorch, S.K. and P. Kubes, *An emerging role for neutrophil extracellular traps in noninfectious disease.* Nat Med, 2017. **23**(3): p. 279-287.
298. Erpenbeck, L. and M.P. Schön, *Neutrophil extracellular traps: protagonists of cancer progression?* Oncogene, 2016.

299. Cools-Lartigue, J., et al., *Neutrophil extracellular traps sequester circulating tumor cells and promote metastasis.* J Clin Invest, 2013.
300. Nie, M., et al., *Neutrophil extracellular traps induced by IL-8 promote diffuse large B cell lymphoma progression via the TLR9 signaling.* Clin Cancer Res, 2018.
301. Kim, T.Y., et al., *Elevated extracellular trap formation and contact system activation in acute leukemia.* J Thromb Thrombolysis, 2018. **46**(3): p. 379-385.
302. Grabcanovic-Musija, F., et al., *Neutrophil extracellular trap (NET) formation characterises stable and exacerbated COPD and correlates with airflow limitation.* Respir Res, 2015. **16**: p. 59.
303. Gupta, A.K., et al., *Induction of neutrophil extracellular DNA lattices by placental microparticles and IL-8 and their presence in preeclampsia.* Hum Immunol, 2005. **66**: p. 1146-1154.
304. Clark, S.R., et al., *Platelet TLR4 activates neutrophil extracellular traps to ensnare bacteria in septic blood.* Nat Med, 2007. **13**: p. 463-469.
305. Döring, Y., O. Soehnlein, and C. Weber, *Neutrophil Extracellular Traps in Atherosclerosis and Atherothrombosis.* Circ Res, 2017. **120**(4): p. 736-743.
306. Kimball, A.S., et al., *The Emerging Role of NETs in Venous Thrombosis and Immunothrombosis.* Front Immunol, 2016. **7**: p. 236.
307. Langseth, M.S., et al., *Markers of neutrophil extracellular traps are associated with adverse clinical outcome in stable coronary artery disease.* Eur J Prev Cardiol, 2018. **25**(7): p. 762-769.
308. Borissoff, J.I., et al., *Elevated levels of circulating DNA and chromatin are independently associated with severe coronary atherosclerosis and a prothrombotic state.* Arterioscler Thromb Vasc Biol, 2013. **33**(8): p. 2032-2040.
309. de Boer, O.J., et al., *Neutrophils, neutrophil extracellular traps and interleukin-17 associate with the organisation of thrombi in acute myocardial infarction.* Thromb Haemost, 2013. **109**(2): p. 290-7.
310. Leppkes, M., et al., *Externalized decondensed neutrophil chromatin occludes pancreatic ducts and drives pancreatitis.* 2016. **7**: p. 10973.
311. Dwivedi, N. and M. Radic, *Burning controversies in NETs and autoimmunity: The mysteries of cell death and autoimmune disease.* Autoimmunity, 2018: p. 1-14.
312. Lee, K.H., et al., *Neutrophil extracellular traps (NETs) in autoimmune diseases: A comprehensive review.* Autoimmun Rev, 2017. **16**(11): p. 1160-1173.
313. Sur Chowdhury, C., et al., *Enhanced neutrophil extracellular trap generation in rheumatoid arthritis: analysis of underlying signal transduction pathways and potential diagnostic utility.* Arthritis Res Ther, 2014. **16**(3): p. R122.
314. Wang, W., W. Peng, and X. Ning, *Increased levels of neutrophil extracellular trap remnants in the serum of patients with rheumatoid arthritis.* Int J Rheum Dis, 2018. **21**(2): p. 415-421.
315. Leffler, J., et al., *Degradation of neutrophil extracellular traps co-varies with disease activity in patients with systemic lupus erythematosus.* Arthritis Res Ther, 2013. **15**(4): p. R84.
316. Hu, S.C., et al., *Neutrophil extracellular trap formation is increased in psoriasis and induces human beta-defensin-2 production in epidermal keratinocytes.* Sci Rep, 2016. **6**: p. 31119.
317. Schön, M.P. and L. Erpenbeck, *The Interleukin-23/Interleukin-17 Axis Links Adaptive and Innate Immunity in Psoriasis.* Frontiers in immunology, 2018. **9**: p. 1323-1323.

318. Kessenbrock, K., et al., *Netting neutrophils in autoimmune small-vessel vasculitis.* Nat Med, 2009. **15**(6): p. 623-5.
319. Rojas, M., et al., *Molecular mimicry and autoimmunity.* Journal of Autoimmunity, 2018. **95**: p. 100-123.
320. Munoz, L.E., et al., *The role of defective clearance of apoptotic cells in systemic autoimmunity.* Nat Rev Rheumatol, 2010. **6**(5): p. 280-9.
321. Mahajan, A., M. Herrmann, and L.E. Muñoz, *Clearance Deficiency and Cell Death Pathways: A Model for the Pathogenesis of SLE.* Frontiers in immunology, 2016. **7**: p. 35-35.
322. Carmona-Rivera, C. and M.J. Kaplan, *Detection of SLE antigens in neutrophil extracellular traps (NETs).* Methods Mol Biol, 2014. **1134**: p. 151-61.
323. Sangaletti, S., et al., *Neutrophil extracellular traps mediate transfer of cytoplasmic neutrophil antigens to myeloid dendritic cells toward ANCA induction and associated autoimmunity.* Blood, 2012. **120**(15): p. 3007-18.
324. Lande, R., et al., *Neutrophils activate plasmacytoid dendritic cells by releasing self-DNA-peptide complexes in systemic lupus erythematosus.* Science translational medicine, 2011. **3**(73): p. 73ra19-73ra19.
325. Gestermann, N., et al., *Netting Neutrophils Activate Autoreactive B Cells in Lupus.* J Immunol, 2018. **200**(10): p. 3364-3371.
326. Lande, R., et al., *Plasmacytoid dendritic cells sense self-DNA coupled with antimicrobial peptide.* Nature, 2007. **449**(7162): p. 564-9.
327. Carmona-Rivera, C. and M.J. Kaplan, *Low-density granulocytes: a distinct class of neutrophils in systemic autoimmunity.* Semin Immunopathol, 2013. **35**(4): p. 455-63.
328. Wang, H., et al., *Neutrophil Extracellular Trap Mitochondrial DNA and Its Autoantibody in Systemic Lupus Erythematosus and a Proof-of-Concept Trial of Metformin.* Arthritis Rheumatol, 2015. **67**(12): p. 3190-200.
329. Yasutomo, K., et al., *Mutation of DNASE1 in people with systemic lupus erythematosus.* Nat Genet, 2001. **28**(4): p. 313-4.
330. Martinez-Valle, F., et al., *DNase 1 activity in patients with systemic lupus erythematosus: relationship with epidemiological, clinical, immunological and therapeutical features.* Lupus, 2009. **18**(5): p. 418-23.
331. Hakkim, A., et al., *Impairment of neutrophil extracellular trap degradation is associated with lupus nephritis.* Proc Natl Acad Sci U S A, 2010. **107**(21): p. 9813-8.
332. Leffler, J., et al., *Neutrophil Extracellular Traps That Are Not Degraded in Systemic Lupus Erythematosus Activate Complement Exacerbating the Disease.* The Journal of Immunology, 2012. **188**(7): p. 3522-3531.
333. Eyerich, S., et al., *Cutaneous Barriers and Skin Immunity: Differentiating A Connected Network.* Trends in Immunology, 2018. **39**(4): p. 315-327.
334. Gueymard, C.A., D. Myers, and K. Emery, *Proposed reference irradiance spectra for solar energy systems testing.* Solar Energy, 2002. **73**(6): p. 443-467.
335. Anderson, R.R. and J.A. Parrish, *The optics of human skin.* J Invest Dermatol, 1981. **77**(1): p. 13-9.
336. Igarashi, T., K. Nishino, and S.K. Nayar, *The Appearance of Human Skin.* New York: Columbia University, 2005: p. 1-85.
337. Svobodova, A. and J. Vostalova, *Solar radiation induced skin damage: review of protective and preventive options.* Int J Radiat Biol, 2010. **86**(12): p. 999-1030.

338. Anderson, R.R., J. Hu, and J.A. Parrish, *Optical radiation transfer in the human skin and applications in in vivo remittance spectroscopy.* Marks R., Payne P.A. (eds) Symposium Bioengineering and the Skin, 1981.
339. Hammel, H.T., J.D. Hardy, and D. Murgatroyd, *Spectral transmittance and reflectance of excised human skin.* J Appl Physiol, 1956. **9**(2): p. 257-64.
340. Hasselbaich, K.A., *Quantitative Untersuchungen über die Absorption der menschlichen Haut von ultravioletten Strahlen.* Skand Arch Physiol 1911. **25**(2): p. 5-68.
341. Ha, R.Y., et al., *Analysis of facial skin thickness: defining the relative thickness index.* Plast Reconstr Surg, 2005. **115**(6): p. 1769-73.
342. Sandby-Moller, J., T. Poulsen, and H.C. Wulf, *Epidermal thickness at different body sites: relationship to age, gender, pigmentation, blood content, skin type and smoking habits.* Acta Derm Venereol, 2003. **83**(6): p. 410-3.
343. Fritsch, P. and T. Schwarz, *Dermatologie Venerologie. Grundlagen. Klinik. Atlas. (3th ed.).* Berlin/Heidelberg: Springer-Verlag, 2018(3): p. 101-15.
344. Clydesdale, G.J., G.W. Dandie, and H.K. Muller, *Ultraviolet light induced injury: immunological and inflammatory effects.* Immunol Cell Biol, 2001. **79**(6): p. 547-68.
345. Pattison, D.I. and M.J. Davies, *Actions of ultraviolet light on cellular structures.* EXS, 2006(96): p. 131-57.
346. Nakashima, Y., S. Ohta, and A.M. Wolf, *Blue light-induced oxidative stress in live skin.* Free Radic Biol Med, 2017. **108**: p. 300-310.
347. Kulms, D. and T. Schwarz, *Molecular mechanisms of UV-induced apoptosis.* Photodermatol Photoimmunol Photomed, 2000. **16**(5): p. 195-201.
348. Nishisgori, C., *Current concept of photocarcinogenesis.* Photochem Photobiol Sci, 2015. **14**(9): p. 1713-21.
349. Aubin, F., *Mechanisms involved in ultraviolet light-induced immunosuppression.* Eur J Dermatol, 2003. **13**(6): p. 515-23.
350. Kim, A. and B.F. Chong, *Photosensitivity in cutaneous lupus erythematosus.* Photodermatology, photoimmunology & photomedicine, 2013. **29**(1): p. 4-11.
351. Li, C., et al., *Ultraviolet light A irradiation induces immunosuppression associated with the generation of reactive oxygen species in human neutrophils.* Journal of Innovative Optical Health Sciences, 2016. **09**(01): p. 1650001.
352. Sweeney, J.F., et al., *Ultraviolet irradiation accelerates apoptosis in human polymorphonuclear leukocytes: protection by LPS and GM-CSF.* J Leukoc Biol, 1997. **62**(4): p. 517-23.
353. Frasch, S.C., et al., *p38 mitogen-activated protein kinase-dependent and -independent intracellular signal transduction pathways leading to apoptosis in human neutrophils.* J Biol Chem, 1998. **273**(14): p. 8389-97.
354. Azzouz, D., et al., *Two-in-one: UV radiation simultaneously induces apoptosis and NETosis.* Cell Death Discov, 2018. **4**: p. 51.
355. Mario, M., et al., *Near infrared laser irradiation induces NETosis via oxidative stress and autophagy.* Lasers Med Sci, 2018.
356. Swerlick, R.A., *The structure and function of the cutaneous vasculature.* J Dermatol, 1997. **24**(11): p. 734-8.
357. Lee, P.L., H. van Weelden, and P.L. Bruijnzeel, *Neutrophil infiltration in normal human skin after exposure to different ultraviolet radiation sources.* Photochem Photobiol, 2008. **84**(6): p. 1528-34.

358. Strickland, I., et al., *TNF-alpha and IL-8 are upregulated in the epidermis of normal human skin after UVB exposure: correlation with neutrophil accumulation and E-selectin expression.* J Invest Dermatol, 1997. **108**(5): p. 763-8.
359. Oka, M., et al., *Phospholipase Cε has a crucial role in ultraviolet B-induced neutrophil-associated skin inflammation by regulating the expression of CXCL1/KC.* Laboratory Investigation, 2011. **91**: p. 711.
360. Rijken, F., R.C. Kiekens, and P.L. Bruijnzeel, *Skin-infiltrating neutrophils following exposure to solar-simulated radiation could play an important role in photoageing of human skin.* Br J Dermatol, 2005. **152**(2): p. 321-8.
361. Hoffman, T. and E.F. Lizzio, *Albumin in monocyte function assays. Differential stimulation of superoxide or arachidonate release by calcium ionophores.* J Immunol Methods, 1988. **112**(1): p. 9-14.
362. David, S.A., P. Balaram, and V.I. Mathan, *Characterization of the interaction of lipid A and lipopolysaccharide with human serum albumin: implications for an endotoxin carrier function for albumin.* Journal of Endotoxin Research, 1995. **2**(2): p. 99-106.
363. Nimeri, G., et al., *The influence of plasma proteins and platelets on oxygen radical production and F-actin distribution in neutrophils adhering to polymer surfaces.* Biomaterials, 2002. **23**(8): p. 1785-95.
364. Knox, P., *Kinetics of cell spreading in the presence of different concentrations of serum or fibronectin-depleted serum.* Journal of Cell Science, 1984. **71**(1): p. 51-59.
365. Erpenbeck, L., et al., *Effect of Adhesion and Substrate Elasticity on Neutrophil Extracellular Trap Formation.* bioRxiv, 2019: p. 508366.
366. Katz, J., G. Bonorris, and A.L. Sellers, *Extravascular albumin in human tissues.* Clin Sci, 1970. **39**(6): p. 725-9.
367. Butcher, D.T., T. Alliston, and V.M. Weaver, *A tense situation: forcing tumour progression.* Nat Rev Cancer, 2009. **9**(2): p. 108-22.
368. Healy, L.D., et al., *Activated protein C inhibits neutrophil extracellular trap formation in vitro and activation in vivo.* J Biol Chem, 2017. **292**(21): p. 8616-8629.
369. Mohanty, T., et al., *A novel mechanism for NETosis provides antimicrobial defense at the oral mucosa.* Blood, 2015. **126**(18): p. 2128-37.
370. Khan, M.A., et al., *Regulating NETosis: Increasing pH Promotes NADPH Oxidase-Dependent NETosis.* Front Med (Lausanne), 2018. **5**: p. 19.
371. Behnen, M., et al., *Extracellular Acidification Inhibits the ROS-Dependent Formation of Neutrophil Extracellular Traps.* Frontiers in Immunology, 2017. **8**(184).
372. Naffah de Souza, C., et al., *Alkaline pH Promotes NADPH Oxidase-Independent Neutrophil Extracellular Trap Formation: A Matter of Mitochondrial Reactive Oxygen Species Generation and Citrullination and Cleavage of Histone.* Front Immunol, 2017. **8**: p. 1849.
373. Uotila, L.M., et al., *Filamin A Regulates Neutrophil Adhesion, Production of Reactive Oxygen Species, and Neutrophil Extracellular Trap Release.* J Immunol, 2017.
374. Kim, H. and C.A. McCulloch, *Filamin A mediates interactions between cytoskeletal proteins that control cell adhesion.* FEBS Lett, 2011. **585**(1): p. 18-22.
375. Sun, C., et al., *Filamin-A regulates neutrophil uropod retraction through RhoA during chemotaxis.* PLoS One, 2013. **8**(10): p. e79009.
376. Kiema, T., et al., *The molecular basis of filamin binding to integrins and competition with talin.* Mol Cell, 2006. **21**(3): p. 337-47.
377. Brinkmann, V. and A. Zychlinsky, *Neutrophil extracellular traps: is immunity the second function of chromatin?* J Cell Biol, 2012. **198**(5): p. 773-83.

378. Friedl, P., K. Wolf, and J. Lammerding, *Nuclear mechanics during cell migration.* Curr Opin Cell Biol, 2011. **23**(1): p. 55-64.
379. Gesson, K., et al., *A-type lamins bind both hetero- and euchromatin, the latter being regulated by lamina-associated polypeptide 2 alpha.* Genome Res, 2016. **26**(4): p. 462-73.
380. Thiam, H.-R., et al., *Perinuclear Arp2/3-driven actin polymerization enables nuclear deformation to facilitate cell migration through complex environments.* Nature communications, 2016. **7**: p. 10997-10997.
381. Schreiner, S.M., et al., *The tethering of chromatin to the nuclear envelope supports nuclear mechanics.* Nature Communications, 2015. **6**: p. 7159.
382. Olins, A.L., et al., *The human granulocyte nucleus: Unusual nuclear envelope and heterochromatin composition.* Eur J Cell Biol, 2008. **87**(5): p. 279-90.
383. Bonne-Année, S., et al., *Extracellular traps are associated with human and mouse neutrophil and macrophage mediated killing of larval Strongyloides stercoralis.* Microbes and infection, 2014. **16**(6): p. 502-511.
384. Harada, T., et al., *Nuclear lamin stiffness is a barrier to 3D migration, but softness can limit survival.* The Journal of Cell Biology, 2014. **204**(5): p. 669-682.
385. Raab, M., et al., *ESCRT III repairs nuclear envelope ruptures during cell migration to limit DNA damage and cell death.* Science, 2016. **352**(6283): p. 359-62.
386. Shah, P., K. Wolf, and J. Lammerding, *Bursting the Bubble - Nuclear Envelope Rupture as a Path to Genomic Instability?* Trends Cell Biol, 2017. **27**(8): p. 546-555.
387. Gray, R.D., et al., *Delayed neutrophil apoptosis enhances NET formation in cystic fibrosis.* Thorax, 2018. **73**(2): p. 134-144.
388. Kambara, H., et al., *Gasdermin D Exerts Anti-inflammatory Effects by Promoting Neutrophil Death.* Cell Rep, 2018. **22**(11): p. 2924-2936.
389. Tran, J.R., et al., *Lamin in inflammation and aging.* Curr Opin Cell Biol, 2016. **40**: p. 124-130.
390. Scaffidi, P. and T. Misteli, *Lamin A-dependent nuclear defects in human aging.* Science, 2006. **312**(5776): p. 1059-63.
391. Gaines, P., et al., *Mouse neutrophils lacking lamin B-receptor expression exhibit aberrant development and lack critical functional responses.* Exp Hematol, 2008. **36**(8): p. 965-76.
392. Tibrewal, S., et al., *Hyperosmolar stress induces neutrophil extracellular trap formation: implications for dry eye disease.* Invest Ophthalmol Vis Sci, 2014. **55**(12): p. 7961-9.
393. Csomos, K., et al., *Protein cross-linking by chlorinated polyamines and transglutamylation stabilizes neutrophil extracellular traps.* Cell Death Dis, 2016. **7**(8): p. e2332.
394. Sollberger, G., B. Amulic, and A. Zychlinsky, *Neutrophil Extracellular Trap Formation Is Independent of De Novo Gene Expression.* PLoS One, 2016. **11**(6): p. e0157454.
395. Medicine, I.o., *The Role of Protein and Amino Acids in Sustaining and Enhancing Performance*. 1999, Washington, DC: The National Academies Press. 448.
396. Khan, M.A. and N. Palaniyar, *Transcriptional firing helps to drive NETosis.* Sci Rep, 2017. **7**: p. 41749.
397. Hamam, H.J., M.A. Khan, and N. Palaniyar, *Histone Acetylation Promotes Neutrophil Extracellular Trap Formation.* Biomolecules, 2019. **9**(1).
398. Yasuda, H., Y. Takishita, and E.F. Sato, *P-97 - Epigenetic regulation of neutrophil extracellular traps.* Free Radical Biology and Medicine, 2018. **120**: p. S74.

399. Neumann, A., et al., *Lipid alterations in human blood-derived neutrophils lead to formation of neutrophil extracellular traps.* Eur J Cell Biol, 2014. **93**(8-9): p. 347-54.
400. Brogden, G., et al., *Methods to Study Lipid Alterations in Neutrophils and the Subsequent Formation of Neutrophil Extracellular Traps.* J Vis Exp, 2017(121).
401. Wildhagen, K.C., et al., *Nonanticoagulant heparin prevents histone-mediated cytotoxicity in vitro and improves survival in sepsis.* Blood, 2014. **123**(7): p. 1098-101.
402. Rossaint, J. and A. Zarbock, *Tissue-specific neutrophil recruitment into the lung, liver, and kidney.* J Innate Immun, 2013. **5**(4): p. 348-57.
403. Lewis, H.D., et al., *Inhibition of PAD4 activity is sufficient to disrupt mouse and human NET formation.* Nat Chem Biol, 2015. **11**(3): p. 189-91.
404. Li, P., et al., *PAD4 is essential for antibacterial innate immunity mediated by neutrophil extracellular traps.* J Exp Med, 2010. **207**(9): p. 1853-62.
405. Inoue, M., et al., *Plasma redox imbalance caused by albumin oxidation promotes lung-predominant NETosis and pulmonary cancer metastasis.* Nat Commun, 2018. **9**(1): p. 5116.

Acknowledgements

The completion of this thesis would not have been possible without the support of such a vast number of people that it is impossible for me to mention them entirely. However, I would like to express special thanks to some people who particularly encouraged this work.

First of all, I want to commemorate my deep appreciation to my supervisors Dr. Luise Erpenbeck and Dr. Sebastian Kruss as well as my first referee and mentor Prof. Michael P. Schön for their support far beyond pure scientific advising! Your close personal guidance and scientific passion incredibly encouraged me during my dissertation and augmented my personal development to an extent I would have never expected. Thank you for everything!

Additionally, I would like to express my gratitude to Prof. Jürgen Wienands, the second referee of this doctoral thesis, for his scientific support and guidance during my promotion within the thesis committee. In this context, I also would not want to miss the opportunity to thank my mentor Prof. Christian Ammer together with the whole peer coaching group of the *Dorothea Schlözer Mentoring* for our exciting discussions, the personal strength you gave me during my doctoral period and for an unforgettable carriage ride.

Of course, the greatest reward belongs to the entire lab-team of my supervisors. I am extremely grateful to be a member of these groups; you made my doctoral time unforgettable! Particularly, I want to thank Daniel Meyer for his exceptional support as a co-worker and close friend as well as the student-co-worker-team, including Katharina, Susanne, Anja, Sophie, Julia, Antonia, Veit and all the other co-authors on the publications this thesis is based on. I also want to give my greatest thanks to the diligent proof-readers Aya, Gerda, Verena, Florian, Quinte, Susanne, Meshkat and Gabriele as well as the endless number of blood donors!

I would like to profusely thank the research groups of Prof. Schön and Prof. Janshoff as well as of Prof. Steinem, Prof. Bogeski and Prof. Egner for the interesting cooperations, exceptional technical guidance and support, fascinating discussions, all your suggestions and obviously lots of fun!

And last but certainly not least, I would like to express my endless thanks to my parents, both of my sisters, my entire family and friends for their outstanding support, never-ending patience and love during this challenging life period. I also want to thank my love Quinte and his family for withstanding long nights and supporting me with their affection during the exhausting writing phase. In this context, I further want to express my deepest gratitude to my uncle Michael, my grandfather Reinhart and my second cousin David for their scientific inspiration from childhood on.

List of publications

1. Elsa Neubert*, Daniel Meyer*, Francesco Rocca, Gökhan Günay, Anja Kwaczala-Tessmann, Julia Grandke, Susanne N. Senger-Sander, Claudia Geisler, Alexander Egner, Michael P. Schön, Luise Erpenbeck und Sebastian Kruss; "*Chromatin swelling drives neutrophil extracellular trap release*", Nature Communications, 2018, DOI: 10.1038/s41467-018-06263-5.

2. Elena Polo, Tadeusz T. Nitka, Elsa Neubert, Luise Erpenbeck, Lela Vukovic, Sebastian Kruss; „*Control of integrin affinity by confining RGD peptides on fluorescent carbon nanotubes*", ACS Applied Materials and Interfaces, 2018, DOI: 10.1021/acsami.8b04373.

3. Elsa Neubert*, Susanne N. Senger-Sander*, Veit S. Manzke, Julia Busse, Elena Polo, Sophie E. F. Scheidmann, Michael P. Schön, S. Kruss and L. Erpenbeck; „ Serum and Serum Albumin Inhibit *in vitro* Formation of Neutrophil Extracellular Traps (NETs)", Frontiers in Immunology, 2019, DOI: 10.3389/fimmu.2019.00012.

4. Luise Erpenbeck*, Antonia L. Gruhn*, Galina Kudryasheva, Gökhan Günay, Daniel Meyer, Elsa Neubert, Julia Busse, Michael P. Schön, Florian Rehfeldt, Sebastian Kruss; "*Effect of Substrate Elasticity on Neutrophil Extracellular Trap Formation*", preprint uploaded to bioRxiv, 2019, DOI: 10.1101/508366.

5. SyedSaoud Zaidi*, Mong-Jen Chen*, Daniel T Lee, Elsa Neubert, Pär Ewing, Anna Miller-Larsson, Günther Hochhaus; „*Placental P-glycoprotein Reduces the Placental Transfer of Budesonide but not Fluticasone Propionate: A Study in Mice*", AAPS J., accepted.

6. Elsa Neubert*, Katharina M. Bach*, Julia Busse, Ivan Bogeski, Michael P. Schön, Sebastian Kruss, Luise Erpenbeck; "*Blue and Long-wave Ultraviolet Light Induce in vitro Neutrophil Extracellular trap formation*", prepared for submission to Frontiers in Immunology.

*Authors contributed equally